

CHAPTER I

Introduction and Background: The Convergence of Peptide and Polymer Science toward Novel Antibiotics

Motivation and Objectives

Since the serendipitous discovery of penicillin by Alexander Fleming in 1928,¹ antibiotic drugs have been the standard in treatment for infectious disease, saving countless lives worldwide. Unfortunately, widespread use has led to evolution of microbial strains that resist the action of antibiotics.^{2,3} Notable examples of antibiotic-resistant bacteria that currently pose a significant threat to public health include methicillin-resistant *Staphylococcus aureus* (MRSA),⁴ extensively drug-resistant tuberculosis (XDR-TB),^{5,6} and vancomycin-resistant *Enterococci* (VRE).⁷ A steady supply of new antibiotics, which work by novel mechanisms of action, is therefore requisite to keep pace with the constant proliferation of antibiotic-resistant bacteria. However, an alarming trend has recently emerged: while resistance continues to spread prodigiously, the number of new antibiotic drugs approvals has been declining.⁸

As a result, there is currently an urgent need for new anti-infective strategies, which are not susceptible to the existing mechanisms of resistance. The chief objective is to obtain compounds that would fulfill the following design objectives:

- Potent activity against a broad spectrum of bacterial strains, to ensure applicability against a wide variety of infections
- Rapid bactericidal kinetics, to avoid loss of activity by degradation
- Little or no toxicity to human cells, to minimize side effects during treatment
- Reduced likelihood of inducing bacterial resistance, to ensure that the drugs will remain useful for an extended period of time
- Reasonable manufacturing cost, to ensure affordability

Novel compounds which fulfill the above criteria are expected to advance the field of antimicrobials by circumventing the current resistance mechanisms, and will thereby aid in the treatment of infectious disease. This dissertation focuses on using new design principles that mimic the antibacterial function of natural peptides to optimize the activity of polymers as antimicrobial agents which fulfill the criteria listed above. The central goal of this bio-mimetic design approach is to capture the specific structural features of the peptides which control their activity using synthetic polymers, rather than the conventional approach of exactly copying their chemical structure.

Host Defense Peptides

Host defense peptides (HDPs) are a class of compounds found in nature that function as a part of the innate immune system to defend the host against invasion by harmful bacteria.⁹ These peptides primarily act by direct killing of bacteria cells, and by induction of immune response.¹⁰ Hence, the term “host-defense” is derived from their protective function in the body. Focusing on the ability of these natural peptides to directly kill bacteria, they are often referred to as “antimicrobial peptides (AMP)” in the literature.¹¹ Because the AMPs kill bacteria without harming host cells, they are particularly attractive as potential new antibiotics. The peptides can kill a broad spectrum of bacterial strains, exert rapid bactericidal kinetics, are non-toxic to host cells. Additionally, they are less prone to resistance by bacterial cells due to their mechanism of action, which putatively relies on membrane disruption.¹²

Since the 1950's, it has been known that normal tissues and secretions possess the ability to inhibit the growth of microbes and that these substances play a role in the innate immunity of host cells.¹³ The identity of the active antimicrobial compounds in these tissues remained elusive for many decades. In 1987, Zasloff discovered one of the earliest known HDPs in the skin of the African clawed frog *Xenopus laevis*.¹⁴ *Xenopus* does not show signs of infection in microbially contaminated pond water, even after undergoing surgery without antibiotics, which prompted Zasloff to search for an active antimicrobial compound in their skin. He isolated two short peptides from the frog skin secretions and determined their sequences, which are rich in hydrophobic and cationic residues. The peptides displayed potent activity against a panel of fourteen gram-positive

and gram-negative bacteria, including *E. coli* and *S. aureus*. They were named magainin-1 and -2 (from the Hebrew *magain*, meaning “shield”). The sequence and secondary structure of magainin-2 are shown in Figure I-1.

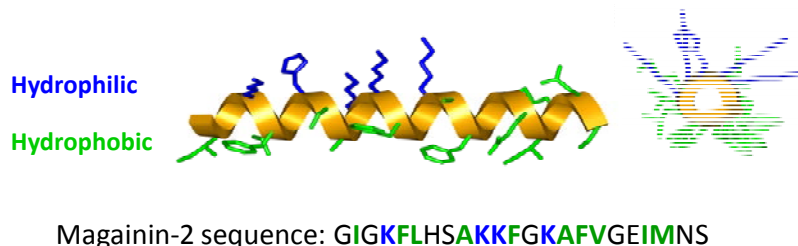


Figure I-1. Sequence and secondary structure of magainin-2, a prototypical host defense peptide.

Other early pioneers in the HDP field include Boman and Lehrer, who independently isolated antimicrobial cecropins from insects¹⁵ and defensins from humans,^{16, 17} respectively. Since these early discoveries, it has been shown that HDPs are present in all multi-cellular organisms,⁹ as a part of immune system to combat invading pathogens.¹⁴ Since their discovery, HDPs have attracted intense scientific and commercial interest.^{18, 19} For example, omiganan (MBI-226) is a cationic, amphiphilic peptide isolated from bovine neutrophils which recently passed Phase III clinical trial for preventing catheter-related infections.²⁰ This demonstrates the potential for host defense peptides to serve as novel antibiotic drugs.

Host defense peptides are characterized by extraordinary diversity in origin, primary sequence, and secondary structure.⁹ Despite the lack of homology, there appear to be certain features which are common to a vast majority of antimicrobial peptides.¹⁸ Wang and co-workers have compiled an exhaustive database of more than seventeen hundred known antimicrobial peptides (AMPs).^{21, 22} The most up-to-date version of this database can be accessed at the following URL: <http://aps.unmc.edu/AP/main.php>. Analysis of the AMP database reveals that the vast majority of antimicrobial peptides possess the following characteristics in terms of their amino acid sequences:

- Net cationic charge at neutral pH (average +3.8)
- Amphiphilicity (average 44% non-polar residues)
- Low molecular weight (average 30.6 amino acids)

These properties are thought to play a key role in the mechanism of antimicrobial action exerted by the peptides. Determining the mechanism by which HDPs exert their

bactericidal effects has been a main focus in the field.^{23, 24} Once the active peptides were isolated, it was found that the all-D and all-L enantiomeric forms express similar antimicrobial activity, which indicates the absence of a specific receptor-mediated interaction (not a “lock-and-key” type mechanism).²⁵ Considering their amphiphilic nature, Matsuzaki and others hypothesized that the mechanism of antimicrobial action exerted by HDPs involves disruption of the bacterial cell membrane.^{26, 27} Even before the discovery of magainins, it was proposed that the antimicrobial components in normal tissue act by damaging bacterial membranes.^{28, 29} Indeed, magainin-2 induces leakage of entrapped contents from within model lipid vesicles, which mimic the phospholipid composition of bacterial cell membranes.²⁶

A large body of work has been directed at analysis of the details of this membrane disruption event.³⁰⁻³⁷ Magainin-2, an extensively studied prototypical HDP, exists as a random coil in solution. Because bacterial membranes display a greater density of anionic lipids on their membranes, relative to mammalian cells, electrostatic attraction favors selective binding of the cationic peptides to bacteria versus mammalian cells (Figure I-2). Additionally, mammalian cells contain cholesterol, which increases the rigidity of the membranes and are therefore believed resist the insertion by antimicrobial peptides.³⁸

Upon binding to bacterial cell membranes, it adopts an α -helical structure, in which cationic residues are displayed on one “face” of the helix, while the non-polar side chains are on the opposing face.^{38, 39} This motif is known as “facial amphiphilicity” and has been observed in a variety of α -helical antimicrobial peptides.⁴⁰⁻⁴³ The helix formation of peptides is induced by the complexation of cationic groups with lipid headgroups, whereas the hydrophobic face of the helix is localized in the non-polar membrane core (Figure I-3).^{42, 44} Other antimicrobial peptides form β -sheet structures, in which cationic and hydrophobic residues are displayed on opposite sides, and the backbone is stabilized by disulfide bonds.⁴⁵ In addition, certain peptides can form irregular conformations (lacking the helical or sheet motif) which nevertheless segregate cationic and hydrophobic residues into different domains.⁴⁶ This suggests that the facially amphiphilic nature, rather than specific structural elements such the α -helix, is the chief determinant of antimicrobial activity.

without lipid reorientation.^{37, 45, 51} Finally, peptides may accumulate on the outer surface of the membranes and completely disrupt the lipids via the “carpet model”.³⁵ For large a quantity of peptide bound to the membrane, solubilization of the membranes could be dominant (Figure I-3). It is generally accepted that the increased membrane permeability leads to loss of the transmembrane potential, leakage of cytoplasmic contents or osmotic lysis, and ultimately cell death.

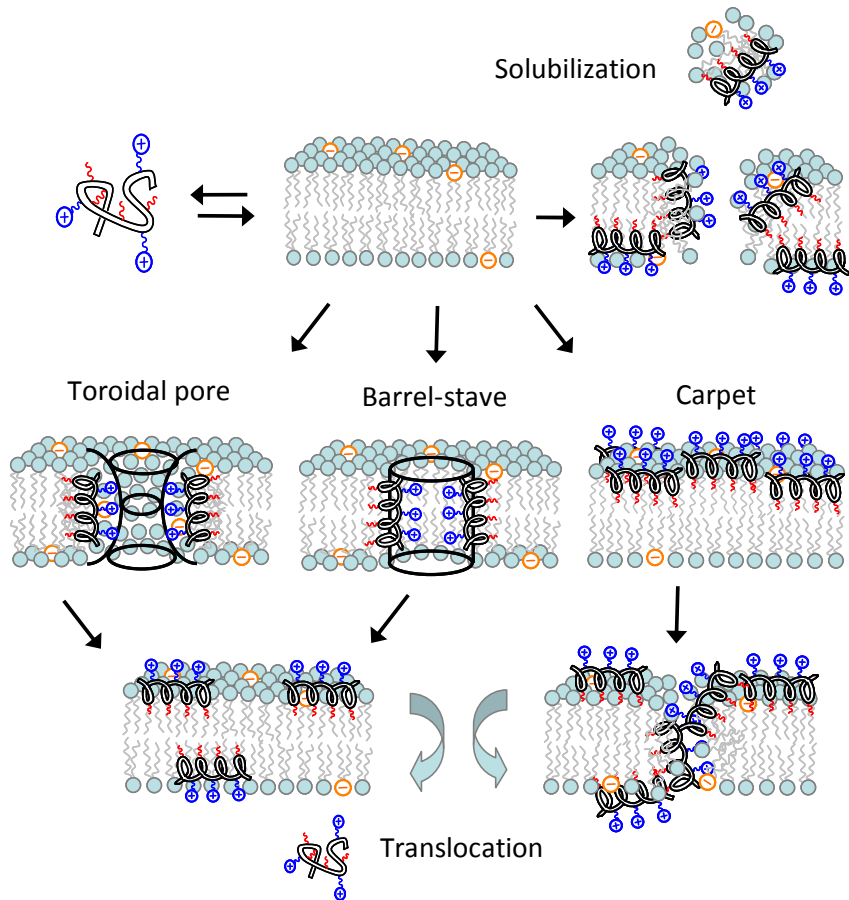


Figure I-3. Proposed mechanisms of membrane disruption exerted by antimicrobial peptides

While HDPs are very promising candidates in pharmaceutical applications, several obstacles continue to plague the realistic outlook for their widespread use as drugs.⁵² The methods required to synthesize sequence specific peptides are often cost- and labor-intensive relative to traditional antibiotics.⁵² Furthermore, HDPs being considered for clinical trials have encountered obstacles including proteolysis, reduced activity *in vivo*, and poor pharmacokinetics.⁵² Proteolysis, the degradation of peptide chains by enzymes in the body, reduces the number of active compounds available to kill

bacteria. Pharmacokinetics, the time-dependent distribution of a drug in the body after administration, are hampered by removal of the peptides from the site of infection prior to killing the bacteria. Activity can be further hindered *in vivo* due to screening of the electrostatic attraction by salts or inactivation of the peptides by serum.

It has been hypothesized that the antimicrobial mechanism of HDPs can be generalized to non-natural (synthetic) peptides, because their function is controlled by facial amphiphilicity and cationic charge, rather than highly specific receptor-mediated interactions. Synthetic α -helical peptides which can adapt facially amphiphilic structures, such as the magainin derivative MSI-78, have shown superior antimicrobial activity relative to the natural peptide magainin-2.^{12, 53} In addition to the peptides based on naturally-occurring α -amino acids (Figure I-4, structure A), peptidomimetics have been also examined. For example, β -peptides consisting of β -amino acids (Figure I-4, structure B), have been shown to kill bacteria without harming human cells.^{54, 55} Peptoids are another class of peptidomimetics in which the side chains are attached to the amide nitrogen atom (Figure I-4, structure C). Peptoids lack a chiral center in the backbone, but the side chains can be designed to induce facially amphiphilic conformations upon membrane binding.⁴³

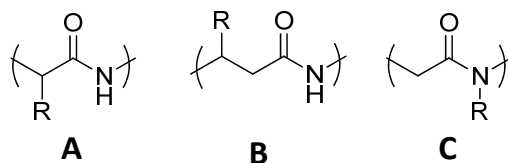


Figure I-4. Structures of (A) peptides, (B) β -peptides, and (C) peptoids

Accordingly, β -peptides⁵⁶ and peptoids⁴³ were shown to kill bacteria without harming human cells, by mimicking the facially amphiphilic helical structure of host defense peptides. These non-natural platforms afford additional advantages such as resistance to proteolysis (degradation by enzymes in the body). Hence, researchers can design the peptides for pharmaceutical applications and indeed many peptide antibiotics such as Omiganan are currently in clinical trials.^{11, 18, 57}

An alternative approach is to utilize synthetic polymers which are not easily recognized by enzymes in the body, thus potentially solving the problem of degradation encountered in the case of peptide drugs. It is quite possible that synthetic polymers, with

access to a nearly limitless range of chemical structures, will be particularly useful in circumventing some of the obstacles which complicate the application of membrane-active antimicrobial peptides.

Synthetic Polymer Biocides

In household cleaning products, benzalkonium chloride surfactant compounds have been used as the active disinfectant since the 1950's.^{58, 59} The chemical structure of these surfactants features a quaternary ammonium salt (QAS) unit attached to a long alkyl chain. In 1983, Ikeda and co-workers reasoned that the activity of these surfactants might be enhanced by incorporation into the side chains of a synthetic polymer, in which the active compound could be locally concentrated into the many repeating units of the polymer chains.⁶⁰ This was readily achieved by introducing a vinyl moiety onto the benzyl group of the surfactant and then polymerizing the obtained styrene by conventional free radical procedures (Figure I-5).

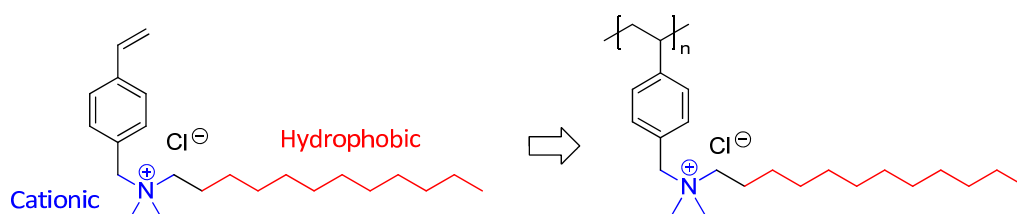


Figure I-5. Polymer disinfectants based on benzyalkonium chlorides, which are surfactants used in household cleaning products. The polymerization of this styrene derivative is a standard thermally initiated free radical process. Figure adopted from Ikeda et al (1983).

These QAS-functionalized polystyrenes were shown to effectively kill bacteria, with potencies dependent on the alkyl side chain length and molecular weight. The field of disinfecting polymers has expanded significantly, with a wide variety of polymer platforms including quaternized vinyl pyridines, vinyl alcohols, and methacrylate derivatives.^{61, 62} It has been asserted that the mechanism of action employed by these polymers involves damage of bacterial cell membranes, causing leakage of cytoplasmic contents or complete lysis of the cells. In contrast to host defense peptides, these surfactant molecules are not expected to adapt facially amphiphilic conformations or to form discrete pores in the membranes.⁶³ The application of these materials involves

immobilization of the polymer chains on surfaces (Figure I-8, structure G) for disinfecting coatings.^{64,65} These polymer biocides are not commonly viewed as potential pharmaceuticals, however, because their surfactant characteristic would likely induce toxicity to human cells as well as combating bacteria.

There is no evidence in the early literature of any conceptual connection between the discovery of host defense peptides (HDPs) and the initial development of polymer disinfectant materials to the author's knowledge. Such a connection is now emerging because, curiously, the polymers appear to have certain features in common with HDPs.^{66,67} In addition, the membrane-disrupting mode of action exerted by the polysurfactants seems analogous to peptide-induced permeabilization, although the former are not cell-type selective.⁶⁸ Indeed, despite some similarities, several key differences between host defense peptides and polymer surfactants should be highlighted (Table I-1).

Table I-1. Structural Features and Activity of Antimicrobial Peptides and Polymers

	Molecular weight	Cationic Groups	Hydrophobic Groups	Activity
Host Defense Peptides	2-5 kDa	Primary amines (K), guanidines (R)	Non-polar amino acids (A,V,L, etc.)	Antimicrobial, non-toxic
Polymer Biocides	10-100 kDa	Quaternary ammonium (QAS)	Long alkyl chains (C ₆ -C ₁₂)	Biocidal
Peptide-mimetic Polymers	1-10 kDa	Primary amines	Short alkyl chains (C ₁ -C ₄)	Antimicrobial, lower toxicity

It would be ideal to identify polymers which selectively kill of bacteria cells, without harming human cells, toward novel antibacterial drugs. Polymers which capture the essential features of HDPs are expected to show similar biological activity, because their activity is modulated by physiochemical determinants. Hence, we focus on designing polymers to mimic the salient structural features of HDPs.

Peptide-mimetic Antimicrobial Polymers

Mimicry of host defense peptides using synthetic β -peptides and peptoids has demonstrated that the antibacterial properties typical of HDPs can also be achieved by

synthetic methods without the need to isolate them from natural sources.^{43, 54, 55} Entirely non-biological molecules can also exert a membrane-disrupting antimicrobial mechanism.^{69, 70} Small, rigid oligomers displaying cationic and hydrophobic groups were among the first examples of entirely abiotic compounds which effectively mimic HDP activity (Figure I-8, structure B).^{69, 71} The conformation of these molecules are fixed by rigid arylamide structures stabilized by hydrogen bonding between amide nitrogen atoms and thioether groups in neighboring side chains. The oligomers display their cationic and hydrophobic components on opposite sides of the molecules. This design is intended to reproduce the facial amphiphilicity of HDPs by the simplest chemical structure. Remarkably, an aryl amide oligomer based on the concept of facial amphiphilicity has already passed a phase I clinical trial as an intravenous antibiotic drug to combat MRSA.⁷²

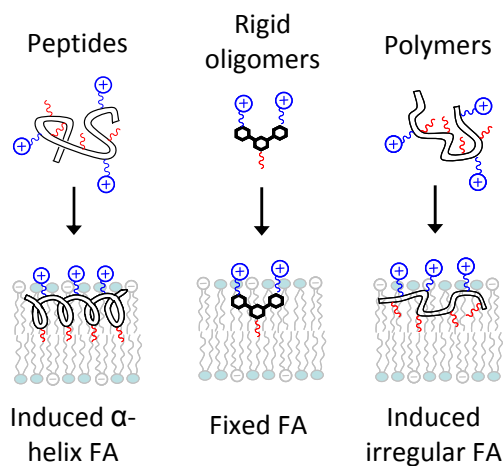


Figure I-6. Chemical structures which possess facially amphiphilic (FA) conformations on bacterial membranes, via induction of the α -helix, fixed rigid structures, and irregular conformations.

Synthetic polymers, including polymethacrylates, nylons and polynorbornenes, are another platform with great promise for mimicry of HDPs.^{66, 67} Unlike disinfecting polymers (surfactant-based biocides), the HDP-mimetic design approach has the potential to endow excellent antimicrobial potency without harming human cells. Although facially amphiphilic secondary structures cannot be readily programmed into synthetic polymers by current methods, a sufficiently flexible polymer chain may adapt irregular but facially amphiphilic conformation upon binding at the membrane-water interface (Figure I-6). This can be achieved by random copolymers with flexible backbones, such as nylons or polymethacrylates, in which the side chains display pendant cationic groups

as well as pendant hydrophobic groups. These heterogeneous polymer chains are expected to form random/irregular conformations in solution. Upon binding to the interfacial membrane surface, however, the conformation may be altered to facilitate interaction between the cationic side chains and anionic lipid headgroups. Simultaneously, the hydrophobic side chains are expected to partition into the non-polar membrane environment, thus giving rise to a facial amphiphilic though conformationally irregular structure (Figure I-6).^{73, 74}

DeGrado and co-workers developed random methacrylate copolymers bearing cationic ammonium groups and hydrophobic groups in the side chains of the two comonomers.⁷⁵ Primary amines were utilized as the cationic groups and butyl side chains as the hydrophobic moieties (C₄). Polymerization was carried out using a thiol compound, which allows tuning of the number average molecular weight by chain transfer polymerization (Figure I-7).

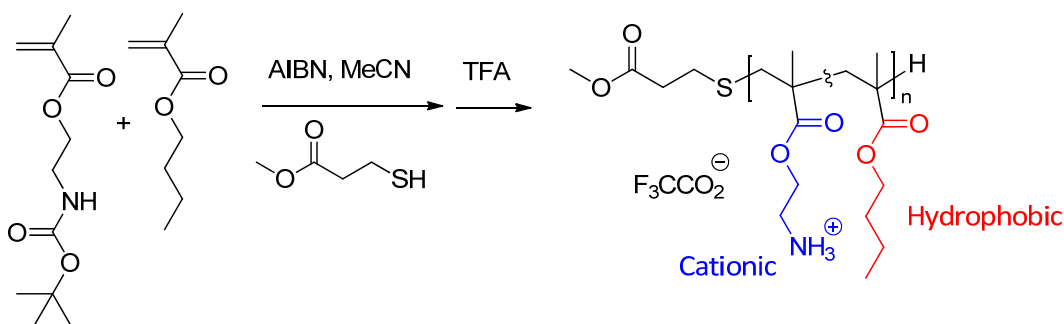


Figure I-7. Synthesis of a peptide-mimetic antimicrobial polymer, adopted from DeGrado and co-workers

Indeed, these polymethacrylate materials exhibited potent activity against *Escherichia coli*, which is normally symbiotic with humans but is sometimes associated with illness due to contaminated food products and urinary tract infections. As the ratio of hydrophobic-to-cationic side chains in the copolymer was adjusted, these materials expressed excellent antimicrobial activity in the micromolar concentration range, which is comparable to the activity of HDPs.⁷⁵ However, the polymers also induced lysis of human red blood cells, which implies that they are toxic. Interestingly, the toxicity was somewhat alleviated in the copolymers with lower molecular weight. They later showed that the optimal balance of potent antimicrobial activity combined with little or no

hemolysis could be achieved in copolymers containing methyl- or ethylmethacrylate (C₁-C₂) instead of butyl methacrylate (C₄) comonomer (Figure I-8, structure D).⁷⁶

Gellman and co-workers have also developed antimicrobial nylon-3 random copolymers (Figure I-8, structure E) intended to mimic HDPs.⁷⁴ In their copolymers, roughly 60% of the repeating units consisted of hydrophobic side chains whereas the remaining side chains were functionalized with primary amino groups. The average degree of polymerization was in the range of 10-30 repeating units, which is also in the range of most HDPs.^{21, 22} The polymers could be tuned to express selective activity against bacteria while minimizing hemolytic activity.⁷³

Tew and co-workers developed an extensive library of antimicrobial polymers based on amphiphilic norbornene derivatives (Figure I-8, structure C).^{77, 78} On one side of the amphiphilic repeating units, non-polar substituents are displayed, whereas primary amino groups are pendant on the other side. Their library also contains examples of compounds which exert excellent antimicrobial efficacy with little or no hemolytic action.⁷⁹

The HDP-mimetic polymers reported so far have required extensive optimization in order to identify just a few examples with low micromolar antimicrobial activity with no hemolysis up to the millimolar concentration range. Most examples are either ineffective at killing bacteria, or else they kill both bacteria and human cells indiscriminately. Only by finely tuning the structural parameters, certain synthetic polymers displayed selective activity against bacteria but not human cells. The best examples have common features which are listed in Table I-1. These features which are common among the best examples of antimicrobial polymers are evocative of HDP characteristics. Hence, it can be appreciated that the convergence of peptide and polymer sciences will be particularly useful in the development of novel materials for biomedical applications.

Extensive studies have revealed the structural characteristics of the polymers which play a key role in controlling the antimicrobial activity. It has been widely realized that optimization of the balance between cationic charge and hydrophobicity, referred to as the “amphiphilic balance,” is requisite for the judicious design of antimicrobial polymers.⁶⁷ Highly cationic peptides may bind to bacterial cell surfaces; however, their

hydrophilicity likely precludes insertion into the hydrophobic core of the membranes, which limits their activity. On the other hand, when peptides contain a high fraction of hydrophobic residues, they are indiscriminately toxic to both human and bacteria cells, because their hydrophobic nature enables binding and insertion into human cell membranes. When the cationic and hydrophobic residues in antimicrobial peptides are present in the appropriate ratio, the peptides can selectively kill bacteria without harming human cells^{32,35} due to the optimal balance of cationic and hydrophobic groups, resulting in selective binding to bacteria and ability of polymers to insert into and disrupt cell membranes.

Three main strategies for optimizing the amphiphilic balance in these polymers have been employed: adjusting the ratio of hydrophobic and cationic side chains in random copolymers,^{74, 75, 80, 81} adjusting the identity of hydrophobic moieties in random copolymers or amphiphilic homopolymers,^{77, 78} and reducing the hydrophobicity of polymer disinfectants by conjugation with electrically neutral, hydrophilic groups such as polyethylene glycol.⁸² In each case, finely tuning the amphiphilic balance is a particularly effective method to obtain biocompatible antimicrobial polymers. Because various polymer backbone structures were explored, it appears that amphiphilic balance is a universal or general design requirement.

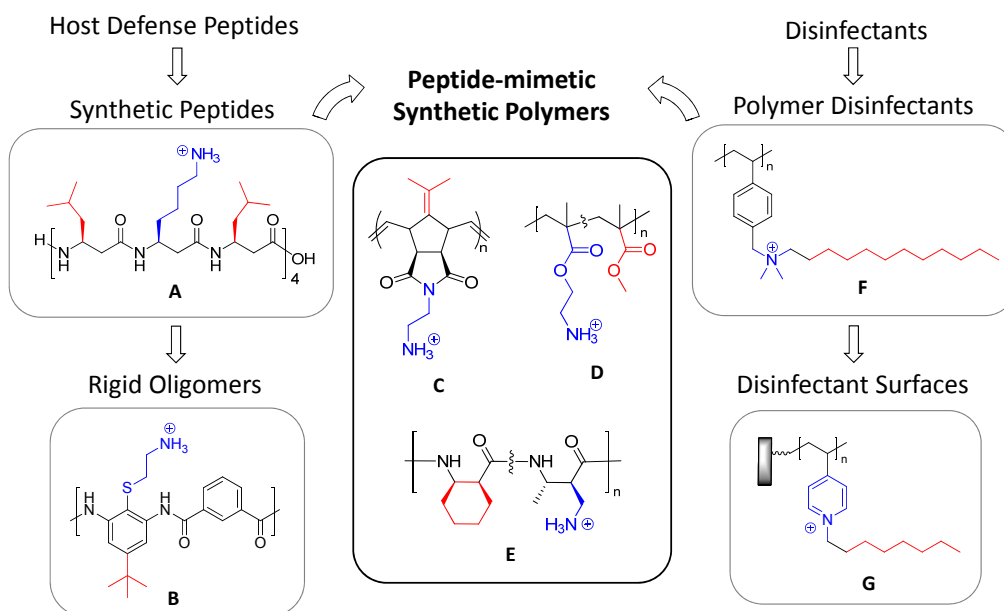


Figure I-8. Peptide-mimetic antimicrobial polymers are obtained by the convergence of peptide and polymer science.

Modulating the average molecular weight of the polymers enables tuning the total number of biologically active groups in each polymer chain. Increasing molecular weight in amphiphilic copolymers of methacrylate derivatives has been shown to enhance their antimicrobial activity; however, the high MW polymers exhibit markedly increased hemolytic properties.⁷⁵ Mimicking the small size of host defense peptides, low molecular weight nylon-3 polymers (1-4 kDa) were found to express low micromolar antimicrobial activity combined with minimal hemolysis: higher MW polymers were strongly hemolytic whereas the MIC values are not dependent on the MW.⁷³ In the same report, it was shown that dialyzed MW fractions > 2 kDa of an amphiphilic nylon-3 copolymer population are more hemolytic than the MW fractions < 2 kDa.⁷³ Hence, it would appear that low MW oligomers, which reflect the small size of host defense peptides, are a more suitable design choice for non-hemolytic antimicrobials relative to high MW polymeric biocides.

In summary, cationic and amphiphilic polymers have been effectively designed and synthesized to mimic the structural features and antimicrobial mechanism of host defense peptides (Figure I-8). Key structural determinants of activity have been delineated: amphiphilic balance, cationic charges, and molecular weight have been shown to modulate the observed antimicrobial and hemolytic activities (Table I-1).

While these design principles have provided a basic foundation for the development of antimicrobial polymers, the roles played by the structure of the cationic groups, the polymer backbone identity, and the groups which attach the cations to the backbone, were not explored in the prior literature. To that end, this dissertation focuses on establishing the role of salient structural activity determinants, and on probing the mechanism of antimicrobial activity exerted by synthetic polymer mimics of host defense peptides.

CHAPTER II

Effect of Cationic Group Structure on Antimicrobial and Hemolytic Activity of Amphiphilic Copolymers

Introduction

Synthetic polymers containing quaternary ammonium salts (QAS) attached to long hydrophobic alkyl side chains, or polysurfactants, have been studied extensively in the development of antimicrobials.^{61, 62, 64, 83-90} Polysurfactants putatively bind to bacterial cell membranes and disrupt the barrier function of the membrane, leading to loss of the transmembrane potential, leakage of cytoplasmic contents, and concomitant cell death.⁶² The purpose of incorporating cationic charges in these polymers is to enhance their affinity to anionic components of the bacterial cell membranes by electrostatic attraction.⁸³ Synthesis of such compounds is not labor-intensive or costly, rendering their production feasible on the industrial scale. As examples, poly(vinyl alcohol)s,⁸⁵ polyacrylates,⁸⁶ polyimines,⁸⁷ polystyrenes,^{62, 83} polysiloxanes⁹⁰ and polyurethanes⁹¹ have been functionalized with QAS groups and successfully used as bactericides. Polymers containing QAS and hydrophobic groups have shown great promise for application as permanently disinfecting surfaces.^{64, 65, 92-95} On the other hand, if such polymers are to be potentially useful in a broad range of applications, their toxicity to human cells must be considered. It seems that relatively little attention has been paid to the toxicity of polysurfactants to human cells, although a major obstacle in the biomedical application of synthetic polymers is their cytotoxicity or poor biocompatibility. One study systematically examined the effects of spatial distribution of QAS units in relation to the hydrophobic units on the antimicrobial activity as well as toxicity to human cells.⁹⁶ Still, a complete understanding of all the factors that give rise to toxicity has not been reached.

Host defense peptides exhibiting desirable cell selectivity have been found in nature, such as magainins isolated from the skin of the African clawed frog *Xenopus*

laevis.¹⁴ The structural features common to many host defense peptides are the presence of cationic and hydrophobic residues as well as relatively low molecular weight (1-10 kDa).⁹ These common features have recently been incorporated into various cationic, amphiphilic macromolecules which also showed antimicrobial activity with promising selectivity.⁷⁹ For example, tuning the molecular size and number of hydrophobic side chains modestly improves the cell selectivity exhibited by random copolymers of methacrylate derivatives.⁷⁵ Varying the identity of the hydrophobic units in polynorbornenes is another promising avenue toward non-hemolytic antimicrobials.⁷⁷ Substantial cell selectivity has been achieved by tuning the ratio of cationic to hydrophobic units in random copolymers prepared from beta lactams.⁷⁴ Rigid amphiphilic oligomers,⁶⁹ synthetic peptide analogues,¹² β -peptides,^{54, 97} α,β -peptides,⁹⁸ and peptoids⁴³ have also been shown to kill bacteria efficiently while minimizing harm to human cells. Interestingly, these cell-selective synthetic compounds use primary amine groups, which are largely protonated at physiological pH, as the source of cationic charge. In contrast, conventional polysurfactants bear quaternary ammonium groups as the cationic functionality. Gellman and co-workers reported that polymers containing tertiary amines displayed biocidal activity while analogous polymers containing quaternary ammonium salts were inactive.⁶⁸ The fact that compounds containing different cationic groups showed such stark differences in antimicrobial activity and cell selectivity led us to inquire: *What is the role of amine functionality in the antimicrobial and hemolytic activities of amphiphilic polymers?*

Based on previous studies of the mechanism employed by host defense peptides and their synthetic mimics, the cationic groups seem to play a role in two key mechanistic steps: binding of the peptides to the cell membrane and subsequent membrane permeabilization.^{26, 34, 99} It has been proposed that the cationic charge of the peptides enhances the specificity of their binding to bacterial cell membranes relative to human cell membranes^{9, 38} because the former contain a greater amount of anionic lipids on the outer leaflet.^{100, 101} However, excessive hydrophobicity gives rise to non-specific binding, resulting in lysis of human red blood cells.²⁷ Therefore, it has been widely reported that balancing the cationic charge and hydrophobicity of the molecules is requisite to obtain non-toxic antimicrobial peptides.^{99, 102-105}

In the next step of the mechanism, the peptides are inserted into the cell membrane by partitioning of hydrophobic residues into the hydrophobic region of the lipid bilayer.⁴⁸ This causes membrane permeabilization by formation of transmembrane pores resembling ion channels (Figure I-3).^{33, 34} The pores are thought to be lined by hydrophilic amine groups of the peptide ("barrel-stave") and by lipid headgroups ("toroidal pore") to create a hydrophilic environment through which cytoplasmic contents may exit. It has been argued that pore formation is a transient process in which surface-bound peptide aggregates briefly insert into the bilayer and are then redistributed to the inner and outer leaflets.⁵⁰ Alternatively, the membrane may be compromised by accumulation of peptides on the membrane surface via the "carpet" mechanism, which completely disrupts the lipid organization (Figure I-3).¹⁰⁶

Based on these studies of antimicrobial peptides, it is reasonable to speculate that the chemical structure of the cationic groups in an antimicrobial polymer or peptide affects their interaction with lipids in the membrane, thereby influencing the observed activity. One may consider the possibility that the amine groups in the peptides complex with lipid head groups by a combination of electrostatic and hydrogen bonding contributions, enhancing their affinity to the lipids as well as altering the properties of the transient pores. Hence, we hypothesize that it will be possible to modulate the activity of synthetic polymers by varying the chemical structures of the cationic groups in the side chains.

The exact role that cationic functionality plays in the modulating the potency and mode of antimicrobial action have not yet been systematically investigated to our knowledge. Therefore, consideration of the cationic functionality as a parameter in the design rationale of antimicrobials will represent an advancement of the field. Because of the chemical diversity of polymer structures reported in the literature, it is difficult to quantify the extent to which different ammonium groups are responsible for the observed differences in activity by comparison of reported values. For that reason, a more direct comparison of structures with different ammonium groups is desirable. In this Chapter, we present a systematic analysis of antimicrobial and hemolytic activities in amphiphilic copolymers bearing primary, tertiary, and quaternary ammonium groups in the side chains.

Polymer Design, Synthesis and Characterization

We synthesized random copolymers containing primary, tertiary, or QAS groups in the side chains by slight modification of literature procedures (Appendix A). Amphiphilic polymethacrylate derivatives have shown potent antimicrobial activity and varying degrees of toxicity to human red blood cells, depending on hydrophobicity.⁷⁶ We chose the polymethacrylate platform for this study because structural parameters including the degree of polymerization (DP), mole fraction of hydrophobic repeat units, and the identity of the side chain groups, can be readily tuned.

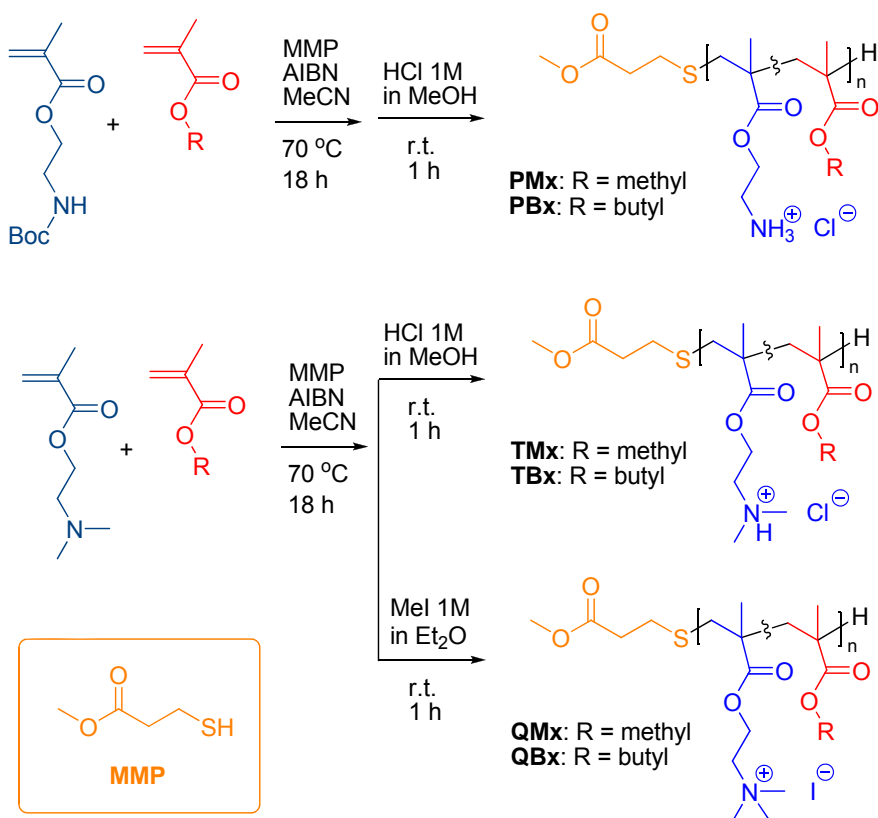


Figure II-1. Synthesis of amphiphilic random copolymers bearing primary, tertiary, or quaternary ammonium salts. The subscript x refers to the mole % of hydrophobic (MMA or BMA) repeating units in the copolymer. AIBN: Azobisisobutyronitrile, MMP: methylmercaptopropionate. The mole fraction of methyl side chains, f_{methyl} , was varied from 0.0 to ~0.7. Copolymers were prepared with DP values of 6-11 repeat units

Copolymers were prepared with DP values of 6-11 repeat units because this range was previously shown to give favorable activity against bacteria cells without causing

lysis of human red blood cells.¹⁰⁷ In the copolymers containing methyl groups, the mole fraction of methyl side chains, f_{methyl} , was varied from 0.0 to ~ 0.7 . Copolymers containing butyl groups, the mole fraction of butyl side chains, f_{butyl} , was varied from 0.0 to ~ 0.4 . Copolymers with higher fractions of the non-polar groups displayed little or no water solubility and were therefore impractical for the antimicrobial or hemolytic assays, which are done in aqueous buffers. Characterization data are given in Table II-1.

Prior to evaluation of the biological activity of the copolymers, we examined the extent of ionization of some representative polymers by potentiometric titration. Since the primary or tertiary amine groups in polymers exist in equilibrium between deprotonated (basic) and protonated (cationic) forms, knowledge of the extent of ionization of these polymers at a given buffer pH is requisite for quantifying the effect of the number of cationic charges or basic groups on their activity. For several representative polymers in our library, we assessed the effect of pH on the extent of ionization, α (Figure II-2).

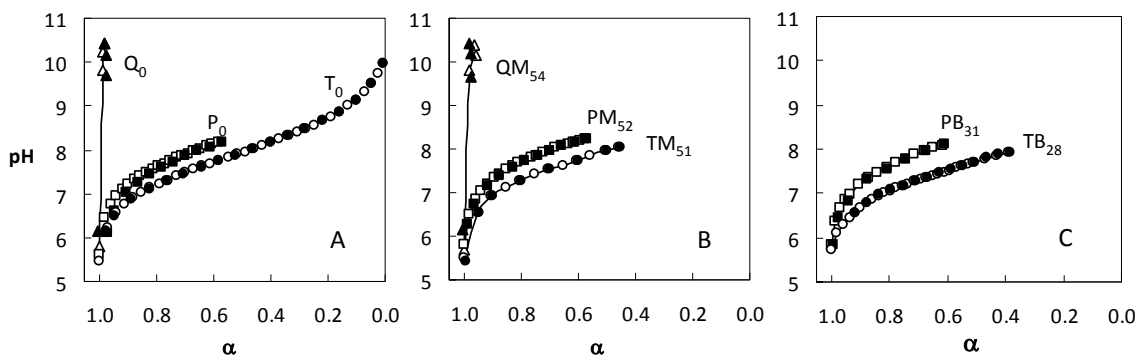


Figure II-2. Titration of amphiphilic random copolymers bearing primary, tertiary, or quaternary ammonium salts; (A) no hydrophobic comonomer, (B) MMA comonomer, and (C) BMA comonomer.

The homopolymer containing primary amines, P_0 , was initially titrated with NaOH to the equivalence point at approximately pH 11 and then back-titrated with HCl. The back-titration trace deviated significantly from that of forward titration as α approached ~ 0.8 , likely due to chemical changes of the P_0 structure in basic conditions. It is well known that amine-functionalized methacrylates isomerize to methacrylamides at high pH.¹⁰⁸ We also confirmed that the monomer (1-aminoethyl)methacrylate isomerized to hydroxyethyl methacrylamide; the ^1H NMR spectra indicated quantitative isomerization after stirring in $\text{K}_2\text{CO}_3(\text{aq})$, pH 10.2, for 24 hours at room temperature

(Appendix B). The ^1H NMR spectra of P_0 indicated multiple changes, including the formation of methacrylamides. Since the side chains are concentrated in the polymer relative to free monomer in solution, multiple different chemical reactions are possible, including formation of amide groups within the same repeat unit and between different side chains, as well as the formation of carboxylic acid groups by hydrolysis of the esters.¹⁰⁸ Despite the chemical changes observed at high pH, the ^1H NMR spectrum of P_0 after stirring at pH 8 for 1 hr displayed no changes, suggesting that the polymer is chemically stable in this condition. In addition, titration of P_0 up to pH 8 showed good agreement with back-titration data (Figure II-2). Similarly, the copolymers PM_{52} and PB_{31} showed good agreement between forward and back-titration traces when the titrations were limited to pH 8. The titration data of P_0 , PM_{52} and PB_{31} are practically indistinguishable, suggesting that the introduction of hydrophobic side chains does not significantly alter the basicity of neighboring primary amine groups.

The monomer *N,N*-dimethylaminoethylmethacrylate (DMAEMA) was titrated and found to have a pK_a value of 8.48, which agrees closely with the published value ($\text{pK}_a = 8.44$).¹⁰⁹ The homopolymer of DMAEMA prepared in this study, T_0 , was also titrated with NaOH aq. to the equivalence point at approximately pH 10 and then back titrated with HCl aq. in good agreement (Figure II-2). This suggests that the polymer is chemically stable in the entire range of pH. In comparison to DMAEMA, the tertiary amine groups in the T_0 polymer were less basic with a degree of ionization α of 0.5 at pH 7.94. In general, the basicity of amine groups attached to the polymer chains differ from those of the free monomer in solution due to differences in the microenvironment surrounding each group in the polymer, due to Columbic repulsion of neighboring cationic groups and local dielectric effects in the polymer chains.¹¹⁰ Although T_0 appears to be fully water soluble in the range of pH 6-10, solutions of the copolymers TM_{51} and TB_{28} became turbid beyond pH 9. Increased hydrophobicity of these copolymers is likely responsible for the precipitation from aqueous solution at higher pH. For this reason, partial titration curves were obtained for the copolymers TM_{51} and TB_{28} in the range of pH 6 to 8, giving good agreement with back-titration curves (Figure II-2) and maintaining solution clarity throughout. The titration traces of T_0 and TM_{51} are practically identical, indicating that the incorporation of methyl side chains does not affect the basicity of

neighboring tertiary amine groups. On the other hand, TB₂₈ is significantly less basic than TM₅₁, possibly due to a reduction in the polarity of their microenvironments associated with the hydrophobicity of the butyl groups in the polymer.

Knowledge of the relationships between pH and α for these selected polymers will prove useful in the quantitative interpretation of results from biological assays performed in buffers of various bulk pH, as described in later sections of this report.

Antimicrobial Activity

Antimicrobial activity of the copolymers against *Escherichia coli* were tested for all polymers. *E. coli* is the most populous bacterium in the normal human intestinal flora and is normally symbiotic; however in some cases *E. coli* cause food poisoning and urinary tract infections. For each polymer, the minimal inhibitory concentration (MIC) was determined as the lowest polymer concentration which completely prevents the growth of bacteria, measured as optical density increase, after overnight incubation in broth. The details of the antimicrobial activity assay procedure are given in Appendix A. The MIC values for all of the polymers are given in Tables II-1 and II-2.

The antimicrobial activities of the polymers are strongly dependent on the chemical structure of the ammonium groups when the hydrophobic groups are methyl esters. The primary amine side chains confer relatively high antimicrobial potency on the copolymers, whereas the polymers with tertiary amines showed weak activity and those with quaternary ammonium groups were completely inactive. Notably, the PM and TM polymers displayed different dependencies of their MIC values on f_{methyl} values (Figure II-3).

Table II-1. Characterization and biological activities of random copolymers containing different amine functional groups. R = methyl.

Polymer	$f_{\text{methyl}}^{\text{a}}$	DP ^a	M_n^{a} (kDa)	MIC ^b		HC ₅₀ ^b		HC ₅₀ / MIC
				μM	μg/mL	μM	μg/mL	
P ₀	0.00	7.4	1.4	> 1400	> 2000	> 1400	> 2000	--
PM ₁₈	0.18	6.2	1.1	930	1000	> 1800	> 2000	> 2
PM ₂₃	0.23	7.5	1.2	270	320	> 1700	> 2000	> 6
PM ₂₉	0.29	6.5	1.1	50	55	> 1800	> 2000	> 36
PM ₄₀	0.40	6.4	1.0	21	21	> 2000	> 2000	> 95
PM ₄₇	0.47	6.2	1.0	16	16	> 2000	> 2000	> 125
PM ₅₂	0.52	10.3	1.5	11	17	460	680	42
PM ₅₉	0.59	8.2	1.2	9.0	11	210	260	24
PM ₆₅	0.65	7.6	1.1	7.4	8.1	95	100	13
T ₀	0.00	7.7	1.6	> 1300	> 2000	> 1300	> 2000	--
TM ₁₉	0.19	7.8	1.5	920	1400	> 1300	> 2000	> 1
TM ₂₆	0.26	7.6	1.4	490	690	> 1400	> 2000	> 3
TM ₃₈	0.38	8.2	1.4	240	340	> 1400	> 2000	> 6
TM ₄₆	0.46	6.7	1.0	260	260	> 2000	> 2000	> 8
TM ₅₁	0.51	7.1	1.1	220	242	1400	1500	6
TM ₅₂	0.52	7.1	1.1	290	319	1100	1200	4
TM ₆₁	0.61	7.9	1.2	700	840	340	410	0.5
TM ₇₁	0.71	9.5	1.3	> 1500	> 2000	97	130	< 0.1
Q ₀	0.00	7.4	2.3	> 870	> 2000	> 870	> 2000	--
QM ₂₃	0.23	7.0	1.9	> 1100	> 2000	> 1100	> 2000	--
QM ₃₀	0.30	6.4	1.7	> 1200	> 2000	> 1200	> 2000	--
QM ₃₈	0.38	6.6	1.6	> 1300	> 2000	> 1300	> 2000	--
QM ₄₈	0.48	6.7	1.5	> 1300	> 2000	> 1300	> 2000	--
QM ₅₄	0.54	7.1	1.5	> 1300	> 2000	> 1300	> 2000	--
QM ₅₇	0.57	6.5	1.3	> 1500	> 2000	> 1500	> 2000	--
QM ₆₃	0.63	6.6	1.3	> 1500	> 2000	> 1500	> 2000	--
QM ₆₅	0.65	6.8	1.3	> 1500	> 2000	> 1500	> 2000	--
		melittin	2.8	4.4	12.5	0.6	1.4	0.1
		magainin-2	2.5	51	125	> 100	> 250	> 2

a) Calculated from ¹H NMR spectra, as described in Appendix B.

b) Experimental details of the MIC and HC₅₀ are described in Appendix A.

Table II-2. Characterization and biological activities of random copolymers containing different amine functional groups. R = butyl.

Polymer	$f_{\text{butyl}}^{\text{a}}$	DP ^a	M_n^{a} (kDa)	MIC ^b		HC ₅₀ ^b		HC ₅₀ / MIC
				μM	μg/mL	μM	μg/mL	
PB ₂₀	0.20	11.4	2.0	4.0	8.0	100	200	25
PB ₃₁	0.31	8.2	1.4	5.5	7.7	22	31	4
PB ₃₄	0.34	6.8	1.2	6.5	7.8	29	35	4
PB ₃₇	0.37	10.7	1.8	4.3	7.7	7.6	14	2
PB ₄₀	0.40	8.4	1.4	5.4	7.6	9.1	13	2
PB ₄₂	0.42	9.0	1.5	5.1	7.7	9.6	14	2
TB ₁₂	0.12	8.1	1.6	15	24	970	1600	65
TB ₁₉	0.19	9.3	1.8	4.4	7.9	100	180	23
TB ₂₃	0.23	8.6	1.6	2.4	3.8	40	64	17
TB ₂₆	0.26	9.1	1.7	2.3	3.9	36	60	16
TB ₂₈	0.28	8.4	1.6	2.5	4	42	670	17
TB ₃₆	0.36	8.8	1.6	4.8	7.7	19	30	4
TB ₄₂	0.42	8.2	1.5	16	24	13	20	1
QB ₂₂	0.22	11.8	3.5	490	1700	> 570	> 2000	> 1
QB ₂₆	0.26	9.8	2.7	110	300	> 740	> 2000	> 7
QB ₃₁	0.31	7.0	1.9	24	46	630	1200	26
QB ₃₅	0.35	13.4	3.5	27	95	320	1100	12
QB ₃₇	0.37	9.3	2.4	14	34	90	220	6
QB ₃₉	0.39	6.0	1.5	17	39	56	130	3
QB ₄₄	0.44	8.9	2.3	17	39	29	67	2
		melittin	2.8	4.4	12.5	0.6	1.4	0.1
		magainin-2	2.5	51	125	> 100	> 250	> 2

a) Calculated from ¹H NMR spectra, as described in Appendix B.

b) Experimental details of the MIC and HC₅₀ are described in Appendix A.

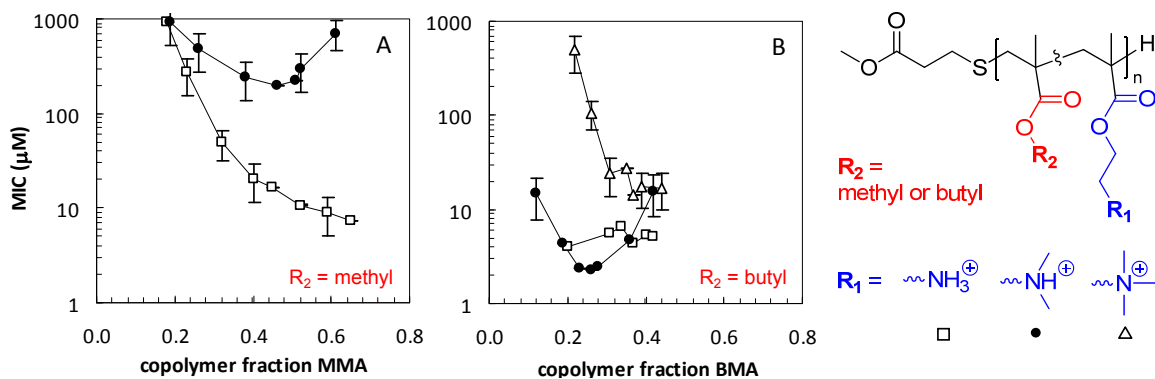


Figure II-3. Antimicrobial activities (MIC) of random copolymers. The side chains contain (A) methyl or (B) butyl groups as the hydrophobic side chains and primary (empty squares), tertiary (filled circles), or quaternary (empty triangles) amine groups against *E. coli*. The MIC values of the QM series are not shown because inhibition of bacteria was not observed up to the highest polymer concentration tested (2000 μg/mL).

In the PM polymer series, the MIC decreased by orders of magnitude as f_{methyl} was increased, approaching a minimum MIC value $< 10 \mu\text{M}$, which is lower than natural host-defense peptide magainin 2 (MIC = $50 \mu\text{M}$) in this assay. The MIC values in the TM series decreased to reach a minimum of $\sim 200 \mu\text{M}$ at $f_{\text{methyl}} = 0.5$ and then increased as f_{methyl} was further increased. The increased hydrophobicity of the PM and TM polymers seems to be responsible for an enhancement of antimicrobial activity with increasing f_{methyl} in the range of 0 to 0.5. However, excessive hydrophobicity of polymers in the high f_{methyl} range may cause aggregation, reducing the number of polymers available to interact with the bacteria cells. Also, increasing f_{methyl} requires decreasing the number of amine groups in the copolymer, reducing the number of cationic charges. This would diminish the electrostatic attraction to bacterial cell membranes. A combination of these factors may be responsible for the observation that the MIC values plateau in the PM series and go through a local minimum for TM polymers when f_{methyl} is increased beyond 0.5. The differences in MIC dependence on f_{methyl} might arise from a greater propensity of TM polymers to undergo aggregation relative to the PM polymers, perhaps due to the fact that the deprotonated (basic) tertiary amine groups are more hydrophobic than basic primary amine groups.

We also investigated the activity of random copolymers containing butyl side chains as the hydrophobic group. Since hydrophobicity is an important factor in the

antimicrobial activity of polymeric biocides,⁸³ methyl groups might not be sufficiently hydrophobic for polymers containing quaternary ammonium groups to gain substantial antimicrobial activity, although they were shown to be effective in combination with primary and tertiary amine groups. It has long been known that polymers with quaternary ammonium salts in the side chains require long alkyl groups to impart substantial antimicrobial activity.^{61, 62, 64, 83-90} In this work, copolymers containing butyl groups showed lower MIC values than those containing methyl groups (Figure II-3). The PB polymer series displayed MIC values of approximately 5 μM in the range $f_{\text{butyl}} = 0.20$ to 0.42. The MIC values of TB polymers were orders of magnitude lower than those of the TM polymers, reaching a minimum MIC value of 2 μM at $f_{\text{butyl}} = 0.25$. The QB series exhibited substantial antimicrobial activity when f_{butyl} was increased from 0.35 to 0.44, and the MIC values approached a plateau of about 20 μM in the higher f_{butyl} region. Regardless of the cationic functionality, the MIC of all series of polymers seemed to approach a comparable range (5-20 μM) when f_{butyl} was increased to about 0.4, which perhaps represents the limit of activity (lowest MIC) that can be achieved by this library of polymethacrylate derivatives. The f values at which the MIC dependence undergoes a transition (approaches a plateau or goes through a local minimum) is lower for polymers with butyl groups than for those with methyl groups. This is consistent with the notion that, although increasing the hydrophobicity enhances antimicrobial potency, excessive hydrophobicity limits activity.

Hemolytic Activity

As a measure of biocompatibility, we report the lysis of human red blood cells (RBCs) induced by the polymers. The hemolytic activity was determined as the polymer concentration which induced 50% release of hemoglobin (HC_{50}) from the RBCs relative to the positive control, Triton X-100. This assessment of toxicity is the most commonly employed for membrane-disrupting peptides, because human RBCs are particularly fragile. The details of the hemolysis assay procedure are given in Appendix A.

The hydrophilic PM and TM polymers ($f_{\text{methyl}} < 0.4$) and all of the QM polymers were non-hemolytic up to the highest polymer concentration tested. As the f_{methyl} was increased from 0.4 to 0.7 in the PM and TM series, hemolytic potency increased by an

order of magnitude (Figure II-4). Interestingly, the HC_{50} values of PM polymers are only about two-fold lower than those of the TM polymers, while the MIC values in the PM series were orders of magnitude lower than in the TM series. In addition, the HC_{50} of the TM series monotonically decreased with increasing f_{methyl} , while the MIC trend exhibited a minimum. These results imply that tuning of hydrophobicity and prudent choice of ammonium functionality are necessary steps to maximize antimicrobial potency and minimize the hemolytic activity.

The HC_{50} values for TB and PB polymers are similar, decreasing with increasing f_{butyl} to a minimum of $\sim 10 \mu\text{M}$ (Figure II-4). The QB series are highly hemolytic around $f_{\text{methyl}} = 0.4$, with HC_{50} values of $\sim 20 \mu\text{M}$. This indicates that the polymers containing quaternary ammonium groups require a greater number of hydrophobic groups and longer alkyl side chains in order to lyse RBCs compared with polymers containing primary and tertiary amines.

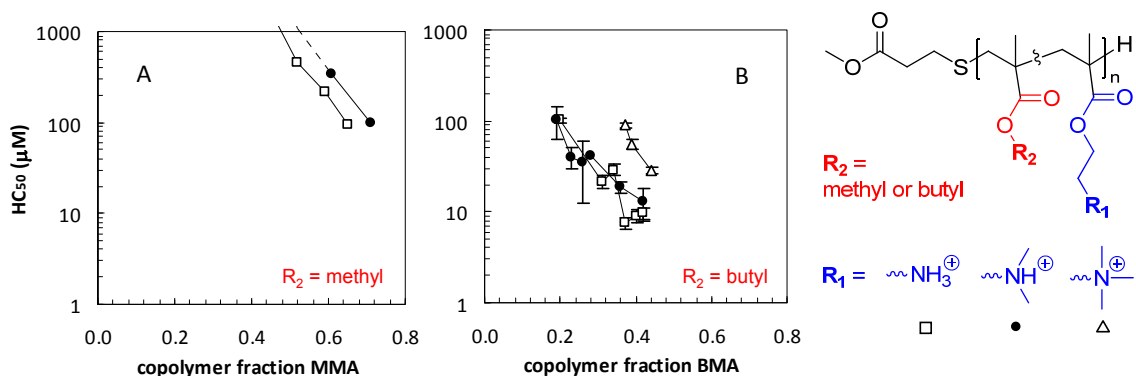


Figure II-4. Hemolytic activities (HC_{50}) of random copolymers. Side chains contain methyl (empty symbols) or butyl (filled symbols) as the hydrophobic groups and primary (squares), tertiary (circles), or quaternary (triangles) ammonium salts as the cationic groups.

Selectivity

The selectivity index value ($SI = HC_{50}/MIC$) of antimicrobial compounds in the literature has been used to describe the cell specificity towards bacteria vs. red blood cells. Since the MIC and HC_{50} values depend on the factors such as sample preparation, the number of cells in assay solution, solvent, pH, salt concentration, microplate material, and the choice of the assay medium, it is difficult to assess the absolute cell specificity of antimicrobials based on the SI value alone. We used the natural host defense peptide

magainin 2 (MIC = 51 μM , HC₅₀ > 100 μM , SI >2) and the bee venom toxin melittin (MIC = 4.4 μM , HC₅₀ = 0.6 μM , SI = 0.1) as standards for comparison since these are membrane-active compounds with selective and non-selective activity to bacteria over RBCs.

The selectivity of the polymers decreases monotonically with increasing f values (Figure II-5) in the region $f_{\text{methyl}} = 0.40$ to 0.52. PM polymers displayed MIC values of ~ 10 -20 μM and HC₅₀/MIC greater than at least 10, which is orders of magnitude more selective than the standard biocide melittin (SI = 0.1). Among these polymers, the best example is PM₄₀, which showed an MIC value of 20 μM and an HC₅₀ value > 2000 μM . This gives an outstanding selectivity index value of >100. In addition, the polymer TB₁₂ has an MIC of 15 μM and an HC₅₀ of 970 μM , which gives a selectivity index of 66. These polymers are more potent in the antimicrobial assay against *E. coli* compared to magainin 2 and display excellent SI values. Hence, selectivity can be optimized by tuning the properties of the polymers.

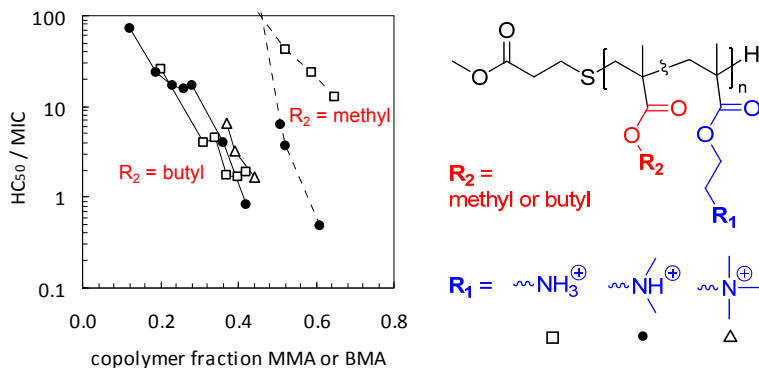


Figure II-5. Selectivity Indices (HC₅₀/MIC) of random copolymers. Side chains contain methyl (dotted lines) or butyl (solid lines) side chains as the hydrophobic groups and primary (squares), tertiary (circles), or quaternary ammonium groups. HC₅₀/MIC values for polymers with low f values, and all of the polymers in the QM series, are not determined because of lack of HC₅₀ and/or MIC.

Importantly, the chemical structure of the cationic group is a key determinant of the maximum selectivity that can be achieved. The polymers containing primary or tertiary amines are promising candidates for a broad range of applications, including biomedical fields. The polymers containing quaternary ammonium groups were not as potent antimicrobials unless hydrophobicity was increased, in which case they displayed rather poor SI values. This suggests that QAS polymers are more appropriate for

disinfecting applications, where lysis of human red blood cells is less of a concern relative to biomedical applications.

Bactericidal Activity vs. pH

Based on our potentiometric titration data, a fraction of the amine groups in PM₅₂ and TM₅₁ are deprotonated (basic) at pH 7 (Figure II-2). On the other hand, 100% of the quaternary ammonium groups in QM₅₄ can be regarded as cationic charges regardless of the solution pH. In light of these facts, we wondered whether the deprotonated form of amine groups in PM₅₂ and TM₅₁ play a role in their biological activities. Also, we wondered whether differences in activity would persist in a condition where 100% of the primary and tertiary amine groups are protonated (*e.g.* pH 6). Gellman and co-workers found that poly(*N,N*-dimethylaminomethylstyrene), which contains pendant tertiary amine groups, displayed biocidal activity comparable to that of the toxin melittin, while analogous polymers containing QAS groups were inactive.⁶⁸ This suggests that the difference in activity arose from the differences between reversible *N*-protonation and *N*-quaternization of the tertiary amine groups. Their titration experiments suggested that a fraction of the tertiary amine groups in the polymer were deprotonated in the physiological pH condition, giving rise to an amphiphilic structure. Similarly, we found that polymethacrylates containing primary and tertiary amine groups displayed greater antimicrobial activity than an analogous polymer containing quaternary ammonium salts. Therefore, we performed assays in buffers of pH varying from 6 to 8 using the selected polymers PM₅₂, TM₅₁, and QM₅₄, which have comparable f_{methyl} (0.51-0.54) and DP (7.1-10.3) values.

The degree of ionization of PM₅₂ and TM₅₁ polymers had a profound impact on bactericidal activity, while QM₅₄ displayed no detectable MBC up to 1400 μM in buffers ranging from pH 6 to 8 (Figure II-6). Interestingly, the polymers displayed differences in their antimicrobial activity at pH 6 wherein nearly all of the amine groups in each of the polymers are cationic, $\alpha \sim 1.0$ (Figure II-2). This shows that the chemical structure of the ammonium groups, and not simply their cationic charge, plays an important role in the bactericidal action. The bactericidal mechanism of polymers may involve complexation of ammonium groups to anionic components of the membrane, such as anionic

headgroups of the lipids (*e.g.* phosphatidyl glycerol) and lipopolysaccharides, which contain sulfonic acid in the side chains (see Figure I-2 for the chemical structures of lipids). The protonated ammonium groups may hydrogen-bond with lipids, in addition to electrostatic attraction, possibly enhancing the activity. The hydrophobicity of the ammonium groups depends on their chemical structure,¹¹¹ which may further contribute to the observed activities. The tertiary and quaternary ammonium groups have additional methyl appendages, which may influence solvation and thereby alter the amphiphilic structures of the polymer chains.

As the buffer pH is increased from 6 to 8, the polymers containing primary or tertiary amine groups in solution are effectively ternary systems containing hydrophobic groups, cationic ammonium groups, and basic amine groups. With the fraction of methyl side chains fixed, the MBC of PM₅₂ decreased by more than an order of magnitude as the pH was increased from 6 to 8 (Figure II-6).

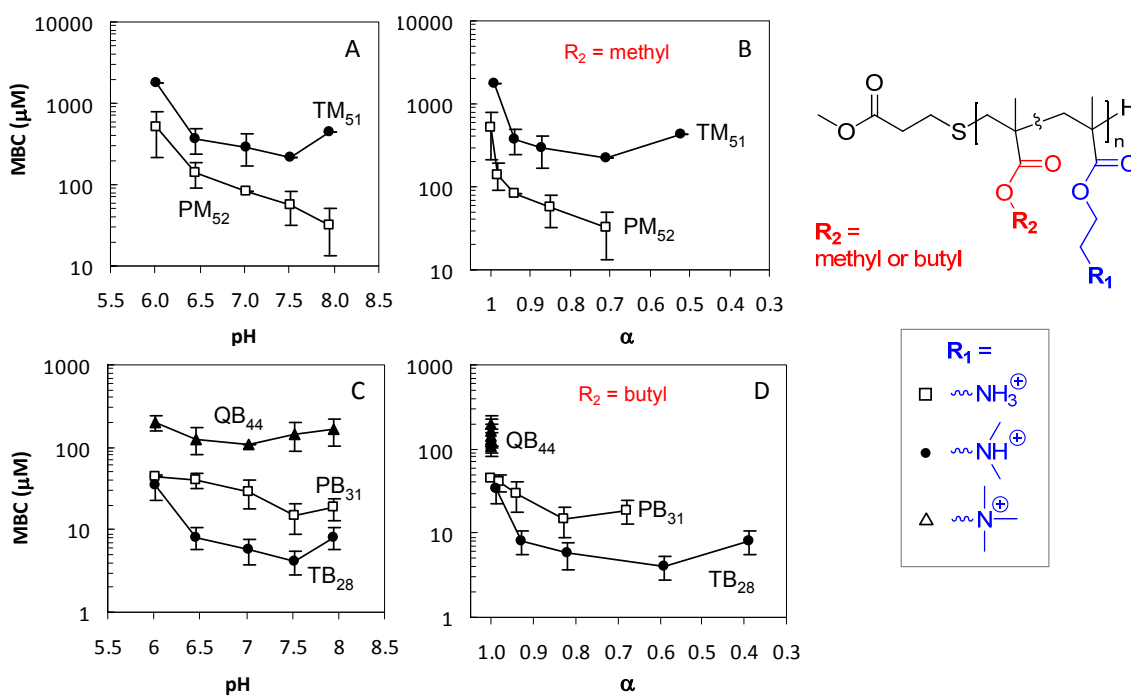


Figure II-6. Bactericidal activity (MBC) as a function of pH and extent of ionization, α , for copolymers with (A and B) MMA and (C and D) BMA. QM₅₄ showed no detectable bactericidal effect up to 1400 μM in all buffers from pH 6 to 8. No significant effect on the viability of *E. coli* ATCC 25922 in the given assay conditions with the pH range used here was observed.

This implies that increasing the number of basic amine groups, at the expense of cationic charges, enhances the antimicrobial potency of PM₅₂. The MBC of TM₅₁ also decreased dramatically as the pH was increased from 6 to 7.5. As the pH was increased to 8, however, a slight loss of activity was observed. This effect may be due to increased hydrophobicity of the polymers at higher pH or the basic amines might play an active role in the antimicrobial mechanism.

It has been shown that changing the number of cationic residues in antimicrobial peptides affects their antimicrobial activity and ability to lyse model lipid vesicles.¹¹²⁻¹¹⁴ Decreasing α in our polymers reduces their net charge, which may cause a decrease in their electrostatic attraction to anionic components of the bacterial cell membrane. This effect may contribute to the loss of bactericidal activity displayed by TM₅₁ in pH 8 ($\alpha \sim 0.5$).

Alternatively, the reduction of activity shown by TM₅₁ in high pH may be attributed to the polymer favoring the aggregated state, owing to increased hydrophobicity and decreased cationic charge. It was shown previously that the antibacterial and membrane-lytic activities of histidine-rich peptides are enhanced in acidic pH^{115,116} and this effect may be related to the formation of nano-scale aggregates at physiological pH.¹¹⁷

The MBC values of polymers with butyl side chains (PB₃₁, TB₂₈, and QB₄₄) showed less pronounced sensitivity to solution pH, compared to the MBC values of polymers with methyl side chains (Figure II-6). Although PB₃₁ and TB₂₈ polymers showed almost the same MBC value at pH 6 ($\alpha = 1.0$), TB₂₈ became roughly three-fold more potent than PB₃₁ as the pH was increased to 7. Interestingly, QB₄₄ showed substantial bactericidal activity in this assay independent of solution pH. Recalling that polymers in the QM series showed no activity at any pH studied, it seems that longer alkyl chains are required for polymers containing quaternary ammonium salts to demonstrate bactericidal action.

In summary, the bactericidal activity of polymers containing primary or tertiary amines showed marked dependence on ionization state. We observed enhancement of activity with increasing pH in the region $\alpha > 0.8$, which we attribute to increased hydrophobicity. We observed a loss of activity by polymers in this study when the

number of charged groups was substantially reduced by increasing pH to 8. This reduction of activity may be due to aggregation of polymers in the high pH condition. Alternatively, substantial reduction in the number of cationic charges on the polymer might mitigate electrostatic attraction to the bacterial membrane. On the other hand, the bactericidal activity of polymers containing quaternary ammonium salt groups showed no significant pH dependence.

Hemolytic Activity vs. pH

We further examined the effect of the degree of ionization of polymers on their hemolytic activity. The hemolysis induced by PM₅₂ and TM₅₁ at 500 $\mu\text{g}/\text{mL}$ exhibited a strong dependence on pH (Figure II-8), while QM₅₄ failed to show any appreciable hemolytic activity across the entire pH range. The fraction of hemolysis induced by PM₅₂ monotonically increased as pH was increased from 6 to 8, indicating that increasing the fraction of deprotonated amine groups or increasing the hydrophobicity of the polymer causes enhanced hemolysis. On the other hand, hemolysis induced by TM₅₁ increased from pH 6 to 7 and then decreased as the pH was further increased to 8, giving a maximum fraction of hemolysis of ~ 0.5 (Figure II-8). Considering the hydrophobic nature of the neutral tertiary amine groups, this is considered evidence that aggregation of the TM₅₁ polymer curtails its membrane activity at pH 8 ($\alpha \sim 0.7$). The polymers containing butyl side chains (PB₃₁, TB₂₈, and QB₄₄) caused practically complete hemoglobin release at 500 $\mu\text{g}/\text{mL}$ regardless of pH.

We observed a sigmoidal increase in hemolysis fraction as the polymer concentration was increased in the semi-log plots. The hemolysis curves shift to lower polymer concentration as pH is increased in the case of PM₅₂. With the TM₅₁ polymer, on the other hand, the shape of the curves were different depending on the pH; the curves for pH 7.5 and 8 increase more gradually than those in lower pH and seem to approach a maximum hemolysis fraction lower than 1.0 in high polymer concentrations. This behavior is indicative of a reduced number of hemolytically active TM₅₁ polymer chains in solution, possibly due to the hydrophobic aggregation induced by deprotonation of the tertiary amine groups as the solution pH increases.

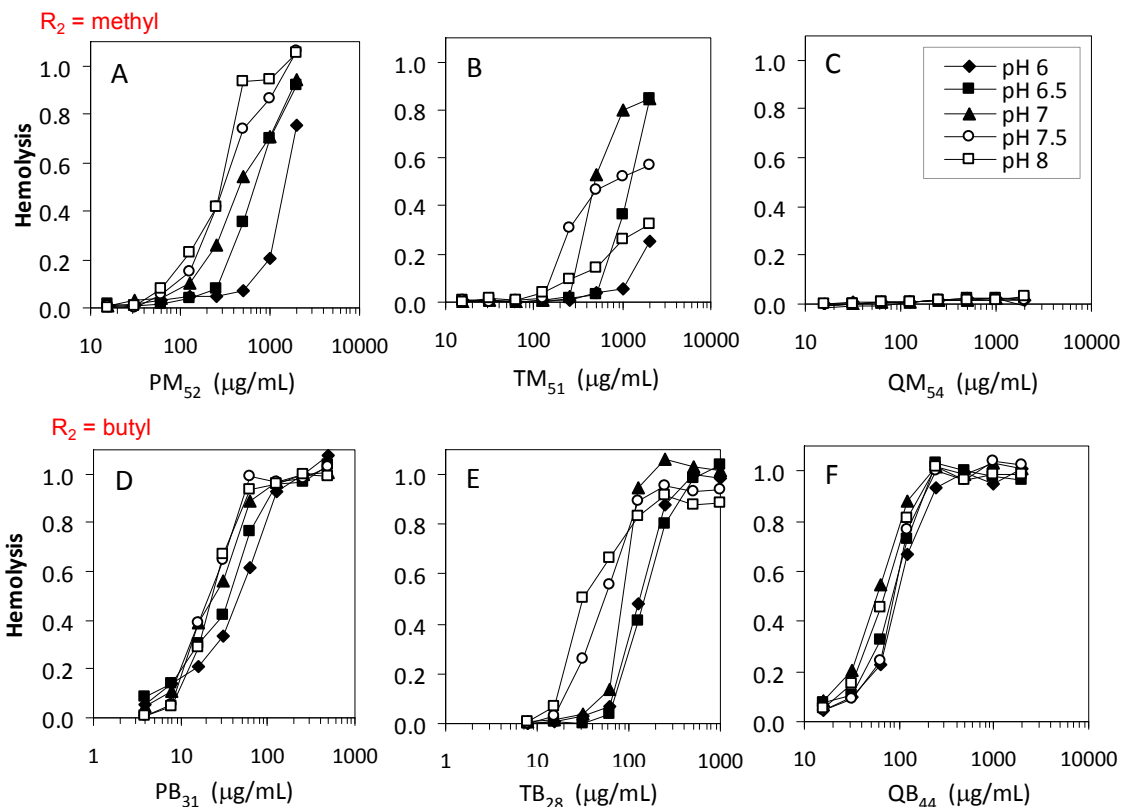


Figure II-7. Hemolysis as a function of pH. The fraction of hemolysis induced by the representative copolymers at the fixed concentration of $500 \mu\text{g/mL}$ in buffers ranging from pH 6 to 8.

Furthermore, we examined the HC_{50} values obtained from the dose-response curves (Figure II-8) for each polymer. The HC_{50} values for PM_{51} decreases with increasing α , reaching a plateau of about $200 \mu\text{M}$ as α approaches 0.8 (Figure II-8), which we attribute to increased hydrophobicity at high pH, which enhances the activity of each polymer chain but also causes aggregation, reducing the number of polymer chains available for membrane interaction. The HC_{50} values of TM_{52} could not be determined in pH 6 or 8 because the hemolysis did not surpass 50% up to the highest polymer concentration tested ($2000 \mu\text{g/mL}$).

Compared to the polymers containing methyl side chains, the HC_{50} values for the polymers containing butyl groups are lower and less sensitive to changes in pH or α . Increasing pH from 6 to 7 caused the HC_{50} of PB_{31} to decrease by less than three fold. Further increase to pH 8 caused no significant change, which is similar to the HC_{50} profile of PM_{51} . The HC_{50} of TB_{28} monotonically decreased with increasing pH by four

fold. Because the butyl groups are more intensely hydrophobic than methyl groups, it is possible that the contributions from the amine groups are less pronounced.

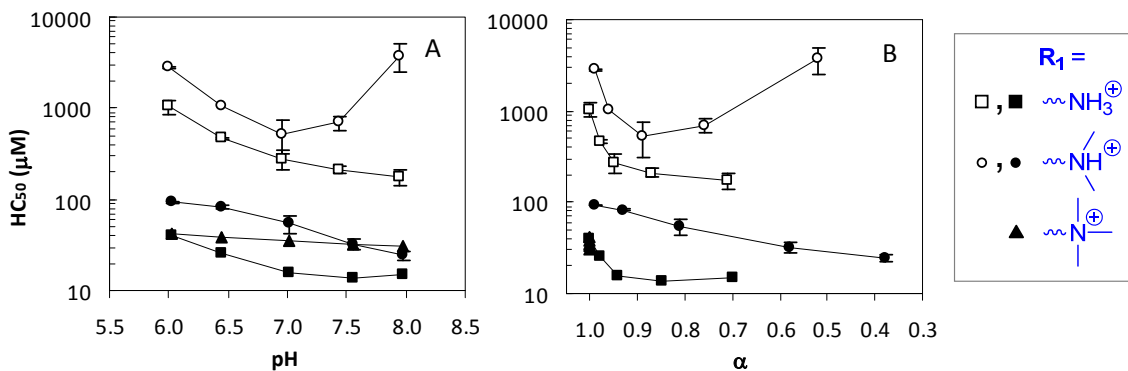


Figure II-8. Hemolytic activity (HC_{50}) as a function of pH and extent of ionization. Dependence on (A) buffer pH and (B) extent of ionization α , for the copolymers containing various ammonium moieties indicated in the caption and MMA (empty symbols) or BMA (filled symbols).

Enhanced membrane association and subsequent disruption induced by poly(2-ethylacrylic acid) (PEAA) has been attributed to increasing the polymer hydrophobicity as pH is decreased.¹¹⁸⁻¹²⁰ In this dissertation, we examined polymers which undergo deprotonation of cationic amine groups in $pH > 7$, leading to an enhancement of the hemolytic action. This mirrors the action mechanism of PEAA with respect to the pH-sensitivity of hemolysis, although the precise details of how amine groups participate in the membrane-disruption mechanism remains unclear at present. PEAA induced pH-dependent hemolysis with a sharp transition near $pH 6.5$,^{121, 122} whereas the pH dependence of our polymers showed a gradual transition across $pH 6$ to 8 (Figure 7). The polymers in this study are oligomeric in terms of size, whereas the PEAA polymers are high molecular weight. Changes in pH likely have a more dramatic effect on high molecular weight polymers because these contain a larger number of ionizable amine groups.

It has also been reported that the hemolysis induced by poly(2-propylacrylic acid) (PPAA) increases as the pH of the buffer is varied from 5 to 6 but as the pH is further increased to 7, hemolysis decreases.¹²³ The authors mention that PPAA may form microaggregates in the low pH region, curtailing their activity. Our results show a loss of hemolytic activity when the α value of TM₅₁ was decreased substantially. We also

speculate that aggregation of the polymers contributes to the observed loss. The reports on poly(2-alkylacrylic acid)s were aimed at gene delivery through endosomes where the polymers are activated to disrupt the lipid membranes and escape from the endosomes.¹²⁴ The same scientific concepts can be applied to the action of antimicrobial compound that target bacterial cell membranes.

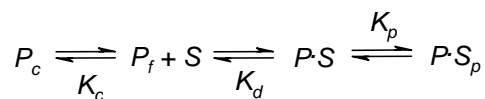
Conclusions

In this Chapter, we reported a library of amphiphilic random copolymers containing primary or tertiary amines, or quaternary ammonium groups, as a source of cationic charge. We examined the relationship between the biological activity and the amine functionality towards an understanding of the biological function of the amine groups. The copolymer series having primary amine groups displayed potent antimicrobial activity and selectivity against *E. coli* over RBCs. The copolymers containing quaternary ammonium groups showed activity against *E. coli* only when the hydrophobic content of the polymers was increased and these copolymers were limited in their cell selectivity, suggesting that reversibly *N*-protonated amines are a more appropriate design choice for the cationic groups in the development of non-toxic antimicrobial polymers.

The pH dependence experiments indicated that the amine groups provide cationic charges as well as play an important role in the antimicrobial action and hemolysis, which we hypothesized. These results suggested that the antimicrobial and hemolytic activities of polymers depend on the properties of amine side chains as well as the hydrophobic nature of polymers, which will allow creation of polymers with desired activities by choosing appropriate amine and hydrophobic side chains. The pH-sensitive antimicrobial and hemolytic action of the copolymers containing primary or tertiary amines can be tuned by changing the amount and identity of hydrophobic comonomer. This degree of freedom in the design of biologically active polymers is inaccessible to polymers containing quaternary ammonium groups.

The effect of hydrophobicity and cationic groups in the polymers on their membrane activity can be interpreted using a schematic model of the polymer-lipid interaction, as discussed previously¹⁰⁷ (Scheme II-1). Polymers free in solution, P_f , and

binding sites on the membrane, S , are in equilibrium with a polymers bound to sites on the membrane, $P \cdot S$. Subsequent to initial binding, we hypothesize the formation of polymer-lipid complexes on the cell membrane, $P \cdot S_p$, which are associated with membrane permeabilization. However, P_f is also in equilibrium with aggregated polymers, P_c , which we regard as a membrane-inactive species.



Scheme II-1. Proposed Model of Polymer-Membrane Interaction

Increasing hydrophobicity of the polymer enhances the observed activity due to increased amount of bound polymers, $P \cdot S$ (lower K_d) and increased population of active species, $P \cdot S_p$ (higher K_p). On the other hand, excessive hydrophobicity drives the equilibrium towards the inactive P_c species, curtailing the observed activity. Increasing the number of cationic charges on the polymer enhances the binding affinity (decreases K_d) to the membrane by electrostatic attraction to anionic lipids in the bacterial surface and also disfavors the P_c state because of higher water solubility. However, the membrane permeabilization is compromised. The chemical structure of the amine groups also seems to play a critical role in the polymer-lipid interaction, as evidenced by profound differences in activity observed for polymers containing different amine groups. The protonated or quaternized ammonium groups provide cationic charge thought to enhance the electrostatic contribution to the binding of polymers to anionic lipids in the bacterial cell membrane. However, the role of the amine functionality in the insertion and permeabilization events remains unknown to our knowledge. The amine groups are possibly involved in the formation of polymer-lipid complexes, which affect the disruption mechanism. To explore this hypothesis, we further examined the interaction of polymers with model lipid vesicles, which is described in the following Chapter.

CHAPTER III

Role of Cationic Group Structure in Membrane Binding and Disruption by Amphiphilic Copolymers

Introduction

Structure-activity relationships highlighted the importance of the choice of amine groups in the biological activity of polymethacrylates which mimic host defense peptides, as detailed in Chapter II. An interesting feature of host defense peptides and their synthetic polymer mimics is the source of their cationic charge: they contain primary amine groups which are protonated at physiological pH, while polysurfactants typically contain permanently charged quaternary ammonium salt (QAS) groups. In the previous Chapter, we described a direct comparison of polymethacrylate derivatives containing either protonated amines or quaternary ammonium units, which revealed that the primary amines are most effective at conferring favorable antimicrobial properties.⁸⁰ Additionally, polystyrenes⁶⁸ and polydiallylamines¹²⁵ have shown greater antimicrobial activity when functionalized with tertiary ammonium, rather than QAS groups. Based on the structure-activity data, we hypothesized that the polymer interaction consists of a binding equilibrium and subsequent membrane permeabilization, which is profoundly impacted by the chemical structure of the cationic ammonium groups. This led us to inquire: *what is the role of cationic groups in the binding and membrane disruption processes?*

The central hypothesis of this field is that cell membrane-disruption induced by amphiphilic polymers leads to the observed biocidal activities.^{61, 66, 67} Although a great deal of effort has focused on the interaction of high molecular weight polymers with model membranes,¹²⁶ relatively little is known about the membrane disruption induced by this emerging class of low molecular weight amphiphilic polymers, which mimic host defense peptides. Accordingly, recent investigations on the propensity of such

antimicrobial polymers to permeabilize model membranes have been carried out. Recently, the effect of lipid composition on the ability of antimicrobial oligomers to induce dye leakage from lipid bilayers by forming transmembrane pores was reported.¹²⁷ Epanand et al demonstrated that peptide-mimetic antimicrobial nylon-3 polymers induce leakage from liposomes which mimic the lipid composition of bacterial cell membranes, but not from those which mimic that of mammalian cell membranes.¹²⁸ In general, the bacterial cells contain more anionic lipids such as phosphatidyl glycerol (PG). The authors concluded that the charge interaction between cationic polymers and anionic lipids drives the binding and membrane disruption events. In addition, we recently showed that amphiphilic copolymers based on methacrylamides induced leakage from liposomes depending on the lipid composition and hydrophobicity of the polymers, which correlated well with their antimicrobial and hemolytic activities (these results are discussed in detail in Chapter IV).⁸¹ However, a complete understanding of the structural features of the polymers, rather than the lipids, which control the membrane activity has not been achieved to date. Particularly, it would be interesting to assess the role of cationic group structure in the membrane disruption process, as a representative structural difference between peptide-mimetic and conventional polysurfactant antimicrobials.

Due to the complexity of cell membrane structures, it is challenging to elucidate the molecular mechanism of membrane disruption exerted by polymers, which we hypothesize is central to their antimicrobial activity. Therefore, the model membranes will be able to provide a pure biophysical system to clearly demonstrate the interaction of polymers with membranes. Understanding the role of cationic groups in the disruption of these model membranes will provide a biophysical basis for understanding their observed hemolytic activities. This knowledge will aid in the future design of antimicrobial polymers with a minimal propensity to disrupt mammalian cells. Additionally, understanding the role of cationic group structure in the polymer-membrane interaction will demonstrate why primary amines, utilized in nature by host defense peptides, appear to be the optimal choice of cationic groups in antimicrobial polymers. The investigation will also augment the design principles of polymers toward materials with controlled membrane activities by controlling the properties of their cationic amine structures.

In this Chapter, we quantify the membrane-binding of representative dye-labeled copolymers which contain different ammonium structures (primary, tertiary, or quaternary). We further quantified the effect of amine structures of the polymers on the mechanism of the membrane disruption. We examined the molecular interactions between the ammonium groups and the phosphate groups of lipids by solid-state NMR and water-octanol partitioning. We chose to investigate the binding of amphiphilic polymers to vesicles composed of 1-palmitoyl-2-oleoyl-sn-glycero-3-phosphocholine (POPC, chemical structure shown in Figure III-4) a zwitterionic lipid which is a major component of mammalian cell membranes. Furthermore, we present the damage to POPC vesicles induced by the polymers by a fluorescence de-quenching experiment, as well as the disordering of lipid orientation by solid state NMR.

Dansyl-labeled Polymer Synthesis and Characterization

We prepared three model polymethacrylate derivatives, each containing a different type of ammonium group as the source of cationic charge. The polymer side chains consist of hydrophobic groups and primary, tertiary or quaternary ammonium salt groups (Figure III-1).

The mole fraction of methyl groups in the side chains, f_{methyl} , and the degree of polymerization (DP) values are similar in the three polymers, such that the effect of the cationic group structure can be investigated directly. We chose to prepare relatively short polymers ($M_n = 2\text{-}4$ kDa) with an average mole fraction of methyl methacrylate relative to all monomer units in a polymer chain, f_{methyl} of 0.56-0.57 for this study (Table III-1) because similar parameters gave rise to hemolytic polymers in our previous work.⁸⁰

The polymer end groups are conjugated to dansyl, a fluorophore which can be exploited as a probe of the microenvironment polarity.¹²⁹ The fluorescence from dansyl groups increases upon transfer from an aqueous to a non-polar microenvironment. Hence, the fluorescence will be increased when the dansyl groups are inserted into the hydrophobic region of lipid bilayers upon polymer binding. Titration of a polymer solution by liposomes could thereby provide binding isotherms of the polymers to model vesicles, enabling quantification of the dissociation constants.

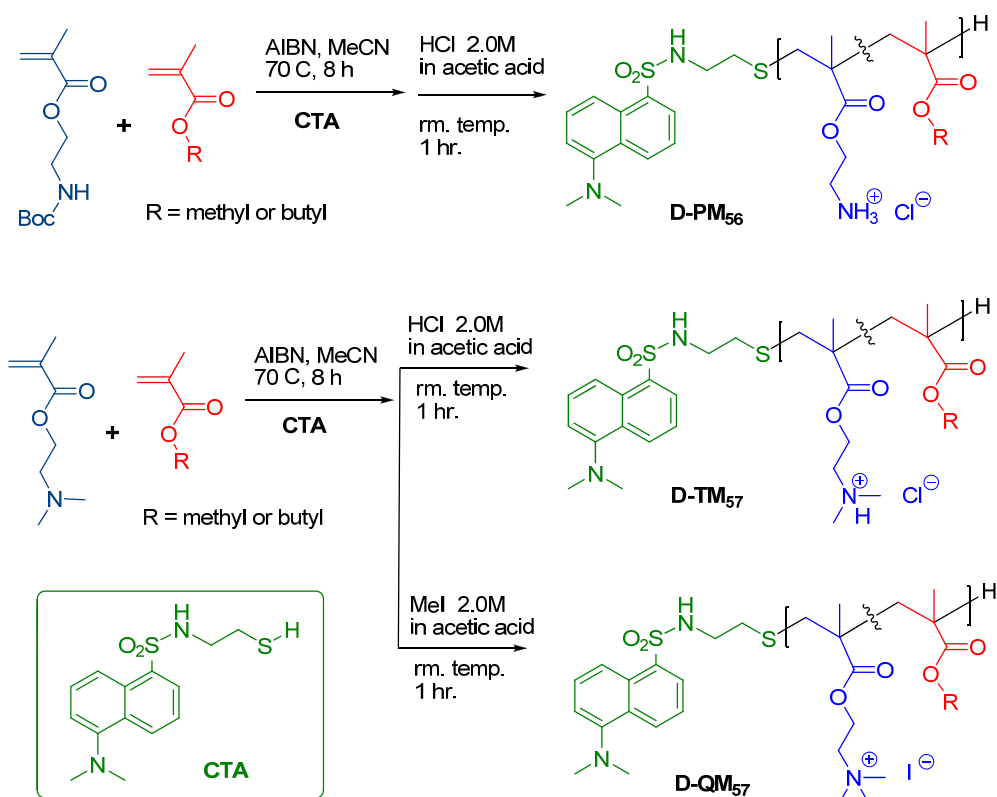


Figure III-1. Synthesis of amphiphilic random copolymers bearing primary, tertiary, or quaternary ammonium salts and dansyl end groups. Synthesis of the dansyl-functionalized chain transfer agent is described in Appendix A.

Table III-1. Characterization of random copolymers with dansyl end groups

Polymer	$f_{\text{methyl}}^{[a]}$	DP ^[a]	$M_n^{[a]}$ (kDa)	$\epsilon^{[b]}$ (M ⁻¹ cm ⁻¹)	$\lambda_{\text{max}}^{[b]}$ (nm)		HC ₅₀ (μM , $\mu\text{g/mL}$)
					Abs.	Em.	
D-PM₅₆	0.56	20	2.6	4700	334	508	36, 94
D-TM₅₇	0.57	19	2.7	4400	336	512	230, 620
D-QM₅₆	0.56	22	4.2	4600	339	511	>480, >2000

[a] Mole fraction of methyl repeat units (f_{methyl}), number average degree of polymerization (DP) and molecular weight (M_n) determined by peak integration analysis of the ¹H NMR spectra in methanol-d₄.

[b] Molar extinction coefficient, ϵ , at the wavelength of maximum absorbance, Abs. λ_{max} , and wavelength of maximum fluorescence emission intensity, Em. λ_{max} , recorded in methanol

The molecular weights were determined by comparing the integrated areas in the ¹H NMR spectra (Appendix B). The wavelengths of maximum absorbance and fluorescence emission of the polymers in methanol, in which the polymer chains are expected to be well solvated, were in the ranges of 334-339 and 508-512 nm, respectively. The molar extinction coefficients (ϵ) of the polymers in methanol were in the range of

4400-4700 $M^{-1}cm^{-1}$. These values are comparable to free dansyl as well as dansyl-conjugated proteins reported in the literature,^{130, 131} indicating that the attachment to these polymers did not diminish the absorbance and emission properties of the dansyl end groups.

The hemolytic properties of the polymers followed the same trend as the polymers without dansyl labels.⁸⁰ Polymer D-PM₅₆ showed the lowest HC₅₀ value of 36 μM while D-TM₅₇ was less hemolytic with an HC₅₀ value of 230 μM . The QAS-containing polymer 3 did not induce any observable hemolysis up to the highest concentration tested (480 μM). In exactly the same assay conditions, the bee venom toxin melittin showed an HC₅₀ value of 4.4 μM . Based on their characterization and hemolytic activities, the representative copolymers in this study are suitable for investigating the role of cationic group structure in the membrane binding and disruption exerted by amphiphilic polymethacrylates.

Before studying the interaction of the polymers with lipid vesicles, we performed potentiometric titrations of D-PM₅₆ and D-TM₅₇ in order to quantify their extent of ionization (α) in buffers of various pH. The polymers were titrated to pH 8 and 7.5, respectively, in good agreement with the back-titration data, indicating that the polymers are stable in this pH range (Figure III-2).

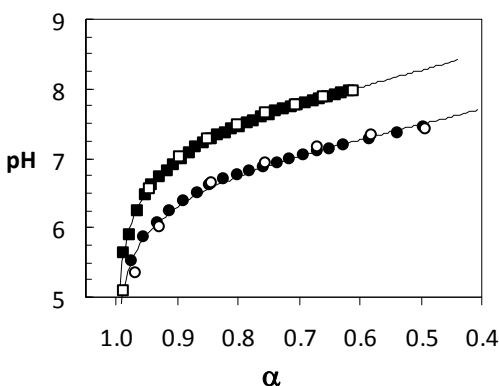


Figure III-2. Potentiometric titration curves for the representative copolymers, D-PM₅₆ (squares) and D-TM₅₇ (circles). Filled symbols represent the forward titration with NaOH aq. and empty symbols denote the back-titration with HCl aq. in good agreement. The curves are best fits to the generalized Henderson-Hasselbalch equation for polyelectrolytes.

The apparent pK_a values of D-PM₅₆ and D-TM₅₇ are 8.3 and 7.5, respectively, according to extrapolation of curve fits to the generalized Henderson-Hasselbalch

equation (Appendix A). At pH 6, the α values of D-PM₅₆ and D-TM₅₇ are > 0.95 whereas, at pH 7, the α value of D-PM₅₆ was about 0.9 and that of D-TM₅₇ decreased to about 0.7, indicating these polymers display a fraction of neutral amine groups at physiological pH.

Water-Octanol Partition Coefficients

In the design of polymers that exert their effect on membranes by disruption or pore formation, the importance of striking a fine-tuned balance between hydrophobic and hydrophilic components, known as “amphiphilic balance”, has been widely appreciated.^{67, 132} When the components are present in the appropriate ratio, favorable antimicrobial activity and low toxicity to human cells can be observed.^{67, 73} When the polymers are too hydrophilic, only weak activity is observed due to limited insertion into the hydrophobic membranes. On the other hand, toxicity to both bacterial and human cells is observed when the polymers are excessively hydrophobic. The overall hydrophobicity of amphiphilic polymers has been largely limited to qualitative or indirect descriptions of the chemical structure of polymers, such as comonomer ratios^{74, 75} and the lengths of alkyl side chains.¹⁰⁷ We determined the water-octanol partition coefficient ($\log P$) by measuring the equilibrium concentration of polymers in water and octanol phases based on the fluorescence intensities of the dansyl-labeled polymers in methanol. The $\log P$ is a quantitative measure of the overall hydrophobicity or amphiphilic balance, which encompasses the cationic ammonium group structure, degree of ionization, type and mole fraction of hydrophobic groups, and molecular weight. Traditionally, $\log P$ values have been used to predict the ability of small compounds and drugs to permeate cell membranes in pharmaceutical applications and environmental science, which assess the penetration of pollutants to ground water.¹³³ In this work, we extend that rationale to include polymeric molecules with the potential to act as pharmaceuticals in the future.

The $\log P$ of the polymers containing primary or tertiary amines were found to depend on pH, while those polymers containing quaternary ammonium groups were pH-independent as expected (Figure III-3). The polymers D-PM₅₆ and D-TM₅₇ displayed similar $\log P$ values of about -0.5 at pH 6, a condition in which nearly all of the amine groups are protonated according to the titration data (Figure III-2), implying that the

copolymers are hydrophilic in this condition. The $\log P$ for the polymer D-PM₅₆ increased gradually to about 0.0 as the pH was increased to 8. On the other hand, the $\log P$ value of D-TM₅₇ increased dramatically around pH 7 and reached a plateau at higher pH, toward a $\log P$ value of about +2.0. When the pH axis is re-scaled to the extent of ionization α , the $\log P$ values of D-PM₅₆ and D-TM₅₇ increase linearly with decreasing α . This indicates that deprotonation of the ammonium groups in the side chains renders the partitioning of polymer into the octanol phase more favorable, within the physiological pH range. The linear relationship suggests that the incremental contribution of deprotonation of ammonium groups to the partitioning of polymers into octanol is constant. The slope for polymer D-TM₅₇ is roughly three-fold greater in magnitude than that of D-PM₅₆. These results indicate that the deprotonated (neutral) tertiary amines impart significantly greater hydrophobicity to the polymers relative to the primary amines, as would be expected from the less polar structure of the former. Hence, the chemical structure of the cationic groups, and not simply their positive charge, profoundly impacts the amphiphilic balance.

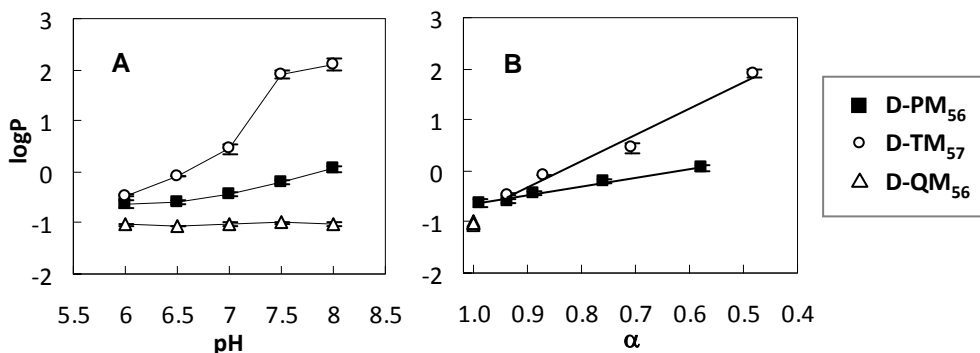


Figure III-3. Partition coefficients of each polymer between octanol and aqueous phase (HEPES or MES 10mM, NaCl 150 mM) as functions of (A) buffer pH and (B) extent of ionization α

The $\log P$ of D-QM₅₆ is about -1.0 across the entire pH range studied, implying that the polymer containing quaternary ammonium salts is predominantly hydrophilic and pH insensitive. Interestingly, the $\log P$ values of D-PM₅₆ and D-TM₅₇ in the pH 6 buffer are roughly -0.5, which suggests slightly lower hydrophilicity relative to D-QM₅₆, even though D-PM₅₆ and D-TM₅₇ are almost completely ionized. This demonstrates that the overall hydrophilicity is not a simple function of the number of cationic ammonium groups, but also depends on their chemical structure. Amphiphilic copolymers

containing QAS groups are more hydrophilic than analogous polymers containing the same number of cationic primary or tertiary ammonium groups. This observation agrees with simulations on the solvation of glycine derivatives containing primary, tertiary, and quaternary ammonium groups in their side chains.¹¹¹

Polymer-Liposome Dissociation Constants

We exploited the environmentally sensitive dansyl end groups to detect the partitioning of polymers into the hydrophobic region of Zwitterionic lipid bilayers. The polymers are weakly fluorescent in aqueous buffer due to quenching of the dansyl end-groups exposed to water. Upon addition of liposomes, the polymer may partition into the non-polar membrane environment, resulting in enhancement of the fluorescence intensity (Figure III-4).

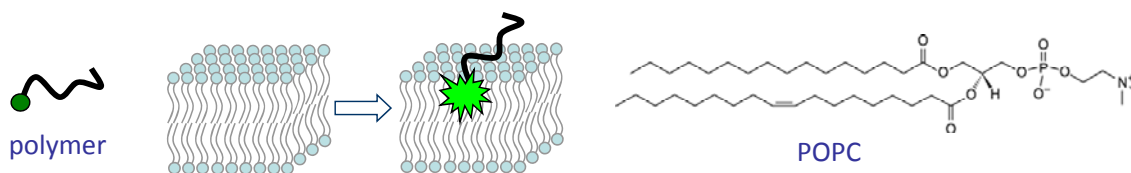


Figure III-4. Fluorescence enhancement of dansyl-labeled polymers upon partitioning into the hydrophobic membrane environment, and the chemical structure of the lipid POPC.

In the absence of POPC (structure in Figure III-4) each of the polymers exhibited fluorescence emission in phosphate buffered saline (F_0 , where $[\text{POPC}] = 0 \mu\text{M}$). As the pH was elevated from 6 to 8, the initial fluorescence intensities F_0 of D-PM₅₆ and D-QM₅₆ did not change significantly. On the other hand, the polymer D-TM₅₇ showed an F_0 value of about 9.4 at pH 6 but increased markedly to about 20.2 in the pH 8 buffer, which suggests that the dansyl end group was transferred to a less polar microenvironment. Such an observation is consistent with the formation of hydrophobic polymer aggregates of D-TM₅₇ in the aqueous environment when the pH is elevated (pH = 8, $\log P = +2.0$).

Upon titration of the polymer solutions with aliquots of POPC stock solution, changes in the fluorescence intensity were monitored in buffers ranging from pH 6 to 8 (Figure III-5).

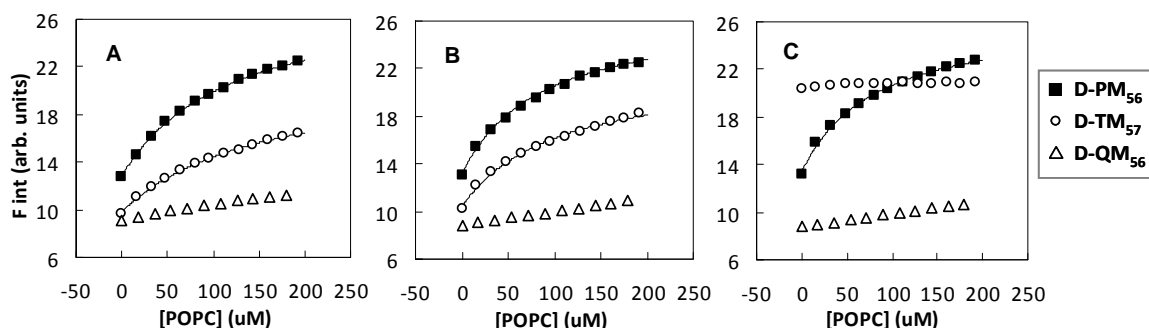


Figure III-5. Binding isotherms of polymers to POPC vesicles as a function of pH. D-PM₅₆ (filled squares), D-TM₅₇ (empty circles), and D-QM₅₆ (empty triangles) were titrated with 5 μ L aliquots vesicles of POPC in buffer of pH (A) 6, (B) 7, and (C) 8. The initial polymer concentration was 1 μ M. Fluorescence intensities are corrected for dilution and the inner filter effect. The curves represent best fits to the single-site binding model (Appendix A) with $n = 6$.

The fluorescence intensity of polymer D-PM₅₆ increased roughly 1.8 fold when saturated with liposomes ($[POPC] = 192 \mu\text{M}$). At the same POPC concentration, the fluorescence intensity of polymer D-TM₅₇ increased about 1.6 fold at pH 6 and 1.7 fold at pH 7. However, at pH 8, the D-TM₅₇ emission was unaltered by the liposomes, implying that the hydrophobic aggregates did not bind to POPC liposomes appreciably. Hence, excessively hydrophobic ($\log P \sim +2.0$) copolymers are not effective membrane active compounds due to the diminished propensity of their aggregates to insert into lipid bilayers. This supports the hypothesis put forth in the preceding Chapter.

The QAS-containing polymer D-QM₅₆ showed only slight changes upon liposome titration, regardless of buffer pH, which implies that the polymers did not significantly partition into the hydrophobic region of POPC lipid bilayers. This shows that excessively hydrophilic ($\log P \sim -1.0$) copolymers are favorably solvated in the external aqueous environment and likewise ineffective as membrane active compounds. Between these extremes, copolymers with a $\log P$ value near 0.0, such as D-PM₅₆ at pH 7.5, appear to exert superior membrane-binding affinity, which implies that membrane activity can be tuned by quantitatively adjusting the amphiphilic balance. We show for the first time that this adjustment could be made by judiciously choosing the structure of the cationic appendages, in addition to the traditional approach of tuning the hydrophobic groups. This pivotal result may aid in explaining the superior membrane activity of polymers containing protonated, rather than quaternized, ammonium groups in the side chains, such as polymethacrylates,⁸⁰ polystyrenes,⁶⁸ and polydiallylamines.¹²⁵

To quantify binding affinity, curve-fitting was performed on the isotherm data using equation 4 for the single-site binding model, as described previously, to obtain dissociation constants (K_D) for polymer-liposome binding (Figure III-6A). It is interesting that the K_D of polymer D-TM₅₇ was about 1.7-fold higher than that of D-PM₅₆ in pH 6, although nearly all of the amine groups in both polymers were protonated and their $\log P$ values were nearly identical at that pH. This indicates that the absolute number of cationic charges in the polymers and the $\log P$ value do not uniquely determine the binding affinity to POPC vesicles. The K_D values of polymer D-PM₅₆ and D-TM₅₇ decreased with increasing pH and approached $\sim 12 \mu\text{M}$, indicating that the binding of polymers might be predominantly determined by their hydrophobicity at high pH. We further examined the effect of hydrophobicity on the binding of polymers by re-scaling the pH axis to $\log P$ (Figure III-6B). The K_D values decreased with increasing $\log P$ values, indicating that an increase in the overall hydrophobicity drives the partitioning of the polymers to lipid bilayers. In the $\log P$ range of -0.7 to 0, polymer D-PM₅₆ showed lower K_D values than D-TM₅₇. The difference between values of $\ln(K_D)$ for D-PM₅₆ and D-TM₅₇ was roughly constant at ~ 0.7 , corresponding to $\Delta\Delta G \sim 0.43 \text{ kcal/mol}$ of polymer. This implies that the binding of polymer D-PM₅₆ to POPC vesicles is slightly more favorable than that of D-TM₅₇.

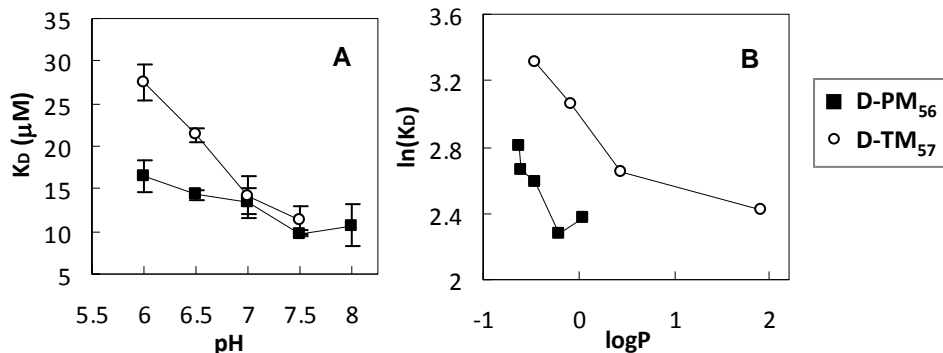


Figure III-6. Dissociation constants for polymer-POPC vesicle binding monitored by dansyl fluorescence, (A) as a function of pH and (B) water-octanol partition coefficient in the log-log plot. The error bars represent the standard deviation of three K_D values calculated from independent binding isotherm measurements.

We hypothesized that the lower K_D values of D-PM₅₆ to POPC, relative to those of D-TM₅₇, arise from greater affinity of the primary amine groups for the phosphate lipid headgroups, relative to that of tertiary amines. To test this hypothesis, the water-octanol

partition coefficients were measured for each of the polymers in the presence of the surfactant dodecylphosphate (DDP) in the pH 6 buffer (Figure III-7). The surfactant was added to a final concentration of 0.1 or 1 mM. This is well below the critical micelle concentration (CMC) for DDP, which is in the range of 10-60 mM depending on the counter-ion and temperature.¹³⁴ Therefore, we assume that the polymers form a complex with monomeric DDP, rather than micelles.

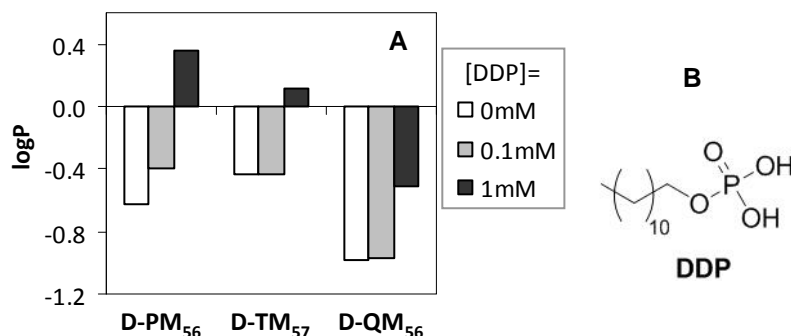


Figure III-7. Partition coefficients of the polymers in the presence of anionic detergent. Partitioning between aqueous buffer (10 mM MES, 150 mM NaCl, pH 6) and octanol was measured for each of the copolymers in the presence of 0, 0.1, and 1 mM dodecylphosphate (DDP). The total polymer concentration was 0.1 mM.

The log P values of each of the copolymers were sensitive to the presence of 1mM dodecylphosphate (DDP), although the magnitude of change in log P upon addition of surfactant depended on the identity of the cationic groups. The log P values of D-PM₅₆ displayed the most pronounced sensitivity to the addition of DDP. The magnitude of change in log P for D-PM₅₆ (+0.99) exceeded that of D-TM₅₇ (+0.54) and D-QM₅₆ (+0.46) upon addition of 1mM DDP. Since the pK_a values of the phosphate group in DDP are reportedly 2.8 and 7.2,¹³⁵ the mono-anion of DDP is the predominant species at pH 6. Therefore, we speculate that the cationic ammonium groups of polymer and the phosphate groups of DDP form a non-polar amine-phosphate complex. Such complexation would be expected to enhance the partitioning of the polymer to the non-polar octanol phase and, in that context, the primary amine groups appear to have the greatest affinity for phosphate headgroups in the surfactant.

On the other hand, the log P of the polymer with quaternary ammonium salt groups, D-QM₅₆, which is expected to have electrostatic interaction with anionic DDP, was less affected by the presence DDP. This result suggests that the interaction between

primary ammonium groups and anionic phosphate groups are driven by a combination of electrostatic and hydrogen bonding interactions. Furthermore, this outcome supports the notion that the insertion of dansyl groups on D-PM₅₆ into the hydrophobic core of phospholipid membrane is facilitated by hydrogen bonding to the phosphates in the lipid headgroups, which are reflected by the lower K_D values (higher binding affinity) of polymer D-PM₅₆. Because guanidinium groups are known to form more robust complexes with phosphate groups, relative to primary amines, it is reasonable to hypothesize from this result that amphiphilic copolymers displaying guanidine moieties in the side chains would partition into lipid bilayers as well. Although the cell-penetrating ability of arginine-rich macromolecules is well known,^{136, 137} relatively little attention has been paid to amphiphilic guanidine-containing copolymers in the design of membrane-disrupting polymers as antimicrobial agents.

At pH 7, D-PM₅₆ and D-TM₅₇ showed the same K_D , which implies that the total binding energies to POPC vesicles are equivalent. However, the relative contributions of overall hydrophobicity ($\log P$) and amine-phosphate complexation to the overall binding energy differed. In other words, the amine-phosphate complexation presented in Figure III-7 appears to enhance the binding to lipid bilayers for polymer D-PM₅₆ relative to D-TM₅₇ to compensate for the hydrophobicity difference between the polymers although the apparent binding energy is same.

Polymer-Induced Liposome Leakage

In order to assess the ability of the polymers in this study to disrupt the integrity of model membranes, we monitored the leakage of an entrapped fluorophore from within large unilaminar vesicles of POPC upon polymer addition. Liposomes are prepared with a self-quenching fluorescence dye entrapped above the quenching concentration. Upon polymer addition, the liposomes are permeabilized and the dye is diluted into solution, resulting in fluorescence enhancement (Figure III-8). This is the standard method to quantify the permeabilization of membranes.¹³⁸

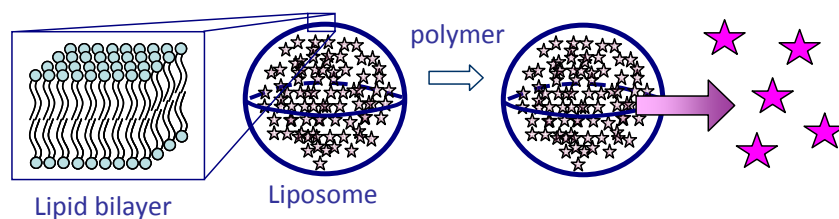


Figure III-8. Schematic of polymer-induced leakage of entrapped, self-quenching fluorophore from within liposomes, as a model system for membrane disruption.

The polymers D-PM₅₆ and D-TM₅₇ induced dye efflux from the liposomes in a pH-dependent manner, while the polymer D-QM₅₆ was not significantly membrane-lytic regardless of the buffer pH (Figure III-9). At pH 6, the polymers have the same number of cationic charges and similar log *P* values. However, they showed marked differences in their ability to induce dye leakage from vesicles of POPC. This demonstrates that not only the net cationic charge and hydrophobicity, but also the chemical structure of the cationic groups, are important determinants of membrane-lytic potency.

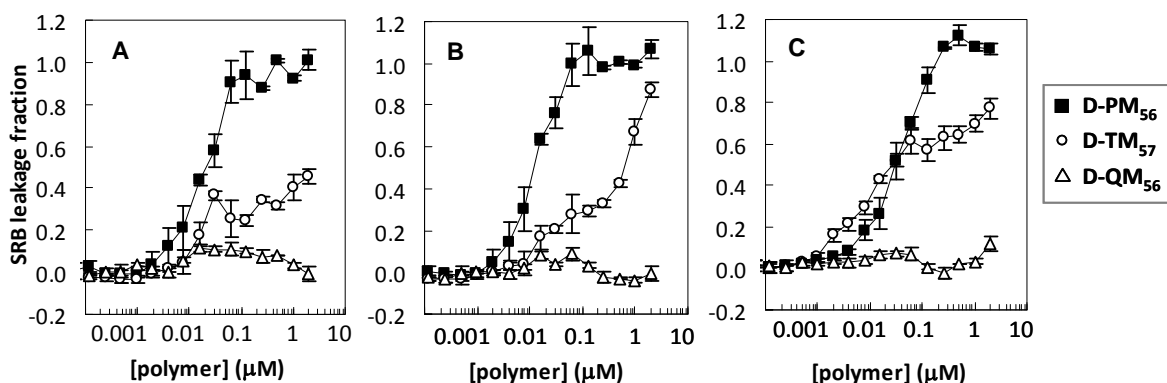


Figure III-9 Sulforhodamine B (SRB) leakage from POPC liposomes induced by the copolymers as a function of pH. Phosphate buffered saline solutions of pH (A) 6, (B) 7, and (C) 8 were used in the microplate assay. The total lipid concentration was fixed at 10 μM. The error bars represent standard deviation of the triplicate measurements.

Interestingly, the polymer containing primary amines, D-PM₅₆, retained its membrane-lytic property in buffers ranging from pH 6 to 8. On the other hand, the membrane damage caused by D-TM₅₇ was enhanced by increasing pH in this range. Recalling that the *K_D* value of D-TM₅₇ was enhanced by approximately two-fold upon increasing pH from 6 to 7, it is interesting that the concentration of this polymer which induced ~50% dye leakage seemed to increase by orders of magnitude as the pH was varied in this range. Regardless of pH, the polymer with QAS moieties, D-QM₅₆, did not

induce dye leakage from POPC vesicles. This is likely due to little or no binding affinity of D-QM₅₆ to POPC since the polymer is highly hydrophilic ($\log P \sim -1$). Membrane disruption by polymer containing QAS units is indeed possible when longer alkyl chains are attached in order to increase the hydrophobicity; however, as we show here by direct comparison, the QAS units are less effective at conferring membrane-disrupting ability relative to protonated (primary or tertiary) ammonium groups. In addition to the binding curves, this result further corroborates several reports on the enhanced antimicrobial and hemolytic activity of polymers bearing protonated, rather than QAS, ammonium groups.^{68, 80, 125}

At pH 7, polymers D-PM₅₆ and D-TM₅₇ have the same K_D value (Figure III-5), which suggests that the same concentration of polymers bound to the POPC membranes. However, in the same condition of pH 7, D-PM₅₆ was much more lytic than D-TM₅₇ (Figure III-9). This indicates that the membrane-permeabilization ability of the bound polymers depends on the structure of their cationic groups, rather than the mass action (total bound amount) of polymers on the membrane. We speculate that this is due to the differences in amine-phosphate interactions: the formation of complex between primary ammonium groups and phosphate lipid head groups might facilitate the insertion of polymers into the lipid membrane such that the membrane permeabilization is enhanced.

Solid-state NMR

In order to further probe the role of cationic group structure in the interaction of polymers with model membranes at high-resolution, ³¹P NMR spectra of mechanically aligned POPC bilayers were obtained. The ³¹P spectrum of mechanically aligned lipid bilayers is sensitive to the orientation of the lipid molecules, the phase of lipids, and the interaction between lipid molecules and additives such as peptides.^{139, 140} The pure POPC bilayers (0 mole % polymer) showed a single sharp peak at 31.7 ppm, which is indicative of the well-aligned sample with the orientation of the lipid bilayer normal parallel to the external magnetic field. Increasing the mole percentage of bound polymer relative to lipid in each case caused spectral changes indicative of electrostatic interactions between the phosphate group of POPC and the amine group of polymers leading to disruption in the lipid bilayers (Figure III-10).

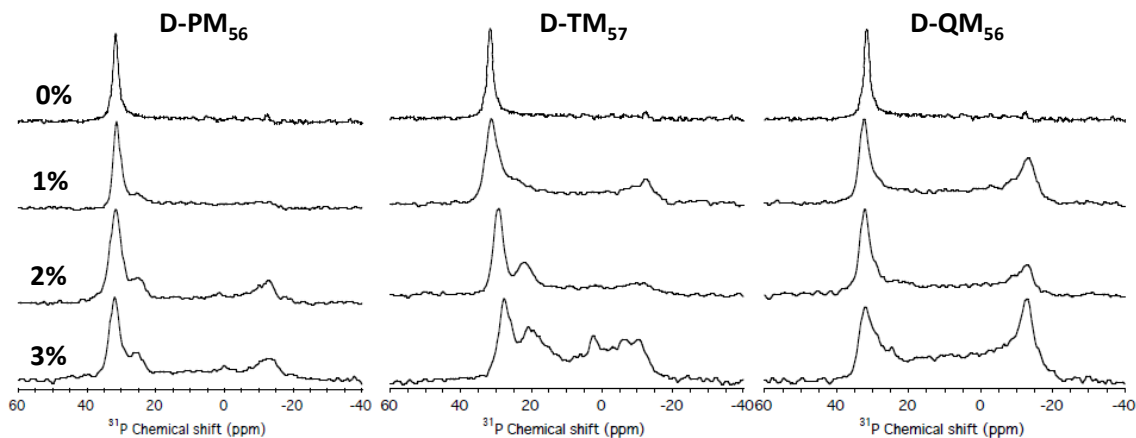


Figure III-10. Experimental ^{31}P chemical shift spectra of mechanically-aligned POPC bilayers with the copolymers incorporated. Mole percentages of polymer relative to lipid of 0, 1, 2, and 3 mol % as indicated. All NMR experiments were performed with the bilayer normal was set parallel to the external magnetic field of the spectrometer.

The presence of the intense peak at 31.7 ppm for lipid bilayers with the polymers D-PM₅₆ or D-QM₅₆ incorporated suggest that a majority of the lipid populations are in lamellar phase and not perturbed by the polymer interaction.^{140, 141} On the other hand, POPC bilayers incorporated with the polymer D-TM₅₇ at the concentrations 2 mol% and 3 mol% showed an apparent shift of the main peak to 29.2 ppm and 27.8 ppm, respectively. Since the perpendicular-edge of the spectrum arising from unaligned lipids is unchanged due to polymer D-TM₅₇ interaction, the decreasing frequency of the intense peak (~31.7 ppm) suggests conformational changes of POPC head group induced by the interaction of polymer D-TM₅₇. The spectra of POPC bilayers incorporated with the polymer D-PM₅₆ and D-TM₅₇, additional peaks at 25 ppm for all of the polymer 1 and 22 ppm and 21 ppm for the 2 mol% and 3 mol% of the polymer D-TM₅₇, respectively, are clearly seen in the spectra. A broad intensity over the range of the ^{31}P chemical shifts indicates anisotropy arising from unaligned lipids for most bilayers samples incorporated with polymers. A small isotropic peak at 2 ppm is also seen from the POPC bilayers incorporated with 3 mol% polymer D-TM₅₇. The polymer D-QM₅₆ sample did not give extra peaks, but only a broad powder pattern. These results suggest that polymers D-PM₅₆ and D-TM₅₇ alter the head group conformation of POPC leading to polymer-rich and polymer-poor lipid domains. For example, a peak at 25, 22, or 21 ppm may be attributed to the POPC bilayers containing polymer-rich domains.¹⁴⁰

Polymer D-PM₅₆, which contains primary ammonium appendages, caused a broadening of the peak near 31 ppm and also gave rise to two distinct peaks near 25 and -13 ppm when the mole percent of bound polymer was 2 or 3%. These changes demonstrate that the polymer alters the conformation of the POPC lipid headgroups. The development of a spectral feature near -13 ppm is indicative of lipid headgroups aligned perpendicular to the membrane, which may result from the formation of pores. The amine-phosphate interactions may enhance the reorganization of lipids upon the insertion of polymers to lipid bilayer.

Mixing of polymer D-TM₅₇ into the POPC bilayers also caused distinct changes in the ³¹P spectra. As with D-PM₅₆, features also appeared near 25 and -13 ppm, which suggests that mechanism of membrane disruption employed by D-PM₅₆ and D-TM₅₇ are similar to some extent. However, at 3 mole % of D-TM₅₇, the POPC bilayers displayed a very broad spectral feature spanning from 31 to -13 ppm due to polymer-induced disordering of lipids as seen in the case of polymer D-QM₅₆. It is likely that such gross disorganization of the lipid headgroups arises from irregular aggregate of lipids with the hydrophobic polymer D-TM₅₇.

Finally, it is interesting that the polymer D-QM₅₆, which contains quaternary ammonium salt groups, exerted a fundamentally different effect on the POPC bilayers compared to D-PM₅₆ and D-TM₅₇. The peak near -13 ppm appears more prominent at lower polymer content and the feature observed around 25 to 20 ppm is not evident at all. This suggests that structure of the cationic groups in the polymer modulates the polymer interaction with lipid bilayers. Although D-QM₅₆ clearly disrupts POPC bilayers when binding is forced, the polymer binds only weakly to POPC vesicles in solution and hence does not induce appreciable dye leakage. This shows that the QAS-containing polymers could potentially form pores and thereby permeabilize POPC bilayers, if the binding was enhanced by increasing the overall hydrophobicity.

Membrane Disruption Mechanism

The results from the series of experiments on partitioning and membrane binding of polymers indicated that the interaction of polymer D-PM₅₆ with lipid bilayers likely involves complexation between the primary ammonium groups of the polymers and

phosphate head groups of lipids. In addition, while polymer D-TM₅₇ showed the same binding affinity for liposomes at pH 7, polymer D-PM₅₆ displayed a much greater ability to permeabilize lipid bilayers. This indicates that the dye leakage occurs as a result of molecular interactions of the polymer within the lipid bilayers after initial binding, which likely involves amine-phosphate complexation. The solid-state NMR study likewise indicated that the ammonium groups interact with lipid head groups to induce a reorganization of the lipid bilayer structure, including perpendicular alignment of the lipid head groups. Further analysis of these spectra suggests that the polymer D-PM₅₆ induced the formation of polymer-rich and poor domains.

It has been proposed that the membrane-lytic peptides, which often display primary amino functionality, operate by the formation of “barrel-stave” or “toroidal” pores in cell membranes,³⁷ in which a fraction of the lipid headgroups are oriented perpendicular to membrane surface. Alternatively, peptides may induce total disruption resulting from accumulation of peptides on the membranes via the “carpet” mechanism.¹⁰⁶ The synthetic polymers in this report also efficiently induced the permeabilization of model membranes, when the cationic groups were protonated primary amines rather than quaternary ammonium salt groups. However, the exact mechanism(s) of their membrane-disruption action remains unclear at present and is currently being investigated. Probing the details of the membrane disruption mechanism exerted by polymers containing the primary amines would be highly desirable in the future.

In order to design non-hemolytic antimicrobial polymers, it has been established that minimization of hydrophobicity is a requirement.¹⁰⁷ This is largely due to the fact that the partitioning of polymers into zwitterionic membranes is mainly driven by hydrophobic effects, which were quantified in this study. Interestingly, we also found that the structure of the cationic groups contributes to the membrane association even when hydrophobicity is fixed. The ability of host defense peptides to selectively kill bacteria without harming human cells has been ascribed, at least in part, to electrostatic attraction of the cationic peptides to the anionic bacterial membranes.³⁸ While the polymers in this study apparently permeabilize mammalian cell membranes depending on their hydrophobicity, it remains unclear whether the pore formation in bacterial cell

membranes is responsible for their antimicrobial activity. For this reason, given that cell membranes of bacteria and mammalian cells consist of distinctively different types and composition of lipids, quantitative studies on the role of the lipid structure in the polymer-lipid interaction will also be important in the future to clarify the design principles for obtaining selective antimicrobials.

Polymers containing primary amines can be tuned to kill bacteria while causing no hemolysis, by reducing the fraction of hydrophobic side chains.⁸⁰ This method is ineffective for QAS-containing polymers, which require longer alkyl side chains as the hydrophobic groups in order to express antimicrobial activity as well as hemolytic activity.⁸⁰ Clarifying the mechanism of their antimicrobial action will therefore enable a complete understanding of the role played by cationic groups in the membrane activity of these emerging new materials.

Conclusions

This study demonstrated that the polymers containing primary amines are more potent hemolytic agents due to their enhanced ability to bind and disrupt the organization of lipid bilayers, relative to polymers with tertiary or quaternary ammonium groups. We found that the cationic group structure affects the apparent pK_a values of the polymers by decreasing the solubility of the polymers in water, leading to aggregation, when methyl groups are attached (tertiary amines) to the primary amines. In turn, the changes in pK_a affect the overall hydrophobicity, which increases upon deprotonation of the ammonium groups. Because the neutral tertiary amines are less polar than the neutral primary amines, the former become highly hydrophobic ($\log P > 2$) when the polymers are more than 50% deprotonated. The dissociation constants of polymers to lipid bilayers decreased in response to pH increase (polymer side chain deprotonation) which seems to rely on hydrophobicity combined with hydrogen-bonding effects. Furthermore, interaction of the polymer side chains with the lipid headgroups as revealed by ^{31}P NMR experiments appears to modulate the lipid head group conformation that results in membrane-disrupting behavior of polymers.

While disinfecting synthetic polymers have traditionally employed quaternary ammonium salt (QAS) moieties as their cationic units, primary amines endow a wide

variety of host defense peptides with a net cationic charge. The importance of lysine residues (which display primary amines in their side chains) has been established in the case of antimicrobial peptides.¹¹² Increasing the number of lysine residues enhanced the binding to anionic lipid bilayers, the membrane disruption, and the observed antimicrobial activities. Furthermore, substitution of lysine residues with histidines, which display imidizoles in the side chains (neutral at pH 7.4), caused a reduction in the activity of several synthetic antimicrobial peptides.¹¹⁵⁻¹¹⁷ These results suggest that primary amines are essential to the function of the host defense peptides.

We hypothesized moreover that this design principle could be generalized to synthetic polymers; that is, the activity of primary amine-containing polymers was expected to outperform analogues bearing tertiary or quaternary ammonium units. In this Chapter, the membrane disrupting ability of polymers is indeed enhanced by using primary amines, rather than QAS units, as the cationic groups at physiological pH. This appears to highlight the design rationale of membrane-disrupting macromolecules found in nature. Such information is expected to prove useful in the future development of non-hemolytic antimicrobials.

CHAPTER IV

Amphiphilic Polymethacrylamides as an Antimicrobial Design Platform

Introduction

Systematic studies have provided descriptions of some parameters that modulate antimicrobial and hemolytic activity of synthetic polymers, toward a design rationale for future development.^{80, 81} In the literature, a variety of polymer backbone structures were employed and activities were discussed largely in terms of the side chain properties.^{74, 76-78} It has been postulated that increasing hydrophobicity leads to lysis of human cells because the polymers bind indiscriminately to membranes regardless of subtle differences in anionic charge. Therefore, we hypothesized that a more hydrophilic backbone would reduce the global hydrophobicity of the polymers and thereby reduce the toxicity to human cells. In related polymers, the overall hydrophobicity, estimated as the summation of logP values for all the side chains was shown to monotonically increase the hemolytic toxicity.⁷⁶

Host defense peptides and synthetic peptide mimics possess a backbone connected by amide linkages, which are considerably more polar than the backbones of most vinyl polymers. In the previous Chapters, we have explored activity determinants in amphiphilic polymethacrylate derivatives, a prototypical class of antimicrobials^{75, 107, 142} containing ester groups in the side chains. These groups could readily be replaced with more hydrophilic amide linkages in order to demonstrate the effect of increased polarity near the polymer backbone (Figure IV-1).

Kopeček and coworkers extensively studied the polymerization of N-(2-hydroxypropyl) methacrylamide in the presence of butanethiol to control molecular weight by chain transfer polymerization.¹⁴³ They obtained a variety of biocompatible methacrylamide polymers conjugated to fluorophores, peptides, and other biologically active compounds, for applications including cancer therapy.¹⁴³⁻¹⁴⁵ Hence, it seemed that

hemocompatible antimicrobials could be developed using a polymethacrylamide platform including cationic and hydrophobic side chains. Accordingly, we systematically analyzed the structure-activity relationships in this class of materials.

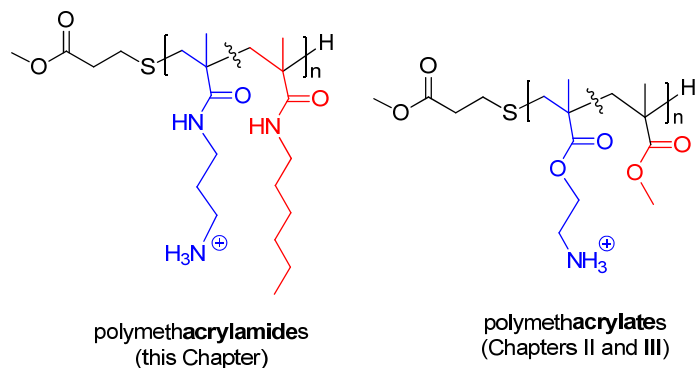


Figure IV-1. Comparison of chemical structures for polymethacrylates and polymethacrylamides

Polymer Synthesis and Characterization

We prepared methacrylamide copolymers containing primary ammonium chloride groups and hydrophobic alkyl groups. Two series of random copolymers containing hydrophobic alkyl groups and primary amine groups were prepared in one step by free radical polymerization in methanol/ethanol mixtures (Figure IV-2) This scheme is slightly modified from a report by Kopeček and co-workers on the polymerization of N-(2-hydroxypropyl)methacrylamide.¹⁴³ The details of the polymerization method and the characterization of polymers by NMR are described in Appendices A and B, respectively.

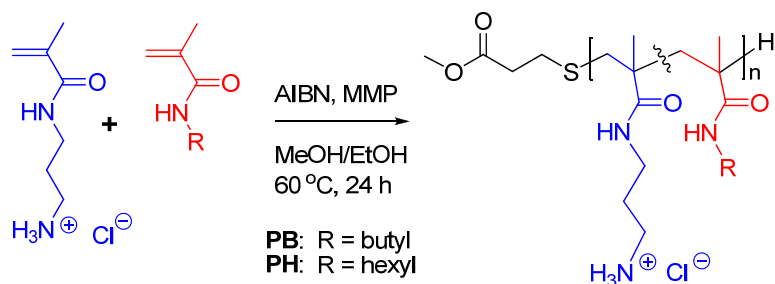


Figure IV-2. Synthesis of the amphiphilic methacrylamide random copolymers

Methylmercaptopropionate (MMP) was employed as a chain transfer agent in order to control the number average degree of polymerization (DP). The mole ratio of chain transfer agent to total monomer concentration was 0.1, giving short oligomers with

DP values in the range of 14-20 (Table IV-1). The feed ratio of comonomers was varied in order to tailor the average mole fraction of alkyl side chains in the copolymers, f_{alkyl} . Peak integrations in the ^1H NMR spectra were analyzed to determine the values of DP and f_{alkyl} for each polymer (Appendix B).

This low molecular size range (2.4-3.6 kDa) is similar to previously described polymers^{74, 77, 107} and peptides⁹ which are known to possess antimicrobial and non-hemolytic properties. The f_{alkyl} values ranged from 0 to 0.78 in the PB series (R = butyl) and 0 to 0.63 in the PH series (R = hexyl), in good correlation with the comonomer feed compositions used in the polymerizations (Appendix B). The chemical stability of the polymers in basic aqueous solution was examined by ^1H NMR (spectra shown in Appendix B). The amine-functionalized side chains in P_0 were unaltered by stirring at pH 10 for 24 hours. In contrast, primary amine-functionalized polymethacrylates were previously found to undergo multiple chemical changes due to isomerization and hydrolysis.^{108, 142, 146} Hence, this class of cationic, amphiphilic polymethacrylamides possesses improved chemical stability relative to the well-studied polymethacrylate derivatives.

Table IV-1. Characterization of methacrylamide random copolymers

Polymer	R =	f_{alkyl}	DP	M_n (kDa)
P_0	–	0.00	17	3.1
PB ₂₀	butyl	0.20	20	3.6
PB ₃₆	butyl	0.36	14	2.4
PB ₅₄	butyl	0.54	15	2.4
PB ₇₈	butyl	0.78	14	2.3
PH ₁₈	hexyl	0.18	19	3.5
PH ₃₃	hexyl	0.33	17	3.0
PH ₅₁	hexyl	0.51	16	2.9
PH ₆₃	hexyl	0.63	16	2.9

The ionization behavior of the polymers in this study was examined by means of potentiometric titration using a previously described procedure.¹⁴⁷ Establishing the extent of ionization in the polymers is requisite for the proper interpretation of structure-activity data because the protonated (cationic) and deprotonated (neutral) amine groups may play different roles in their antimicrobial or hemolytic action. It is well known that

pH influences the activity of membrane-lytic peptides¹¹⁵ and polymers^{122, 124, 148} bearing ionizable groups in the side chains. The cationic homopolymer P_0 was titrated to the equivalence point with NaOH and subsequently back-titrated with HCl in good agreement with each other (Figure IV-3).

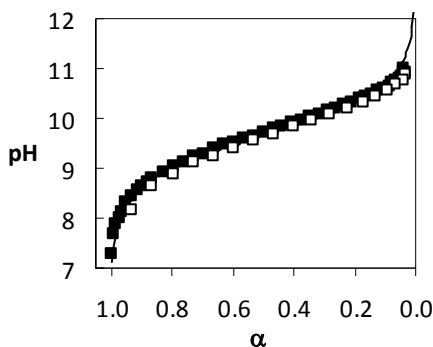


Figure IV-3. Potentiometric titration data for the cationic homopolymer, P_0 in aqueous 150mM NaCl solution. Solid symbols denote the forward titration with NaOH and empty symbols denote the back-titration with HCl.

The extent of ionization α for this polymer is >0.98 at pH 6 to 8. This indicates that nearly all of the primary amine groups in the P_0 side chains are protonated (cationic) in the physiologically relevant pH range. The α value for this polymer reaches 0.5 when the pH is increased to about 9.7. Hence, the polymer can be considered a two-component system of cationic ammonium groups and hydrophobic alkyl groups in buffer of pH 7.4.

Relative to P_0 , low molecular weight polymers of aminoethylmethacrylate, poly(AEMA), were previously shown to be significantly less basic: whereas 99% of the amine groups in P_0 are cationic at pH 7.4, only 72% of those in poly(AEMA) are cationic in that condition.¹⁴² This difference may be related to the difference in polymer polarity. The amide groups in P_0 provide more polar microenvironment surrounding the dye relative to the polymethacrylates, which contain less polar ester linkages. P_0 may therefore adopt a more extended chain conformation, minimizing Coulombic repulsion of cationic charges and thereby increasing basicity.¹¹⁰ The cationic groups in P_0 are attached to the polymer backbone by a propyl linker, whereas those of poly(AEMA) are separated by an ethyl linkage, which would also likely relieve Coulombic repulsions. Also, the increased dielectric of the microenvironment surrounding the amine groups in

the polymethacrylamides would increase basicity relative to the lower dielectric environment in polymethacrylates.¹⁴⁷

Antimicrobial Activity

We quantified the antimicrobial activity of the polymers as the minimum inhibitory concentration (MIC) values, as described in Appendix A. The amphiphilic, cationic copolymers completely inhibited the growth of *E. coli* and *S. aureus* in the micromolar concentration range of polymers, with MIC values that depend on f_{alkyl} and the length of the alkyl group (Figure IV-4). In the same assay conditions, the host defense peptide magainin-2 and the bee venom toxin peptide melittin showed MIC values against *E. coli* of 51 and 4 μM , respectively. Against *S. aureus*, the MIC values of magainin-2 and melittin were found to be $> 100 \mu\text{M}$ and 2 μM , respectively. Hence, the copolymers in this study showed antimicrobial potency comparable to that of peptides found in nature.

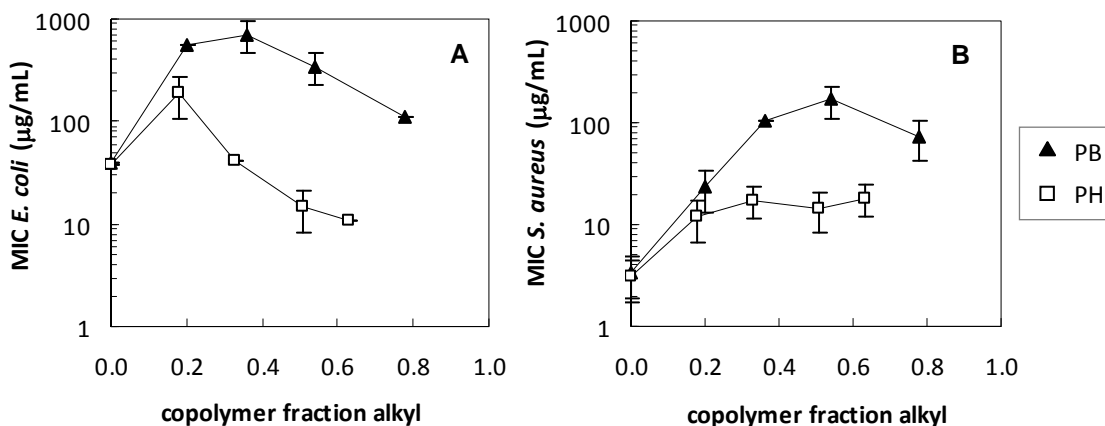


Figure IV-4. Antimicrobial activities (MIC) of methacrylamide random copolymers. MIC values plotted as functions of f_{alkyl} for the random copolymers against (A) *E. coli* and (B) *S. aureus*.

Figure IV-4 illustrates that the copolymers in the PH series, which contain hexyl side chains, showed MIC values as much as an order of magnitude lower than those of the PB copolymers, which have butyl groups. This difference in MIC values increased with increasing f_{alkyl} . Against *E. coli*, PB₅₄ had an MIC value of 340 μM (833 $\mu\text{g/mL}$) while PH₅₁ had an MIC of 14 μM (42 $\mu\text{g/mL}$). These two polymers have similar DP and f_{alkyl} , which indicates that longer hydrophobic alkyl side chains impart more potent

antimicrobial activity. Hence, it appears that increasing the hydrophobicity of side chains in the antimicrobial polymers enhances activity. As previously discussed in the literature, increasing the mole fraction of hydrophobic repeating units in random copolymers increases the antimicrobial and hemolytic activities.^{74, 77, 107}

In both polymer series, the MIC values against *E. coli* went through local maxima as f_{alkyl} was varied in the range of 0-0.8. When f_{alkyl} was increased from 0 to ~ 0.2 , the MIC values increased, which implies a loss of antimicrobial activity. Apparently, the antimicrobial action depends on the cationic charges in the polymer, which are diluted in the polymer chains by including a small fraction of hydrophobic repeat units. Increasing f_{alkyl} beyond 0.2 caused a decrease in MIC, implying that increasing the hydrophobicity enhances antimicrobial activity in the higher f_{alkyl} range. Hence, we consider that the cationic homopolymers and the hydrophobic copolymers may exert different mechanisms of antimicrobial action.

Against *S. aureus*, the MIC values went through a maximum as f_{alkyl} was increased in the PB series. In the PH series, the MIC values against *S. aureus* approached a plateau with increasing f_{alkyl} . Interestingly, the maximum in the PB series against *S. aureus* occurred at higher f_{alkyl} (~ 0.55) compared to the *E. coli* MIC data, which went through a maximum near $f_{\text{alkyl}} = 0.2$. This suggests that *S. aureus* cells are more sensitive to the effect of cationic charge density in the copolymers, while *E. coli* cells are more susceptible to the action of the hydrophobic groups. This distinction may arise from the differences in membrane structures between the two tested microorganisms. Gram negative bacteria such as *E. coli* possess two lipid bilayer membranes, separated by a thin layer of peptidoglycan (a three-dimensional cross-linked polymer network of peptides and sugar units which gives the membrane rigidity and shape). On the other hand, Gram-positive bacteria such as *S. aureus* possess only a single lipid bilayer membrane, protected by a comparably thick peptidoglycan layer. Tew and co-workers have shown that antimicrobial polymers can distinguish between gram-positive and gram-negative bacteria because of these structural differences in the membranes.¹⁴⁹

In the context of other primary amine containing polymers discussed in the literature, the polymethacrylamides in this work displayed anomalous activity minima (MIC maxima) as the hydrophobic comonomer content was increased. DeGrado and co-

workers found that the antimicrobial activity of polymethacrylates was enhanced by increasing the mole fraction of butyl groups in the copolymer side chains.⁷⁵ Antimicrobial activity of polymethacrylates increased sigmoidally with increasing fraction of hydrophobic comonomer, and was fit to the empirical Hill equation.¹⁰⁷ Mowery et al described antimicrobial random copolymers of beta lactams (Figure I-8, structure C) which showed increasing activity as the fraction of hydrophobic comonomer was increased.⁷⁴ Ilker et al likewise demonstrated that the antimicrobial activity of polynorbornenes (Figure I-8, structure D) was enhanced by increasing the hydrophobicity of the side chains.⁷⁷ The MIC values often display local minima with increasing hydrophobicity, which can be ascribed to the formation of micro-aggregates in the aqueous environment in the case of excessively hydrophobic polymers. Antimicrobial peptides rich in histidine form aggregates in water by hydrophobic association, observed by light scattering, which reduces their activity and membrane disruption ability.^{116, 117} For the polymers in this study, the MIC values going through a local maximum (antimicrobial activity at a minimum) with increasing hydrophobic comonomer in random copolymers bearing primary amines has not been previously reported to the best of our knowledge.

The MIC values increased from 30 to 500 $\mu\text{g/mL}$ as the mole percent of butyl groups increased from 0 to 20% (Figure IV-4). This suggests that decreasing MIC values with increasing hydrophobicity has been reported in the case of polymers bearing quaternary ammonium salts (QAS), such as copolymers of quaternized pyridine and alkylmethacrylates.⁹⁶ Additionally, studies on surface-bound QAS-polymers have shown that potent antimicrobial activity requires high cationic charge density.^{92, 150, 151} Reduction of the cationic charge density with increasing f_{alkyl} may be related to the observed loss of activity in the random copolymers presented here. However, whether these polymers exert their antimicrobial effects by a mechanism similar to that of QAS-polymer surfaces remains unclear at present.

A significant factor that distinguishes polymethacrylamides in this work from previously studied polymethacrylates (Figure IV-1) is their ionization behavior: in pH 7.4, only about 72% of the amine groups in the polymethacrylates are protonated¹⁴² while 100% of the amines in P_0 are cationic. In our prior studies on polymethacrylates, we

found that the antimicrobial and hemolytic activities were significantly reduced when the experiments were performed in pH 6, in which 100% of the amine groups are protonated.¹⁴² It is possible that the presence of neutral amines enhances activity, which implies that we can tune the activity of amphiphilic polymers by choosing ionizable groups with various pKa values.

Hemolytic Activity

To examine the biocompatibility of the polymers, hemoglobin release from human red blood cells was measured after incubation with each of polymers at various concentrations, as described in Appendix A. The extent to which copolymers in this study lysed human red blood cells depended on the polymer concentration as well as the identity and mole fraction of the hydrophobic side chains (Figure IV-5).

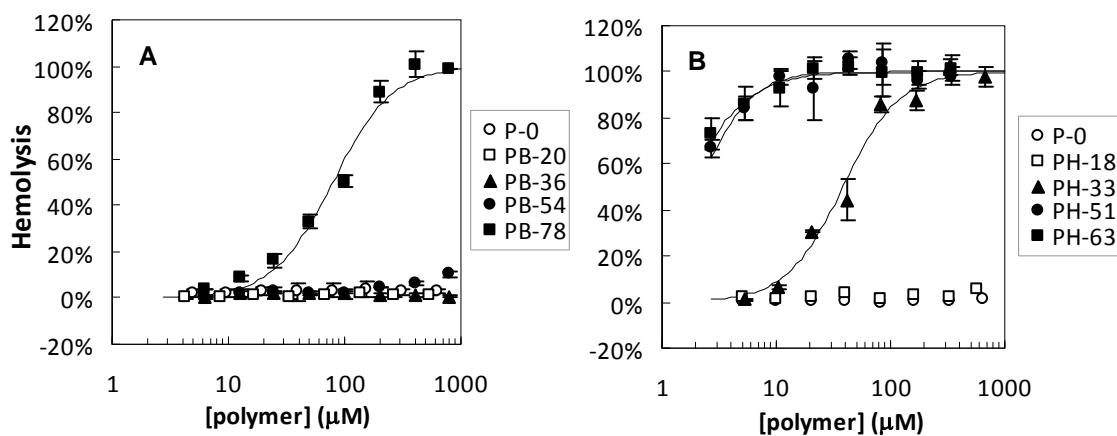


Figure IV-5. Hemolysis dose-response curves for the methacrylamide copolymers, in the (A) PB series and (B) PH series. The symbols represent experimental data and the curves are best fits to the Hill equation. Error bars represent the standard deviation from triplicate measurements.

In the PB series, polymers with $f_{alkyl} < 0.55$ showed no significant hemolysis up to roughly 570-670 μM (2000 $\mu\text{g/mL}$), which is comparable to the non-hemolytic property of magainin-2, which induced less than 10% hemolysis up to 100 μM in the same assay conditions. The data shown here indicate that the PB polymers are non-hemolytic, but rather antimicrobial. This demonstrates the validity of our initial hypothesis: non-hemolytic antimicrobials were by using a hydrophilic methacrylamide as a polymer platform in this study. On the other hand, the PH showed highly hemolytic compared to PB (Figure IV-5), which shows that increasing the hydrophobicity of the side chains did

eventually lead to increased hemolysis (Figure IV-5). PB₇₈ induced a significant amount of hemolysis ($HC_{50} = 79 \mu\text{M}$) and the polymers in the PH series were even more hemolytic. PH₃₃ showed an HC_{50} value of $36 \mu\text{M}$ and PH₅₁ and PH₆₃ showed HC_{50} values lower than $5 \mu\text{M}$, which is comparable to the highly hemolytic property of the bee venom peptide melittin ($HC_{50} = 0.7 \mu\text{M}$). Based on these observations, it seems that increasing f_{alkyl} , or increasing the length of the alkyl side chains, monotonically enhances hemolytic activity (Figure IV-6). This suggests that the overall hydrophobicity appears to be one of the major determinants of hemolysis. This hydrophobicity effect was also demonstrated for polymethacrylates, which showed a correlation between hydrophobicity of the side chains and hemolysis (HC_{50}). The increased hemolysis with increasing hydrophobicity defined by reverse phase HPLC was also reported.¹⁵² This seems to be general trend of the effect of hydrophobicity on hemolysis, which is in agreement with previous reports on polymethacrylates¹⁰⁷ as well as host defense peptides.³⁹

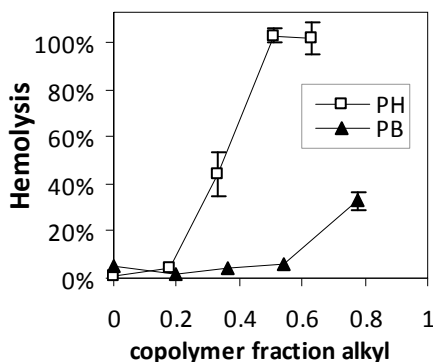


Figure IV-6. Hemolysis as a function of hydrophobic comonomer content, at a fixed polymer concentration of $125 \mu\text{g/mL}$.

DeGrado and co-workers found that increasing the hydrophobic comonomer fraction in polymethacrylates enhanced hemolytic activity.¹⁰⁷ These authors developed a theoretical model demonstrating that the hemolytic activity can be described as a partitioning of hydrophobic side chains in the non-polar region of red blood cell membranes in competition with polymer-polymer aggregation in the aqueous environment. It is hypothesized that the insertion of polymer chains into the membrane leads to membrane permeabilization, causing hemolysis. The results herein regarding polymethacrylamides follow the same trends in general. However, compared to polymethacrylates, it appears that the polymethacrylamides in this work require much

higher percentages of hydrophobic groups in the side chains to display hemolytic potency. Random copolymers containing roughly 20% butylmethacrylate are potent antimicrobials (MIC = 4 μM) and are somewhat hemolytic (HC_{50} = 100 μM).¹⁴² In this study, we showed that the copolymer containing a similar percentage of butylmethacrylamide PB₂₀ was only modestly active against *E. coli* (MIC = 560 μM) and non-hemolytic up to 556 μM (2000 $\mu\text{g/mL}$). It is possible that such stark differences in hemolysis arise from the hydrophilic nature of the methacrylamide units relative to methacrylates. Assuming that the partitioning of polymer chains to membranes is the major driving force of membrane permeabilization or hemolysis, more hydrophobic polymers are expected to be more hemolytic. Because the methacrylamides have a more polar backbone structure, a greater percentage of alkyl units and longer alkyl chains must be present in order for the polymers are hydrophobic enough overall to partition into the hydrophobic region of the red blood cell membranes.

Cytotoxicity

In addition to hemolysis, which measures leakage of hemoglobin from red blood cells, cytotoxicity testing using viable human cells will aid in assessing the potential for polymers in therapeutic or pharmaceutical applications. Accordingly, cytotoxicity of the polymers in this study to human epithelial HEP-2 cells was quantified by the XTT colorimetric assay, as described in Appendix A. Cytotoxicity was quantified as the reduction in the metabolic activity of the cells (indicative of cell viability) relative to the positive control surfactant Triton X-100. The polymer concentration which caused 50% reduction in cell viability after 1 or 24 hours incubation was defined as the IC_{50} value. Because the cells were exposed to polymer in serum-free medium, the confluence of cells was less than 80% after the 24 hour exposure time, which ensures that cell growth does not obscure the results. The monomer 3-aminopropylmethacrylamide did not affect the viability of the HEP-2 cells up to the highest concentration tested, which was 2800 μM (500 $\mu\text{g/mL}$). Since the maximum amount of unreacted monomer in the assay solution was 700 μM (125 $\mu\text{g/mL}$) the effect of the unreacted monomer can be considered negligible.

The host defense peptide magainin-2 showed less than 10% reduction in cell viability up to the highest concentration tested (100 μM), indicating low cytotoxicity, and the bee venom toxin peptide melittin showed an IC_{50} value of approximately 0.5 μM . All of the copolymers in this study induced substantial reduction of HEP-2 metabolic activity at concentrations below 10 μM , indicating that their cytotoxicity to human carcinoma cells is comparable to that of melittin (Figure IV-7).

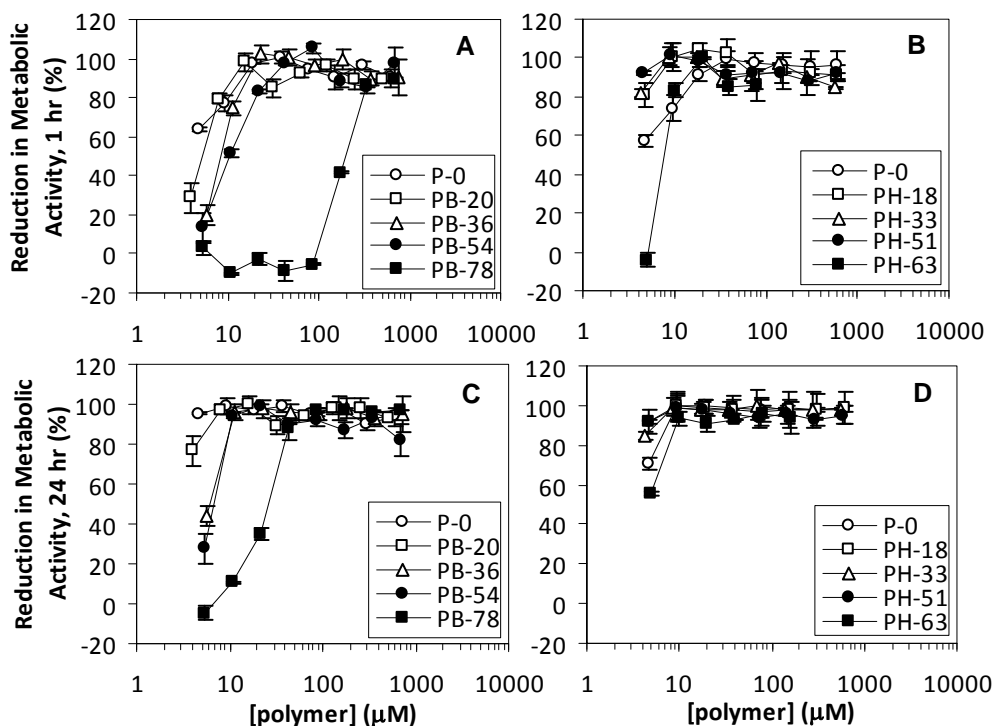


Figure IV-7. Cytotoxicity of the copolymers against HEP-2 cells by the XTT assay, measured as reduction in metabolic activity after incubation with the copolymers for 1 hour (A, B) and 24 hours (C, D).

The reduction in metabolic activity caused by the polymers depended on the copolymer composition. As f_{alkyl} was increased in the PB series, the polymers induced reduction in metabolic activity at higher polymer concentration. This shows that the polymers containing a greater number of the cationic primary ammonium groups were the most potent cytotoxic agents. This result corroborates prior work on the *in vitro* cytotoxicity of a wide variety of polycationic compounds such as polylysine and polyethyleneimine, which showed increasing toxicity with increasing cationic charge density.¹⁵³

Strikingly, the PB polymers with mostly cationic contents ($f_{\text{HB}} = 0\text{--}0.6$) induced less than 10% hemolysis up to the highest concentration, but they caused 100% reduction of HEp-2 cell viability. This result indicates that the polymers in the PB series are non-toxic to RBCs but nevertheless are highly toxic to HEp-2 cells. It seems that increasing the f_{alkyl} value reduces the cytotoxicity of the polymers in the PB series (Figure IV-8). This trend is opposite the trend in hemolytic activity, which was found to be more potent in the hydrophobic copolymers with higher f_{alkyl} values (Figure IV-6). Based on the hemolysis data, increasing the hydrophobicity in the side chains exacerbated the lysis of human red blood cells. In the case of HEp-2 cells, it was apparent that increasing the number of cationic charges in the polymers increased the cytotoxicity.

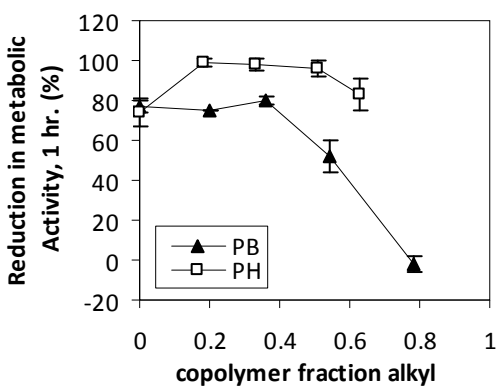


Figure IV-8. Cytotoxicity as a function of hydrophobic comonomer content. Reduction of metabolic activity in HEp-2 cells after incubation with the polymers for 1 hour at a fixed polymer concentration of $31.25 \mu\text{g/mL}$ as functions of f_{alkyl} .

The ratio of the HC_{50} to the MIC value of a given polymer is often reported as a measure of the ability to inhibit bacterial growth while minimizing leakage of hemoglobin from erythrocytes. Analogously, we report the ratio of IC_{50} (the polymer concentration which causes a 50% reduction in HEp-2 cell viability) to MIC as a measure of the ability to inhibit bacterial growth while minimizing the impact on human epithelial cell viability.

The cationic homopolymer P_0 showed an $\text{HC}_{50}/\text{MIC}$ value of > 54 against *E. coli* and > 640 against *S. aureus*. In the context of other polymers in the literature,⁷⁸ the latter value is remarkably high, which implies that P_0 is an excellent non-hemolytic antibacterial agent against *S. aureus*. As we hypothesized, the more polar methacrylamide platform afforded polymers which do not lyse human red blood cells.

On the other hand, the HC_{50}/MIC values of the copolymers decrease with increasing hydrophobic content. While the HC_{50}/MIC values of PH_{18} were > 11 for *E. coli* and > 170 for *S. aureus*, those of PH_{33} were 0.92 for *E. coli* and 2.2 for *S. aureus*. This shows that increasing the hexylmethacrylamide content by only 15% negates the selectivity for bacteria vs. red blood cells.

Despite the hemocompatibility of P_0 , the polycation is highly cytotoxic to HEP-2 cells. The value of IC_{50}/MIC for P_0 was < 1.3 , which implies no selectivity for bacteria over human epithelial cells. Although the polycation in this study is quite promising based on its potent antimicrobial and non-hemolytic properties, its toxicity to human epithelial cells may limit its therapeutic or pharmaceutical usefulness. Increasing f_{alkyl} in the copolymers gave rise to modest improvements in the IC_{50}/MIC values.

Cationic polymers have long been studied in the field of non-viral gene-delivery¹⁵⁴⁻¹⁵⁶ and it is well known that they are cytotoxic to human cells.¹⁵³ This presents a dilemma for the design of biocompatible amphiphilic methacrylamide copolymers: increasing the hydrophobic content aggravates hemolysis whereas increasing the cationic charge density leads to cytotoxicity. This means that the polymers would be of limited utility in applications where toxicity is a primary concern.

Liposome Dye Leakage

Because the putative antimicrobial mechanisms of many polymers involve disruption of biomembranes, we probed the ability of the polymers in this study to induce leakage from phospholipid vesicles. The cytoplasmic membrane of *E. coli* is rich in phosphatidylethanolamine (PE) and anionic phosphatidylglycerol (PG) lipids, which are present in a roughly 4:1 ratio.¹⁰¹ The lipids found in the cell membrane of *S. aureus* are mainly PG, phosphatidyl-lysyl-glycerol (Lysyl-PG), and cardiolipin (CL) in roughly a 12:7:1 ratio, according to recent studies.^{157, 158} Lysyl-PG carries a net positive charge of +1 while cardiolipin, a dimer of PG lipids, bears a net negative charge of -2. The outer leaflet of human red blood cell membranes contain Zwitterionic phosphatidylcholine (PC) lipids as the major component, while the anionic lipid phosphatidylserine is sequestered almost entirely in the inner leaflet.¹⁰⁰

In order to mimic the phospholipid composition of *E. coli*, *S. aureus*, and human red blood cell membranes, we prepared liposomes consisting of POPE/POPG (4:1), DOPG/Lysyl-DOPG/CL (12:7:1), and POPC. We then assessed the extent to which the copolymers in this study induce leakage of an entrapped dye from the model vesicles. The amount of dye leakage induced by the copolymers at a fixed concentration (1 μ M) depended on f_{alkyl} , the length of the alkyl groups, and the chemical structure of the lipids (Figure IV-9).

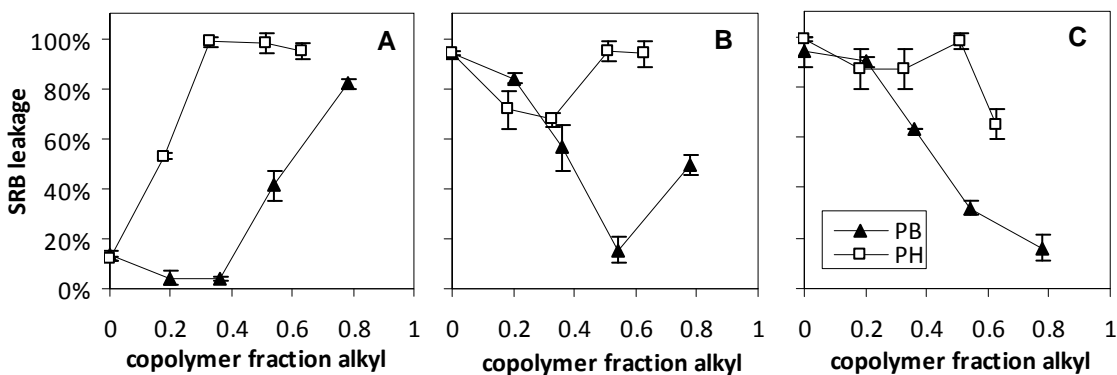


Figure IV-9. Sulforhodamine B (SRB) leakage from liposomes induced by the copolymers as a function of lipid composition. Effect of f_{alkyl} on the amount of SRB leaked from vesicles composed of (A) POPC, (B) POPE/POPG, and (C) DOPG/Lysyl-DOPG/CL at a fixed polymer concentration of 1 μ M. The legend in panel C applies to the entire figure.

In general, the ability of polymers to disrupt vesicles of POPC increased with increasing f_{alkyl} as well as increasing length of the alkyl side chains (Figure IV-9A). In the PB series, polymers with $f_{\text{alkyl}} = 0.00$ to 0.36 induced relatively little dye efflux from the POPC liposomes. PB₅₄ caused modest dye leakage and only PB₇₈ induced nearly complete lysis of the vesicles. The polymers in the PH series showed much more potent ability to permeabilize membranes: PH₁₈ induced modest SRB leakage, while PH₃₃, PH₅₁, and PH₆₃ all induced nearly complete leakage at a concentration of 1 μ M. These results show that increasing the hydrophobicity of the polymers, either by increasing f_{alkyl} or the alkyl chain length, enhances the ability of the polymers to disrupt Zwitterionic vesicles. Interestingly, these data follow the same general trends as do the hemolytic activities. The polymers which showed potent hemolytic activity are also highly membrane-lytic (Figure IV-9).

It was reported that the lytic activity of antimicrobial peptides against PC vesicles correlate with their hemolytic activity.³⁹ In the case of polymers and peptides, increasing hydrophobic content monotonically increases the hemolytic activity.^{30, 75, 76}

The copolymers in this study displayed the ability to disrupt vesicles of POPE/POPG (Figure IV-9B). In the PB series, the amount of leakage at a polymer concentration of 1 μ M decreased from nearly 100% to less than 20% as f_{alkyl} was increased from 0.00 to 0.54. Further increasing f_{alkyl} to 0.78 caused an increase in the amount of leakage. In the PH series, increasing f_{alkyl} from 0.00 to 0.33 caused a decrease in leakage amount from nearly 100% to roughly 70%, but further increasing f_{alkyl} to 0.51 and 0.63 caused the leakage amount to increase back up to nearly 100% again. The polymer-induced leakage from vesicles of POPE/POPG, which mimic the phospholipid composition of the cytoplasmic membrane in *E. coli* cells, went through local minima with increasing f_{alkyl} . These local minima mirror the non-monotonic trends in activity against *E. coli*, which likewise went through minima with increasing f_{alkyl} . Hence, it is plausible that disruption of the cytoplasmic membrane in bacterial cells plays a crucial role in the observed antimicrobial activity of the polymers.

The copolymers in this study also caused leakage of the SRB dye from vesicles of PG/Lysyl-PG/CL, a simplified model for the *S. aureus* cell membrane (Figure IV-9C). Increasing f_{alkyl} causes a loss of membrane lytic activity in both the PB and PH series. In the PB series, increasing f_{alkyl} from 0 to 0.78 caused the leakage amount to decrease from 100% to less than 20%. These polymers showed activity against *S. aureus* which also declined with increasing f_{alkyl} (Figure IV-3B).

In order to examine the membrane disruption process in greater detail, we studied the kinetics of dye leakage from the model vesicles induced by representative polymers in this study (Figure IV-10).

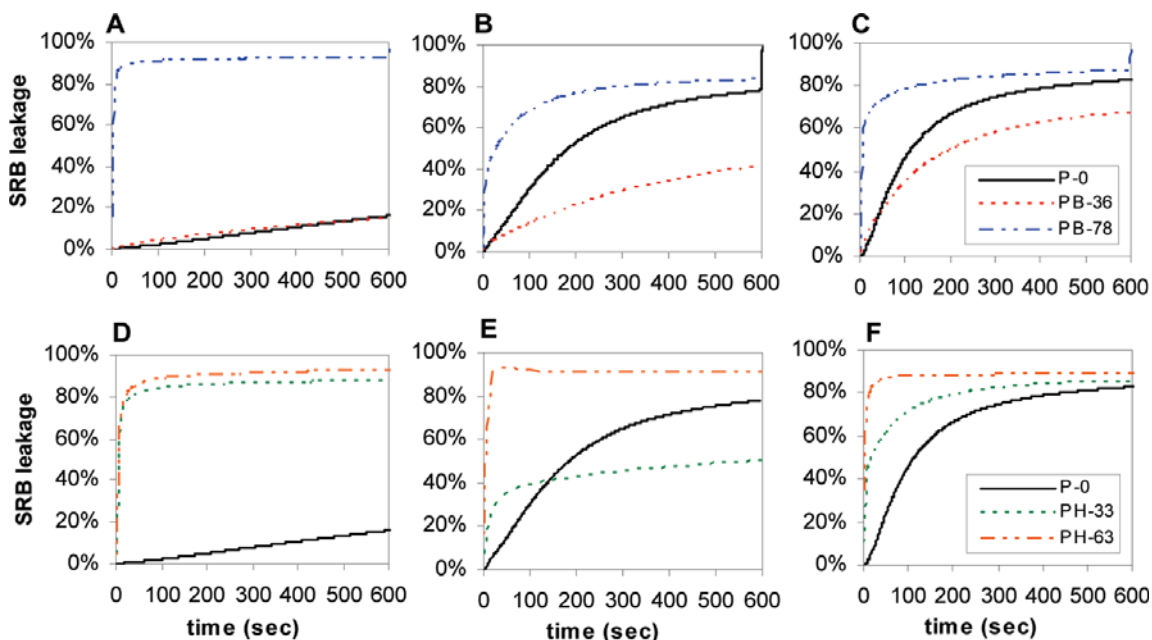


Figure IV-10. Kinetics of sulforhodamine B (SRB) efflux from liposomes. Large unilamellar vesicles composed of (A,D) POPC, (B,E) POPE/POPG, and (C,F) DOPG/Lysyl-DOPG/CL induced by representative polymers. The polymer concentration was $2 \mu\text{M}$ and the lipid concentration was $10 \mu\text{M}$ in all cases. The legend in panel C applies also to A and B, while the legend in panel F applies also to D and E.

From the POPC vesicles, P_0 induced less than 20% dye leakage after ten minutes. In contrast, the more hydrophobic compounds PB_{78} , PH_{33} , and PH_{63} induced rapid dye leakage, exceeding 80% within 30 seconds. From POPE/POPG vesicles, the homopolymer P_0 and the copolymers PB_{78} and PH_{63} each induced roughly 80-90% total leakage after the ten minute time course. Although the total amount of leakage induced by these polymers was comparable, the leakage kinetics are different. While the hydrophobic copolymer PH_{63} induced rapid leakage, nearly complete within 30 seconds, the polycation P_0 caused a comparatively much more gradual increase in fluorescence intensity. The polymer PH_{33} , which is intermediate in terms of hydrophobicity, caused rapid leakage up to $\sim 30\%$, followed by a more gradual leakage curve.

The kinetics of dye leakage from vesicles composed of DOPG/Lysyl-DOPG/CL also demonstrated a marked dependence on f_{alkyl} and the length of the alkyl chains. As in the case of POPE/POPG, the homopolymer P_0 induced nearly complete lysis of the DOPG/Lysyl-DOPG/CL vesicles by a gradual leakage process. On the other hand, the hydrophobic copolymers PB_{78} and PH_{63} induced rapid dye leakage, exceeding 70 and 80% leakage within 30 seconds, respectively. The polymer PH_{33} , which is intermediate

in hydrophobicity, caused rapid leakage up to ~ 45%, followed by a more gradual leakage process.

Apparently, the hydrophobic groups of the polymer exert leakage behavior that is characterized by the rapid dye release process, while the cationic groups give rise to a slower leakage. When anionic lipids are present in the membranes, the cationic polymers have an electrostatic attraction to the vesicles, leading to the observed lytic event. This observation suggests that the copolymer charge facilitates the membrane permeabilization, which may in turn impact the observed antimicrobial activity. Based on the ability of polymers to induce dye leakage from liposomes shown in figure IV-9, the copolymers in this study possibly exert their antimicrobial effect by a mechanism that involves membrane disruption, causing inhibition of cell growth or cell death.

The literature is replete with hypotheses regarding the mechanism of antimicrobial action employed by polymers and peptides: it is well-appreciated that polymers and peptides containing hydrophobic side chains possess the ability to disrupt lipid bilayers^{26, 33, 89} and may exert their antimicrobial effects by forming pores¹²⁶ or other permeable defects in the cytoplasmic membrane.³⁴ Bacteria may adsorb to cationic polymer surfaces, releasing divalent metal ions that are essential to outer membrane integrity.⁹² Polycations such as poly-L-lysine induce disruption of lipid bilayers by a mechanism involving phase segregation of anionic phospholipids in model membranes¹⁵⁹ and this effect has been implicated in the antimicrobial action of peptides¹⁶⁰ and amphiphilic random copolymers as well.¹²⁸ *In vitro* cytotoxicity of cationic polymers studied in the field on non-viral gene delivery is known to depend on their cationic charge density.¹⁵³ One or a combination of these proposed mechanisms may explain the activity of the copolymers in this study. Elucidating the details of the antimicrobial mechanism, however, would require further biophysical studies in the future.

The activity of the copolymers in this study against *E. coli*, *S. aureus*, human red blood cells, and human epithelial cells were shown to depend on the type of alkyl groups and the f_{alkyl} value. Activity against bacteria decreased as f_{alkyl} increased up to a certain critical value, beyond which activity was enhanced with increasing f_{alkyl} . Membrane damage to human red blood cells increased with increasing f_{alkyl} monotonically, while cytotoxicity to HEp-2 cells decreased with increasing f_{alkyl} . Dye leakage from model

vesicles provided evidence that the mechanism of antimicrobial activity employed by the copolymers in this study involves disruption of biomembranes. Leakage from POPC liposomes followed trends in hemolysis, while leakage from POPE/POPG and DOPG/Lysyl-DOPG/CL liposomes, which are mimics of cell membranes found in *E. coli* and *S. aureus*, followed trends similar to their MIC values against those microorganisms.

Conclusions

We quantified the structural characteristics that modulate the antimicrobial, hemolytic, and cytotoxic properties of cationic, amphiphilic random copolymers of methacrylamides. The results demonstrated that the polarity of the polymerizable units has a profound impact on the hydrophobic/hydrophilic balance. Relative to polymethacrylates, which have less polar ester groups, the polymethacrylamides required much higher percentages of hydrophobic comonomer in order to induce hemolysis. In agreement with other reports,¹⁰⁷ we found that the hydrophobicity of the polymers was the main determinant of hemolytic activity. The cationic homopolymer of 3-aminopropylmethacrylamide P₀ showed potent antimicrobial activity against *E. coli* and *S. aureus* but did not induce appreciable hemolysis. As we hypothesized, the more polar methacrylamide design platform can be exploited to obtain non-hemolytic antimicrobial polymers ($HC_{50}/MIC > 640$). However, the polycation showed very potent cytotoxicity against human epithelial cells ($IC_{50}/MIC < 1.3$), which limits its pharmaceutical potential. High cationic charge density is likely responsible for this observed cytotoxicity, based reports of other polycations such as polylysine and polyethyleneimines which showed increasing toxicity with increasing charge.¹⁵³ The polymers in this study are almost 100% ionized in pH 7.4, which contrasts with previously studied polymethacrylates (Figure IV-1), which were shown to be only ~ 72% cationic in that condition.¹⁴²

Increasing the mole fraction of hexyl- or butylmethacrylamide repeat units in the random copolymers led to anomalous local minima in the antimicrobial activity trends. Based on dye leakage experiments using liposomes as model membranes, it seems that the cationic homopolymer and hydrophobic copolymers employ different mechanisms of membrane disruption. The polymers with more than 50% hexylmethacrylamide units showed very potent antimicrobial activity against *E. coli* and *S. aureus*, however, these

compounds were also highly hemolytic. This presented a dilemma in the design of biocompatible antimicrobial polymethacrylamides: dense cationic charge leads to cytotoxicity whereas excessive hydrophobicity leads to hemolysis. The cytotoxicity could possibly be tuned by choosing side chain groups with different pK_a values in order to control the cationic charge density. Also, incorporation of neutral hydrophilic groups in the side chains, as done previously with vinyl pyridine derivatives,^{82, 161, 162} may enhance biocompatibility in this system.

Because these copolymers are chemically stable and contain pendant amine groups, we envision that they could be used for conjugation with a wide variety of other functional groups. In the future, the polymethacrylamides presented in this work could be used as surface coatings that kill bacteria on contact and can be further functionalized with other moieties that resist biofouling or bacterial accumulation on surfaces.

CHAPTER V

Role of Cationic Side Chain Spacer Groups in Activity and Mechanism of Antimicrobial Action by Amphiphilic Copolymers

Introduction

In the design of antimicrobial polymers, the diversity of structures available in polymer science allows a wide variety of potential design choices. Tuning the hydrophobic/hydrophilic character of the polymers, known as “amphiphilic balance,” has been the most widely applied in the design of antimicrobial polymers.^{73, 78, 81, 107} Additional studies have established the roles played by cationic charge density,¹⁶³ molecular weight,⁷⁵ geometrical arrangement of cationic charges and hydrophobic groups,⁹⁶ and the structure of cationic groups.¹⁴² Still, a comprehensive design rationale remains elusive, with many potential activity determinants as yet unexplored. Hence, it is necessary to judiciously explore the design parameters in this field, toward a more nuanced understanding of the activity determinants and the ultimate goal of utilizing polymers in pharmaceutical applications.

One of the key parameters which remain to be systematically studied is the identity of the groups which connect the primary amines to the polymer backbone, or the “spacer groups”. Beyond adjusting the ratio of hydrophilic to hydrophobic groups in the copolymers, the spacer groups are expected to provide more precise control of the global amphiphilic balance as well as control of the binding to and permeabilization of cell membranes. Because the amphiphilic copolymers likely undergo conformational changes upon binding to the interfacial membrane environment, with cationic groups projected into the aqueous phase and hydrophobic groups inserted into the non-polar membrane region,⁷⁴ we expect that there would be an optimal spacer length for effective polymer-membrane interactions (Figure V-1). A similar concept has been utilized for tuning the activity of cell-penetrating peptoids, which showed improved cell uptake as the spacer

lengths were increased from 3 to 6 carbon alkyl linkers.¹³⁷ Hence, it would be a significant advance in the field of antimicrobial polymers to delineate the role of the cationic side chain spacer groups. In the previous Chapters, we discussed the role of structural parameters such as cationic charges, polymer backbone, and hydrophobic percentage. Here, we examine the role of the geometrical arrangement of the charged groups, which are expected to influence their conformations in the membrane.

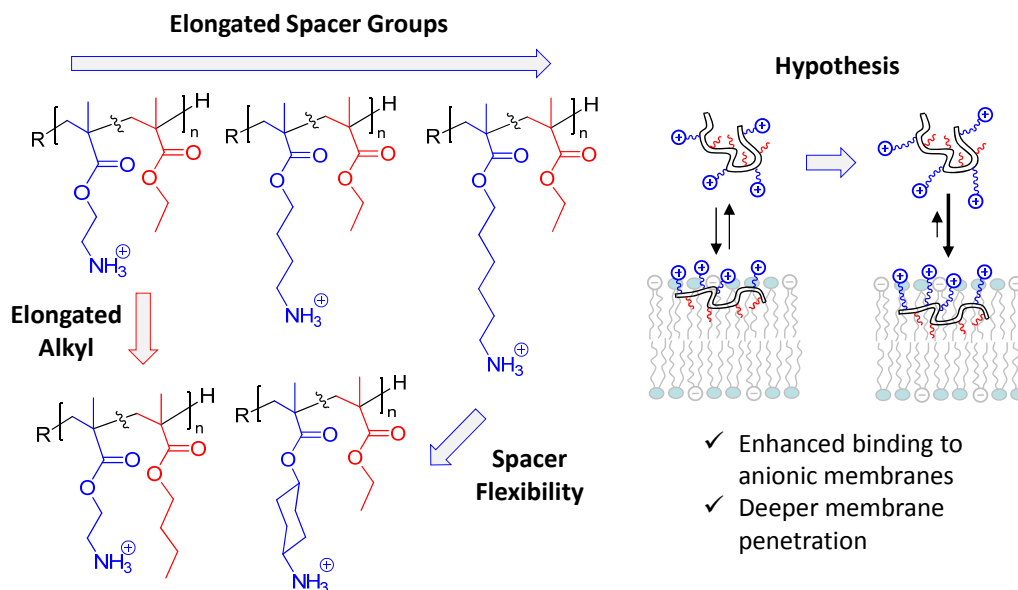


Figure V-1. Spacer arm design strategy and hypothesis: the copolymers may adopt facially amphiphilic conformations upon membrane binding, wherein the pendant amino groups (blue) interact with lipid headgroups and the non-polar side chains (red) partition into the hydrophobic membrane environment. Extension of the “spacer arms” is expected to facilitate such segregation.

In this Chapter, we demonstrate the role played by the spacer groups in terms of antimicrobial and hemolytic activities of synthetic polymethacrylate derivatives. Polymers in which primary amine groups are attached to a non-polar methacrylate backbone via alkyl linkages of various lengths (ethylene, butylene, hexylene, and cyclohexylene) are systematically assessed for antimicrobial and hemolytic activity. We further investigated the mechanism of antimicrobial action to assess whether precise control of structures can effectively mimic the antimicrobial mechanism exerted by peptides, in contrast to a surfactant-like mode of action, in which the lipids are completely disordered or solubilized. We employ fluorescence imaging and flow cytometry analyses of FITC-labeled polymers, osmoprotection assays using PEGs, as

well as an enzyme activity assay to test permeabilization of the inner and outer membranes of *E. coli*. Molecular dynamics simulation of the polymer binding to anionic and zwitterionic lipid bilayers establishes the role of spacer groups in the membrane association event. Combined, the results will examine the membrane disruption antimicrobial mechanism, and the extent to which the spacer arm adjustment strategy modulates the polymer-induced membrane disruption event.

Polymer Synthesis and Characterization

Random copolymers of amino-functionalized methacrylate derivatives with various spacer arms and ethylmethacrylate (EMA) or butylmethacrylate (BMA) were prepared by free radical polymerization using a thiol chain transfer agent to control molecular weight (Figure V-2) by a modification of the previously described method (Appendix A).⁷⁵

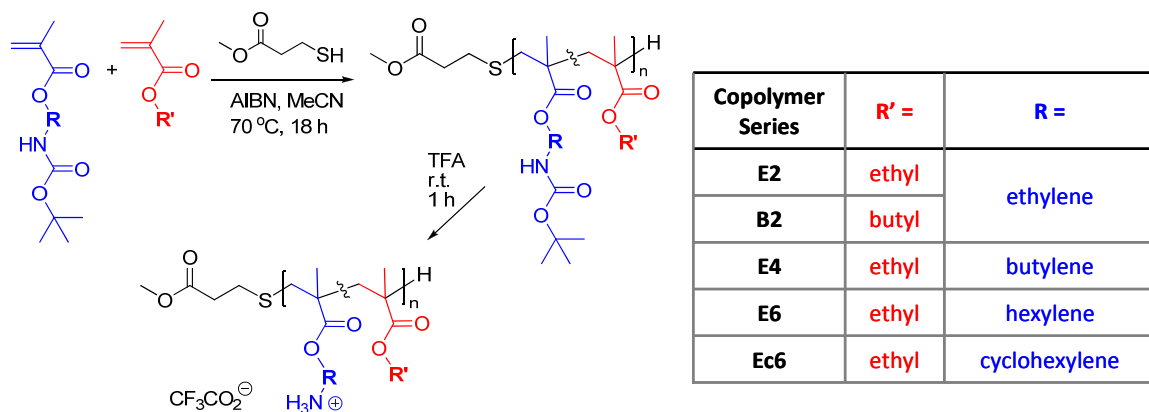


Figure V-2. Generalized synthetic route and chemical structures of the amphiphilic polymethacrylate derivatives with different side chain groups connecting the amines to the polymer backbone, referred to as the cationic “spacer arm groups” (E2, E4, Ec6, E6), and a homologue with elongated hydrophobic alkyl groups (B2). AIBN: Azobisisobutyronitrile, MMP: methyl mercaptopropionate, TFA: trifluoroacetic acid

For each copolymer series, the fraction of hydrophobic repeat units in the copolymer, f_{HB} , was varied in the range of 0.0 to 0.6. The average degrees of polymerization (DP) were constrained to the range of 12-15 (Table V-1), because low MW polymers and peptides in this range have been previously shown to give potent antimicrobial activity with minimal hemolysis, whereas increasing MW generally aggravates hemolysis.¹⁰⁷ The f_{HB} values of each of the polymers are indicated by the subscript for each sample; for example, the copolymer in the E4 series containing 29 mol % EMA units is referred to as E4₂₉. Each series of copolymers is based on the same

structural motif, except that the moieties which connect the cationic ammonium groups to the polymer backbone, or the “spacer arm groups”, were varied from ethylene (E2), butylene (E4), hexylene (E6), to cyclohexylene (Ec6).

Table V-1. Characterization of methacrylate random copolymers containing different cationic side chain spacer groups. Biological activity data for the library of copolymers in this study, with magainin-2 and melittin as standards for comparison.

	f_{HB}^a	DP ^a	M_n^a (kDa)	MIC ^b (μM)		HC ₅₀ ^c (μM)	HC ₅₀ /MIC		Comments <i>E. coli</i>
				<i>E. coli</i>	<i>S. aureus</i>		<i>E. coli</i>	<i>S. aureus</i>	
Homopolymers ($f_{HB} = 0$)									
E2₀	0	12.3	3.1	645	33.6	> 630	> 1.0	> 19.2	Weak
E4₀	0	10.6	3.0	668	83.5	> 668	> 1.0	> 8.0	Weak
E6₀	0	11.0	3.4	2.3	2.3	0.8	0.3	0.3	Biocidal
Ec6₀	0	10.1	3.1	428	60.2	> 641	> 1.5	> 9.6	Weak
B2₀	0	15.3	3.9	260	16	> 519	> 2	> 32	Weak
Copolymers ($f_{HB} = 0.26-0.29$)									
E2₂₈	0.28	13.5	2.9	85.8	42.9	> 686	> 8.0	> 16.0	Moderate
E4₂₉	0.29	12.5	2.9	7.1	21.3	444	62.7	20.9	Selective
E6₂₇	0.27	12.6	3.3	2.4	2.4	0.9	0.4	0.4	Biocidal
Ec6₂₈	0.28	11.5	2.9	7.1	10.7	292	41.2	27.4	Selective
B2₂₆	0.26	13.6	3.1	5.1	5.1	11.0	2.2	2.2	Biocidal
Copolymers ($f_{HB} = 0.40-46$)									
E2₄₅	0.45	16.2	3.1	4.2	13.4	24.5	5.8	1.8	Biocidal
E4₄₆	0.46	17.6	3.6	2.9	5.8	14.7	5.1	2.5	Biocidal
E6₄₀	0.40	14.5	3.4	1.9	2.3	0.7	0.4	0.2	Biocidal
Ec6₄₄	0.44	12.7	2.9	2.7	7.3	10.0	3.7	1.4	Biocidal
B2₄₀	0.40	19.6	4.1	3.8	3.8	2.1	0.6	0.6	Biocidal
Peptides									
magainin-2	--	2.5		51	> 100	> 100	> 2	--	Selective
melittin	--	2.8		4.4	2.0	0.6	0.1	0.3	Biocidal

a. The mole fraction of hydrophobic repeat units EMA or BMA (f_{HB}), the average degree of polymerization (DP), and the number-average molecular weight (M_n) were obtained by end-group analysis of the ¹H NMR spectra and MALDI-TOF-MS (Appendix B)

b. Minimum inhibitory concentration (MIC), the concentration of polymer which completely inhibited growth of the bacteria after incubation in MH broth for 18 hr at 37 °C

c. Polymer concentration which induced 50% leakage of hemoglobin from human red blood cells (HC₅₀) relative to the positive control surfactant Triton-X-100

Comparison of the activities of E2, E4, and E6 will elucidate the effect of spacer arm elongation. Ec6 contains spacer groups are less flexible due to the cyclic structure, which constrain their conformation, compared to corresponding linear alkyl side chains.

The conventional approach of tuning amphiphilic balance involves adjusting the comonomer ratios and length of hydrophobic alkyl groups. In contrast, this Chapter will elucidate the role of the geometrical arrangement of cationic and alkyl groups. In the comparison, E4 and B2 each have the same number of additional carbon atoms relative to E2, but the connectivity has been altered.

Structure-Activity Relationships

The antimicrobial activities of the polymers were quantified as the concentrations which completely inhibited bacterial growth (MIC) and toxicity to human red blood cells was quantified as the polymer concentration which induces 50% hemoglobin release (HC_{50}). The copolymers in this study exhibited inhibitory effects against Gram-negative *E. coli* and Gram-positive *S. aureus*, and hemolysis of human red blood cells to varying extents, which depended on their cationic side chain spacer arm groups and their f_{HB} values (Table V-1 and Figure V-3).

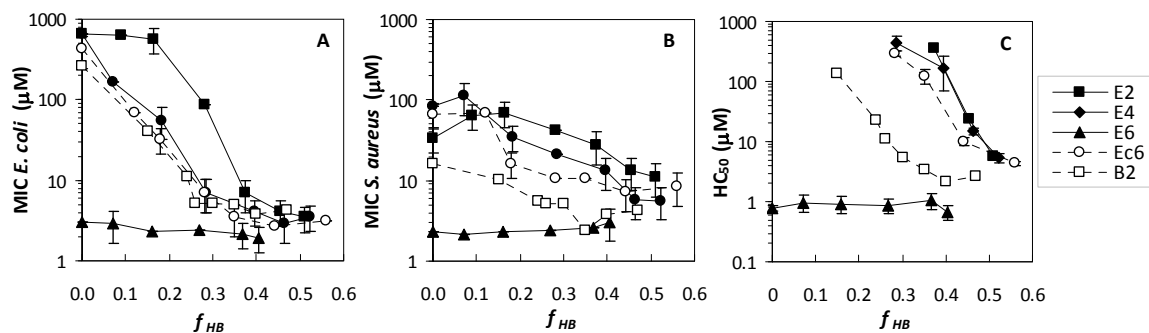


Figure V-3. Optimization of the antimicrobial efficacy in methacrylate copolymers. Minimum inhibitory concentrations, MIC, of the polymethacrylates against (A) *E. coli* and (B) *S. aureus* and (C) hemolytic concentrations, HC_{50} .

Against *E. coli*, the cationic homopolymers E2₀ and E4₀ ($f_{HB} = 0$, Table V-1), showed weak antimicrobial activity ($MIC > 600 \mu\text{M}$) and non-hemolytic activity ($HC_{50} > 600 \mu\text{M}$), likely due to their hydrophilic nature, which precludes partitioning into non-polar membranes.^{107, 142} Further elongation of the spacer arms to hexylene E6₀ caused a dramatic enhancement of antimicrobial activity ($MIC = 2.3 \mu\text{M}$), with concomitant hemolytic toxicity ($HC_{50} = 0.8 \mu\text{M}$), which represents potency similar to that of melittin ($HC_{50} = 0.6 \mu\text{M}$).

The spacer groups profoundly impacted the antimicrobial activity of random copolymers containing various fractions of hydrophobic moieties. In general, the copolymers displayed lower MIC values ($\text{MIC} < 10 \mu\text{M}$, $f_{\text{HB}} > 0.4$) than corresponding homopolymers (Figure V-3A), showing that the copolymers are more potent antimicrobials. The MIC values against *E. coli* decreased with increasing f_{HB} . All the copolymer series reach a plateau in $\text{MIC} < 10 \mu\text{M}$ when $f_{\text{HB}} > 0.4$. Hence, the hydrophobicity of side chains can be considered a chief driving force of activity, as previously shown.¹⁰⁷ In addition to the effect of increasing f_{HB} , the spacer arm elongation greatly enhanced the activity of the copolymers. For example, E4₂₉ ($\text{MIC} = 7.1 \mu\text{M}$) was about 12-fold more active than E2₂₈ ($\text{MIC} = 86 \mu\text{M}$) and the natural peptide magain-2 ($\text{MIC} = 51 \mu\text{M}$), which shows that extension of the spacer arm groups enhances the antimicrobial activity (Table V-1).

The spacer groups also impacted the toxicity to human cells (Figure V-3C). The HC_{50} values generally decreased with increasing f_{HB} in agreement with previous studies.¹⁰⁷ The polymer E4₂₉ showed potent antimicrobial activity but was relatively non-hemolytic ($\text{HC}_{50} = 444 \mu\text{M}$), giving a selectivity index ($\text{HC}_{50}/\text{MIC}$) of 62.7, the best example in this study (Table V-1). In the E2 series, the best example was E2₃₇, which showed potent antimicrobial activity ($\text{MIC} = 7 \mu\text{M}$) and relatively weak hemolytic activity ($\text{HC}_{50} = 363 \mu\text{M}$), giving a selectivity index of 52. This implies that the copolymers with moderate spacer arm length (ethylene, butylene) can be tuned to selectively inhibit *E. coli* without lysis of human red blood cells. Interestingly, the E4 series yielded improved selectivity relative to the best example in the E2 series, demonstrating that the spacer arm parameter is an essential determinant for selectivity optimization. Given that most antimicrobial polymers in the literature display short cationic spacer groups, we expect these findings to facilitate activity improvements across a wide variety of structures in the future. The E6₂₇ copolymer maintained excellent antimicrobial potency ($\text{MIC} = 2.4 \mu\text{M}$) but was also strongly hemolytic ($\text{HC}_{50} = 0.9 \mu\text{M}$), similar to the biocidal bee venom peptide melittin ($\text{MIC} = 4.4$ and $\text{HC}_{50} = 0.6$). The relative ranking of antimicrobial and hemolytic activity in the copolymers was $\text{E6}_{27} > \text{E4}_{29} > \text{E2}_{28}$, which demonstrates the activity enhancement by increasing the length of the spacer arms, in this f_{HB} range. When the hydrophobic comonomer ratio was increased

excessively ($f_{HB} = 0.44-0.47$), the MIC values against *E. coli* were uniformly in the range of 2-4 μM , regardless of the spacer arm groups. The hemolytic activities of these polymers were also aggravated by this excessive increase in hydrophobic content ($\text{HC}_{50} = 0.7-25\mu\text{M}$).

The E4 and B2 polymers have the same number of additional carbon atoms relative to E2, but the additional atoms reside on different chemical centers: on the cationic side chains in E4 as opposed to the hydrophobic side chains in B2. Interestingly, activities against *E. coli* for these polymers are comparable across the entire range of f_{HB} studied. However, utilizing butyl groups generated hemolytic copolymers such as B2₂₆ ($\text{HC}_{50} = 11 \mu\text{M}$), while the E4₂₉ copolymer was much less hemolytic ($\text{HC}_{50} = 444 \mu\text{M}$). In addition, the Ec6 copolymer was less active against *E. coli* relative to E6, but the activity was similar to that of the E4 copolymers. While E6 and Ec6 contain the same number of additional carbon atoms in their spacer groups relative to E2, the cyclic homologue is apparently a less potent antimicrobial. This indicates that the properties of fine structures (cyclic vs. linear alkyl) profoundly impact the observed activities. Because the cyclic spacer arms are fixed in an extended conformation, the insertion of polymers into the hydrophobic region of the membrane may be inhibited relative to the polymers bearing flexible, linear amino hexylene moieties.

Against *S. aureus*, the MIC values of the E2 series were in the range of 10-70 μM , with the highest activity observed for the copolymers with high f_{HB} values, indicating that hydrophobicity affects the antimicrobial ability of these polymers (Figure V-3B). For the copolymers with moderate hydrophobic content ($f_{HB} = 0.27-0.30$), the activity of the polymers increased with increasing spacer group size (activity ranking: E6₂₇ > E4₂₉ > E2₂₈). Among these polymers, the best example was Ec6₁₈, which showed an MIC of 16.3 μM but was non-hemolytic up to 628 μM ($\text{HC}_{50}/\text{MIC} > 38$). These results demonstrate that the activity against Gram-positive *E. coli* as well as Gram-negative *S. aureus* can be controlled by tuning the spacer arm groups in the cationic side chains, in addition to the conventional approach of tuning amphiphilic balance. This further supports our hypothesis that the spacer arm optimization strategy is an effective method to obtain non-hemolytic antimicrobial polymers.

In random copolymers reported so far in the literature, optimization of activity was achieved by tuning the identity and percentage of hydrophobic groups in the side chains of antimicrobial polymethacrylates. In those studies, the spacer arms were not altered. Recently, Sambhy et al showed that the geometrical arrangement of cationic and hydrophobic groups on the same chemical center facilitated the optimization of non-hemolytic antimicrobial poly(vinyl pyridine-co-methacrylate)s.⁹⁶ The results obtained here also confirm that spatial arrangement of the alkyl substituent, in the spacer arms or in the hydrophobic side chains, plays an important role in the selectivity of polymers against different cell types.

Synthesis of Fluorophore-Labeled Polymers

To examine the localization of polymers on live bacterial cells, we adopted a slightly modified polymerization procedure (Figure V-4) which enables reaction of the polymer end terminus to a functionalized dye, fluorescein isothiocyanate (FITC).

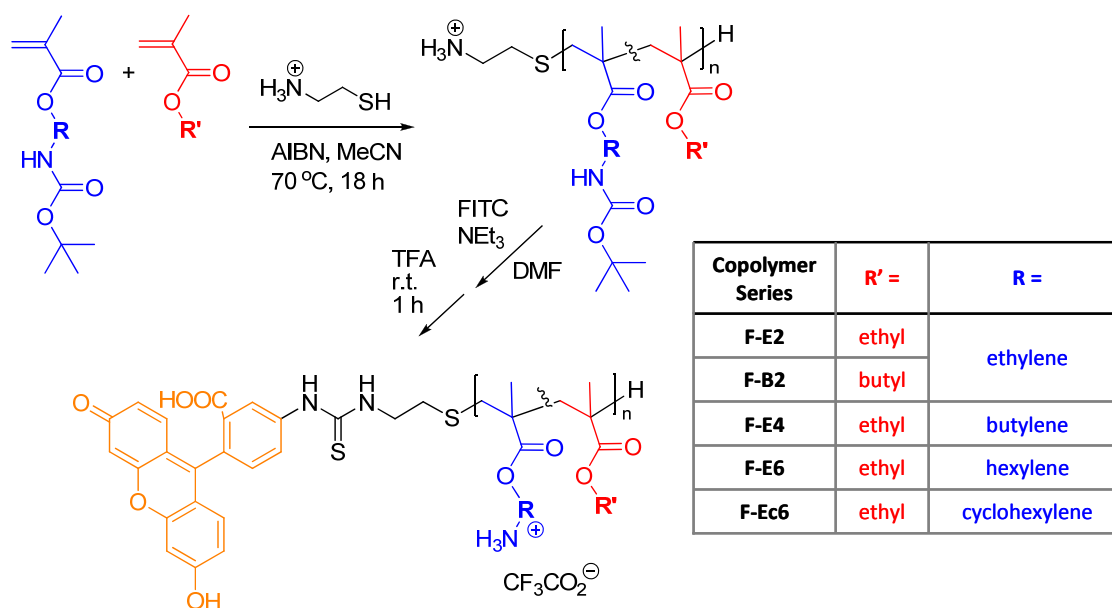


Figure V-4. Generalized synthetic route and chemical structures of the amphiphilic polymethacrylate derivatives with different spacer arms and a fluorophore in the polymer end group. After polymerization, the end groups are coupled to FITC for imaging and flow cytometry analysis. AIBN: Azobisisobutyronitrile, MMP: methyl mercaptopropionate, FITC: fluorescein isothiocyanate, TFA: trifluoroacetic acid

Dye-labeled polymers with various cationic side chain spacer groups were readily obtained and purified by this method, confirmed by absorbance and emission spectra, ^1H NMR spectroscopy and MALDI-TOF-MS. Details of the synthesis and characterization methods are given in Appendices A and B, respectfully.

Fluorescence Imaging of Bacteria Cells

While structure-activity relationships aid in identifying the optimal structures of polymers for potent activity, it is also highly desirable to understand the mechanism(s) by which these polymers exert their antimicrobial effects, toward increasingly nuanced design rationale. To that end, we first examined the localization of representative FITC-labeled copolymers on live *E. coli* cells. The FITC-labeled copolymers stained *E. coli*, indicating that polymers effectively bind to the cells (Figure V-6A). Interestingly, two distinct populations are evident in the micrographs: a fraction of the *E. coli* cells incubated with FITC-labeled E2₃₂ polymer (F-E2₃₂; MIC = 12.5 μM) showed a green fluorescent pattern concentrated along the rod-shaped cell perimeter, whereas the remainder of cells showed bright green fluorescence throughout the entire cell area. This indicates that polymer accumulated on the membranes of the cells with a green fluorescent perimeter, whereas polymer was internalized by the remaining cells. Many of the cells with F-E2₃₂ internalized showed brighter green fluorescence near the ends of the rod shaped cells, indicating that polar localization occurs within the cytoplasm.

To assess the membrane-damage induced by the polymers in this study, the nucleic acid stain propidium iodide (PI, structure in Figure V-5) was added to the *E. coli* suspension after incubation with polymers (Figure V-6B). PI is unable to translocate intact cell membranes but it can penetrate readily into cells with damaged membranes, wherein its fluorescence intensity is greatly enhanced by DNA intercalation. The cells with green fluorescence also showed bright red PI fluorescence throughout the cytoplasm in nearly every case. On the other hand, all of the cells with only membrane-bound polymers lacked noticeable PI fluorescence (Figure V-6C). Similar results were obtained with other FITC-labeled copolymers, containing various spacer groups (see Appendix B, Figures B-16 to B-25).

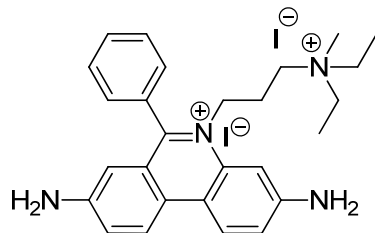


Figure V-5. Chemical structure of propidium iodide (PI), the nucleic acid stain used to detect membrane damage or bacterial cell death

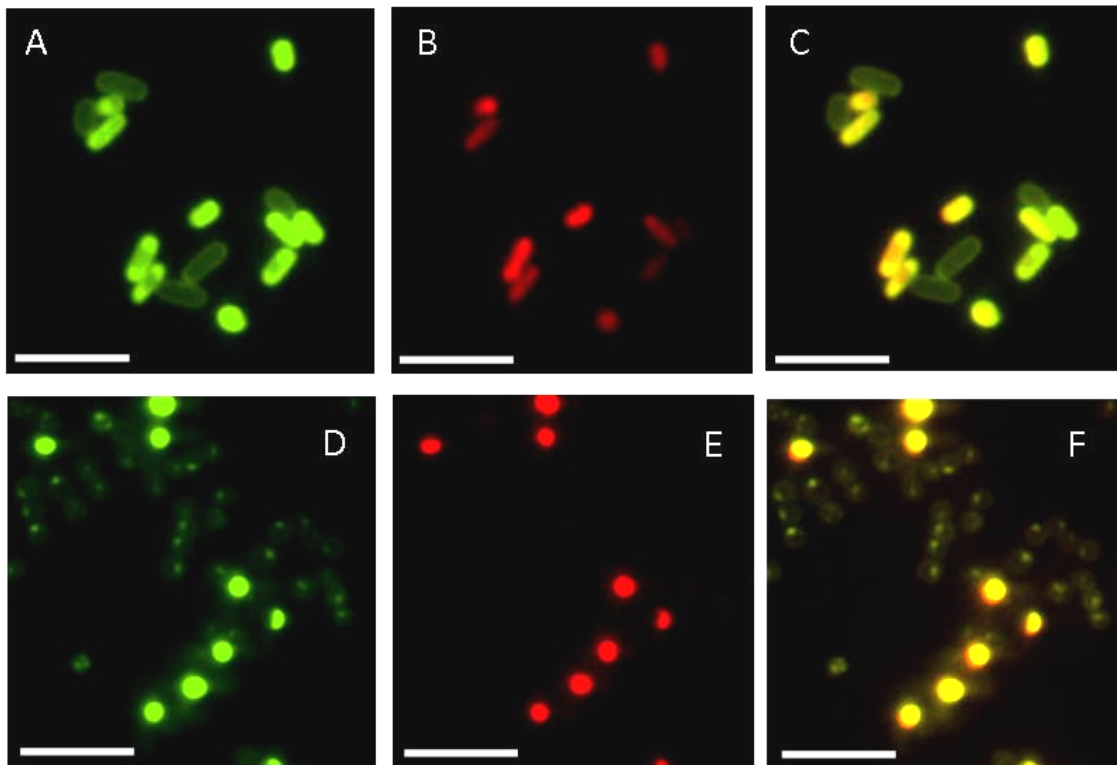


Figure V-6. Fluorescence microscopy images of fluorophore-labeled polymer incubated with live bacteria cells. (A,B,C) *E. coli* and (D,E,F) *S. aureus* incubated for 45 min with 10 μM F-E2₃₂ and an additional 15 min with 1.5 μM propidium iodide. The fluorescent signal from (A,D) the FITC-labeled polymers is shown in green, (B,E) the propidium iodide in red, and (C,F) both color images superimposed. The white scale bar represents 5 μm in each figure.

Each of the FITC-labeled polymers in this study also effectively stained *S. aureus* (Figure V-6,D-F). The polymers accumulated on the cell membranes with polar localization, and in a fraction of the cases, the FITC-polymers penetrated the *S. aureus* cells. The cells that internalized the polymer also showed uptake of the PI stain, implying membrane disruption. These results are qualitatively the same as with *E. coli* cells, indicating that the cationic, amphiphilic copolymers permeabilize both Gram-positive and Gram-negative bacterial membranes. These results suggest that the

polymers initially bind to and accumulate on the bacterial cell envelope, followed by membrane damage with concomitant polymer internalization and PI uptake, which is likely to cause cell death. Because the cells stained with PI retained their characteristic shape, it would appear that the membrane-damaged cells are not entirely destroyed by complete cell lysis or solubilization.

Flow Cytometry Analysis

In addition to the qualitative fluorescence images, the effect of the spacer arms on the polymer-cell association was quantified by flow cytometry. Accumulation of polymer to *E. coli* cells was markedly increased by the elongation of the spacer arm groups although the association to *S. aureus* was relatively unaffected by the modifications (Figure V-7).

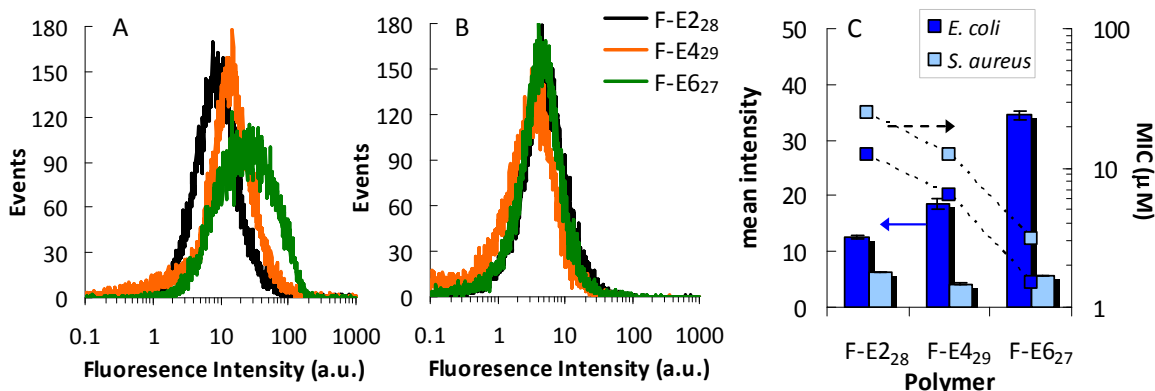


Figure V-7. Flow cytometry histograms of fluorophore-labeled polymer incubated with live bacteria cells (A) *E. coli* and (B) *S. aureus* and (C) the calculated mean intensity for each histogram and MIC values of the FITC-labeled polymers.

Accumulation of FITC-labeled polymers on *E. coli* cells was enhanced by 2.7 fold upon elongation of the spacer groups from ethylene to hexylene spacer groups (Figure V-7C). On the other hand, the enhancement of activity (MIC value) is about 8-fold. This suggests that the more potent antimicrobial activity expressed by copolymers with extended spacer arms may be due to facilitation of the polymer-*E. coli* binding as well as enhanced membrane disruption after binding. In the case of *S. aureus*, the histograms are mostly over-lapping for copolymers with each of the three spacer arm groups (Figure V-7B). Although elongation of the spacer groups led to an enhancement of the anti-*S.*

aureus activity in terms of MIC values by 8-fold (Figure V-7C), it would seem that this enhancement is not a result of improved binding. Rather, it would seem that the disruption mechanism of the polymers in the cell surfaces is responsible for the activity enhancement. Furthermore, the response of bacteria to bound polymer appear to depend on the bacterial strain, possibly due to differences in their cell membrane structures.

Two-dimensional flow cytometry analysis was also carried out with simultaneous detection of the FITC signal from the polymers as well as internalized PI stain. Plotting the fluorescence intensity at 675 nm (red PI signal) against the intensity at 525 nm (green FITC signal) on a color-coded topographical map reveals two distinct populations (Figure V-8).

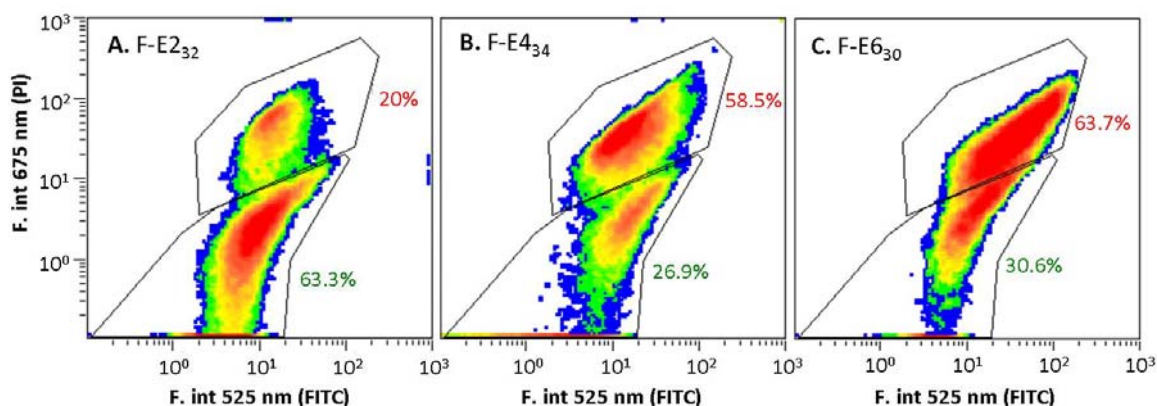


Figure V-8. Two-dimensional flow cytometry analysis showing the binding and membrane damage to *E. coli* cells exerted by polymers. The numbers of events are ranked, from highest to lowest, in the order of red, yellow, green, and blue.

The sub-population (in the upper region of the panels) of cells which exhibit strong green fluorescence intensity while showing relatively weak red fluorescence, indicates *E. coli* cells with FITC-polymer accumulated but little or no PI uptake. In contrast, the sub-population (in the lower region of the panels) which showed strong fluorescence in both colors, corresponds to the cells with both polymer and PI stain present. These results are in very good agreement with the fluorescence images, which qualitatively demonstrated the presence of two such sub-populations of *E. coli* cells. The cells with the same amount of bound polymer (intensity in horizontal axis) showed two different responses in terms of membrane disruption (intensity in vertical axis). Hence, the heterogeneous membrane disruption likely cannot be ascribed entirely to heterogeneous binding across the two sub-populations of *E. coli*; rather it might be due to

the cell-to-cell variation in the susceptibility to the polymers although it is unclear what cellular properties are responsible for the heterogeneous response of cells to the polymers. It also may be due to time dependence of cell lysis. We speculate that polymers accumulate on the cell membranes until a threshold concentration is surpassed, followed by stochastic membrane disruption. Directly observing the kinetics of binding and disruption using single cells will be helpful to further clarify this process in the future.

Interestingly, the proportion of *E. coli* cells in the PI-stained population increased with elongation of the spacer arms (Figure V-8). For F-E2₃₂, 20% of the cells were PI-stained, whereas for F-E4₃₄ and F-E6₃₀ 58.5% and 63.7% were PI-stained, respectively. This further highlights the enhancement of bacterial membrane disruption ability displayed by the copolymers with extended spacer arms. The improved ability to break membranes furthermore follows the same trend as the MIC values for these representative FITC-labeled polymers.

***E. coli* Membrane Permeabilization**

To quantify the outer and inner membrane permeabilization induced by the polymers, the passage of chromogenic enzyme substrates nitrocefin or ONPG across *E. coli* membranes were monitored.¹⁶⁴ These substrate molecules are membrane impermeable molecular analogues for the naturally occurring *E. coli* enzymes β -lactamase (localized in the periplasm) and β -galactosidase (localized in the cytoplasm), respectively. As membrane permeability is increased by exposure to the polymers, the substrates or their enzymes are able to diffuse between the external milieu and the periplasm or cytoplasm more easily, resulting in the production of colored products via the *E. coli* enzymes. Accordingly, this assay demonstrates the permeabilization of outer and inner membranes simultaneously.

For the *E. coli* membrane permeabilization experiments, we chose to study representative copolymers with $f_{HB} = 0.27-0.30$, E2₂₈, E4₂₉, and E6₂₇, because the effect of spacer arm groups on the MIC values is pronounced in this range (Figure V-3). These representative copolymers caused varying extents of permeabilization of *E. coli* outer and inner membranes, depending on the cationic side chain spacer arms (Figure V-9).

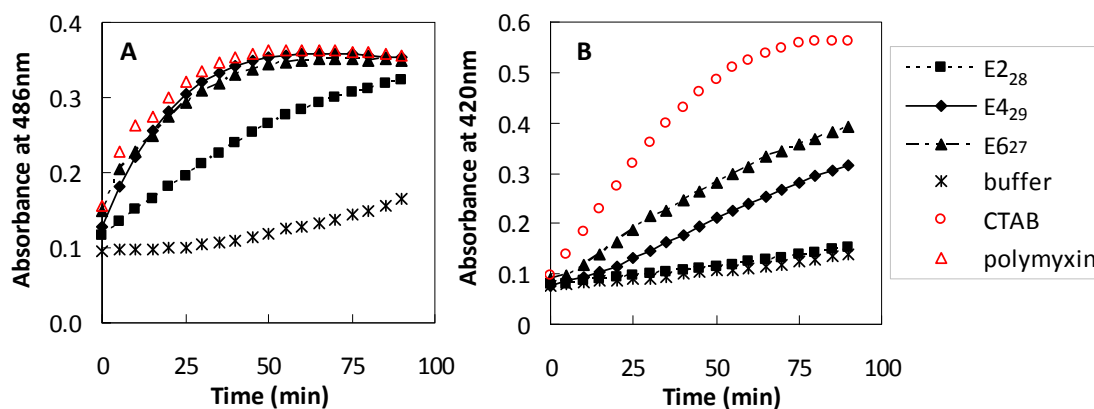


Figure V-9. Permeabilization of *E. coli* outer membrane (OM) and inner membrane (IM) induced by the polymers. Absorbances were measured at (A) 486 nm for the OM and (B) 420 nm for the IM. The concentrations of polymer and polymyxin 6.25 μM , CTAB was 86 μM . Experiments were performed in ambient conditions in buffer (25 mM phosphate, 150 mM NaCl, pH 7.0) on a 96 well microplate.

Since the enzyme reaction was monitored, the rate of increase in absorbance should reflect the amount of enzymes released from cells. The polymers displayed significant OM leakage in the concentration ranges from 3.13 to 100 μM . At a concentration of 6.25 μM , all of the copolymers caused an increase in the absorbance at 486 nm after 90 min incubation (Figure V-9A). This implies significantly increased permeability of *E. coli* outer membranes (OM). The copolymers E6₂₇ and E4₂₉ exhibited OM damage similar to the positive control peptide polymyxin B, which is known to disrupt OM integrity.¹⁶⁵ The polymer with the shortest spacer groups, E2₂₈, displayed a lower rate of formation of product corresponding to OM permeability, although comparable maximum absorbance was achieved after 90 min. This shows that the length of the spacer arm groups is an important determinant of the OM damage process.

The polymers E4₂₉ and E6₂₇ induced a slower rate of IM permeabilization in the concentration range from 6.25 to 100 μM relative to the positive control CTAB, a cationic surfactant known to disrupt bacterial membranes.¹⁶⁶ Although these compounds damaged the OM with the same rate, it appears that the IM damage requires additional challenge from the polymers. This may be due to the cell wall structure inhibiting the access of polymers to the cytoplasmic membrane. E2₂₈ does not significantly affect the integrity of the IM, compared to the negative control, even up to 100 μM . It has been reported that the *E. coli* cells may survive despite OM damage, but permeabilization of

the IM would likely result in cell death.¹⁶⁷ Accordingly, the OM permeabilization induced by E2₂₈ may reflect the relatively high MIC value that polymer (low activity) compared to the other polymers with similar f_{HB} and longer spacer arms.

In terms of their OM- and IM-permeabilization ability, the relative ranking of polymers is E6 > E4 > E2, which is the same trend that their antimicrobial activities follow (Table V-1 and Figure V-3). Considering this result, in addition to the fluorescence imaging and flow cytometry, it is reasonable to propose that the antimicrobial potency of these polymers is due, at least in part, to their bacterial membrane disruption.

Mechanism of Osmotic Lysis

Membrane permeabilization induced by peptides often proceeds by a colloid-osmotic mechanism.^{45, 168, 169} These peptides produce pores in cell membranes which are too small to allow the efflux of macromolecules from the cytosol, but do allow passage of small solutes such as water and ions. The osmolarity of the cytosol exceeds that of the external buffer solution, which contains only the small molecules. This osmotic imbalance (hypotonic condition) causes an influx of water through the small pores, resulting in cell swelling and compromise of the membrane integrity. The hallmark evidence of an osmolytic mode of action is the loss of activity when large osmolytes or “osmo-protectants” are added to the external media because these compounds balance the osmotic pressure across the membrane. While the osmo-protection assay is classically conducted with red blood cells, a recent report suggests that an antimicrobial peptide also kills bacteria by osmolysis.¹⁶⁹ Protegrins are known to form pores in *E. coli* leading to dissipation of the transmembrane potential accompanied by cell volume increase (due to osmotic imbalance) observed by light scattering.¹⁷⁰

We previously reported that the underlying mechanism of hemolysis induced by the amphiphilic polymethacrylates involves colloid-osmolysis.¹⁷¹ We hypothesized that the mechanism of bactericidal action exerted by the amphiphilic copolymers in this study may also involve osmolysis. To address this fundamental query, we adopted an assay for determining the antimicrobial activity in phosphate buffered saline (PBS), which contains well-defined solutes, suitable for assessing the effect of osmolytes. We did not test MIC

values for this purpose because this assay might be obscured by the contents of the MH broth. Since the PBS provides a non-growing condition, the minimum bactericidal concentration (MBC) of the polymers was determined by streaking agar plates and counting colonies after inoculation. When the assay was conducted in PBS without PEGs, the MBC value against *E. coli* of E2₂₈ was 3.9 $\mu\text{g/mL}$; for E4₂₉ and E6₂₇ it was 1.9 $\mu\text{g/mL}$. When PEG (number average Mn = 200 – 6000) was added to the PBS media ([PEG]=15 mM), the MBC increased by 8-fold for both E2₂₈ and E4₂₉ copolymers while the MBC of E6₂₇ was not significantly affected. This suggests that an osmolytic mechanism may indeed be operative. As a control, flow cytometry analysis showed that the FITC-polymer binding to *E. coli* and to *S. aureus* was largely unaffected by the inclusion of PEG 6000. This confirms that PEG does not protect the cells simply by inhibition of binding.

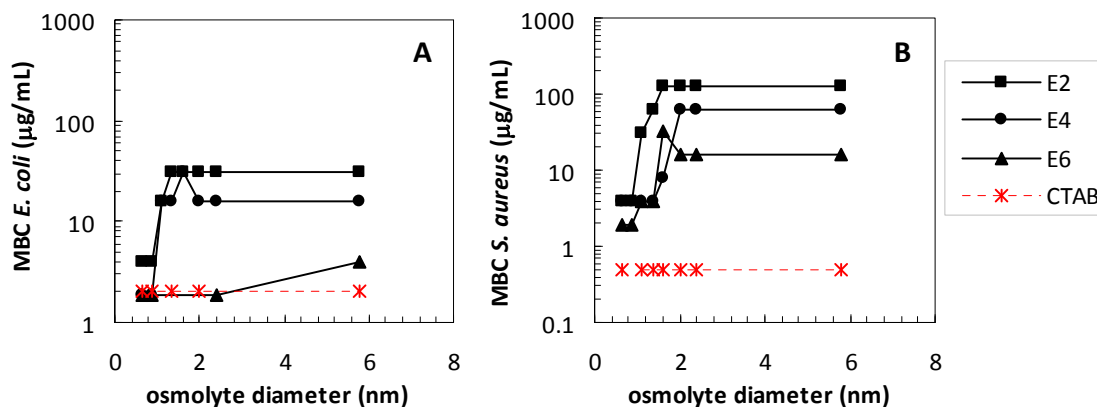


Figure V-9. Effect of external osmolyte diameter on the MBC of copolymers in phosphate buffered saline, a non-growing condition, against (A) *E. coli* and (B) *S. aureus*. The PEG concentration was 15 mM and the buffer was PBS (150 mM NaCl and 10 mM phosphate). Bacteria were incubated with the polymers and PEGs for 2 hours at 37 °C. After a single 10-fold dilution, aliquots were streaked onto agar plates, incubated overnight at 37 °C, and colonies counted. The MBC is the lowest polymer concentration which allows zero colonies to grow from the initial inoculums of 10^6 cfu/mL.

For the E2₂₈ and E4₂₉ copolymers, MBC values in PBS (150 mM NaCl and 10 mM phosphate) and saline media (150 mM NaCl) were the same, indicating the phosphate ions are not effective to protect the cells. The PEGs with Mn > 200 caused a reduction in the bactericidal activity against *E. coli*. This suggests that the copolymers E2₂₈ and E4₂₉ form pores, which are bigger than the phosphate ion (H_2PO_4^- , Stokes diameter = 0.86 nm)¹⁶⁸, but smaller than PEG 200 (hydrodynamic diameter = 1.12 nm).¹⁷² Accordingly, the pore size in *E. coli* membranes can be estimated to be 0.86-1.12

nm. On the other hand, the copolymer E6₂₇ showed little or no change in MBC against *E. coli* with any of the PEGs. CTAB, a cationic surfactant known to kill bacterial cells by membrane disruption, also displayed the MBC values which were independent of the added PEGs: 2.0 $\mu\text{g/mL}$ against *E. coli* and 0.5 $\mu\text{g/mL}$ against *S. aureus*. This indicates that the membrane disruption by CTAB is not osmolysis due to discrete pore formation but rather catastrophic membrane rupture or solubilization typical of surfactants. Since the MBC of E6₂₇ was also relatively independent of PEG addition, this polymer likely also exerts a surfactant-like mechanism of bactericidal action against *E. coli*.

Against *S. aureus*, the MBC values of E2₂₈, E4₂₉ and E6₂₇ were diminished by 32, 16, and 8-fold, respectively, upon the addition of PEGs (Mn > 600). In contrast to *E. coli*, the E6 did not show surfactant-like behavior against *S. aureus*. All the polymers displayed the same MBCs in the PBS and saline media. The MBC values for E2₂₈ increased from 3.9 to 125 $\mu\text{g/mL}$ upon addition of PEGs with MW ranging from 200 to 600 Da. For E4₂₉, the MBC increased from 3.9 to 62.5 $\mu\text{g/mL}$, and for E6₂₇, 1.9 to 15.6 $\mu\text{g/mL}$. This suggests pore diameters in the range of 0.86-1.36 nm for E2₂₈ and of 1.36-2.0 nm for E4₂₉ and E6₂₇. Apparently, the diameter of pores formed in *S. aureus* membranes increased with the elongation of the spacer arms. Overall, the results establish that osmolysis is a reasonable mechanism to consider.

Matsuzaki and co-workers estimated that the pore size induced in *B. megaterium* by magainin 2 is around 2.8 nm.³¹ The peptide CM-15, a melittin derivative, induced pores of about 3.5 nm in *P. aeruginosa* and 2.2-3.8 nm in *E. coli*.¹⁶⁹ Amphotericin B and nystatin form pores with diameters of 0.72-0.74 nm in red blood cells and model vesicles.¹⁶⁸ We recently showed that polymers can form pores in human red blood cells with diameters in the range of 1.6-2 nm.¹⁷¹ In this study, the synthetic polymers appeared to induce pores of varying diameters on *E. coli* (0.86-1.12 nm) and *S. aureus* (0.86-2.0 nm) membranes. Although the polymers are heterogeneous in terms of size and sequence, with flexible backbones and no defined secondary structures, they can nonetheless form discrete nano-scale pores in bacterial membranes.

As PEG size was increased beyond ~1.5 nm, the MBC values of the polymers reached a plateau. Hence, it would appear that above these concentrations, the polymers kill bacteria by a mechanism that is not osmolyte-dependent. All of the polymers may

completely disintegrate the membranes at high concentration by transitioning from a pore-formation to a surfactant-like mode of action. The MBC values at which a plateau is reached are ranked in the order $E2 > E4 > E6 > CTAB$. Hence, elongation of the spacer arms caused a reduction in the threshold for transition to a surfactant-like mode. Because the surfactant mode is expected to be relatively non-specific compared to pore-formation, we speculate that the selectivity (low MIC, high HC_{50}) of polymers with shorter spacer arms (E2, E4) can be ascribed to selective pore formation in bacterial membranes at low concentrations.

Molecular Dynamics Simulation

While the molecular-level details of bactericidal action exerted by polymers and peptides have been elusive experimentally, simulations have provided a wealth of information at this fine scale. Accordingly, we modeled the interaction of representative copolymers with lipid bilayers by molecular dynamics simulation using a previously described method.¹⁷³ A complete description of the experimental methods can be found in Appendix A.

The model E2 and E4 copolymers did not bind to membranes composed of DOPC, a zwitterionic lipid abundant in mammalian cell membranes while E6 and B2 readily inserted into the DOPC bilayers. On the other hand, all of the model polymers readily inserted into lipid bilayers of 1:1 POPC/POPG (Figure V-11), the latter of which is an anionic lipid abundant in bacterial cells. This selective insertion of E2 and E4 into the bacteria-type lipid bilayers, and not zwitterionic bilayers, may aide in explaining the non-hemolytic properties of E2 and E4 relative to B2 and E6. The snapshots display that the polymer chains appear to assume an extended conformation parallel to the membrane surface (Figure V-11A). The cationic ammonium groups are co-localized with the lipid head groups at the lipid-water interface, and the ethyl side chains are buried in the hydrophobic regions of lipid bilayers. It is clear from Figure V-11A that the polymer chains with longer arms (E6) are located more deeply in the hydrophobic regions of bilayers toward the center of lipid bilayer.

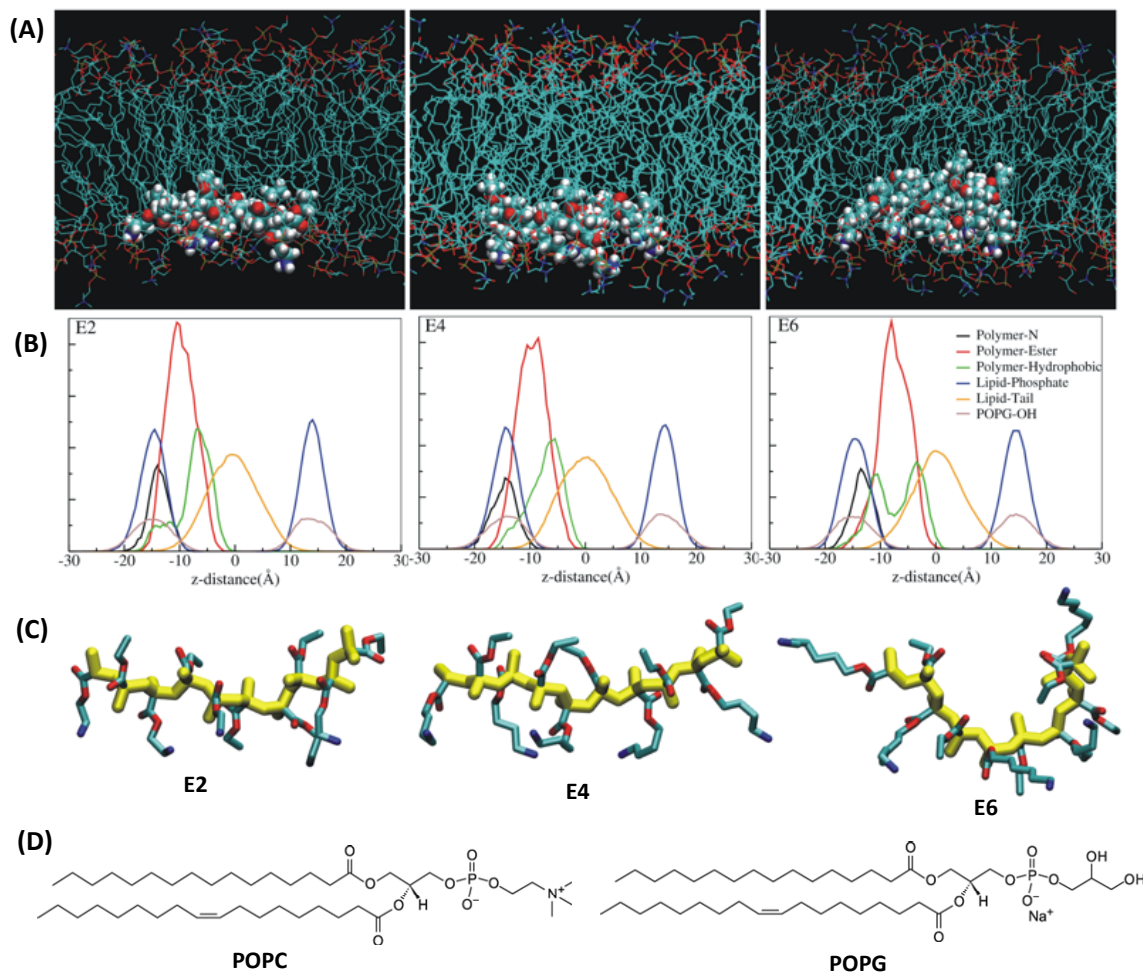


Figure V-11. Molecular dynamics simulation. (A) Snapshots of the model polymers interacting with POPC/POPG (1:1) lipid bilayer at the end of the 50 ns simulation. The blue and red colors of polymer structures represent nitrogen of primary ammonium groups and oxygen of ester group of side chains. Water molecules are omitted for clarity. (B) The unnormalized z-density distributions of chemical groups in the polymers and lipids averaged over the final 40 ns. Polymer nitrogen atoms, ester groups, and hydrophobic side chains are shown in black, red, and green, respectively. Lipid phosphate groups, alkyl tails, and hydroxyl groups of PG are shown in blue, orange, and grey, respectively. (C) The average conformation of the copolymers during the final 10 ns of the simulations. (D) The chemical structures of POPC and POPG.

Quantitative analysis of the results (Figure V-11B) reveals that the distribution peaks of ammonium groups of polymers (black line) are well-aligned with those of the phosphate head groups of both lipids (blue line) and the hydroxyl groups of POPG glycerol (purple line). The radial distribution functions of polymers with the phosphate lipid head groups demonstrate clear interactions. The populations of ammonium groups in the polymers are localized within $\sim 2.5\text{-}3.5$ Å of the phosphate lipid head groups. The peaks of the ethyl side chains (green line) and the lipid acyl chains (orange) also overlap, indicating that the hydrophobic side chains of the polymer are inserted into the

hydrophobic membrane core. The peaks of ammonium groups and ethyl side chains are spatially segregated with respect to the ester groups of polymers (red line) for E2 and E4, indicating that the cationic arms and ethyl side chains are presented on opposite faces of the polymer backbone, *i.e.* a facially amphiphilic arrangement. The average distance between center of mass of the ethyl and amine groups in the polymers are ~ 7 and 9 \AA for E2 and E4, (see Appendix B, Figure B-29) which are substantial given that the theoretical maximum distances are 13 and 16 \AA , respectively, calculated based on the carbon-carbon bond length of 1.54 \AA . Hence, the distance of separation between the cationic and hydrophobic groups of the copolymers in the membrane-bound state can be controlled by fine-tuning the spacer arms. The simulations also confirmed that E2 and E4 adopt relatively extended backbone conformations in the membrane-bound state (Figure V-10C). The average distance between the first and last ester carbon atoms of the polymer is $\sim 20 \text{ \AA}$ (see Appendix B, Figure B-30), indicating a highly stretched conformation, considering that the theoretical length for a polymethacrylate with ten repeating units in a fully extended zig-zag conformation is $\sim 23\text{-}24 \text{ \AA}$.

For E6, the ester groups of the polymer side chains are located on average at a depth (z-distance) of $\sim -14 \text{ \AA}$, compared to the others ($\sim -10 \text{ \AA}$), showing that E6 is inserted more deeply into the hydrophobic regions of lipid bilayers. In contrast to E2 and E4, E6 displayed a crescent-shaped average conformation (Figure V-11C), which reflects the bimodal distribution of ethyl groups with respect to the z-distance. The distance between the polymer ends is $\sim 15 \text{ \AA}$, which is calculated as the distance between the first and last ester groups of the 10-mer, averaged over the last 40 ns of the simulation. This indicates that the E6 conformation is more compact than E2 and E4. This may be due to the flexibility of hexylene arms and high solubility in the membrane core, which provide the polymer backbone with more freedom to adapt different conformations.

These results demonstrate that the polymers are capable of adopting conformations with cationic and hydrophobic groups segregated to opposite faces of the stretched polymer chains upon insertion to the membranes. The conformations of these polymers are evocative of the facially amphiphilic structures of α -helical (Figure I-1) or β -sheet host defense peptides. Despite the lack of any defined secondary structures or rigid/fixed conformations, the polymers nevertheless adapt facially amphiphilic, irregular

structures. In agreement with previous simulations on related polymers, ingrained facial amphiphilicity is therefore not a required design strategy to effectively mimic host defense peptides. Because E2 and E4 adopt extended amphiphilic conformations, while the structure of E6 is somewhat distorted, the spacer arm elongation clearly influences the polymer-membrane interaction. Furthermore, the elongation of the spacer groups seems to facilitate deeper penetration of the polymer side chains into the membrane core. This supports our original hypothesis that the spacer arms could be utilized to tune the depth of polymer penetration into biomembranes.

The simulation results moreover corroborate the structure-activity data. E6 inserts comparably into both zwitterionic and charged bilayers, which reflects the polymers non-specific biocidal activity. E6 adopts a distorted conformation relative to the extended E2 and E4 polymers in the membrane, which may explain the transition from an osmolytic to a surfactant mode of bactericidal action observed in the preceding sections. E2 and E4 insert preferentially into bilayers containing negative charge, which may explain their antimicrobial and non-hemolytic properties considering that human red blood cells do not display anionic phospholipids on the proximal leaflets of their membranes.

Mechanism of Antimicrobial Action

Host defense peptides and their synthetic peptide analogues are believed to form pores in bacterial membranes, leading to permeabilization of cell membranes, leakage of cytoplasmic components, and breakdown of membrane potential, ultimately causing cell death.³⁴ Although the details remain elusive, several models have been proposed for the pore formation process, including transmembrane channels such as the toroidal pore or barrel-stave. Alternatively, the peptides may accumulate on and completely disintegrate the membranes via the “carpet” mechanism. In this study, synthetic polymers were shown to exert many of the hallmarks of peptide activity, including pore formation despite their flexible/irregular structures. The polymers bind the membranes (Figure V-7), induce pore formation followed by osmolysis (Figure V-10), permeabilization (Figures V-8 and V-9), and cell death/inhibition (Figure, V-10 and Table V-1).

Elongating the spacer arms apparently enhanced the binding and membrane disruption events, collectively leading to the dramatic observed activity enhancements in the case of *E. coli*.

Certain peptides, such as buforin (an amphiphilic, 39-amino acid peptide isolated from the Asian toad, *Bufo garagrios*) kill bacteria by a mechanism of cell penetration and subsequent interaction with targets in the cytoplasm, without directly causing membrane damage.¹⁷⁷ In this study, it is shown that polymethacrylates are able to disrupt membranes *and* translocate into the cytoplasm after the disruption event has occurred (Figure V-6). Based on our suite of biophysical studies, it certainly seems plausible that membrane disruption is at least a major, if not the sole, component of their antimicrobial mechanism. Still, the extent to which the mechanism involves intracellular targets remains unexplored to date. Hence, it is not straightforward to assign these polymers a strict mechanistic category such as “cell-penetrating” or “membrane-disrupting” and, in fact, these categories need not be considered as mutually exclusive.¹⁶⁷ In the future, exploring the possibility of polymer interaction with targets in the cytoplasm would be highly interesting.

Conclusions

In this Chapter, the adjustment of spacer arms was shown to greatly augment the conventional approach to amphiphilic balance in random copolymers. The amino spacer length can be tuned to optimize the efficacy of antimicrobial polymers, with a four carbon chain (4-amino butylene) being the most effective. MD simulations revealed that the amino butylene copolymers adopt the most pronounced facially amphiphilic conformation upon binding to POPC/POPG lipid bilayers. We speculate that this design principle could be broadly applied to the various polymeric platforms which exert antimicrobial activity profiles. All of the evidence suggests that polymers, despite their irregular/heterogeneous structures, can mimic the amphiphilic structures in the lipid membranes and antimicrobial functions of host defense peptides, thereby rendering them feasible candidates for a wide variety of applications which require controlling microbial growth.

CHAPTER VI

Conclusions and Future Directions

Structure-Activity Relationships

In this dissertation, several iterations of polymer design and activity evaluation were described. Specific structural determinants of antimicrobial activity and toxicity to human red blood cells were delineated from the structure-activity data. Using a library of random copolymers which display hydrophobic and cationic ammonium groups in the side chains, a collection of key design principles were gleaned from this work. From the extensive library, a select few examples displayed the desirable activity profile, that is, potent activity against bacteria cells with little or no lysis of human red blood cells. The examples from our library which showed the most promising activity possessed the following salient characteristics:

- 1. Low molecular weight.** We synthesized polymers using a thiol chain transfer agent, which ensures that short polymer chains (1-10 kDa) are accessible. This is intended to mimic the small size of host defense peptides. Indeed, prior work indicated that high MW polymers are generally quite toxic.⁷⁵
- 2. Primary Amines.** In Chapter II, we demonstrated the role of ammonium groups in the antimicrobial and hemolytic ability of the copolymers. Primary amines, intended to mimic the side chains of lysine often found in host defense peptides, showed the most promising activity profiles. In Chapter III, we described the enhanced binding and disruption of biomembranes displayed by the polymers bearing primary amines, relative to tertiary and quaternary analogues.
- 3. Amphiphilic Balance.** In each of the Chapters, we varied the mole ratio of hydrophobic to cationic side chains. It was found that cationic homopolymers are relatively weak antimicrobials, whereas excessively hydrophobic copolymers are indiscriminately toxic to both human and bacteria cells. When a fine balance was

achieved, the polymer showed selective toxicity against bacteria, but not human, cells. The optimal ratio was found to be ~45% methylmethacrylate units to ~55% amino-functionalized methacrylate derivative.

- 4. Spacer Arms.** In the lysine residues of host defense peptides, the primary amines are connected to the polymer backbone via a four carbon linear alkyl chain. We found that this C₄ linkage was also the most advantageous in polymethacrylates. The polymers with C₄ spacer arms exhibited the highest selectivity for bacteria over human cells. Moreover, their mechanism of action was found to be rather evocative of the host defense peptides.

All of these characteristics can be considered peptide-mimetic. Hence, we conclude that synthetic polymers, despite their irregular/heterogeneous structures, can be tuned to effectively capture the function of host defense peptides. Judicious application of these design principles is therefore expected to further facilitate the development of novel antimicrobial compounds.

Future Directions in Polymer Chemistry

Synthetic polymers are becoming increasingly utilized in pharmaceutical, therapeutic, dental and biomedical applications due to the ability of researchers to finely tune their chemical and physical properties^{178, 179}. These features have provided an impetus for studying antimicrobial synthetic polymers as mimics of the host defense peptides with potential application to combat infectious disease. While many uses of polymers are found as inert delivery vehicles, such as polymer-drug conjugates or nanoparticles which deliver genes, biological activity can be also derived inherently from the structure of the polymer itself. Copaxone, for example, is a random copolymer currently being used in medicine to treat multiple sclerosis.^{73, 180} Polymer science affords unique advantages in the design of antimicrobials which effectively mimic host defense peptides. Unlike step-wise peptide synthesis, the methods of polymer synthesis enable rapid and readily scalable preparation at reasonable cost.

A plethora of structural features in antimicrobial polymers remain yet to be explored systematically. These include but are certainly not limited to the roles of

polymer backbone structure, flexibility/rigidity, polydispersity, tacticity, copolymer microstructure and macromolecular architecture. More detailed structure-activity studies aimed at delineating the effects of such parameters are expected to advance the field by providing novel activity determinants. The tools to address these fundamental questions are indeed available: polymerization procedures enable tuning the molecular weight and maintaining a narrow molecular weight distribution, with access to a wide array of chemical functionalities and macromolecular architectures¹⁸¹⁻¹⁸⁵.

Reversible addition fragmentation transfer (RAFT) polymerization is expected to be particularly well suited for future development of antimicrobial polymers, although few if any examples can be found in the current literature. In the future, RAFT should be applied to polymerizing libraries of polymers with various polydispersity indices (PDI), for example. The PDI of a polymer population is highly likely to influence activity because higher molecular weight fractions of a disperse population are expected to be more hemolytic. Hence, narrow PDI samples would enable mitigation of the adverse hemolytic toxicity while still retaining excellent antimicrobial potency.

Mechanism of Antimicrobial Action

A suite of biophysical experiments to probe the mechanism of antimicrobial action exerted by the polymers revealed that the likely mode killing involves the disruption of bacteria membranes. Fluorescence imaging of dye-labeled polymers showed their binding to bacterial membranes as well as membrane permeabilization (propidium iodide uptake). Permeabilization of *E. coli* inner and outer membranes was detected by an enzyme activity assay. The antimicrobial activity was dramatically reduced in the presence of PEGs in the external media, strongly suggesting that osmotic lysis is induced by the polymers. Molecular dynamics simulations moreover suggested facially amphiphilic conformations are assumed upon binding to anionic lipid bilayers. Combining the evidence from all of these results, we propose that the polymers exert their antimicrobial effects against Gram negative bacteria via the following pathway:

1. Binding to the external cell envelope lipids, including anionic phospholipids as well as lipopolysaccharides.
2. Rapid outer membrane (OM) permeabilization.

3. Gradual translocation of the periplasmic space to accumulate on the inner membrane (IM). On the IM, the polymer adopt facially amphiphilic (though conformationally irregular) structures.
4. Pore formation (~1nm) on the inner membrane, leading to influx of water and small solutes, cell swelling, and resulting osmotic lysis
5. Polymer internalization within the cells, possibly resulting in secondary killing pathways such as interference with cellular function. This step remains unexplored and should be the topic of future investigations.
6. Cell death

Future Mechanistic Work

Because the polymers are localized inside the cytoplasm after the membrane disruption event takes place (step 5 in the above proposed mechanism), it is not straightforward to assign the precise cause of death. While it is reasonable to argue that disruption of the IM would likely result in loss of viability, it is also possible that the cationic polymers would interfere with intracellular process after internalization, which may also facilitate the microbial inactivation. Hence, it would be interesting in the future to explore whether the polymers target additional cellular components beyond the membrane. In addition, it would highly interesting to explore whether these materials may induce antimicrobial killing *in vivo* by immuno-modulatory effects known to be operative in certain host defense peptides. Finally, the possibility of bacteria developing resistance to polymer attack should be addressed. Unpublished work in the Kuroda laboratory suggests that *E. coli* cannot develop resistance to our polymers after twenty-five sub-inhibitory passages. While this initial finding is promising, it remains possible that other strains may attempt to develop resistance mechanisms. There is some evidence in the literature that bacteria do attempt to develop resistance against antimicrobial peptides. This is done by alteration of their membrane lipid compositions to reduce anionic charge, up-regulation of proteases to degrade the peptides, and the production of efflux pumps to remove the peptides from the cells. Establishing the extent to which such resistance mechanisms are plausible would be needed for this field to progress vertically.

Challenges Remaining

Considering their activity *in vitro*, it is reasonable to propose that the best examples from the library of polymethacrylates studied in the Kuroda lab may have potential for applications such as topical anti-infective creams, antibiotics directly administered to the site of infection, wound dressings, and implants or biomedical devices. Towards utilizing the polymers in practical applications, knowledge of their efficacy, comprehensive toxicity analyses, and studies on any possible mechanisms of bacterial resistance to the polymer attack would be required. Once these issues are fully addressed in the laboratory, the most promising candidates can be confidently identified.

Whether these polymers or related compounds will eventually be used in clinical settings to combat bacterial infections remains to be seen. Toward that ultimate goal, it is essential to prove the concept in animal trials using the most promising compounds from the libraries developed herein and by others. The future of realistic progress of this field indeed hinges on the ability to demonstrate their efficacy *in vivo*.

APPENDICES

APPENDIX A

Materials and Methods

Materials

2,2'-azobisisobutyronitrile (AIBN) was purchased from Sigma and recrystallized prior to use. Methacryloyl chloride was purchased from Acros and distilled prior to each use. *N,N*-dimethylaminoethyl methacrylate (DMAEMA), and methyl iodide were purchased from Sigma-Aldrich and used without further purification. Methylmethacrylate (MMA), butylmethacrylate (BMA), methyl 3-mercaptopropionate (MMP), ethanolamine, 4-aminobutanol, 6-aminohexanol, 4-trans-aminocyclohexanol, di-*tert*-butyldicarbonate, butylamine, hexylamine, dansyl chloride, cystamine, and tricarboxyethylphosphine (TCEP) were purchased from Acros and used without further purification. *N*-(3-aminopropyl)methacrylamide hydrochloride (APMAm·HCl, > 98%) was purchased from PolySciences (Warrington, PA). Reagent grade solvents and trifluoroacetic acid (TFA) were purchased from Fisher and used without further purification. Standardized solutions of 0.100N sodium hydroxide and hydrogen chloride were purchased from Ricca Chemical Company. The bee venom toxin melittin (purity > 85%) was purchased from Sigma and the antimicrobial peptide Magainin-2 (purity > 90%) was purchased from AnaSpec Inc. The lipids 1-palmitoyl-2oleoyl-*sn*-glycero-3-phosphocholine (POPC), 1-palmitoyl-2oleoyl-*sn*-glycero-3-phosphoethanolamine (POPE), 1-palmitoyl-2oleoyl-*sn*-glycero-3-phospho-(1'-*sn*-glycerol) (POPG), 1,2-dioleoyl-*sn*-glycero-3-[phospho-*rac*-(1-glycerol)] (DOPG), 1,2-dioleoyl-*sn*-glycero-3-[phospho-*rac*-(3-lysyl(1-glycerol))] (Lysyl-DOPG), and 1,1',2,2'-Tetraoleoyl Cardiolipin (CL) were purchased as lyophilized powders from Avanti Polar Lipids (Alabaster, AL). Lipid stock solutions (10 mM) in chloroform were kept frozen at -80 °C, under a nitrogen blanket, until use. Solutions containing Lysyl-DOPG were used immediately after preparation according to the recommendations of Avanti. *E. coli* ATCC 25922 and *S.*

aureus ATCC 25923 were purchased from ATCC as lyophilized powders. Human red blood cells (Red Blood Cells Leukocytes Reduced Adenine Saline Added) were obtained from the American Red Cross Blood Services Southeastern Michigan Region.

Monomer Synthesis

To a solution of ethanolamine (42.7 mmol, 2.6 g), in a biphasic mixture of THF (30 mL) and NaOH(aq) (1 M, 50 mL) was added a solution of di-*tert*-butyldicarbonate (42.7 mmol, 9.3 g) in THF (20 mL) drop-wise and the mixture was stirred at room temperature overnight. The resulting *N*-Boc-protected alcohol was extracted in ethylacetate by washing with water, saturated NaCO₃H (aq), and brine. The same procedure was followed in the case of 4-butanolamine, 6-hexanolamine, and trans-4-aminocyclohexanol. Freshly distilled methacryloyl chloride (23 mmol, 2.2 mL) was diluted with dichloromethane (5 mL) and added drop-wise to a solution of the *N*-Boc-protected alcohol (23 mmol) and triethylamine (25 mmol, 3.5 mL) in dichloromethane (50 mL) at 0 °C ice bath, and the mixture was allowed to stir overnight. The solution was then filtered and the filtrate was concentrated under reduced pressure, extracted in ethylacetate by washing with water, saturated NaCO₃H (aq), and brine.

Alkyl methacrylamides were prepared by reaction of hexylamine or butylamine with methacryloyl chloride in dichloromethane with triethylamine. The products were purified by washing with water, saturated NaCO₃H(aq), and brine and then by silica gel chromatography using ethyl acetate/hexanes (1:1).

The monomer 2-(*tert*-butoxycarbonylamino)ethyl methacrylate, **1**, was recrystallized from hexanes at -20 °C to give a white solid in 72% yield. ¹H NMR (400 MHz, CDCl₃): δ 6.09 (s, 1H), 5.55 (s, 1H), 4.73 (bs), 4.17 (t, 2H), 3.40 (q, 2H), 1.91 (s, 3H), 1.41 (s, 9H). ¹³C NMR (100 MHz, CDCl₃): δ 167.27, 156.04, 136.00, 125.89, 79.56, 63.94, 39.67, 28.32, 18.27. Mass spectrometry: ESI calcd for [C₁₁H₁₉NO₄ + Na]⁺, 252.1212; found, 252.1209.

The monomer 4-(*tert*-butoxycarbonylamino)butyl methacrylate, **2**, was purified by silica gel column chromatography (eluent: hexane/ethyl acetate 3:1) to give a colorless, viscous oil in 81% yield. Thin layer chromatography (eluent: hexane/ethyl acetate 3:1) *R_f* = 0.54, I₂ stained. ¹H NMR (300 MHz, CDCl₃): δ 6.09 (s, 1H), 5.55 (s, 1H), 4.54 (bs), 4.15 (t, 2H), 3.15 (q, 2H), 1.93 (s, 3H), 1.8-1.5 (m, 4H), 1.43 (s, 9H). ¹³C NMR (100

MHz, CDCl₃): δ 167.35, 155.92, 136.34, 125.73, 79.16, 64.25, 40.11, 28.26, 26.73, 25.97, 18.21. Mass spectrometry: ESI calcd for [C₁₃H₂₃NO₄ + Na]⁺, 280.1525; found, 280.1529.

The monomer 6-(*tert*-butoxycarbonylamino)hexyl methacrylate, **3**, was purified by silica gel column chromatography (eluent: hexane/ethyl acetate 9:1) to give a colorless, viscous oil in 68% yield. Thin layer chromatography (eluent: hexane/ethyl acetate 9:1) R_f = 0.90, I₂ stained. ¹H NMR (300 MHz, CDCl₃): δ 6.09 (s, 1H), 5.54 (s, 1H), 4.52 (bs), 4.13 (t, 2H), 3.10 (q, 2H), 1.93 (s, 3H), 1.67 (m, 2H), 1.5-1.3 (m, 6H), 1.43 (s, 9H). ¹³C NMR (100 MHz, CDCl₃): δ 167.49, 155.95, 136.46, 125.19, 79.03, 64.58, 40.45, 29.96, 28.52, 28.39, 26.41, 26.67, 18.30. Mass spectrometry: ESI calcd for [C₁₅H₂₇NO₄ + Na]⁺, 308.1838; found, 308.1833.

The monomer *trans*-4-(*tert*-butoxycarbonylamino)cyclohexyl methacrylate, **4**, was purified by re-crystallization from ethyl acetate at -20 °C to give a white solid in 77% yield. Thin layer chromatography (eluent: hexane/ethyl acetate 9:1) R_f = 0.41, I₂ stained. ¹H NMR (300 MHz, CDCl₃): δ 6.08 (s, 1H), 5.54 (s, 1H), 4.74 (tt, 1H), 4.40 (bs), 3.47 (m, 1H), 2.02 (m, 4H), 1.92 (s, 3H), 1.6-1.4 (m, 2H), 1.44 (s, 9H), 1.35-1.15 (m, 2H). ¹³C NMR (100 MHz, CDCl₃): δ 166.88, 155.20, 136.63, 125.21, 79.26, 72.05, 48.46, 30.73, 29.87, 28.37, 18.27. Mass spectrometry: ESI calcd for [C₁₅H₂₅NO₄ + Na]⁺, 306.1681; found, 306.1681.

Polymer Synthesis

Random copolymers containing primary amines were prepared by a previously described technique⁷⁵ with minor alterations. Ethylmethacrylate (EMA) or butylmethacrylate (BMA) was dissolved with N-Boc-protected aminoalkylmethacrylate **1**, **2**, **3**, or **4** (1 mmol total monomers, various ratios) in acetonitrile (0.5 mL). AIBN (0.01 mmol) and MMP (0.1 mmol) were added from concentrated stock solutions. The mixtures were deoxygenated by nitrogen flushing for 2 minutes each and then submerged in a 70 °C oil bath overnight. After concentration under reduced pressure, the Boc-protecting groups were cleaved using trifluoroacetic acid and precipitated from methanol (0.5 mL) into diethyl ether (25 mL) twice. Obtained precipitates were lyophilized to afford the random copolymers as fine white powders. ¹H NMR (300 MHz, methanol-d₄) for the representative copolymer PM₄₇ (47% MMA, 53% AEMA, DP = 6.2): δ 4.264 (bs, 6.39H), 3.679 (s, 3H), 3.625 (bs, 8.89H), 2.8-2.5 (bm, 7H), 2.3-0.8 (bm, 29.67H).

Polymers containing tertiary and quaternary ammonium groups. DMAEMA was copolymerized with an alkyl methacrylate, using the same procedure as described above, to give a series of precursor polymers. A fraction of each precursor was dissolved in 0.1M HCl in acetic acid, concentrated by N₂ flushing, and twice precipitated from methanol into diethylether. The precipitates were collected by centrifugation and lyophilized to afford random copolymers bearing tertiary amine groups as ammonium chloride salts. Copolymers containing tertiary amine groups and methyl or butyl groups are referred to in this study as TM and TB series, respectively. The remaining amount of each precursor was dissolved in methanol. To these solutions, methyl iodide (2.0M in *tert*-butyl methyl ether) was added in ten-fold excess relative to the amount of tertiary amine groups. After 10 min, the solutions became turbid. Methanol or DMSO was added until the solutions became clear again, and the clear solutions were left to stir at room temperature for an additional 2 hrs. Solvents were then evaporated under reduced pressure to give tan-colored powders. The powders were twice precipitated from DMSO/methanol into diethylether to give white powders. The precipitates were collected by centrifugation and lyophilized to afford random copolymers bearing quaternary ammonium iodide groups. ¹H NMR (300 MHz, methanol-d₄) for the representative copolymer TM₄₆ (46% MMA, 54% DMAEMA, DP = 7.8): δ 4.426 (bs, 8.44H), 3.740 (s, 3H), 3.703 (bs, 10.81H), 3.592 (bs, 8.54H), 3.011 (bs, 25.06), 2.8-2.5 (bm, 7H), 2.3-0.8 (bm, 40.90H). ¹H NMR (300 MHz, D₂O) for the representative copolymer QM₄₈ (48% MMA, 52% quaternized DMAEMA, DP = 6.7): δ 4.543 (bs, 7.22H), 3.824 (bs, 6.89H), 3.732 (s, 3H), 3.702 (bs, 9.26H), 3.290 (bs, 32.22), 3-2.6 (bm, 7H), 2.3-0.8 (bm, 30.68H).

For the synthesis of poly(methacrylamide)s, free radical polymerization was carried out using a modified literature procedure.¹⁴³ APMAM·HCl and butyl- or hexylmethacrylamide (0.5 mmol total monomer, various ratios) were dissolved in methanol/ethanol (1:1, 0.5 mL) in borosilicate glass test tubes. AIBN (0.005 mmol, 0.82 mg) and MMP (0.025 mmol, 2.7 μL) were added from concentrated stock solutions and the tubes were sealed with rubber septa and copper wire. After degassing with N₂ for 5 min each, the tubes were submerged in an oil bath set to 60 °C and left to stir for 24 hrs. Then, the polymers were purified by repeated precipitation from methanol into

diethylether. They were subsequently dried under vacuum and then lyophilized to afford white powders.

Dansyl end-labeled polymers were prepared by the same procedure except that the chain transfer agent was a dansyl-functionalized thiol agent, 5-(dimethylamino)-N-(2-mercaptoethyl)naphthalene-1-sulfonamide. After polymerization, the polymers were purified by gel permeation chromatography over Sephadex LH-20 in methanol. The Boc-protecting groups were then cleaved by treatment with TFA. Precipitation of the cationic polymers in diethylether and lyophilization afforded the random copolymers as fine green powders.

FITC end-labeled polymers were prepared by the same procedure except that the chain transfer agent was aminoethanethiol hydrochloride and the solvent was a mixture of acetonitrile and DMF (1:1). After polymerization, the amino-functionalized end groups were mixed with a two-fold excess of fluorescein isothiocyanate (FITC) in DMF for 1 hour and purified by gel permeation chromatography over Sephadex LH-20 in methanol. The Boc-protecting groups were then cleaved by treatment with TFA. Precipitation of the cationic polymers in diethylether and lyophilization afforded the random copolymers as fine yellow/orange powders.

Potentiometric Titration

Polymers in this study were titrated using a procedure from the literature.¹⁴⁷ First, polymers (typically 5-10mg) were dissolved in aqueous saline (10-15 mL, [NaCl] = 150 mM) in a glass scintillation vial to give a polymer concentration of ~ 0.5 mM. The solution was purged with nitrogen gas for 15 minutes with constant stirring in order to remove CO₂. Then the pH electrode was introduced into the solution and sealed with Parafilm. Throughout the titration, a gentle stream of nitrogen gas was maintained in order to exclude CO₂. With rapid stirring, aliquots of standardized 0.100N sodium hydroxide (5 or 10 uL) were injected using a Hamilton syringe. The solution was allowed to chemically and thermally equilibrate for 2 min after each addition and it was confirmed that the pH reading was stable within ± 0.01 pH units. The degree of ionization of the polymer was calculated from the charge neutrality condition, shown below.

$$\alpha = \frac{[\text{amines}H^+]}{[\text{amines}]_{\text{total}}} = \frac{[Cl^-] + [HO^-] - [Na^+] - [H^+]}{[\text{amines}]_{\text{total}}} \quad (1)$$

where, α is the fraction of amine groups in solution that are positively charged, $[\text{amine}H^+]$, and $[\text{amines}]_{\text{total}}$ is the total concentration of all amine groups in the solution. As an internal standard, ethanolamine was titrated using our method and found to have a pK_a of 9.48, which closely agrees with the accepted value ($pK_a = 9.5$).¹⁸⁶

In some cases, polymer precipitated from solution or underwent chemical changes before reaching the equivalence point ($\alpha = 0$). For such polymers, titration was carried out in a limited range of pH values. Back-titration was performed using aliquots of standardized 0.100N hydrogen chloride solution (10 or 20 μL). Close agreement between forward and back titration data points indicated that no chemical or conformational changes resulted from titration in the restricted pH range. Each titration was performed at least twice, in very close agreement, and the $\text{pH}(\alpha)$ data reported are the average of the result from the separate trials.

Water-Octanol Partition Coefficients

Polymer solutions (500 μL , 100 μM) were prepared in aqueous buffer (10 mM HEPES or MES, 150 mM NaCl, pH ranging from 6 to 8) in an Eppendorf centrifuge tube and octanol (500 μL) was added. The tube was vortexed for 5 minutes and then allowed to sit overnight in the dark. After 5 minutes of centrifugation at 3000 rpm, an aliquot of each phase was diluted 100-fold into methanol and the fluorescence spectra were recorded. The concentration of polymer in each phase was determined from comparison to calibration curves obtained by measuring the fluorescence spectra of the polymers at various concentrations in methanol. The partition coefficient was defined as,

$$\log P = \log \left(\frac{[P]_{\text{oct}}}{[P]_{\text{aq}}} \right) \quad (2)$$

where $[P]_{\text{oct}}$ and $[P]_{\text{aq}}$ are the concentration of the polymer in the octanol and aqueous phases, respectively. Measurements were performed three times from each phase. Measurement of $\log P$ in the presence of mono-n-dodecylphosphate(DDP) were performed by the same procedure as above, except that the aqueous buffer (10 mM MES, 150 mM NaCl, pH 6) contained 0, 0.1, or 1 mM DDP surfactant. The concentrations of DDP were well below the literature values of the critical micelle concentration for this

surfactant, which vary from 3 to 9 mM depending on the temperature, salt concentration and pH.

Antimicrobial Activity Assays

The Minimum Inhibitory Concentration (MIC) value of each polymer in this study was determined by a standard microdilution method approved by The National Committee for Clinical Laboratory Standards (NCCLS)¹⁸⁷ with slight modifications.¹⁸⁸ Polymer stock solutions were prepared in 0.01% aqueous acetic acid. Eight two-fold serial dilutions of the stock were prepared in 0.01% acetic acid. A single colony of *Escherichia coli* DH5 α was inoculated in Muller-Hinton (MH) broth at 37 °C with shaking overnight. The turbid suspension was then diluted to OD₆₀₀ = 0.1, re-grown for 90 minutes to the mid-logarithmic phase (OD₆₀₀ = 0.5-0.6) in MH broth of pH 7.4, and finally diluted to OD₆₀₀ = 0.001, which corresponds to $\sim 2 \times 10^5$ cfu/mL based on colony counting after spreading on MH agar plates. The stock suspension (90 μ L) was then mixed with each of the polymer dilutions (10 μ L) on a sterile 96-well round-bottom polypropylene microplate (Corning #3359). In each case, the highest polymer concentration tested was 2000 μ g/mL. The plates were incubated at 37 °C for 18 hours. Then, the OD₅₉₀ of the wells was recorded using a microplate reader (Perkin Elmer Lambda Reader) and any increase in turbidity was considered due to *E. coli* growth, given that the polymer concentration was below its solubility limit in MH broth. The lowest polymer concentration which completely inhibited growth of *E. coli* was defined as the MIC value for that polymer. All experiments were performed three times, each in triplicate, on different days.

Since the MIC values often depend on the assay conditions and bacterial strains, and because many laboratories have developed their own protocols, it would be impractical to compare the MIC values for different compounds reported in the literature. Therefore, we chose the natural host-defense peptide magainin-2 and the bee venom toxin melittin as reference standards in our assays. The MIC values of melittin and magainin-2 were determined to be 4.4 μ M (12.5 μ g/mL) and 51 μ M (125 μ g/mL), respectively, in this assay condition.

To measure the effect of pH on bactericidal activity, *E. coli* ATCC 25922 in the mid-logarithmic stage were diluted in PBS (10mM phosphate, 150mM NaCl), of various

pH values, to $OD_{600} = 0.005$, corresponding to $\sim 10^6$ cfu/mL. This stock (90 μ L) was mixed with polymer dilutions (10 μ L) on a microplate and incubated for 90 minutes at room temperature. The *E. coli* suspensions without polymers were incubated at room temperature for 2 hours in buffers of different pH. An aliquot of the bacteria suspension was taken every 20 min and diluted 10^3 fold, then spread on an agar plate. Plates were incubated at 37 °C overnight and the number of colonies counted to determine the cfu/mL in the original suspension. The results indicated that there is no significant effect of incubation in PBS buffer and pH on the viability of bacteria in the absence of polymer. After incubation with polymer, the polymer/bacteria mixtures were diluted 10^2 fold into MH broth to remove the effect of polymers and allowed to re-grow overnight at 37 °C in an incubator. The minimum polymer concentration required to give no detectable growth in the OD measurement is defined as the MBC in this non-growing condition. The starting suspension on the microplate (10^6 cfu/mL) contained 10^5 cfu per well. A three-log reduction caused by polymer (99.9% killing) would therefore give a population of 10^2 cfu per well. Because the suspension in each well was then diluted 10^2 fold, a three-log reduction in cfu/mL is the detection limit of this assay. Each experiment was repeated in each buffer pH twice, each in duplicate, on different days. The MBC on of each trial was defined as the average of the values in duplicate and values are reported as the average of the two trials.

To measure the osmo-protection by PEGs, the lowest polymer concentration which caused a 3-log reduction in the number of cfu/mL (99.9% killing) of *E. coli* ATCC 25922 in phosphate buffered saline (PBS = 10mM phosphate, 150 mM NaCl, pH 7.2) after 2 hr incubation at 37 °C was defined as the minimum bactericidal concentration (MBC). Midlogarithmic phase *E. coli* was diluted to an OD_{600} of 0.001 in PBS, *i.e.* 10^6 cfu/mL. The suspension contained 16.6 mM poly(ethylene glycol) of various number-average molecular weights ($M_n = 200-6000$ g/mol). This suspension (90 μ L) was mixed with each of eight serial two-fold dilutions of polymer (10 μ L) on a 96-well polypropylene microplate to give a final PEG concentration of 15 mM. After 2 hr incubation at 37 °C, an aliquot (10 μ L) was taken from each well, diluted 10-fold, and spread onto MH-agar plates. The plates were incubated overnight at 37 °C and the number of colonies counted. The lowest polymer concentration which showed zero

colonies grown (at least a 3-log reduction from 10^4 cfu per 10 μ L aliquot) was defined as the MBC. As positive controls, *E. coli* suspensions, with and without PEG, were also mixed with only PBS (10 μ L) and incubated for 2 hr. Then, an aliquot (10 μ L) was diluted by 10^3 -fold and spread onto an agar plate. These plates showed 4-5 colonies, corresponding to $\sim 5 \cdot 10^5$ cfu/mL, which confirmed that the *E. coli* remained viable in PBS, with and without 15mM PEG, but remained in a static (non-growing) condition. The cationic surfactant cetyltrimethylammonium bromide (CTAB) was used a reference standard, which shows the same MBC in the presence and absence of PEG.

Hemolytic Activity Assays

Toxicity to human red blood cells (RBCs) was assessed by a hemoglobin release assay using the same polymer stock dilutions used for the MIC measurement. RBCs (1 mL) were diluted into phosphate buffered saline (PBS: 10mM phosphate, 150mM NaCl, pH 7.4) (9 mL) and then centrifuged at 1000 rpm for 5 min. The supernatant was carefully removed using a pipette. The RBCs were then washed with PBS two additional times. The resulting stock (10% v/v RBC) was diluted three-fold in PBS to give the assay stock (3.3% v/v RBC). The assay stock (90 μ L) was then mixed with each of the polymer dilutions (10 μ L) on a sterile 96-well round-bottom polypropylene microplate to give a final solution of 3% v/v RBC, which corresponds to approximately 10^8 red blood cells per mL based on counting in a hemacytometer. PBS (10 μ L) or Triton X-100 (10 μ L, 1% v/v) were added instead of polymer solution as negative and positive hemolysis controls, respectively. The microplate was secured in an orbital shaker at 37 °C and 250 rpm for 60 min. The plate was then centrifuged at 1000 rpm for 10 min. The supernatant (10 μ L) was diluted into PBS (90 μ L) and the absorbance at 405 nm was observed using a microplate reader (Perkin Elmer Lambda Reader). The fraction of hemolysis was defined as the absorbance reading divided by the average of readings from the positive control wells. Hemolysis was plotted as a function of polymer concentration and the HC_{50} was defined as the polymer concentration which causes 50% hemolysis relative to the positive control. We estimated this value by fitting the experimental data to the function $H = 1/\{1+(HC_{50}/[\text{polymer}])^n\}$, where H is the hemolysis fraction measured and $[\text{polymer}]$ is the total concentration of polymer. The fitting parameters were n and HC_{50} . In some cases, the hemolysis did not reach 50% up to the highest polymer concentration tested

(2000 $\mu\text{g/mL}$) and hence the HC_{50} was not determined. In other cases, the maximum hemolysis was less than 100% but greater than 50% and the HC_{50} value was calculated. All experiments were performed three times, each in triplicate, on different days. The absorbance values recorded in triplicate were averaged and the HC_{50} value was then calculated for each trial. Values reported are the average of the three trials.

As standards, we tested the biocidal peptide melittin and the antimicrobial peptide magainin-2 in this assay condition. It was noted that the hemolytic activity of melittin depends strongly on the concentration of red blood cells on the microplate. Since the method for HC_{50} determination is not standardized between laboratories, direct comparison with literature values may not accurately reflect the absolute hemolytic activity of the compounds. Therefore, we consider hemolysis caused by our polymers relative to that caused by melittin, a well-known biocide. The HC_{50} of melittin was 0.6 μM (1.4 $\mu\text{g/mL}$). Magainin-2 induced less than 10% hemolysis at the highest peptide concentration used here (250 $\mu\text{g/mL}$) and therefore the HC_{50} value cannot be determined.

To determine the effect of pH on hemolytic activity, the HC_{50} values were obtained as described above, using PBS of different pH values in the range of 6 to 8 with no other alteration of the protocol. The susceptibility of human RBCs to lysis by the non-ionic surfactant Triton X-100 ($\text{HC}_{50} = 120 \mu\text{M}$) does not change when buffers of different pH are used. The HC_{50} values of selected polymers were tested in each pH buffer twice, each in duplicate, on different days. The absorbance values recorded in duplicate were averaged and the HC_{50} value was then calculated for each trial. The HC_{50} of each trial was defined as the average of the values in duplicate and values are reported as the average of the two trials.

Liposome-Polymer Binding

A solution of lipid (100 μL , 10 mM) in chloroform was slowly evaporated under a gentle N_2 stream and subsequently dried under vacuum for 12 hours. The lipid film was resuspended in an aqueous buffer (10mM HEPES or MES, pH 6-8, osmolality = 290 ± 5 mmol/kg), agitated on a vortex mixer for 5 minutes, and subjected to ten freeze/thaw cycles between acetone containing dry ice and a 60 $^\circ\text{C}$ water bath. The turbid suspension was then extruded twenty-one times through two stacked polycarbonate membrane with an average pore size of 100 nm, yielding a clear suspension of large

unilaminar vesicles (LUVs). An aliquot of the liposome stock solution (2.5 or 5 μL) was injected into a cuvette containing polymer solution (2 mL, 1 μM) and the fluorescence intensity was recorded after 5 minutes of mixing. An excitation wavelength of 330 nm and an emission wavelength of 510 nm were used. The fluorescence data were corrected for dilution as well as the inner-filter effect. The corrected fluorescence intensities were plotted versus the total concentration of lipid and the dissociation constant was determined by curve-fitting to the following expression for single-site binding isotherm using KaleidaGraph software, according to a previously established method.¹⁰⁷

$$F = F_0 + \left(\Delta F \cdot \frac{[P]_0 + ([L]_0/n) + K_D - \left(([P]_0 + ([L]_0/n) + K_D)^2 - 4 \cdot [P]_0 \cdot ([L]_0/n) \right)^{1/2}}{2 \cdot [P]_0} \right) \quad (3)$$

where F_0 is the fluorescence intensity before the addition of liposomes, ΔF is the change in fluorescence intensity from F_0 to the fluorescence when the lipid concentration approaches infinity, $[P]_0$ is the total polymer concentration, $[L]_0$ is the total lipid concentration, n is the number of lipids per binding site, and K_D is the dissociation constant. The number of lipids per binding site was fixed in every case to $n=6$ to enable accurate curve fitting, although similarly good fits were obtained with $n = 4-9$, as discussed in a previous report.¹⁰⁷

Liposome Dye Leakage

A solution of lipid (100 μL , 10 mM) in chloroform was slowly evaporated under a gentle N_2 stream and subsequently dried under vacuum for 12 hours. An aqueous buffer (10mM HEPES, 50mM sulforhodamine B (SRB), pH 7.4) was adjusted to an osmolarity of 280 ± 5 mmol/kg by addition of saturated NaCl and measured using a vapor-pressure osmometer, so that liposomes could be prepared without initial osmotic pressure across the membranes. The dry lipid film was resuspended in this buffer, vigorously vortexed for 5 min, and subjected to ten freeze/thaw cycles between dry ice in acetone and a 50 $^\circ\text{C}$ water bath. Then it was passed twenty-one times through a mini-extruder equipped with two stacked polycarbonate membranes of 400 nm average pore size. Unincorporated dye was removed by size exclusion chromatography over Sepharose Cl-4B gel from Amersham Biosciences (Uppsala, Sweden) using a buffer containing no dye (10 mM HEPES, 150 mM NaCl, pH 7.4, 280 ± 5 mmol/kg). The concentration of lipid in the obtained suspension was determined by a colorimetric phosphorous assay.¹⁸⁹ This

solution was diluted in the same buffer to a lipid concentration of $11.11\mu\text{M}$. This suspension ($90\ \mu\text{L}$) was mixed with polymer stock solutions ($10\ \mu\text{L}$) on a 96-well black microplate to give a final lipid concentration of $10\ \mu\text{M}$ in each well. The assay buffer ($10\ \mu\text{L}$) and Triton X ($0.1\% \text{ v/v}$, $10\ \mu\text{L}$) were employed as the negative and positive controls. After 1 hour, the fluorescence intensity in each well was recorded using a Thermo Fisher microplate reader with excitation and emission wavelengths of 565 and 586 nm, respectively. The fraction of leaked SRB in each well was calculated according to the expression: $L = (F-F_0)/(F_{\text{TX}}-F_0)$ where F is the fluorescence intensity recorded in the well, F_0 is the intensity in the negative control well, and F_{TX} is the intensity in the positive control well. For the measurement of dye leakage kinetics, the liposome stock was diluted to $10\mu\text{M}$ in a 2mL quartz cuvette and fluorescence signal was monitored. Then, an aliquot of polymer solution was injected into the cuvette *via* a syringe port in the spectrofluorometer lid and fluorescence intensity was recorded every 2 seconds for 10 minutes. Triton X-100 solution ($4\% \text{ v/v}$, $5\ \mu\text{L}$) was injected as the positive lysis control at the end of the time course.

Cell Culture and XTT Assay

Cytotoxicity experiments were carried out using the HEP-2 cell line, which are human epithelial cells isolated from larynx carcinoma. It should be noted that the HEP-2 cell line is likely contaminated with HeLa cells derived from cervical cancer.¹⁹⁰ Cells were grown in minimum essential medium (MEM) supplemented with 10% heat-inactivated fetal bovine serum (FBS), 1mM pyruvate, and 0.1mM non-essential amino acids at 37°C , $5\% \text{ CO}_2$, and 95% relative humidity. The doubling time of the HEP-2 cells in this supplemented medium is about 22-24 hr. In medium without added serum, the cells generally proliferate only with difficulty.

HEP-2 cells were seeded into the 96-well cell culture plates (Falcon # 3072, USA) at a density of 10^4 cells per well. After 24 hours incubation, the cell confluence was about 50-60%, and the culture medium was replaced with serial dilutions of polymer stock solutions in an antibiotic- and serum-free MEM. The viability of cells exposed to the polymers was assessed using a commercial kit (Cell Proliferation Kit II, Roche, USA). After 4 or 24 hr exposure to polymers, the cells were washed with PBS and MEM without phenol red and serum was added ($75\ \mu\text{L}$). A solution of sodium 3'-[1-

(phenylaminocarbonyl)-3,4-tetrazolium]-bis (4-methoxy-6-nitro) benzene sulfonic acid hydrate (XTT) and an electron-coupling reagent N-methyl dibenzopyrazine methyl sulfate (PMS) were added to each well to give the final concentration of 0.2 mg/mL, and 1.5 μ g/mL, respectively. To assess the effect of polymers on the conversion of substrate, control wells containing only medium, polymer, and XTT with PMS were included. After 4-h incubation at 37 °C in the presence of 5% CO₂, the amount of the orange colored formazan derivative produced by the metabolic cellular activity was determined by the absorbance at 450 nm (test wavelength) and 750 nm (background wavelength). The spectrophotometer was calibrated to zero absorbance using medium without cells. The cell viability was determined relative to that of a control containing intact cells which were exposed to only solvent. All samples were run in triplicate.

Fluorescence Imaging

A culture of *E.coli* ATCC 25922 and *S.aureus* ATCC 25923 cells grown overnight were washed with PBS buffer two times by centrifuging at 6,000 rpm for 5 min. Cells were resuspended in the same volume of PBS buffer. FITC-labeled polymers were added to a final concentration of 10 μ M. Mixtures were incubated for 45min in the dark at room temperature before propidium iodide (PI) was added to each mixture at the final concentration of 1.5 μ M and incubated for another 15 min in the dark. Then, a 3 μ l aliquot was spotted on a sterile glass slide, covered with a coverslip, and observed under a fluorescence microscope with appropriate filters. Image acquisitions were performed with Olympus IX71 (Olympus, Center Valley, PA) equipped with detectors and filter sets for monitoring of FITC (490nm/525nm) and PI (536nm/617nm). Images were obtained using an oil immersion 100 \times objective lens. To assess the effect of PEG on the polymer-cell interactions, the assay was repeated with PEG 6k at a final concentration of 15 μ M.

Flow Cytometry Analysis

E. coli and *S. aureus* cells were cultured and treated with polymers as described above. Cells from the same cultures, but without the polymer treatment, served as controls. Analyses were conducted with a flow cytometer (EPICS ALTRA, Beckman Coulter, Brea, CA). Bacteria population was gated based on forward scatter (FS) and side scatter (SS). A discriminator was set on SS to control a lower than 5% background noise level. Cell density was adjusted to approximately 10⁶ cells/ml and flow rate was adjusted

to achieve an analysis data rate of around 4,000 cells per second. A total of 30,000 cells were collected for each analysis. Green fluorescence intensity (525 nm filter) for the gated bacteria population was collected and analyzed. Measurement for each sample was reproduced twice.

***E. coli* Membrane Permeabilization**

E. coli D31 in LB broth supplemented with 100 μ g/mL ampicillin (LB-Amp) was incubated for 18-24 hours at 37° with vigorous shaking. An aliquot of the culture was then diluted 1:500 in fresh LB-Amp media supplemented with 2mM Isopropyl β -D-1-thiogalactopyranoside (IPTG, Research Products International) and incubated at 37° to OD₆₀₀ ~ 0.3. Serial dilutions of the polymers or the detergent cetyl trimethyl ammonium bromide (CTAB) were mixed (10 μ L) with Z-buffer (40mM Na₂HPO₄, 60mM NaH₂PO₄, 10mM KCl, 1mM MgSO₄, 50mM β -mercaptoethanol, pH 7.0, 56.25 μ L) and a 4 mg/mL solution of the chromogenic β -galactosidase substrate ortho-Nitrophenyl- β -galactoside (ONPG, Rockland Immunochemical), also dissolved in Z-buffer (15 μ L). Just prior to measurement, 18.75 μ L *E. coli* culture was added to all 96 wells for a final volume of 100 μ L. Using a Thermo Multiskan instrument, sample absorbance was monitored at 420nm in 5 minute intervals with periodic agitation between readings. All experiments were performed in duplicate or triplicate.

E. coli D31 in LB-Amp was incubated for 18-24 hours at 37° with vigorous shaking. An aliquot of the culture was then diluted 1:500 in fresh LB-Amp media and incubated at 37° C to OD₆₀₀ ~ 0.2. The culture was then centrifuged and resuspended in an equal volume of PBS buffer (25mM phosphate, 150mM NaCl, pH 7.0). Serial dilutions of the polymers and polymyxin (Sigma) were mixed (10 μ L) with *E.coli* D31 in PBS (80 μ L) on a 96-well microplate. Just prior to measurement, nitrocefin (EMD biosciences) was added to each well to a concentration of 50 μ g/mL. Using a Thermo Multiskan instrument, sample absorbance was monitored at 486nm in 5 minute intervals with periodic agitation between readings. All experiments were performed in duplicate or triplicate.

Molecular Dynamics Simulations

Model syndiotactic alternating copolymers with DP = 10 and $f_{HB} = 0.5$ were inserted in aqueous phase above pre-equilibrated DOPC and POPC-POPG (1:1) bilayers

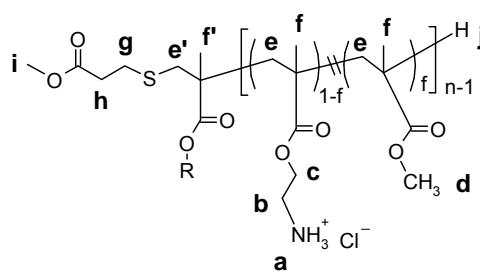
and each system (eight in total) was simulated for 50 ns each. Counterions were added to each system for overall charge neutrality. All the eight systems were simulated under isothermal-isobaric ensemble conditions (305K temperature and 1 atm pressure). The long-range Coulomb interactions were dealt with particle mesh Ewald method. An integration time step of 1.0 fs was used for first 10 ns and a time step of 2 fs was used for all subsequent runs. All the simulations were performed by NAMD2.7.¹⁷⁴ The forcefield parameters for polymers were adopted from our previous simulations¹⁷³ and the latest forcefield of CHARMM36¹⁷⁵ was used for lipids and water was modeled by TIP3P model.¹⁷⁶

APPENDIX B
Polymer Characterization

Characterization of Copolymers by ¹H NMR

Tables B1-B6 show the chemical structure of copolymers in each series and their ¹H NMR peak assignments. For representative polymers, the NMR spectra are also shown (Figures B1-B3) and the analysis of peak integrations to find DP and f_{methyl} or f_{butyl} are described in detail. In each case, the integration of peaks in the region 2.9-2.5 ppm, corresponding to protons in the polymer terminal groups (**h+g+e'+j** in the tables), was normalized to 7.00. Then, the peak integrations arising from the polymer side chains were compared to give the values of DP and f_{methyl} or f_{butyl} . For example, Figure B1 shows the spectrum of copolymer PM₂₉

Table B-1. Characterization of the polymers bearing primary amines and methyl groups, the PM series

	ppm	peak	Assignment
	4.28	bs	c
	3.69-3.63	s & bs overlap	d + i
	3.3	bs	b
	3.0-2.5	mult	h+g+e'+j
	2.5-2	mult	e
	1.5-1.0	mult	f

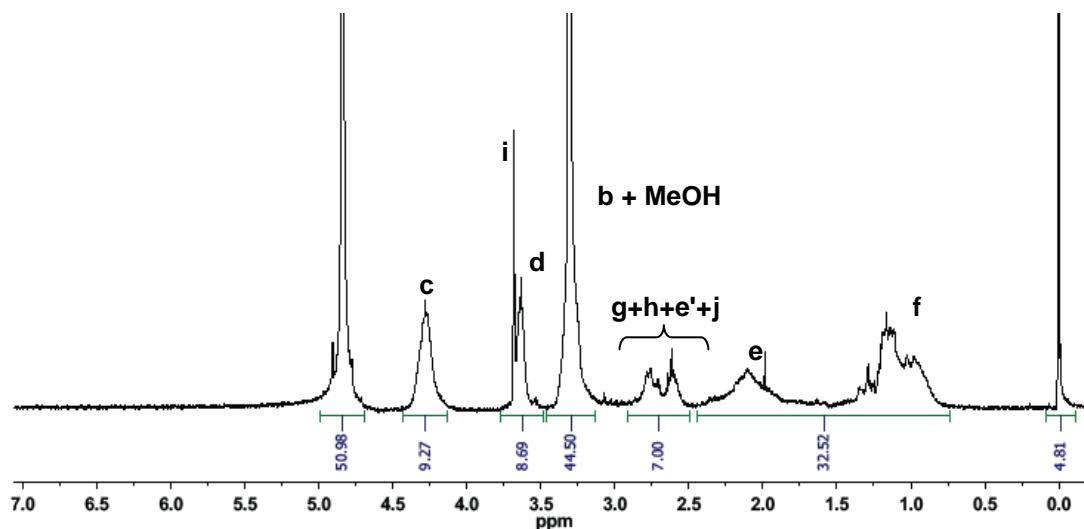


Figure B-1. ^1H NMR spectrum of copolymer with primary amines, PM_{29}

The spectrum contains a broad singlet centered at 4.28 ppm with integration equal to 9.27, which we assign to the methylene protons adjacent to the ester in the amine-functionalized repeat units (**c**). Hence,

$$9.27 = n_{\text{amine}} * 2$$

$$n_{\text{amine}} = 4.635$$

where n_{amine} is the average number of amine-functionalized repeat units per individual polymer chain. The spectrum also shows a sharp singlet overlapping with a broad singlet near 3.6-3.7 ppm. The total integration equals 8.68. The sharp singlet is assigned to the three methyl protons on the polymer end group (**i**), whereas the broad feature represents the three protons of each methyl ester side chain (**d**). Hence,

$$8.68 = 3 + n_{\text{methyl}} * 3$$

$$n_{\text{methyl}} = (8.68-3) / 3 = 1.893$$

where n_{methyl} is the average number of methyl repeat units per individual polymer chain. The number average degree of polymerization (DP) is the sum of n_{amine} and n_{methyl} . The mole fraction of methyl groups in the copolymer, f_{methyl} , equals the number of repeat units with methyl side chains divided by the DP. Hence,

$$\text{DP} = n_{\text{amine}} + n_{\text{methyl}} = 6.528$$

$$f_{\text{methyl}} = n_{\text{methyl}} / \text{DP} = 0.29$$

This is the copolymer PM₂₉ with DP = 6.5. All of the copolymers in this study were characterized by a similar procedure. The peak arising from the *t*-butyl ester protons of the Boc protecting groups (1.4 ppm) is not observed in any of the spectra, indicating quantitative removal of Boc was achieved within the detection limit of the NMR. As additional examples, the ¹H NMR spectra of TM₄₆ (Figure S2) and QB₃₉ (Figure S3) are also shown and the detail of the peak integration analyses are described.

Table B-2. Characterization of the polymers bearing tertiary amines and methyl groups, the TM series

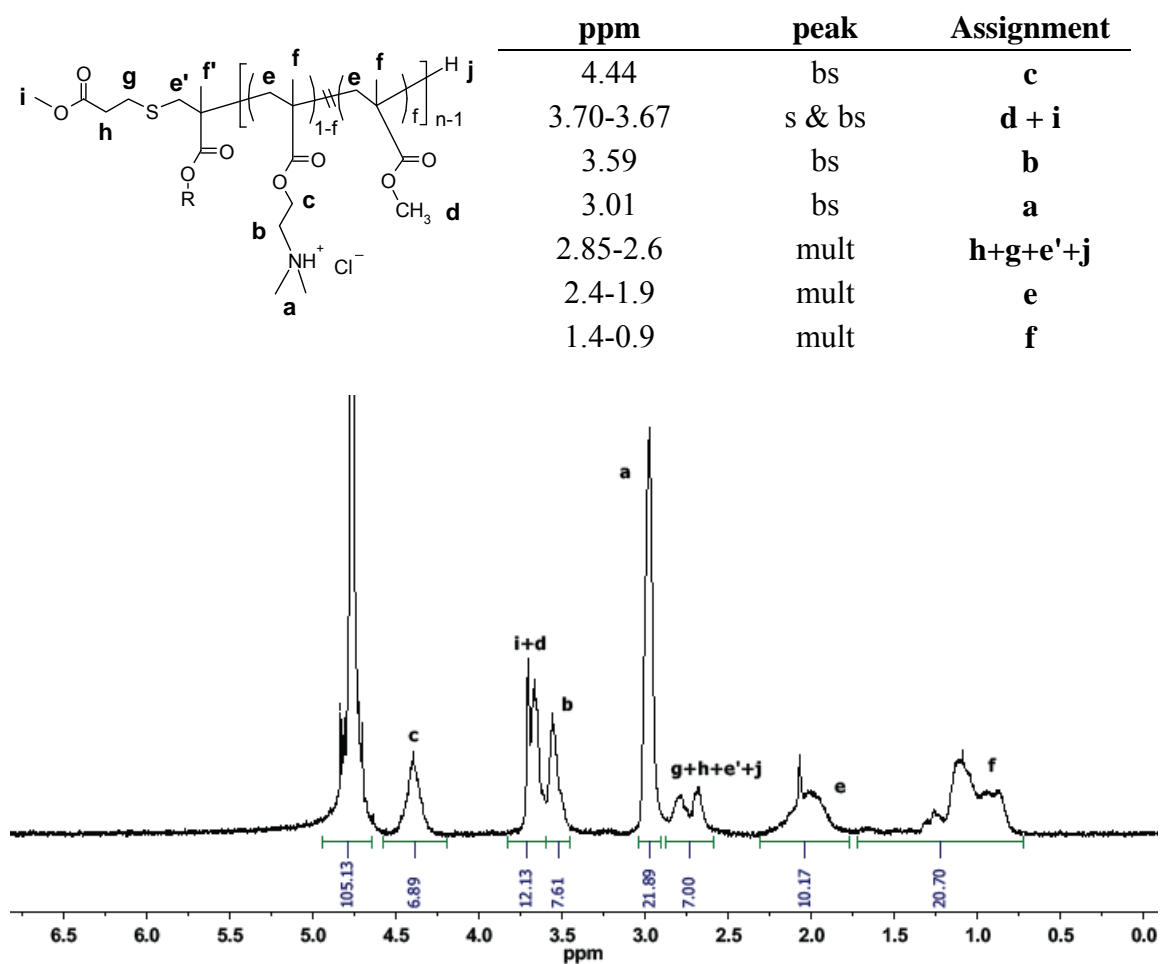


Figure B-2. ¹H NMR spectrum of copolymer with tertiary amines, TM₄₆

The integration of the peak at 4.39 ppm (**c**) and the peak at 3.56 ppm (**b**) each correspond to twice the number of amine side chains per polymer. The integration of the

peak at 2.98 ppm corresponds to six times the number of amine side chains per polymer. We calculate n_{amine} based on each of these peaks and take the average.

$$n_{\text{amine}} = 6.89/2 = 3.445 \text{ or } 21.89/6 = 3.648.$$

The average $n_{\text{amine}} = 3.63$

The broad singlet and sharp singlet overlapping near 3.6-3.7 ppm are the methyl ester end group of the polymer and the methyl ester side chains.

$$n_{\text{methyl}} = (12.13-3)/3 = 3.04$$

$$DP = n_{\text{amine}} + n_{\text{methyl}} = 6.67$$

$$f_{\text{methyl}} = n_{\text{methyl}}/DP = 0.46$$

Table B-3. Characterization of the polymers bearing quaternary ammonium salt groups and methyl groups, the QM series

	ppm	peak	Assignment
	4.55	bs	c
	3.85	bs	b
	3.74-3.70	s & bs	d + i
	3.30	bs	a
	2.9-2.6	mult	h+g+e'+j
	2.4-1.9	mult	e
	1.4-0.9	mult	f

Table B-4. Characterization of the polymers bearing primary amines and butyl groups, the PB series

	ppm	peak	Assignment
	4.28	bs	c
	3.99	bs	d
	3.68	s	i
	2.8-2.5	mult	h+g+e'+j
	2.4-1.9	mult	e
	1.7-0.8	mult	f+k+l+m

Table B-5. Characterization of the polymers bearing tertiary amines and butyl groups, the TB series

	ppm	peak	Assignment
	4.38	bs	c
	4.01	bs	d
	3.68	s	i
	3.54	bs	b
	3.03	bs	a
	2.8-2.5	mult	h+g+e'+j
	2.3-1.9	mult	e
	1.7-0.8	mult	f+k+l+m

Table B-6. Characterization of the polymers bearing quaternary ammonium salt groups and butyl groups, the QB series

	ppm	peak	Assignment
	4.58	bs	c
	4.11	bs	d
	3.85	bs	b
	3.75	s	i
	3.31	bs	a
	2.9-2.6	mult	h+g+e'+j
	2.2-1.8	mult	e
	1.8-0.8	mult	f+k+l+m

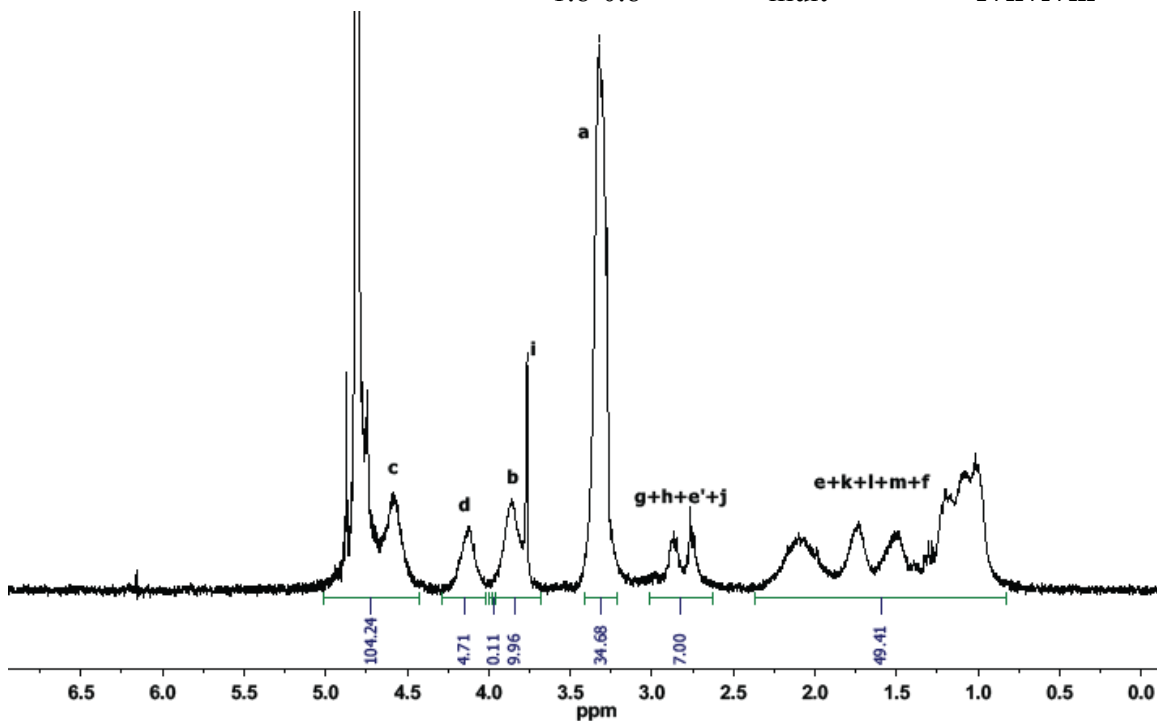


Figure B-3. ^1H NMR spectrum of copolymer with quaternary ammonium salts, QB₃₉

The integration of the peak at 3.31 ppm (**a**) corresponds to nine times the number of amine side chains per polymer. The integration of the peaks near 3.7 ppm correspond to the methyl group of the polymer terminal (**i**) plus the methylene protons adjacent to the QAS groups (**b**).

$$34.68 = 9 \cdot n_{\text{amine}} \text{ or } 9.96 = 3 + 2 \cdot n_{\text{amine}}$$

$$\text{The average } n_{\text{amine}} = 3.667$$

The integration of the peak at 4.11 ppm (**d**) corresponds to twice the number of butyl side chains per polymer.

$$n_{\text{butyl}} = 4.71/2 = 2.355$$

$$\text{DP} = n_{\text{amine}} + n_{\text{butyl}} = 6.02$$

$$f_{\text{butyl}} = n_{\text{butyl}} / \text{DP} = 0.39$$

Notably, no signals appear in the 5.5-6.5 ppm region, indicating that unreacted monomer was completely removed.

For the Dansyl-labeled polymers, similar spectra were obtained (Figure B4).

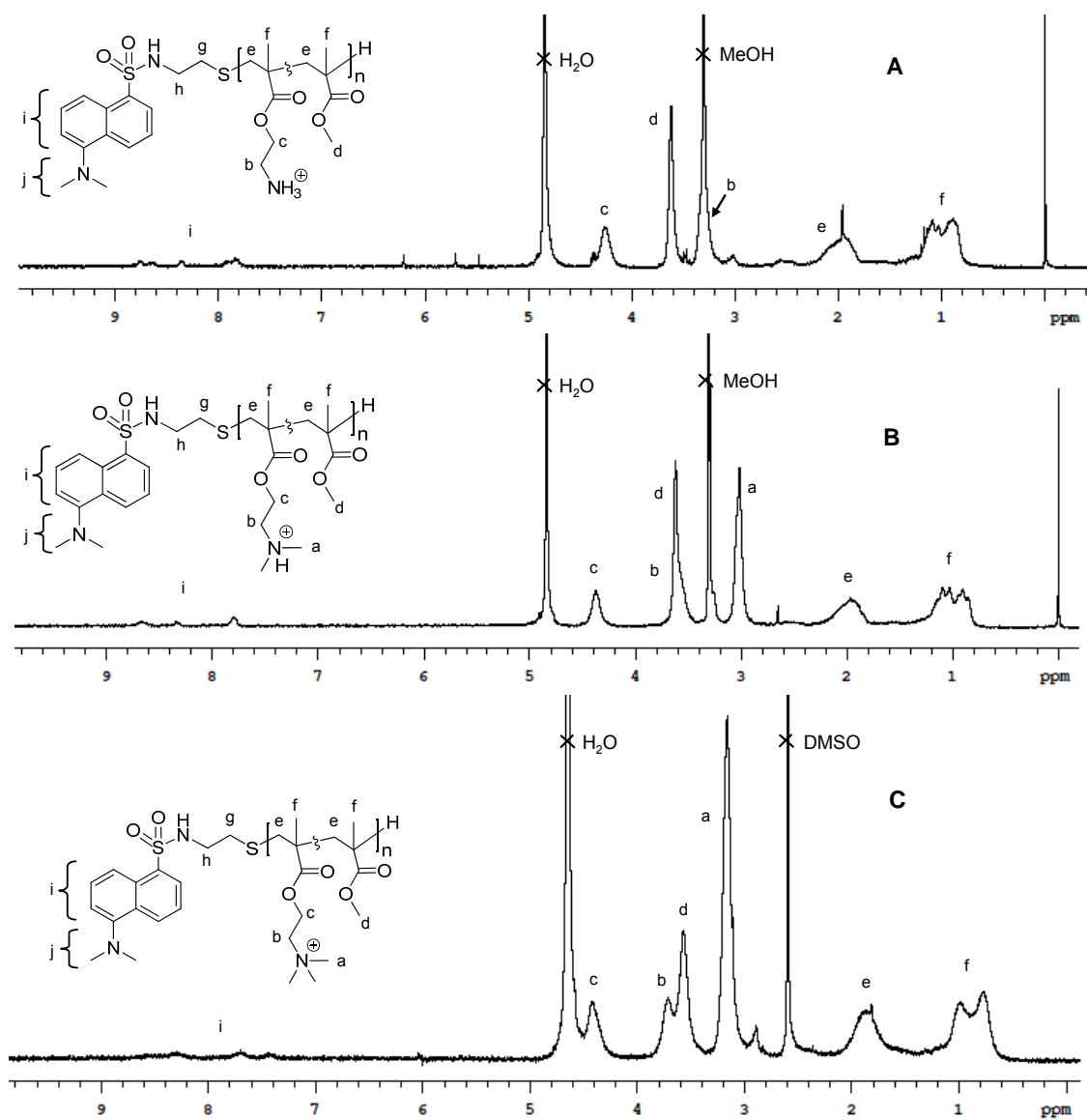


Figure B-4. ^1H NMR spectrum of dansyl-labeled copolymers

Furthermore, a similar analysis was employed for the copolymers with various cationic side chain spacer groups, discussed in Chapter V (Figure B5).

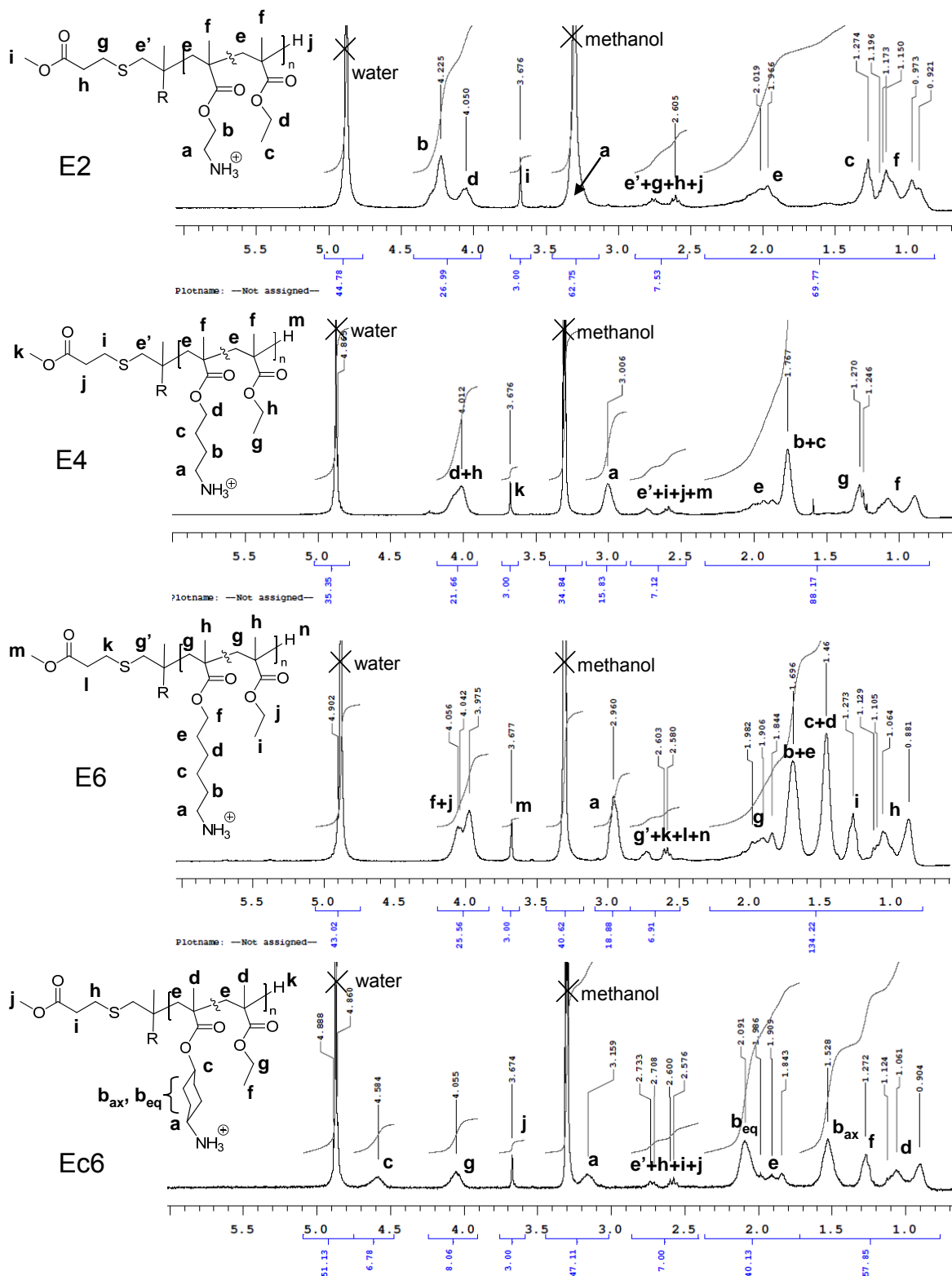


Figure B-5. ¹H NMR spectra of the representative copolymers with varying spacer arms

The stability of the monomer aminoethylmethacrylate was examined by NMR before and after incubating in pH 10 for 1 hour. Boc-AEMA was deprotected to give AEMA HCl. The cationic monomer was precipitated from methanol into diethylether. The precipitate was collected by centrifugation and then lyophilized. It was confirmed that the monomer isomerizes to the corresponding methacrylamide in alkaline conditions.

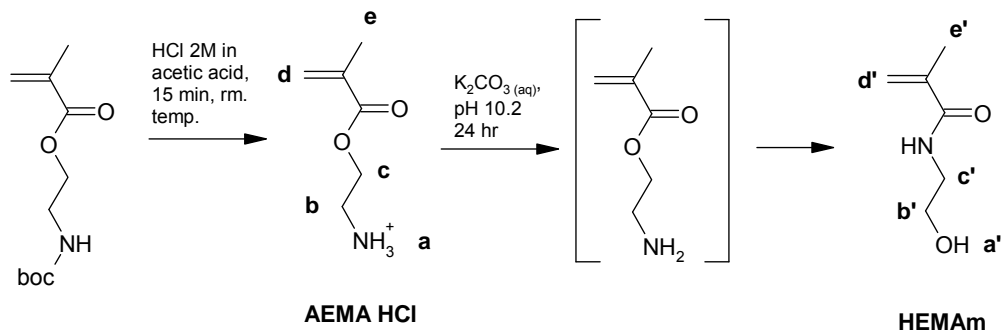


Figure B-6. Base-induced isomerization of the methacrylate containing a primary amine in the side chain

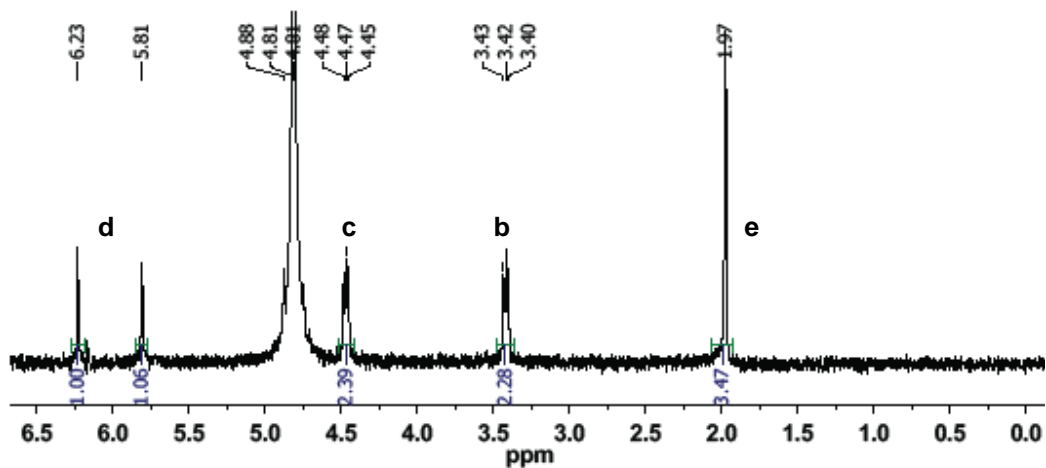


Figure B-7. ^1H NMR of the methacrylate monomer, AEMA HCl (300 MHz, D_2O)

AEMA HCl was then dissolved in 10% $\text{K}_2\text{CO}_3(\text{aq})$, pH 10.2, room temp for 24 hr. The lyophilized powder was added to methanol- d_4 and filtered. NMR was performed on the clear filtrate.

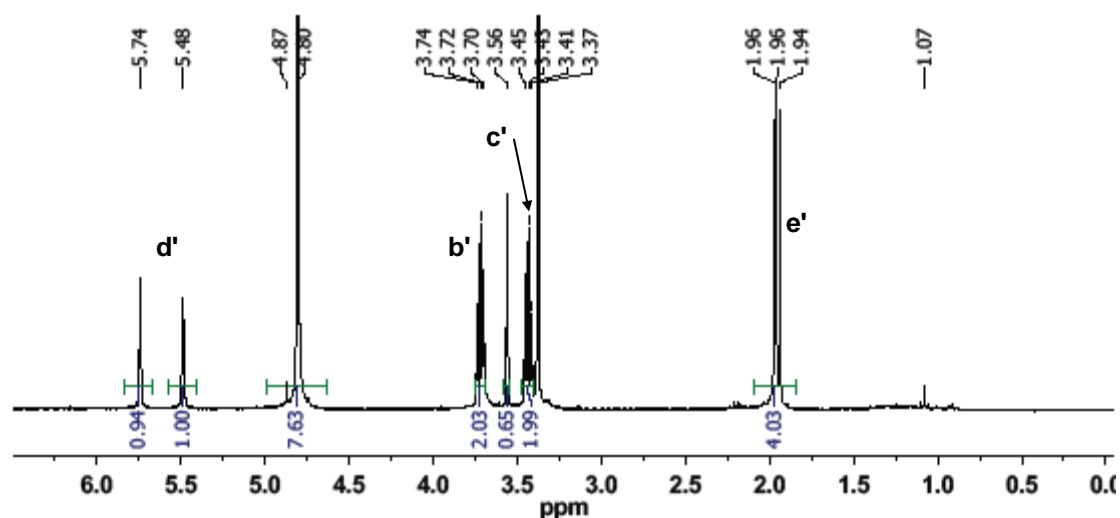


Figure B-8. ^1H NMR of the isomerized methacrylamide monomer, HEMAm (300 MHz, methanol- d_4)

For the methacrylamide platform, discussed in Chapter IV, a slightly modified procedure for the NMR analysis was employed. As an example, the spectrum of the representative copolymer PH₃₃ and the analysis of the relative integrated areas are shown in detail (Figure B9).

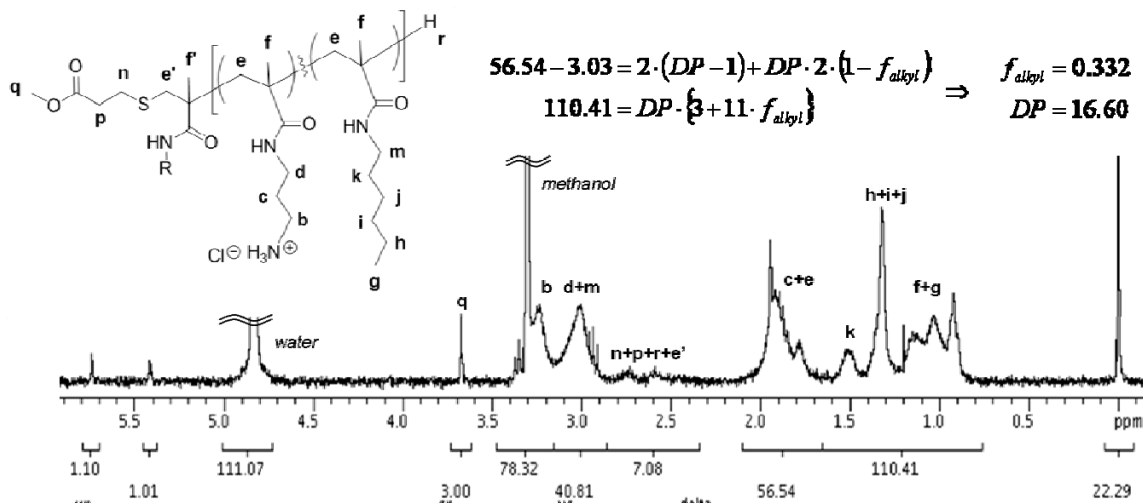


Figure B-9. ^1H NMR spectrum of methacrylamide copolymer, PH₃₃

The NMR spectra revealed that the desired copolymers were obtained in good conversion (> 90%), although some amount of unincorporated amino monomer was detected in all cases. Unfortunately, the unreacted monomer could not be separated from

the polymer by precipitation. It may be possible to remove the unincorporated monomer by dialysis or size exclusion chromatography in future experiments. However, since the monomer displayed no observable antimicrobial, hemolytic activity, or cytotoxicity in control experiments up to the highest concentration, the presence of trace monomer was neglected.

The sharp singlet at 3.67 ppm was assigned to the methyl ester of the polymer terminal group (**q**) and hence the peak integration was normalized to 3.00 protons per polymer chain. The broad features which appear from 2.1-1.6 ppm represent the two methylene backbone protons of each repeat unit, except the one adjacent to the thioether end group, (**e**) plus two of the methylene protons in each of the amine-functionalized repeat units (**c**). These collectively gave an integrated area of 56.54. The methyl protons of the unreacted methacrylamide monomer overlap in this region. Based on the integration of the unreacted alkene proton signal at 5.4 ppm, we subtract 3.03 from the total 56.54 to obtain the integrated area arising only from the polymer. The group of peaks from 1.6-0.9 ppm represents the sum of the three methyl protons of the polymer backbone (**f**) and eleven of the hexyl side chain protons (**g-k**) and showed an integrated area of 110.41. Based on these assignments, two algebraic expressions can be derived and solved simultaneously for DP and f_{alkyl} , as shown in the figure. The solution is $f_{alkyl} = 0.332$ and DP = 16.60, which reflect the values given in Table 1 rounded to two significant figures.

The calculated f_{alkyl} values of the random copolymers were correlated well with the ratio of alkyl methacrylate to total monomer in the feed polymerization mixtures (Figure B-10).

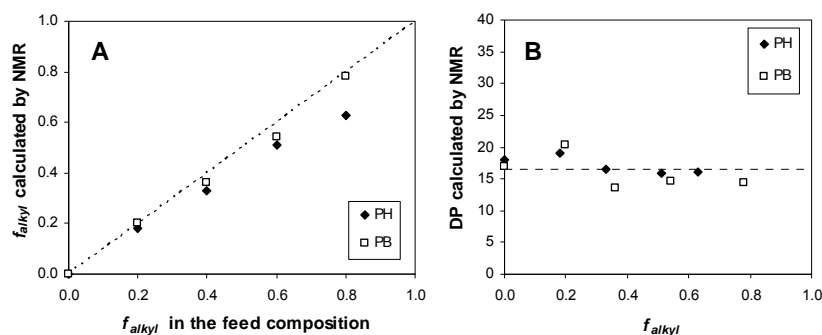


Figure B-10. Calculated mole fractions of hydrophobic comonomer and degree of polymerizations based on interpretation of the ^1H NMR spectra

NMR end-group analysis of all of the copolymers in this study showed that the f_{alkyl} observed was roughly the same as the f_{alkyl} in the feed, suggesting reactivity ratios of each monomer close to unity. The exception to this trend is the polymer PH₆₃, which differs significantly from the feed ratio of 80% hexylmethacrylamide. However, this effect is likely due to the highly hydrophobic nature of that copolymer: when the crude reaction mixture was precipitated from diethylether, copolymers containing higher percentages of hexylmethacrylamide units likely remained in the ether supernatant and thus altered the observed average f_{alkyl} in that case.

In each polymerization, the ratio of thiol chain transfer agent to total monomers was held fixed at $[MMP]/[monomers] = 0.05$. Analysis of the NMR spectra indicated that the DP values range from 14-20. These polymers readily dissolved in 0.01% acetic acid in water at a concentration of 20 mg/mL and Muller Hinton broth at 2 mg/mL. They were also soluble in other polar solvents such as DMF, DMSO, and methanol. Copolymers with higher f_{alkyl} values than those reported were not analyzed due to poor water solubility.

Characterization of the Copolymers by MALDI-TOF-MS

The copolymers with various spacer groups, discussed in chapter IV, were also characterized by MALDI-TOF MS. The chromatographs for the unlabeled copolymers (Figure B-11) are comparable to those of the FITC-labeled polymers (Figure B-12), suggesting similarly low MW materials were obtained by the different thiol chain transfer agents.

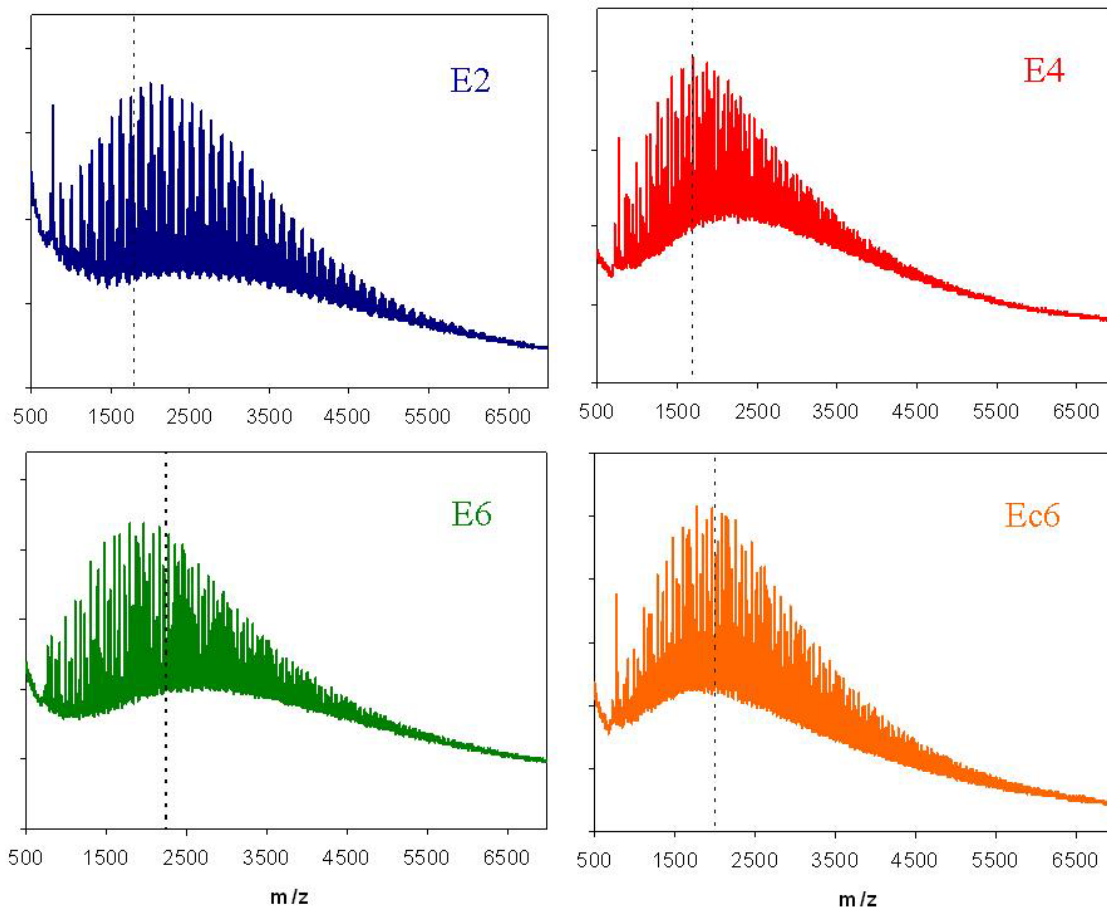


Figure B-11. MALDI-TOF-MS chromatographs of representative copolymers. The vertical dotted lines represent the number average molecular weight calculated from the ¹H NMR spectra (excluding the mass of the TFA counterions).

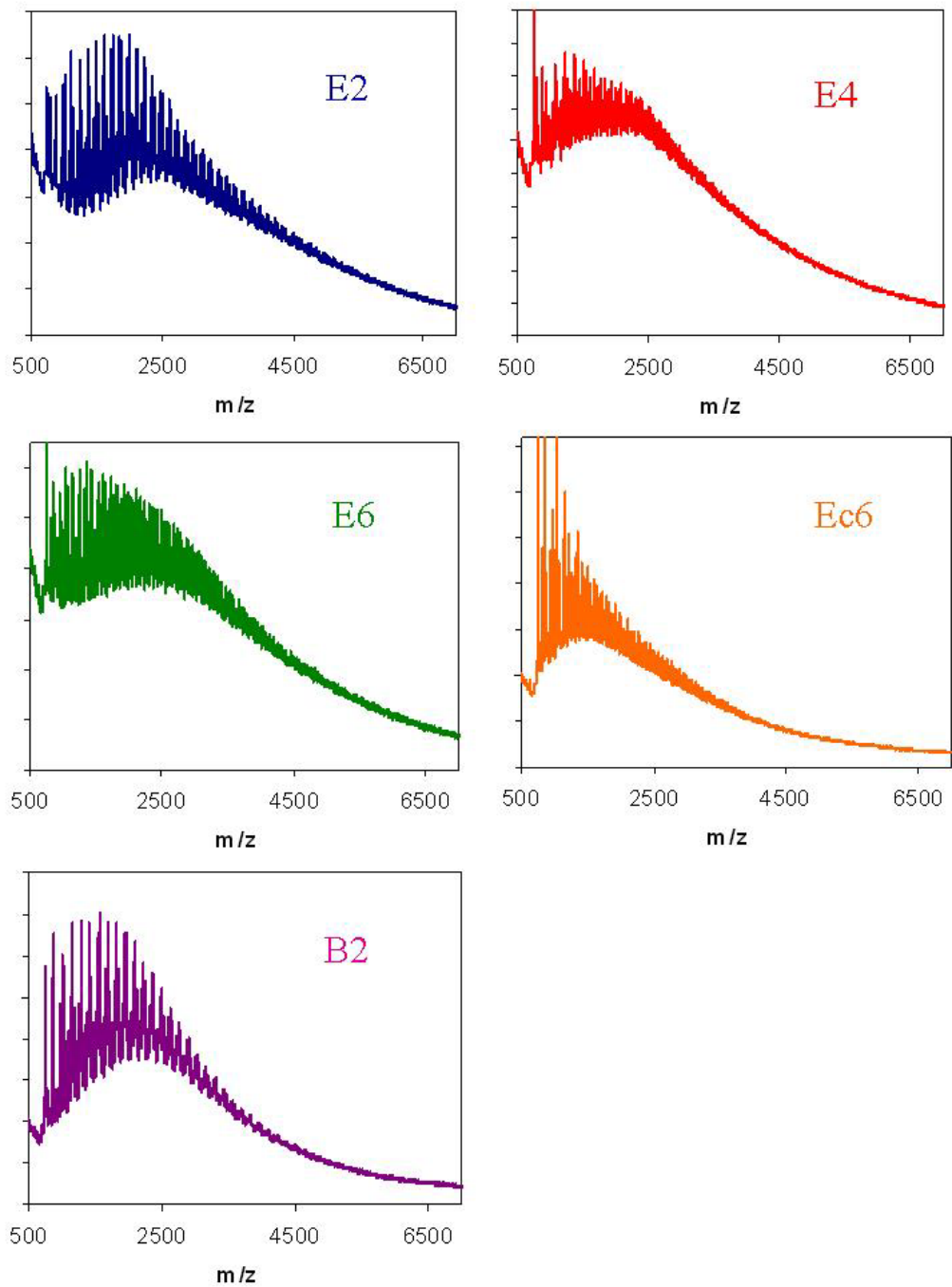


Figure B-12. MALDI-TOF-MS chromatographs of fluorophore-labeled copolymers

Absorbance and Emission of Dye-Labeled Polymers

The dansyl-functionalized copolymers described in Chapter III were characterized by absorbance and emission spectra to give the data shown in Table III-1. The data show that the polymer-bound dye has similar photophysical properties as the unconjugated dye.

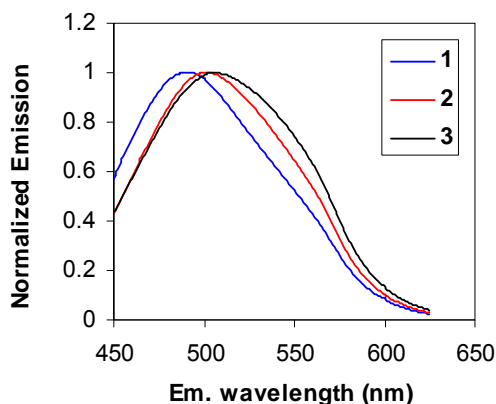


Figure B-13. Normalized emission of the dansyl-labeled polymers, in MES-buffered saline, pH 6.

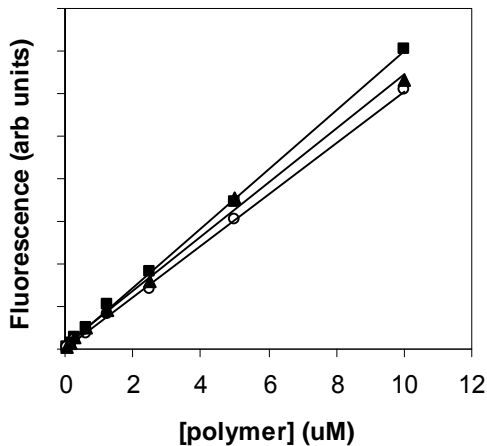


Figure B-14. Fluorescence intensity versus concentration of the polymers in methanol, used as the calibration curves for the calculation of partition coefficients.

The FITC-labeled copolymers described in Chapter V were also characterized by absorbance and emission spectra. The data show that the polymer-bound dye has similar photophysical properties as the unconjugated dye.

Table B-7. Characterization of the FITC-labeled polymers

Polymer	f_{HB}^a	DP ^b	M_n^c (kDa)	Abs. λ_{max} (nm)	Em . λ_{max} (nm)	MIC (μ M)		HC ₅₀ (μ M)
						<i>E. coli</i>	<i>S. aureus</i>	
F-E2 ₃₂	0.32	20.8	4660	498	520	12.5	25	74
F-E4 ₃₄	0.34	15.4	3819	500	521	6.3	12.5	64
F-E6 ₃₀	0.30	18.0	4835	499	521	1.5	3.1	0.51
F-Ec6 ₂₈	0.28	15.7	4340	500	522	6.3	12.5	41
F-B2 ₃₇	0.37	19.7	4527	498	521	3.1	12.5	5.3

- a) Average fraction of the hydrophobic repeat units in the copolymers, based on peak integration of the ¹H NMR spectra
 b) Average degree of polymerization based on peak integration of the ¹H NMR spectra
 c) Number average molecular weight, including the TFA counterions, based on peak integration of the ¹H NMR spectra.

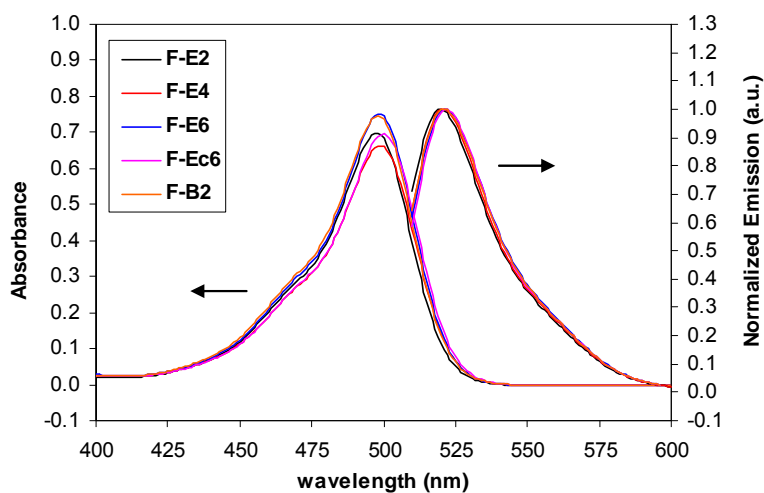


Figure B-15. Absorbance and Emission spectra of the FITC-labeled polymers

Supplemental Fluorescence Images

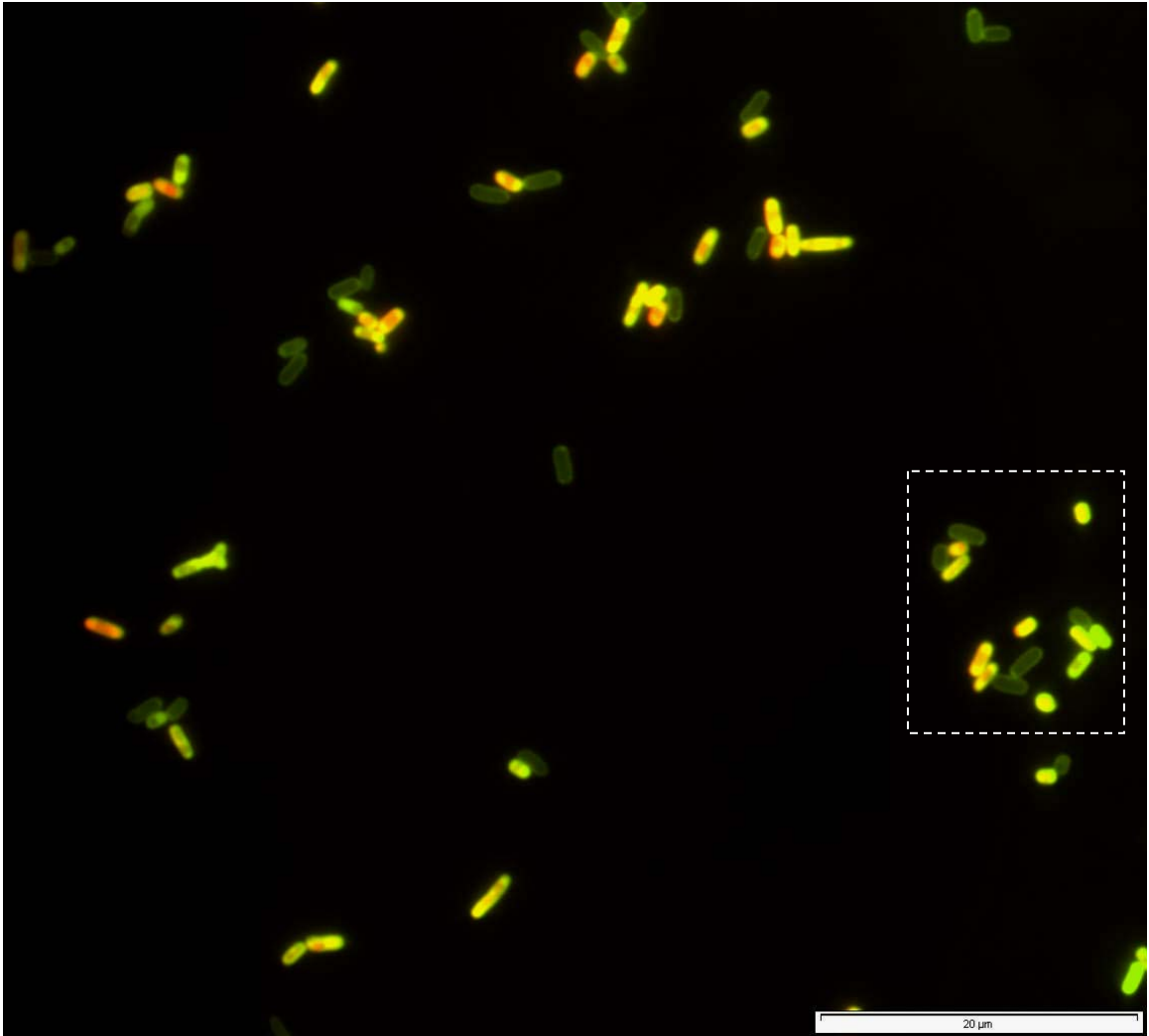


Figure B-16. Epifluorescence image of *E. coli* cells incubated with 10 μM F-E2 (green signal) for 45 min and 1.5 μM PI (red signal) for an additional 15 min. The area of the image within the white dotted line is the cropped image in the text.

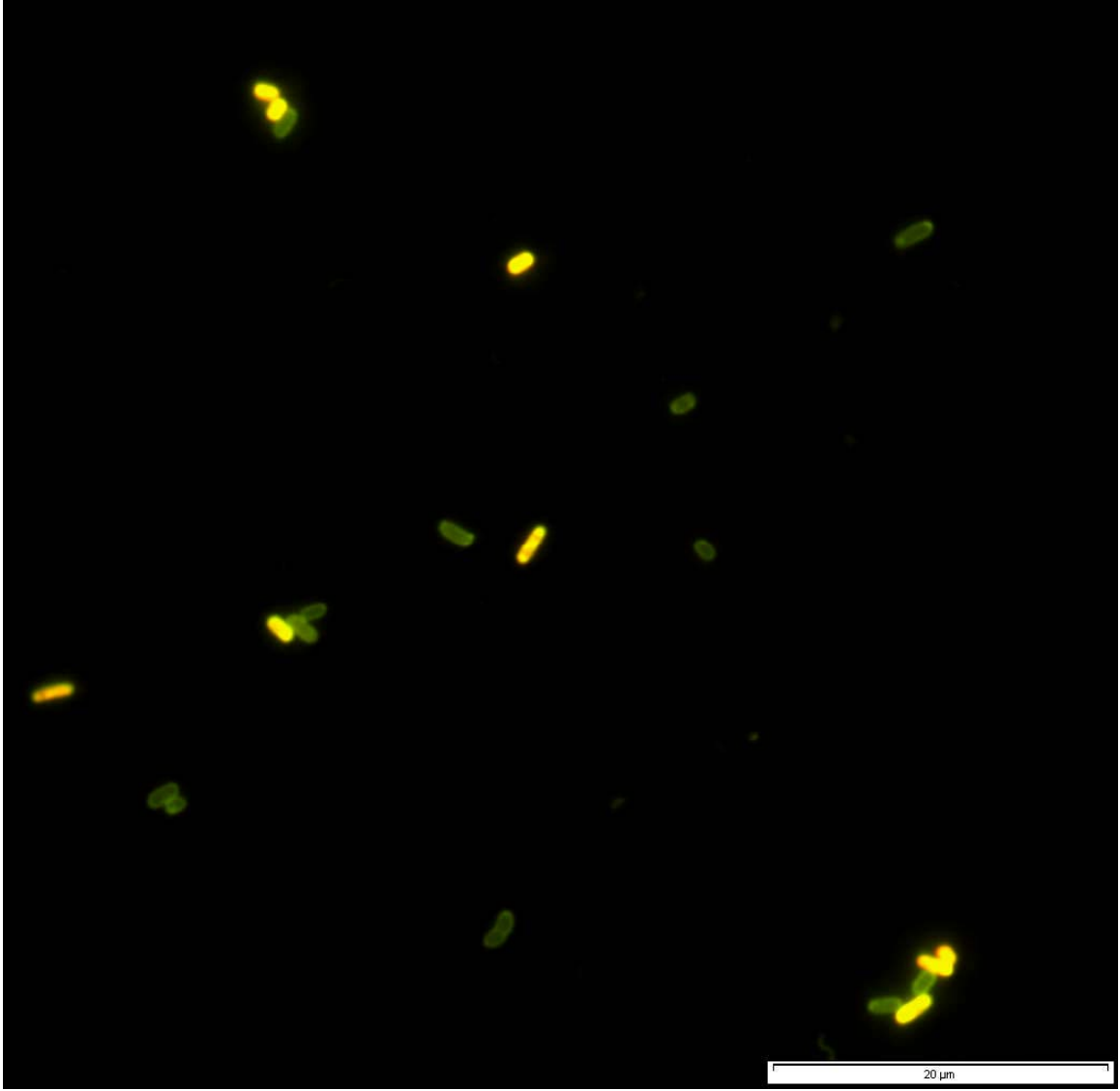


Figure B-17. Epifluorescence image of *E. coli* cells incubated with 10 μM F-E4 (green signal) for 45 min and 1.5 μM PI (red signal) for an additional 15 min.

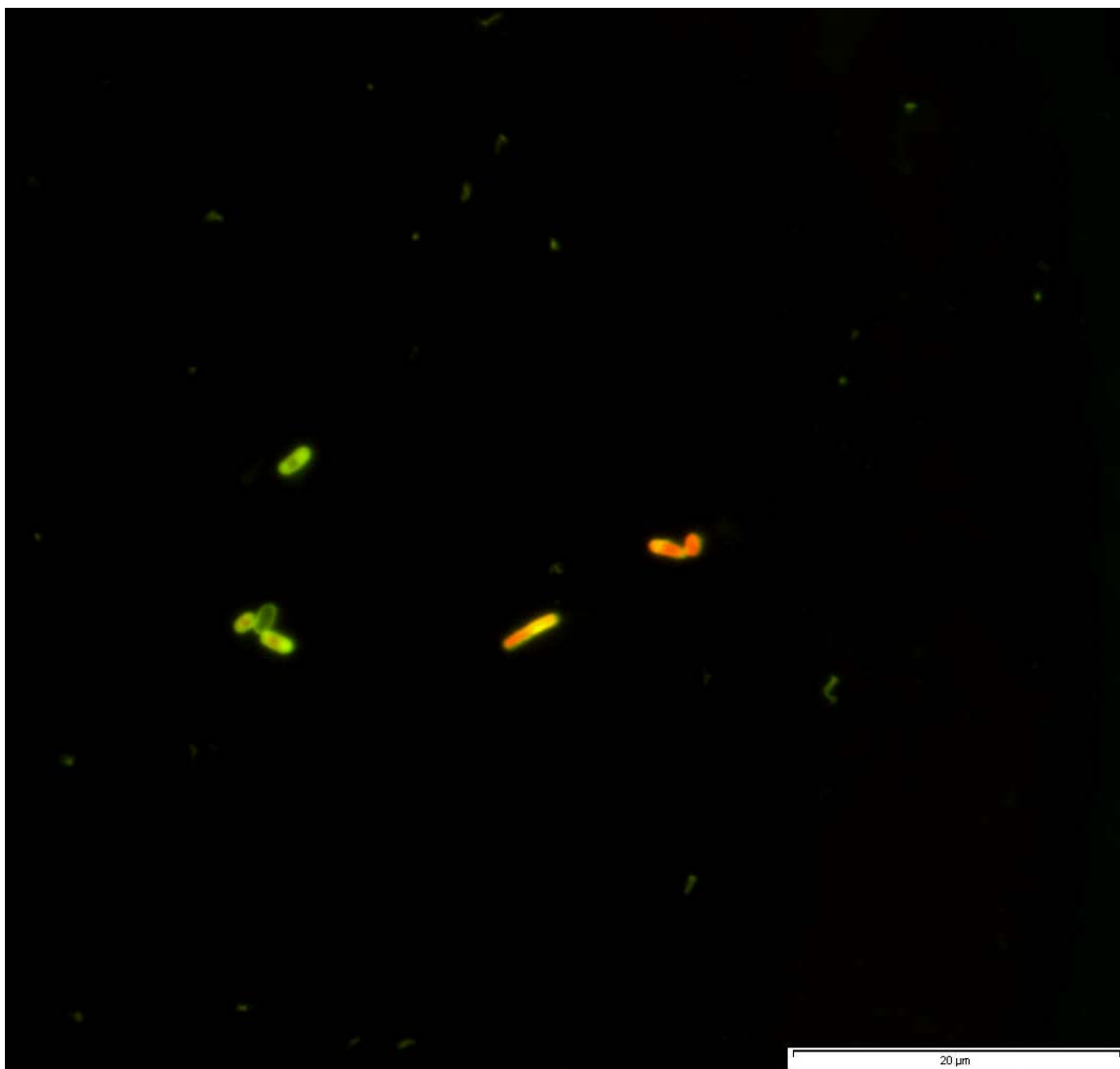


Figure B-18. Epifluorescence image of *E. coli* cells incubated with 10 μM F-E6 (green signal) for 45 min and 1.5 μM PI (red signal) for an additional 15 min. The punctuate green fluorescence seen in the background is likely due to either the debris of dead cells with F-E6 bound or aggregation/precipitation of the hydrophobic polymers.

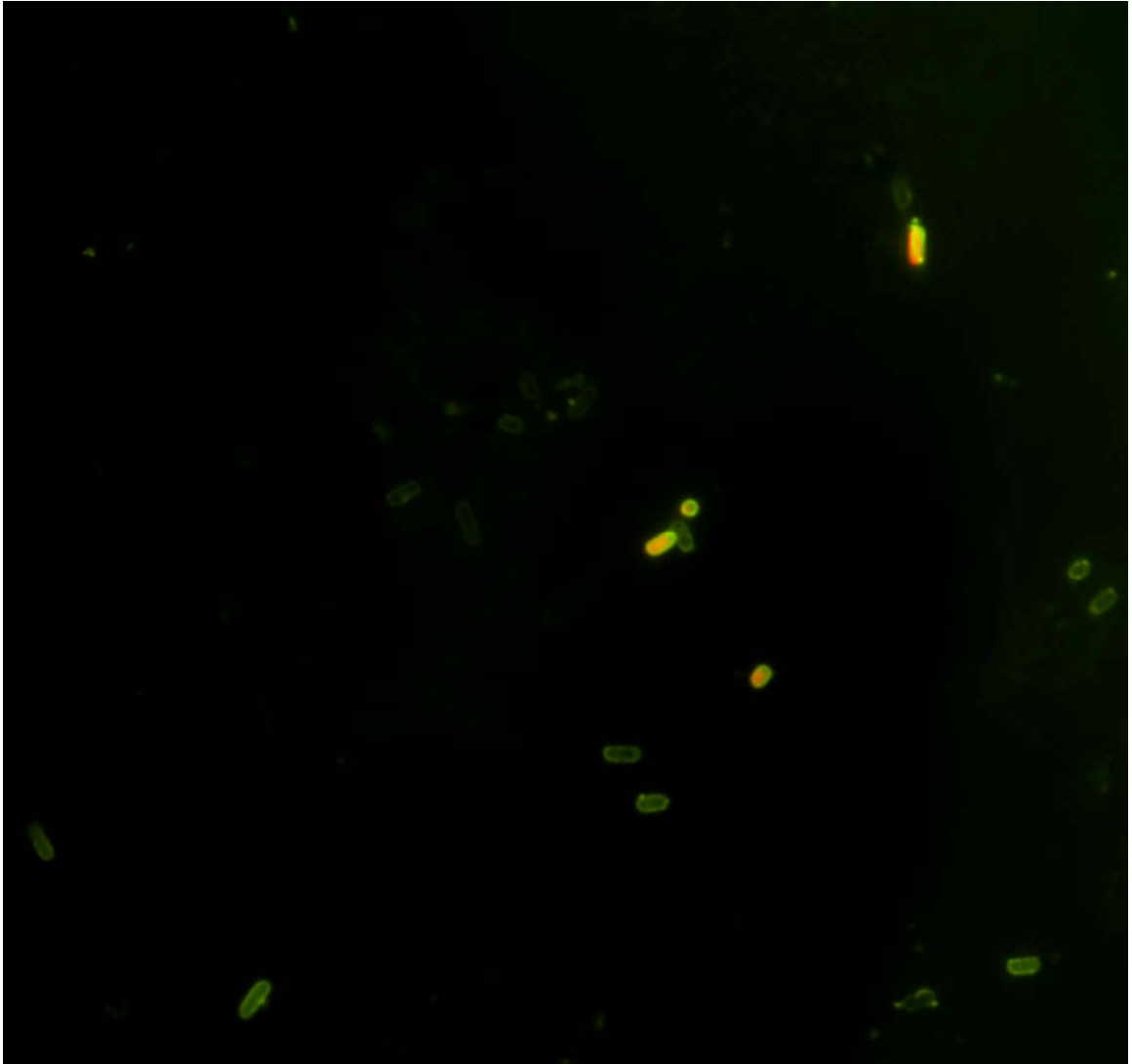


Figure B-19. Epifluorescence image of *E. coli* cells incubated with 10 μ M F-Ec6 (green signal) for 45 min and 1.5 μ M PI (red signal) for an additional 15 min.

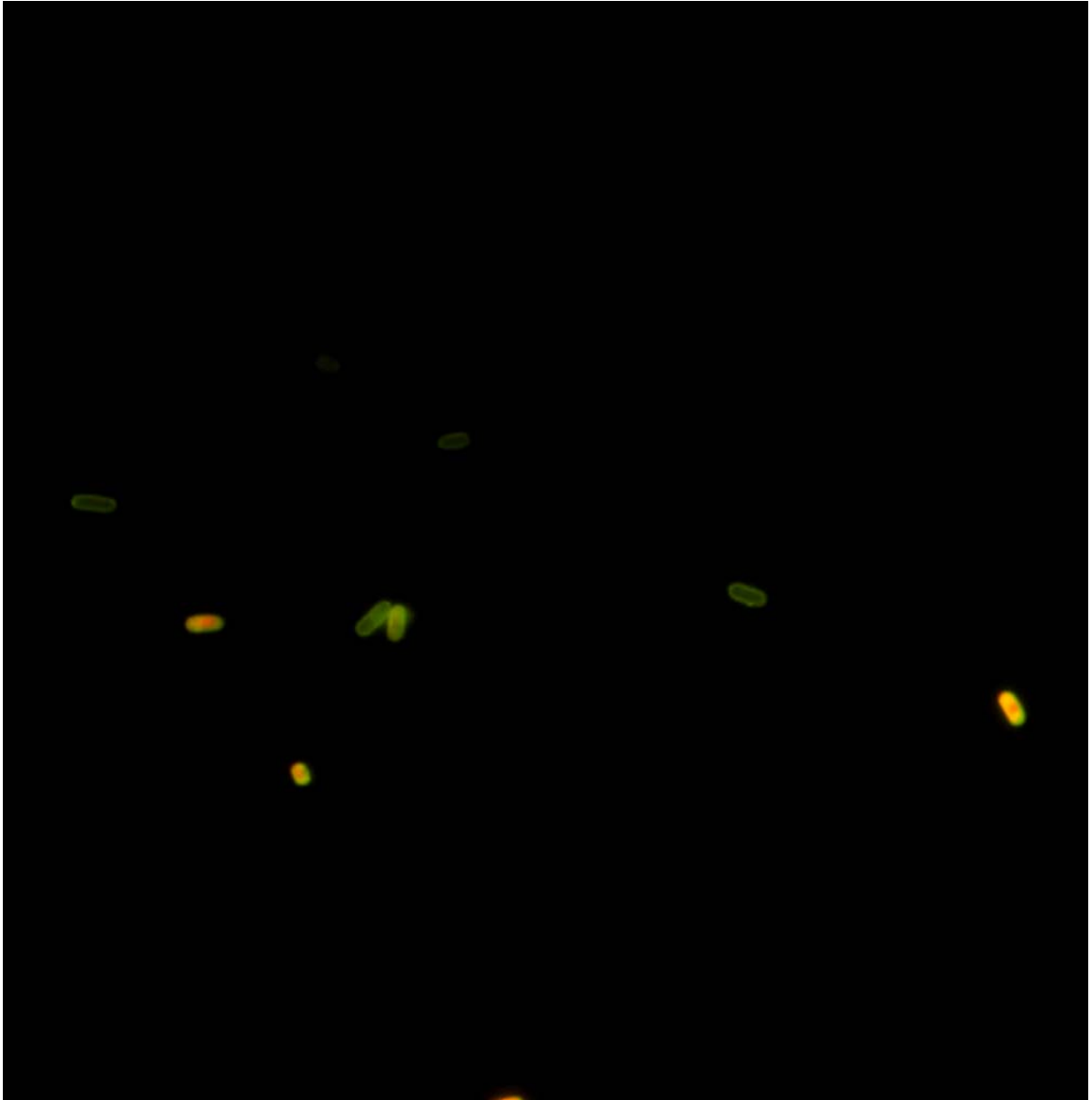


Figure B-20. Epifluorescence image of *E. coli* cells incubated with 10 μ M F-B2 (green signal) for 45 min and 1.5 μ M PI (red signal) for an additional 15 min

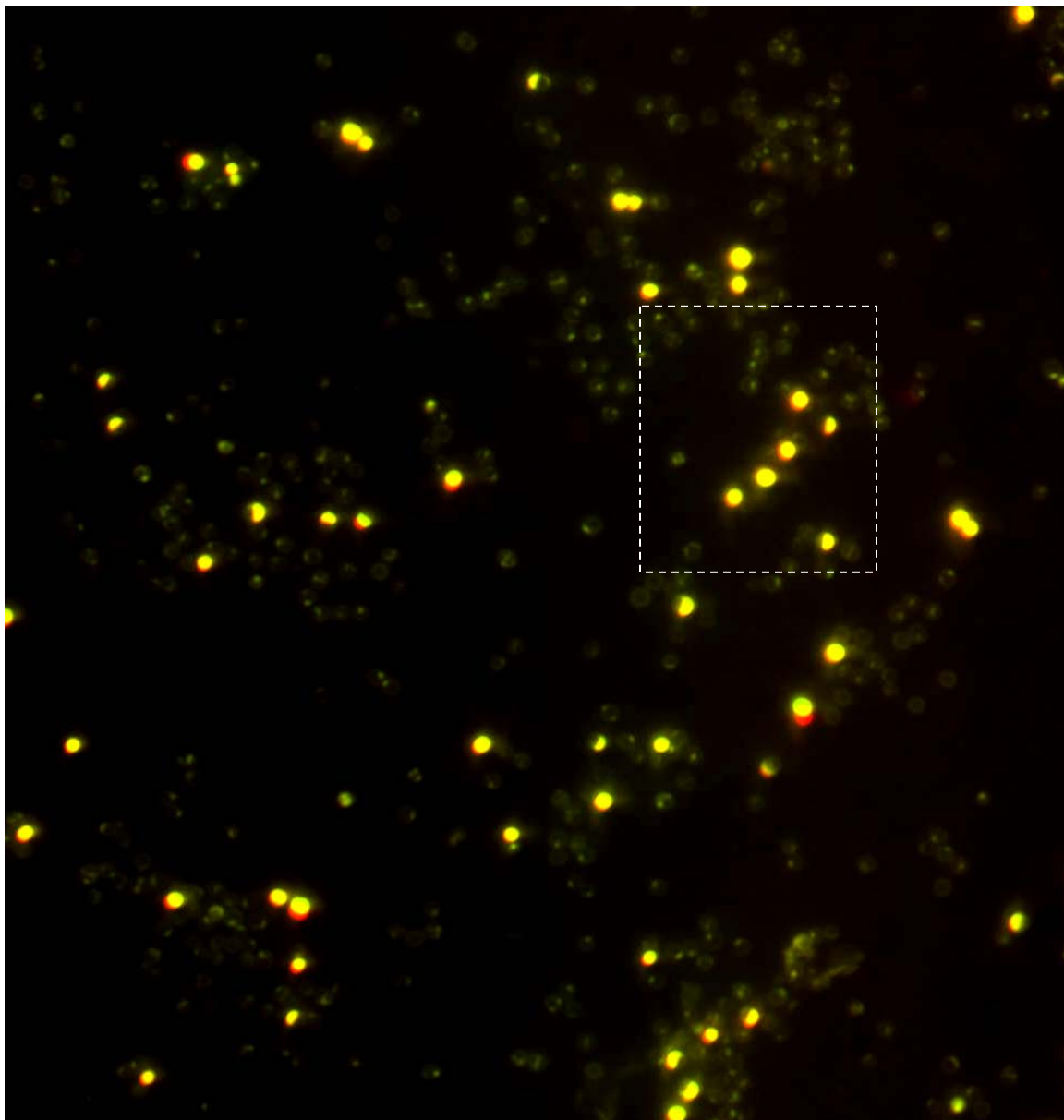


Figure B-21. Epifluorescence image of *S. aureus* cells incubated with 10 μM F-E2 (green signal) for 45 min and 1.5 μM PI (red signal) for an additional 15 min. The area of the image within the white dotted line is the cropped image shown in the text.

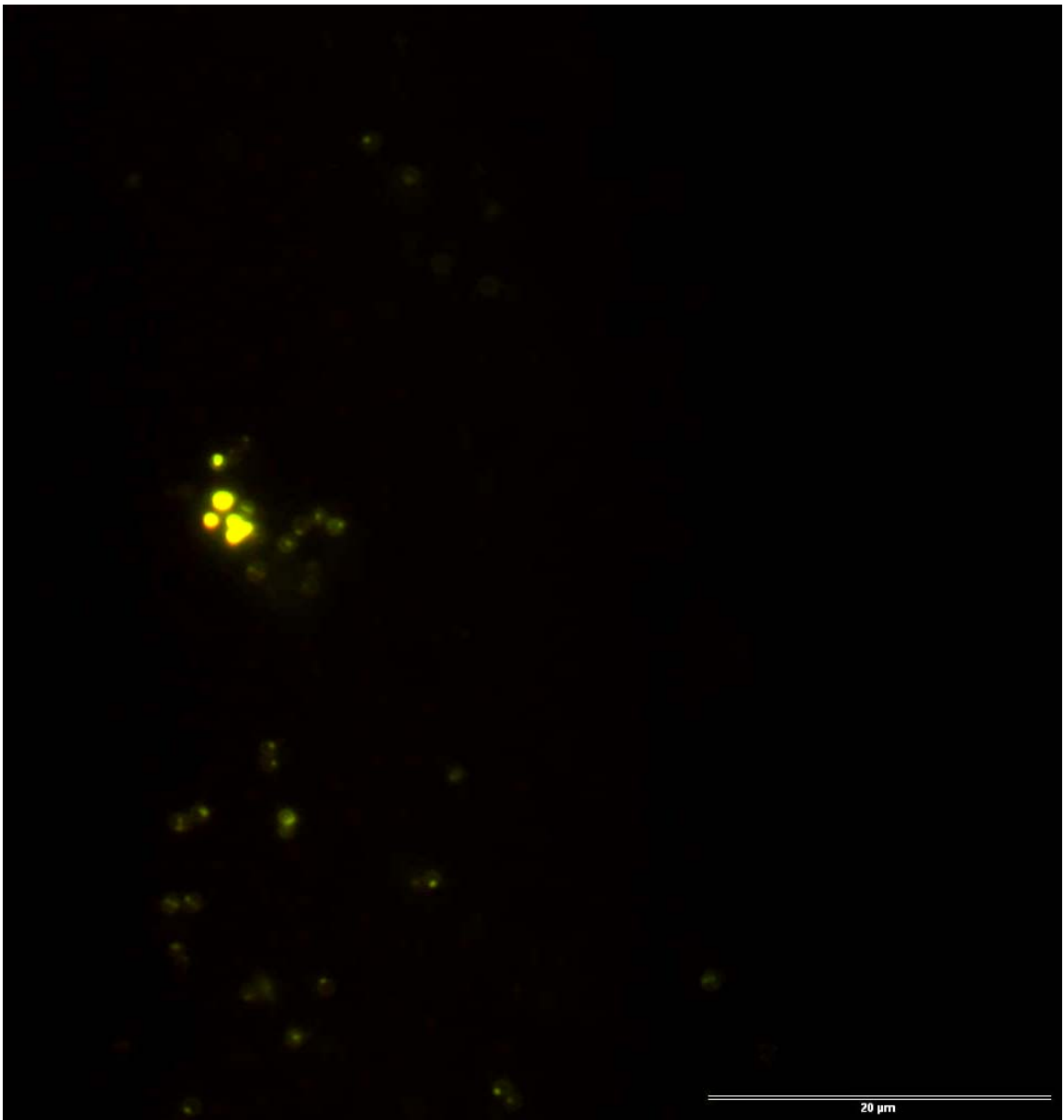


Figure B-22. Epifluorescence image of *S. aureus* cells incubated with 10 μM F-E4 (green signal) for 45 min and 1.5 μM PI (red signal) for an additional 15 min. The area of the image within the white dotted line is the cropped image shown in the text.

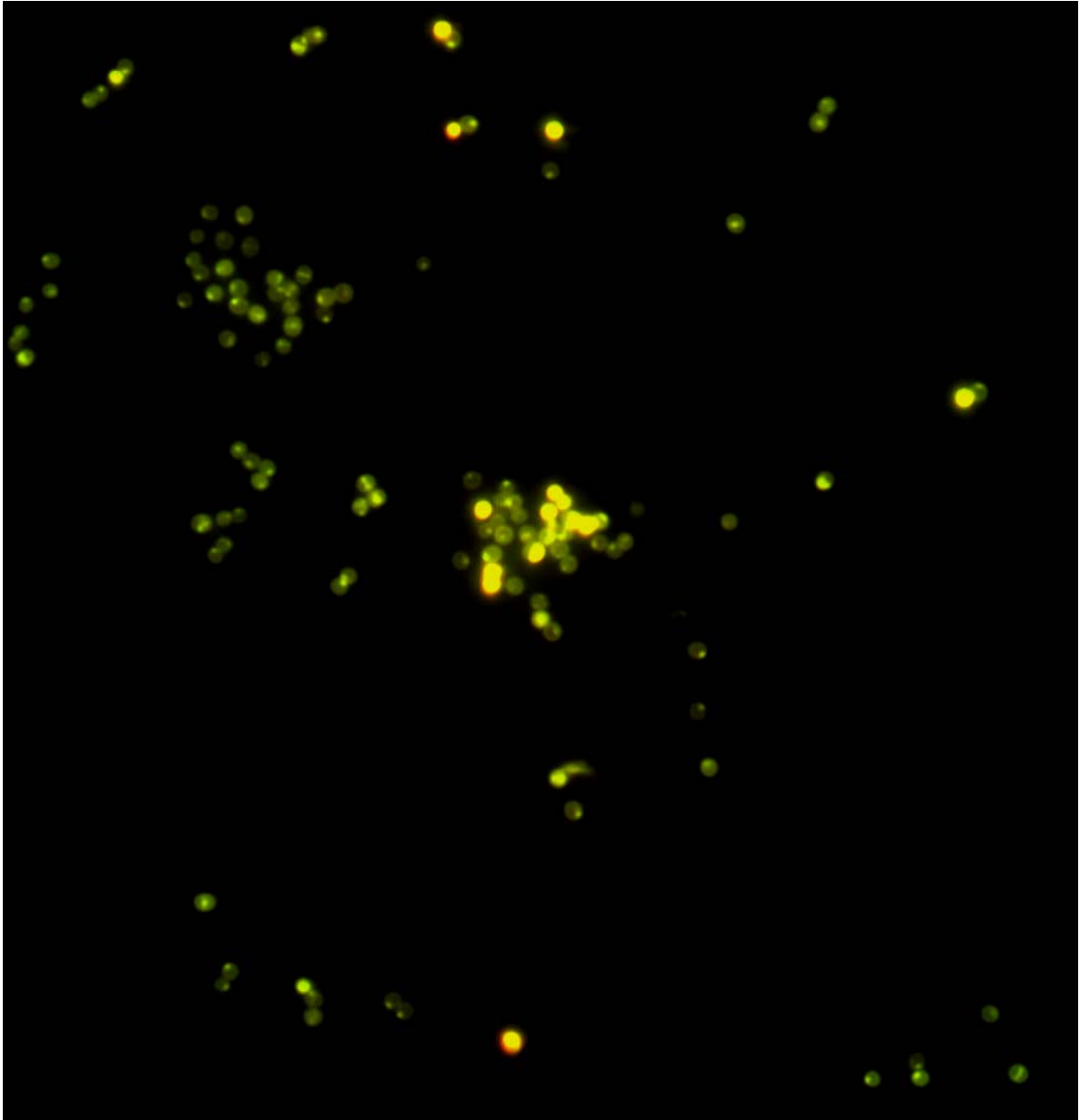


Figure B-23. Epifluorescence image of *S. aureus* cells incubated with 10 μM F-E6 (green signal) for 45 min and 1.5 μM PI (red signal) for an additional 15 min. The area of the image within the white dotted line is the cropped image shown in the text.

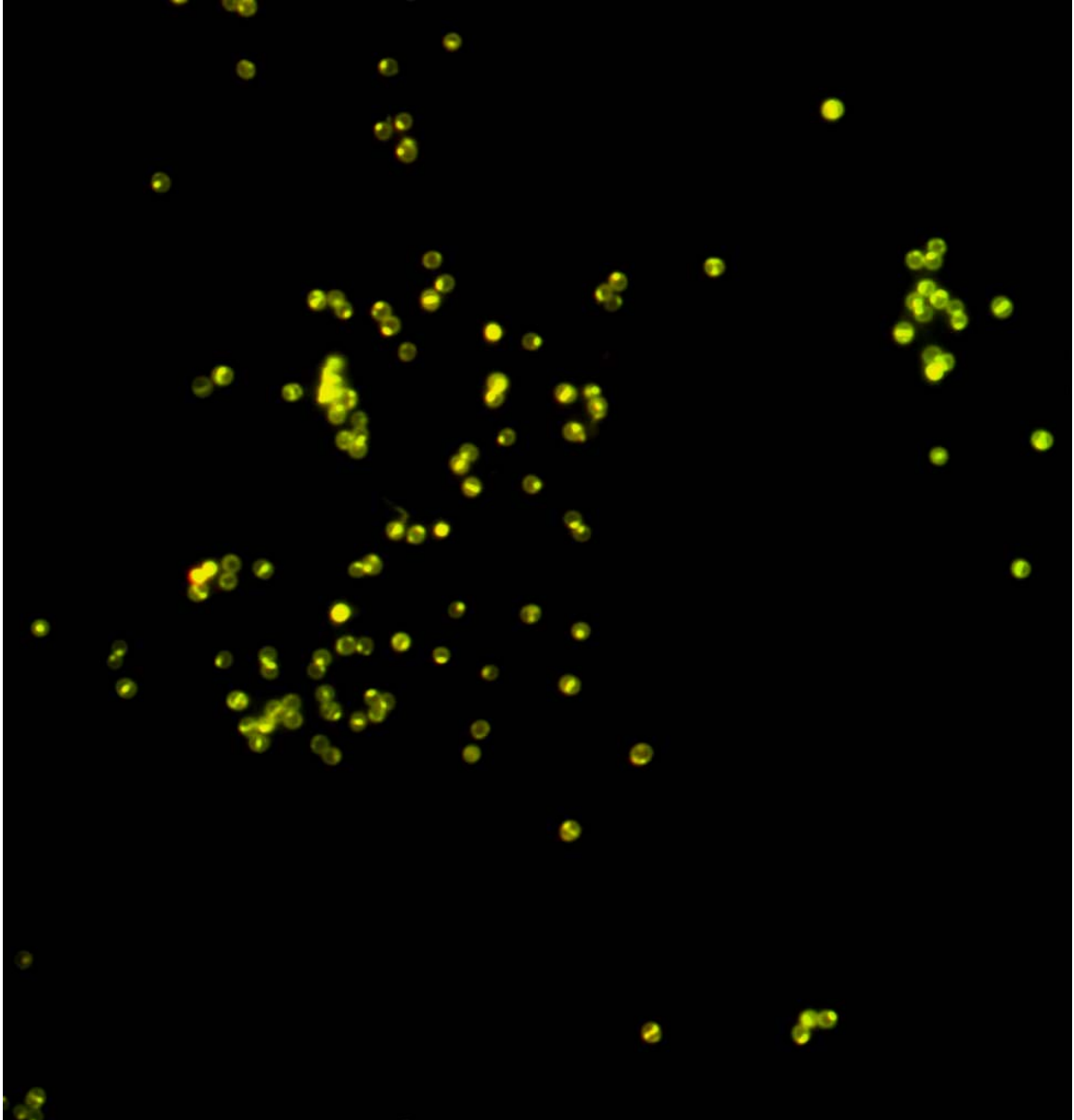


Figure B-24. Epifluorescence image of *S. aureus* cells incubated with 10 μ M F-Ec6 (green signal) for 45 min and 1.5 μ M PI (red signal) for an additional 15 min. The area of the image within the white dotted line is the cropped image shown in the text.

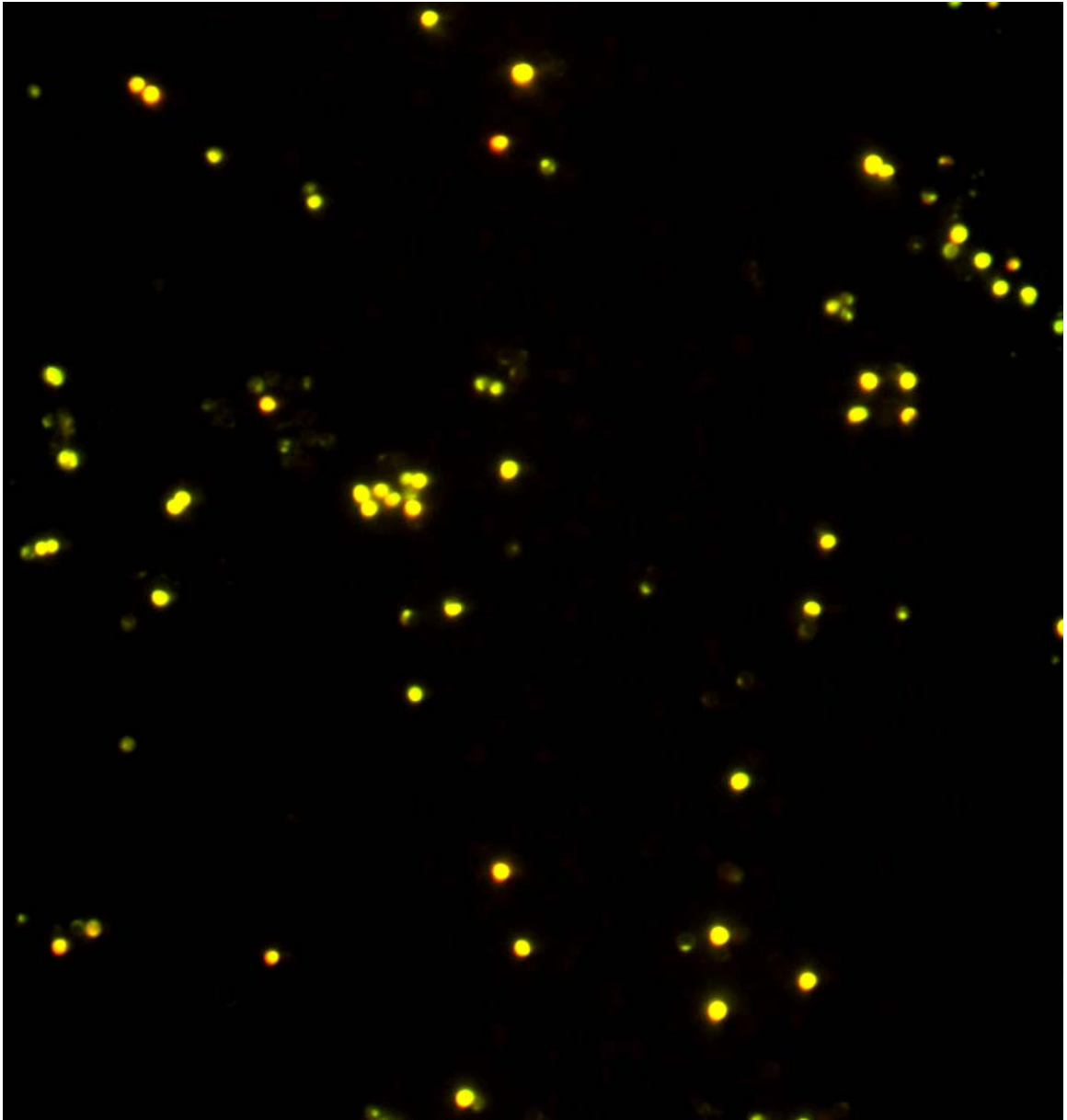


Figure B-25. Epifluorescence image of *S. aureus* cells incubated with 10 μM F-B2 (green signal) for 45 min and 1.5 μM PI (red signal) for an additional 15 min. The area of the image within the white dotted line is the cropped image shown in the text.

Supplemental Molecular Dynamics Simulation Data

For the molecular dynamics simulations, we modeled four representative syndiotactic alternating copolymers with a degree of polymerization of 10 (5 cationic and 5 hydrophobic side chains).

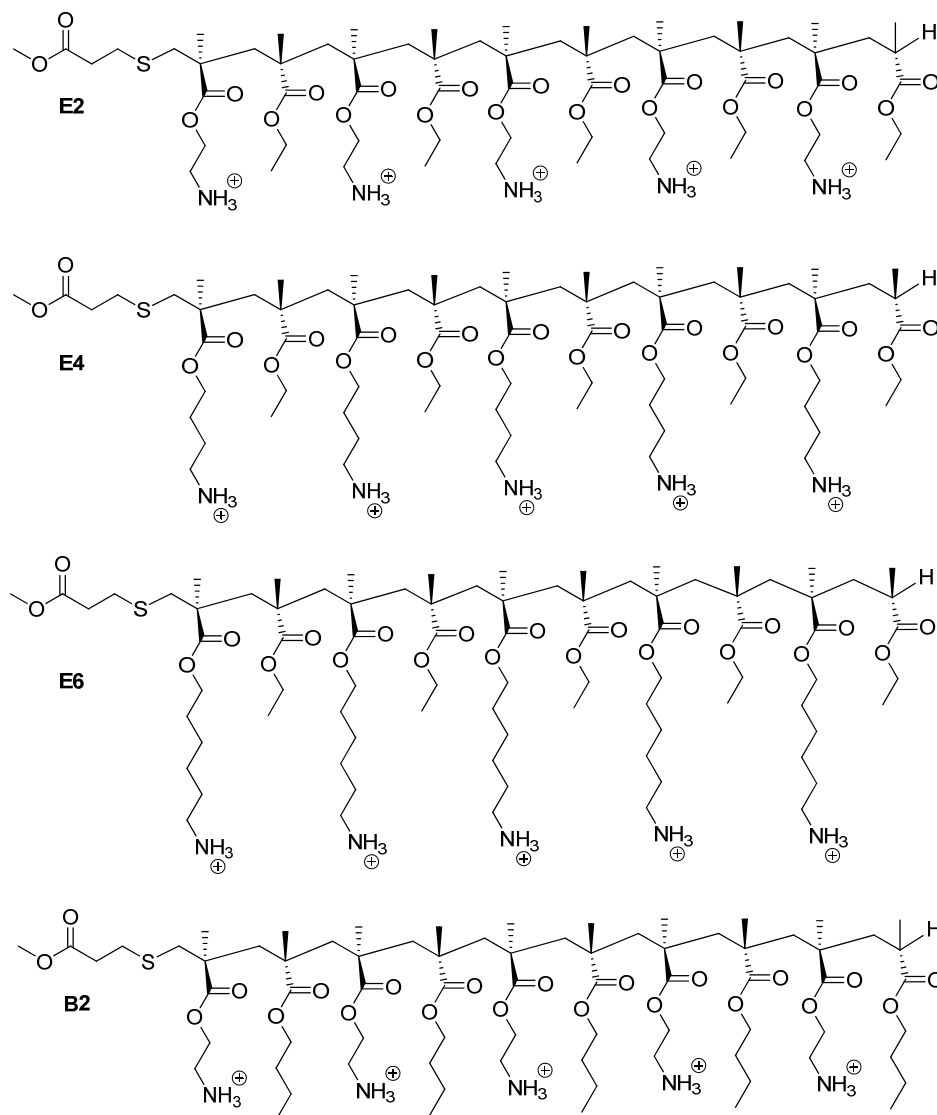


Figure B-26. Chemical structures of model copolymers

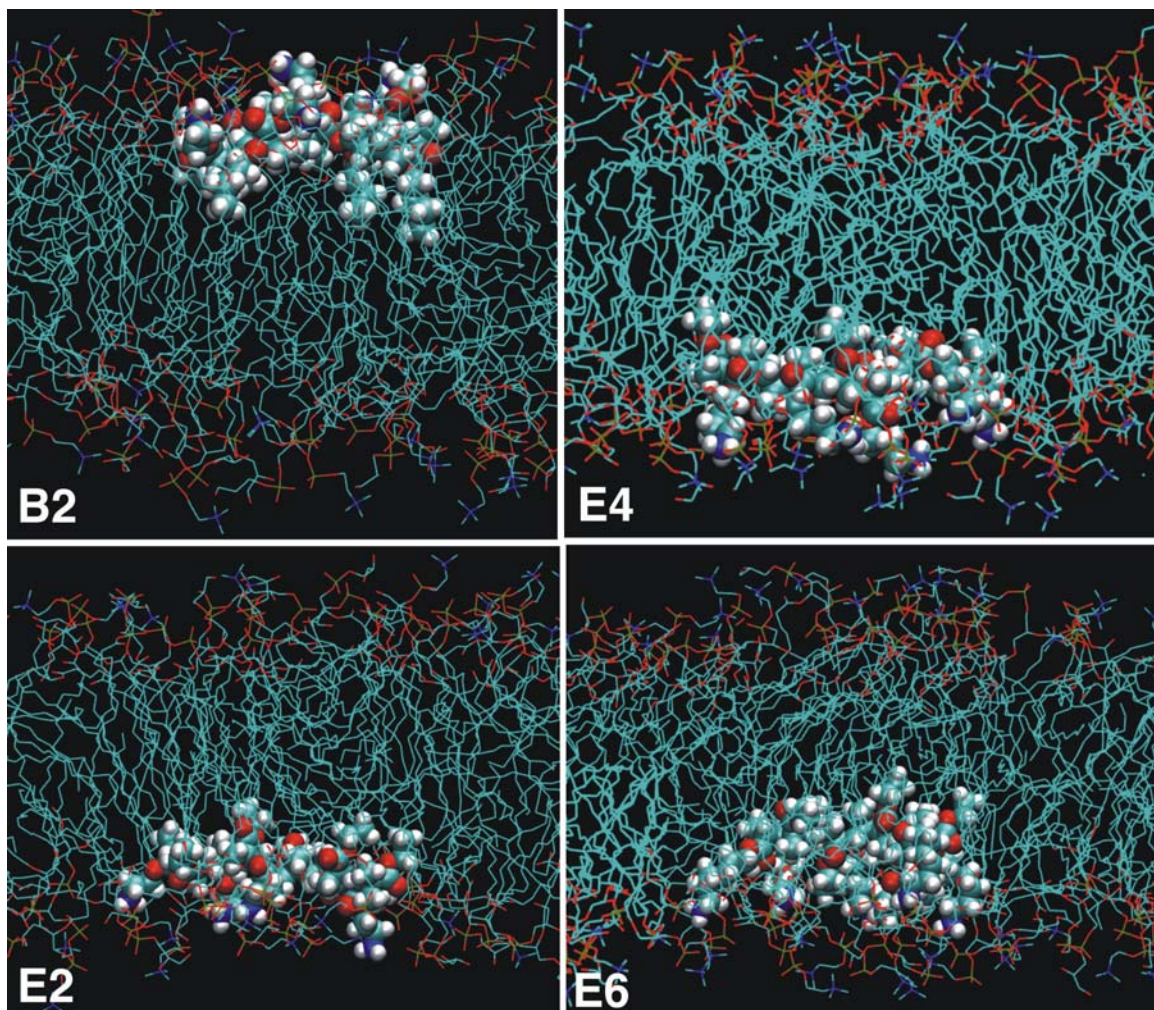


Figure B-27. Snapshots of the four systems at the end of ~50 ns simulations. Water is not shown for clarity. All the four polymers adopt conformations which are parallel to the lipid surface, stretched out. The amine (spacer) groups are interacting strongly with the bilayer headgroup and the hydrophobic groups are interacting with the tail region of the bilayer.

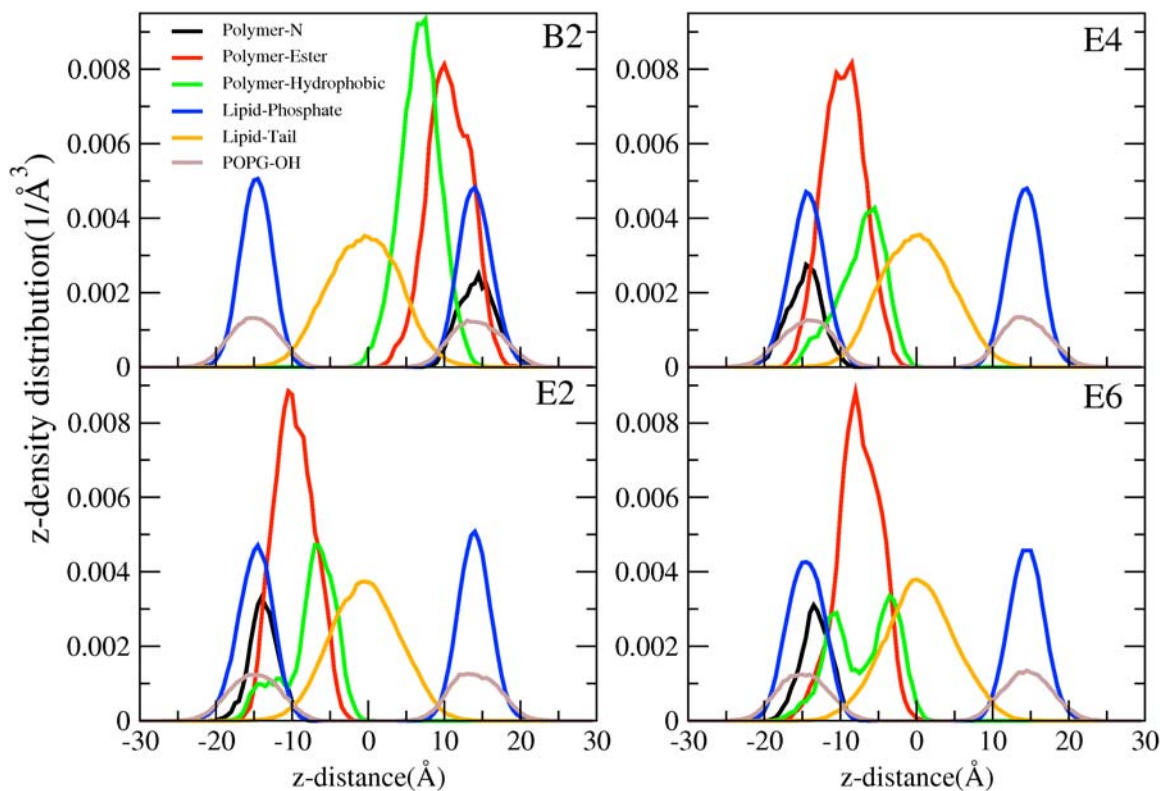


Figure B-28. Z-density profiles of various components of lipid-polymer systems averaged over last 10 ns of MD simulation (40-50 ns). The amine groups interact strongly with the phosphate groups of both POPC and POPG. In case of E4, the amine groups (black) interact equally with phosphate (blue) and hydroxyl groups (of POPG) (brown) as seen from the alignment of the peaks. In case of E6, the amine groups are deeper into the lipid region (due to longer spacer groups), weakening the strong polar interactions with head groups as seen from disalignment of peaks. From E2 to E6, the location of ester group (red) also moves deeper into the bilayer tail region. The location of terminal carbon atoms of the lipid-tail regions are also shown (in orange)

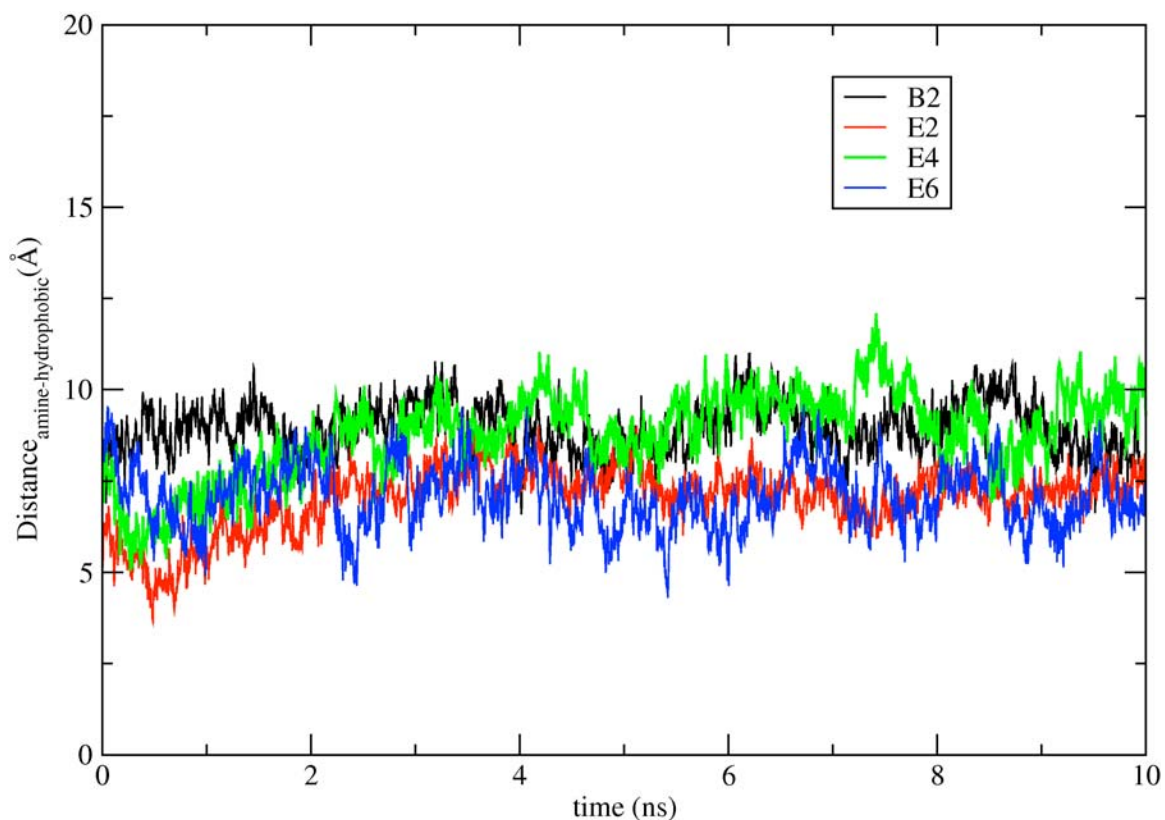


Figure B-29. The distance between center of mass of the hydrophobic and amine groups (suggesting segregation of hydrophobic and charged groups) as a function of time in last 10 ns(40-50ns) of MD simulation. From the figure, the segregation is higher for E4 and B2 ($\sim 9\text{\AA}$) than for E2 and E6 ($\sim 7\text{\AA}$). Increasing the spacer length does not seem to correlate linearly with segregation of the charged and hydrophobic groups (comparing E4 and E6)

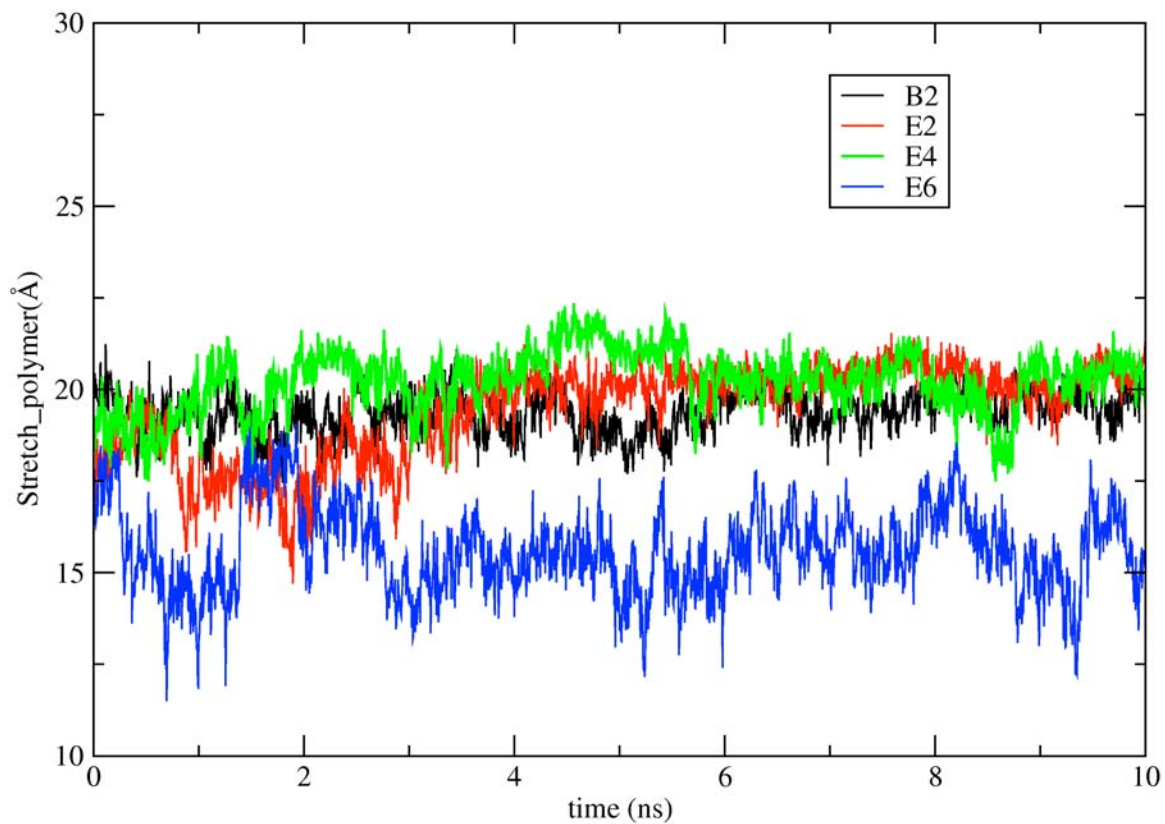


Figure B-30. The stretching of the polymer is measured as the distance between the ester carbons of first and last monomers. This distance is averaged over the last 10 ns. As can be seen from the figure, E6 has a more ‘compact’ structure compared to other structures. Comparatively, E2, E4 and B2 have similar stretching (with E4 stretched the most).

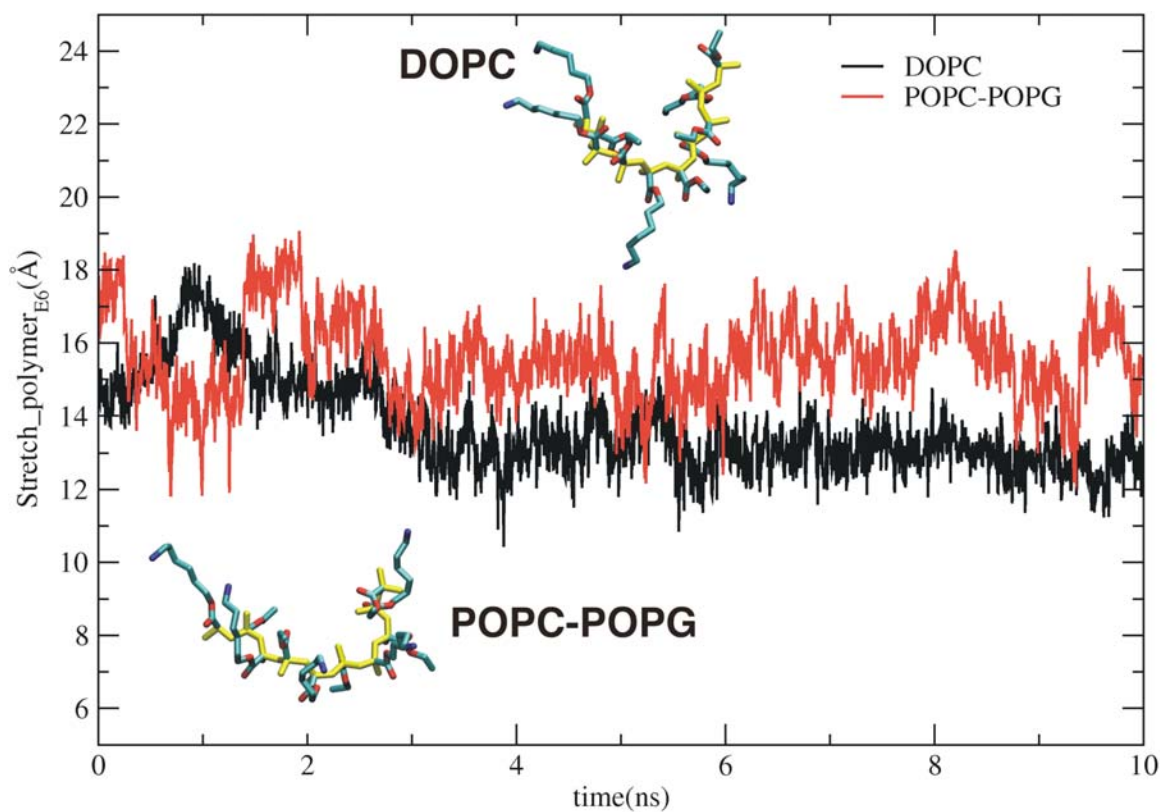


Figure B-31. The stretching of the E6 polymer is measured as the distance between the ester carbons of first and last monomers. This distance is averaged over the last 10 ns of both simulations. In both zwitterionic and charged lipids systems, E6 adopts a compact ‘crescent’ shaped backbone structure. E6 has more compact conformation in the case of zwitterionic lipid system as compared to charged lipids.

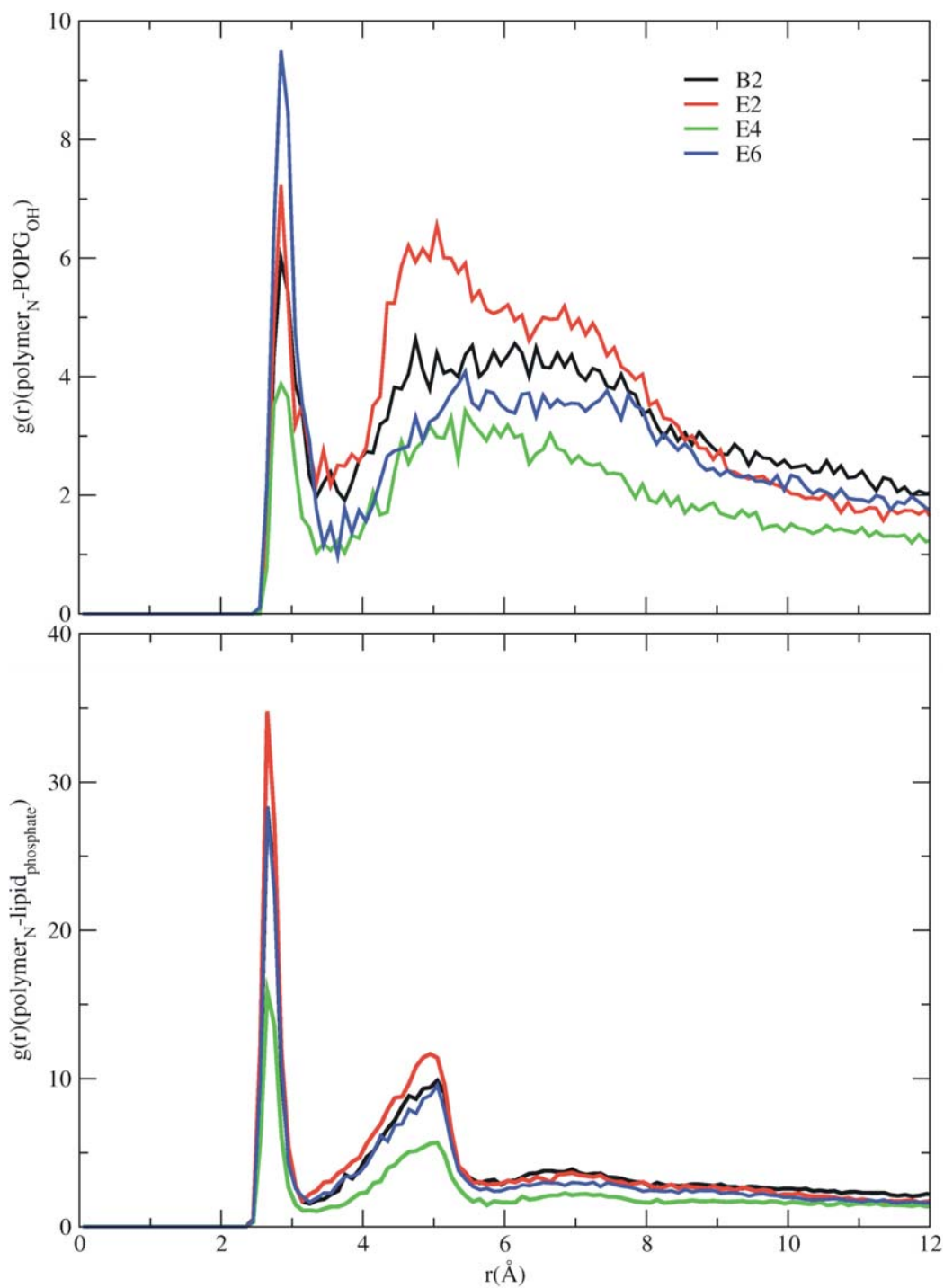


Figure B-32. The radial distribution function of interactions of spacer groups of polymers with charged groups of lipid bilayers. The data is computed over last 10 ns of MD simulation.

REFERENCES

1. Fleming, A., *British Journal of Experimental Pathology* **1929**, 10 (3), 226-236.
2. Boucher, H. W., *Clinical Infectious Diseases* **2010**, 50, S4-S9.
3. Spellberg, B.; Guidos, R.; Gilbert, D.; Bradley, J.; Boucher, H. W.; Scheld, W. M.; Bartlett, J. G.; Edwards, J.; Infect Dis Soc, A., *Clinical Infectious Diseases* **2008**, 46 (2), 155-164.
4. Chambers, H. F.; Deleo, F. R., *Nature Reviews Microbiology* **2009**, 7 (9), 629-641.
5. Jassal, M.; Bishai, W. R., *Lancet Infectious Diseases* **2009**, 9 (1), 19-30.
6. Chan, E. D.; Iseman, M. D., *Current Opinion in Infectious Diseases* **2008**, 21 (6), 587-595.
7. Werner, G.; Strommenger, B.; Witte, W., *Future Microbiology* **2008**, 3 (5), 547-562.
8. Boucher, H. W.; Talbot, G. H.; Bradley, J. S.; Edwards, J. E.; Gilbert, D.; Rice, L. B.; Scheld, M.; Spellberg, B.; Bartlett, J., *Clinical Infectious Diseases* **2009**, 48 (1), 1-12.
9. Zasloff, M., *Nature* **2002**, 415 (6870), 389-395.
10. Bowdish, D. M. E.; Davidson, D. J.; Scott, M. G.; Hancock, R. E. W., *Antimicrobial Agents and Chemotherapy* **2005**, 49 (5), 1727-1732.
11. Hancock, R. E. W.; Sahl, H. G., *Nature Biotechnology* **2006**, 24 (12), 1551-1557.
12. Ge, Y. G.; MacDonald, D. L.; Holroyd, K. J.; Thornsberry, C.; Wexler, H.; Zasloff, M., *Antimicrobial Agents and Chemotherapy* **1999**, 43 (4), 782-788.
13. Hirsch, J. G., *Journal of Experimental Medicine* **1956**, 103 (5), 589-611.
14. Zasloff, M., *Proceedings of the National Academy of Sciences of the United States of America* **1987**, 84 (15), 5449-5453.
15. Steiner, H.; Hultmark, D.; Engstrom, A.; Bennich, H.; Boman, H. G., *Nature* **1981**, 292 (5820), 246-248.
16. Ganz, T.; Selsted, M. E.; Szklarek, D.; Harwig, S. S. L.; Daher, K.; Bainton, D. F.; Lehrer, R. I., *Journal of Clinical Investigation* **1985**, 76 (4), 1427-1435.
17. Selsted, M. E.; Harwig, S. S. L.; Ganz, T.; Schilling, J. W.; Lehrer, R. I., *Journal of Clinical Investigation* **1985**, 76 (4), 1436-1439.
18. Brown, K. L.; Hancock, R. E. W., *Current Opinion in Immunology* **2006**, 18 (1), 24-30.
19. Boman, H. G., *Journal of Internal Medicine* **2003**, 254 (3), 197-215.
20. Francois, B.; Sanchez, M.; Squire, R.; Legras, A.; Minkowitz, H.; Barturen, F.; Breitmeyer, J.; Hardalo, C., *Abstracts of the Interscience Conference on Antimicrobial Agents and Chemotherapy* **2009**, 49, 320.
21. Wang, Z.; Wang, G. S., *Nucleic Acids Research* **2004**, 32, D590-D592.
22. Wang, G. S.; Li, X.; Wang, Z., *Nucleic Acids Research* **2009**, 37, D933-D937.
23. Brogden, K. A., *Nature Reviews Microbiology* **2005**, 3 (3), 238-250.
24. Marcos, J. F.; Gandia, M., *Expert Opinion on Drug Discovery* **2009**, 4 (6), 659-671.

25. Wade, D.; Boman, A.; Wahlin, B.; Drain, C. M.; Andreu, D.; Boman, H. G.; Merrifield, R. B., *Proceedings of the National Academy of Sciences of the United States of America* **1990**, *87* (12), 4761-4765.
26. Matsuzaki, K.; Harada, M.; Handa, T.; Funakoshi, S.; Fujii, N.; Yajima, H.; Miyajima, K., *Biochimica Et Biophysica Acta* **1989**, *981* (1), 130-134.
27. Matsuzaki, K.; Harada, M.; Funakoshi, S.; Fujii, N.; Miyajima, K., *Biochimica Et Biophysica Acta* **1991**, *1063* (1), 162-170.
28. Friedberg, D.; Friedberg, I.; Shilo, M., *Infection and Immunity* **1970**, *1* (3), 311-318.
29. Friedberg, D.; Shilo, M., *Infection and Immunity* **1970**, *1* (3), 305-310.
30. Matsuzaki, K., *Biochimica Et Biophysica Acta-Biomembranes* **2009**, *1788* (8), 1687-1692.
31. Imura, Y.; Choda, N.; Matsuzaki, K., *Biophysical Journal* **2008**, *95* (12), 5757-5765.
32. Dathe, M.; Wieprecht, T., *Biochimica Et Biophysica Acta-Biomembranes* **1999**, *1462* (1-2), 71-87.
33. Shai, Y., *Biochimica Et Biophysica Acta-Biomembranes* **1999**, *1462* (1-2), 55-70.
34. Oren, Z.; Shai, Y., *Biopolymers* **1998**, *47* (6), 451-463.
35. Shai, Y., *Biopolymers* **2002**, *66* (4), 236-248.
36. Imura, Y.; Choda, N.; Fujii, N.; Matsuzaki, K., *Biophysical Journal* **2007**, 199A-199A.
37. Matsuzaki, K., *Biochimica Et Biophysica Acta-Reviews on Biomembranes* **1998**, *1376* (3), 391-400.
38. Matsuzaki, K.; Sugishita, K.; Fujii, N.; Miyajima, K., *Biophysical Journal* **1994**, *66* (2), A223-A223.
39. Matsuzaki, K.; Sugishita, K.; Fujii, N.; Miyajima, K., *Biochemistry* **1995**, *34* (10), 3423-3429.
40. Epand, R. F.; Raguse, T. L.; Gellman, S. H.; Epand, R. M., *Biochemistry* **2004**, *43* (29), 9527-9535.
41. Chen, Y. X.; Vasil, A. I.; Rehaume, L.; Mant, C. T.; Burns, J. L.; Vasil, M. L.; Hancock, R. E. W.; Hodges, R. S., *Chemical Biology & Drug Design* **2006**, *67* (2), 162-173.
42. Fernandez-Vidall, M.; Jayasinghe, S.; Ladokhin, A. S.; White, S. H., *Journal of Molecular Biology* **2007**, *370* (3), 459-470.
43. Patch, J. A.; Barron, A. E., *Journal of the American Chemical Society* **2003**, *125* (40), 12092-12093.
44. White, S. H.; Wimley, W. C., *Annual Review of Biophysics and Biomolecular Structure* **1999**, *28*, 319-365.
45. Langham, A. A.; Ahmad, A. S.; Kaznessis, Y. N., *Journal of the American Chemical Society* **2008**, *130* (13), 4338-4346.
46. Subbalakshmi, C.; Sitaram, N., *Fems Microbiology Letters* **1998**, *160* (1), 91-96.
47. Hale, J. D.; Hancock, R. E., *Expert Review of Anti-Infective Therapy* **2007**, *5* (6), 951-959.
48. Matsuzaki, K.; Murase, O.; Fujii, N.; Miyajima, K., *Biophysical Journal* **1995**, *68* (2 PART 2), A126.
49. Matsuzaki, K.; Murase, O.; Miyajima, K., *Biochemistry* **1995**, *34* (39), 12553-12559.

50. Matsuzaki, K.; Murase, O.; Fujii, N.; Miyajima, K., *Biochemistry* **1996**, *35* (35), 11361-11368.
51. Wimley, W. C.; Selsted, M. E.; White, S. H., *Protein Science* **1994**, *3* (9), 1362-1373.
52. Marr, A. K.; Gooderham, W. J.; Hancock, R. E. W., *Current Opinion in Pharmacology* **2006**, *6* (5), 468-472.
53. Gottler, L. M.; Ramamoorthy, A., *Biochimica Et Biophysica Acta-Biomembranes* **2009**, *1788* (8), 1680-1686.
54. Cheng, R. P.; Gellman, S. H.; DeGrado, W. F., *Chemical Reviews* **2001**, *101* (10), 3219-3232.
55. Porter, E. A.; Weisblum, B.; Gellman, S. H., *Journal of the American Chemical Society* **2002**, *124* (25), 7324-7330.
56. Hamuro, Y.; Schneider, J. P.; DeGrado, W. F., *Journal of the American Chemical Society* **1999**, *121* (51), 12200-12201.
57. Jenssen, H.; Hamill, P.; Hancock, R. E. W., *Clinical Microbiology Reviews* **2006**, *19* (3), 491-+.
58. Klimek, J. W.; Umbreit, L. E., *Soap and Sanitary Chem* **1948**, *24* ((1)), 137-145.
59. Price, P. B., *Archives of Surgery* **1950**, *61* (1), 23-33.
60. Ikeda, T.; Tazuke, S.; Suzuki, Y., *Makromolekulare Chemie-Macromolecular Chemistry and Physics* **1984**, *185* (5), 869-876.
61. Kenawy, E. R.; Worley, S. D.; Broughton, R., *Biomacromolecules* **2007**, *8* (5), 1359-1384.
62. Tashiro, T., *Macromolecular Materials and Engineering* **2001**, *286* (2), 63-87.
63. Vieira, D. B.; Carmona-Ribeiro, A. M., *Journal of Antimicrobial Chemotherapy* **2006**, *58* (4), 760-767.
64. Tiller, J. C.; Liao, C. J.; Lewis, K.; Klivanov, A. M., *Proceedings of the National Academy of Sciences of the United States of America* **2001**, *98* (11), 5981-5985.
65. Lee, S. B.; Koepsel, R. R.; Morley, S. W.; Matyjaszewski, K.; Sun, Y. J.; Russell, A. J., *Biomacromolecules* **2004**, *5* (3), 877-882.
66. Gabriel, G. J.; Som, A.; Madkour, A. E.; Eren, T.; Tew, G. N., *Materials Science & Engineering R-Reports* **2007**, *57* (1-6), 28-64.
67. Palermo, E. F.; Kuroda, K., *Applied Microbiology and Biotechnology* **2010**, *87* (5), 1605-1615.
68. Gelman, M. A.; Weisblum, B.; Lynn, D. M.; Gellman, S. H., *Organic Letters* **2004**, *6* (4), 557-560.
69. Tew, G. N.; Liu, D. H.; Chen, B.; Doerksen, R. J.; Kaplan, J.; Carroll, P. J.; Klein, M. L.; DeGrado, W. F., *Proceedings of the National Academy of Sciences of the United States of America* **2002**, *99* (8), 5110-5114.
70. Liu, D. H.; Choi, S.; Chen, B.; Doerksen, R. J.; Clements, D. J.; Winkler, J. D.; Klein, M. L.; DeGrado, W. F., *Angewandte Chemie-International Edition* **2004**, *43* (9), 1158-1162.
71. Breitenkamp, R. B.; Arnt, L.; Tew, G. N. In *Facially amphiphilic phenylene ethynyls*, 7th International Symposium on Polymers for Advanced Technologies, Ft Lauderdale, FL, Sep 21-24; Ft Lauderdale, FL, 2003; pp 189-194.
72. Tew, G. N.; Scott, R. W.; Klein, M. L.; DeGrado, W. F., *Accounts of Chemical Research* **2010**, *43* (1), 30-39.

73. Mowery, B. P.; Lindner, A. H.; Weisblum, B.; Stahl, S. S.; Gellman, S. H., *Journal of the American Chemical Society* **2009**, *131* (28), 9735-9745.
74. Mowery, B. P.; Lee, S. E.; Kissounko, D. A.; Epanand, R. F.; Epanand, R. M.; Weisblum, B.; Stahl, S. S.; Gellman, S. H., *Journal of the American Chemical Society* **2007**, *129* (50), 15474-+.
75. Kuroda, K.; DeGrado, W. F., *J Amer Chem Soc* **2005**, *127* (12), 4128-4129.
76. Kuroda, K.; Caputo, G. A.; DeGrado, W. F., *Chemistry-a European Journal* **2009**, *15* (5), 1123-1133.
77. Ilker, M. F.; Nusslein, K.; Tew, G. N.; Coughlin, E. B., *Journal of the American Chemical Society* **2004**, *126* (48), 15870-15875.
78. Lienkamp, K.; Madkour, A. E.; Musante, A.; Nelson, C. F.; Nusslein, K.; Tew, G. N., *Journal of the American Chemical Society* **2008**, *130* (30), 9836-9843.
79. Gabriel, G. J.; Maegerlein, J. A.; Nelson, C. E.; Dabkowski, J. M.; Eren, T.; Nusslein, K.; Tew, G. N., *Chemistry-a European Journal* **2009**, *15* (2), 433-439.
80. Palermo, E. F.; Kuroda, K., *Biomacromolecules* **2009**, *10* (6), 1416-1428.
81. Palermo, E. F.; Sovadinova, I.; Kuroda, K., *Biomacromolecules* **2009**, *10* (11), 3098-3107.
82. Allison, B. C.; Applegate, B. M.; Youngblood, J. P., *Biomacromolecules* **2007**, *8* (10), 2995-2999.
83. Ikeda, T.; Tazuke, S.; Suzuki, Y., *Makromolekulare Chemie-Macromolecular Chemistry and Physics* **1984**, *185* (5), 869-876.
84. Nurdin, N.; Helary, G.; Sauvet, G., *Journal of Applied Polymer Science* **1993**, *50* (4), 663-670.
85. Baudrion, F.; Perichaud, A.; Coen, S., *Journal of Applied Polymer Science* **1998**, *70* (13), 2657-2666.
86. Kenawy, E. R.; Abdel-Hay, F. I.; El-Raheem, A.; El-Shanshoury, R.; El-Newehy, M. H., *Journal of Controlled Release* **1998**, *50* (1-3), 145-152.
87. Chen, C. Z. S.; Beck-Tan, N. C.; Dhurjati, P.; van Dyk, T. K.; LaRossa, R. A.; Cooper, S. L., *Biomacromolecules* **2000**, *1* (3), 473-480.
88. Dizman, B.; Elasri, M. O.; Mathias, L. J., *Journal of Polymer Science Part a-Polymer Chemistry* **2006**, *44* (20), 5965-5973.
89. Eren, T.; Som, A.; Rennie, J. R.; Nelson, C. F.; Urgina, Y.; Nusslein, K.; Coughlin, E. B.; Tew, G. N., *Macromolecular Chemistry and Physics* **2008**, *209* (5), 516-524.
90. Rozga-Wijas, K.; Mizerska, U.; Fortuniak, W.; Chojnowski, J.; Halasa, R.; Werel, W., *Journal of Inorganic and Organometallic Polymers and Materials* **2007**, *17* (4), 605-613.
91. Chen, L.; Ma, W. Y.; Yu, X. H.; Yang, C. Z., *Chinese Journal of Polymer Science* **1996**, *14* (3), 205-210.
92. Kugler, R.; Bouloussa, O.; Rondelez, F., *Microbiology-Sgm* **2005**, *151*, 1341-1348.
93. Klibanov, A. M., *Journal of Materials Chemistry* **2007**, *17* (24), 2479-2482.
94. Murata, H.; Koepsel, R. R.; Matyjaszewski, K.; Russell, A. J., *Biomaterials* **2007**, *28*, 4870-4879.
95. Milovic, N. M.; Wang, J.; Lewis, K.; Klibanov, A. M., *Biotechnology and Bioengineering* **2005**, *90* (6), 715-722.
96. Sambhy, V.; Peterson, B. R.; Sen, A., *Angewandte Chemie-International Edition* **2008**, *47* (7), 1250-1254.

97. Porter, E. A.; Wang, X.; Lee, H. S.; Weisblum, B.; Gellman, S. H., *Nature* **2000**, 405 (6784), 298-298.
98. Schmitt, M. A.; Weisblum, B.; Gellman, S. H., *Journal of the American Chemical Society* **2004**, 126 (22), 6848-6849.
99. Dathe, M.; Seydel, J.; Matsuzaki, K.; Beyermann, M.; Krause, E.; Bienert, M., *Biophysical Journal* **1995**, 68 (2 PART 2), A328.
100. Verkleij, A. J.; Zwaal, R. F. A.; Roelofse, B.; Comfuriu, P.; Kastelij, D.; Vandeene, L., *Biochimica Et Biophysica Acta* **1973**, 323 (2), 178-193.
101. Wilkinson, S. G., *Microbial Lipids*. Academic Press: London, England, UK; San Diego, CA, USA, 1988; Vol. 1.
102. Dathe, M.; Schumann, M.; Wieprecht, T.; Winkler, A.; Beyermann, M.; Krause, E.; Matsuzaki, K.; Murase, O.; Bienert, M., *Biochemistry* **1996**, 35 (38), 12612-12622.
103. Powers, J. P. S.; Hancock, R. E. W., *Peptides* **2003**, 24 (11), 1681-1691.
104. Bechinger, B., *Journal of Membrane Biology* **1997**, 156 (3), 197-211.
105. Bechinger, B., *Critical Reviews in Plant Sciences* **2004**, 23 (3), 271-292.
106. Shai, Y., *Biophysical Journal* **2001**, 80 (1), 2A-3A.
107. Kuroda, K.; Caputo, G. A.; DeGrado, W. F., *Chemistry* **2009**, 15 (5), 1123-33.
108. He, L. H.; Read, E. S.; Armes, S. P.; Adams, D. J., *Macromolecules* **2007**, 40 (13), 4429-4438.
109. Sutani, K.; Kaetsu, I.; Uchida, K.; Matsubara, Y., *Radiat. Phys. Chem.* **2002**, 64, 331.
110. Wen, S.; Yin, X. N.; Stevenson, W. T. K., *Journal of Applied Polymer Science* **1991**, 42 (5), 1399-1406.
111. White, A.; Jiang, S., *Journal of Physical Chemistry B* **2011**, 115 (4), 7.
112. Matsuzaki, K.; Nakamura, A.; Murase, O.; Sugishita, K.; Fujii, N.; Miyajima, K., *Biochemistry* **1997**, 36 (8), 2104-2111.
113. Dathe, M.; Nikolenko, H.; Meyer, J.; Beyermann, M.; Bienert, M., *Febs Letters* **2001**, 501 (2-3), 146-150.
114. Jiang, Z. Q.; Vasil, A. I.; Hale, J. D.; Hancock, R. E. W.; Vasil, M. L.; Hodges, R. S., *Biopolymers* **2008**, 90 (3), 369-383.
115. Vogt, T. C. B.; Bechinger, B., *Journal of Biological Chemistry* **1999**, 274 (41), 29115-29121.
116. Mason, A. J.; Gasnier, C.; Kichler, A.; Prevost, G.; Aunis, D.; Metz-Boutigue, M. H.; Bechinger, B., *Antimicrobial Agents and Chemotherapy* **2006**, 50 (10), 3305-3311.
117. Marquette, A.; Mason, A. J.; Bechinger, B., *J. Peptide Sci.* **2008**, 14, 488-495.
118. Thomas, J. L.; Tirrell, D. A., *Accounts of Chemical Research* **1992**, 25 (8), 336-342.
119. Kusonwiriawong, C.; van de Wetering, P.; Hubbell, J. A.; Merkle, H. P.; Walter, E., *European Journal of Pharmaceutics and Biopharmaceutics* **2003**, 56 (2), 237-246.
120. Yessine, M. A.; Lafleur, M.; Meier, C.; Petereit, H. U.; Leroux, J. C., *Biochimica Et Biophysica Acta-Biomembranes* **2003**, 1613 (1-2), 28-38.
121. Murthy, N.; Chang, I.; Stayton, P.; Hoffman, A. In *pH-sensitive hemolysis by random copolymers of alkyl acrylates and acrylic acid*, 40th Microsymposium of the Prauge Meetings on Macromolecules, Prague, Czech Republic, Jul 17-20; Prague, Czech Republic, 2000; pp 49-55.

122. Murthy, N.; Campbell, J.; Fausto, N.; Hoffman, A. S.; Stayton, P. S., *Bioconjugate Chemistry* **2003**, *14* (2), 412-419.
123. Jones, R. A.; Cheung, C. Y.; Black, F. E.; Zia, J. K.; Stayton, P. S.; Hoffman, A. S.; Wilson, M. R., *Biochemical Journal* **2003**, *372*, 65-75.
124. Cheung, C. Y.; Murthy, N.; Stayton, P. S.; Hoffman, A. S., *Bioconjugate Chemistry* **2001**, *12* (6), 906-910.
125. Timofeeva, L. M.; Kleshcheva, N. A.; Moroz, A. F.; Didenko, L. V., *Biomacromolecules* **2009**, *10* (11), 2976-2986.
126. Binder, W. H., *Angewandte Chemie-International Edition* **2008**, *47* (17), 3092-3095.
127. Yang, L. H.; Gordon, V. D.; Trinkle, D. R.; Schmidt, N. W.; Davis, M. A.; DeVries, C.; Som, A.; Cronan, J. E.; Tew, G. N.; Wong, G. C. L., *Proceedings of the National Academy of Sciences of the United States of America* **2008**, *105* (52), 20595-20600.
128. Epand, R. F.; Mowery, B. P.; Lee, S. E.; Stahl, S. S.; Lehrer, R. I.; Gellman, S. H.; Epand, R. M., *Journal of Molecular Biology* **2008**, *379* (1), 38-50.
129. Chen, R. F., *Archives of Biochemistry and Biophysics* **1967**, *120* (3), 609-&.
130. Chen, R. F., *Analytical Biochemistry* **1968**, *25* (1-3), 412-&.
131. Chen, R. F., *Archives of Biochemistry and Biophysics* **1968**, *128* (1), 163-&.
132. Som, A.; Vemparala, S.; Ivanov, I.; Tew, G. N., *Biopolymers* **2008**, *90* (2), 83-93.
133. Leo, A. J.; Hansch, C., *Perspectives in Drug Discovery and Design* **1999**, *17* (1), 1-25.
134. Arakawa, J.; Pethica, B. A., *Journal of Colloid and Interface Science* **1980**, *75* (2), 441-450.
135. Nakayama, K.; Tari, I.; Sakai, M.; Murata, Y.; Sugihara, G., *J. Oleo Sci.* **2004**, *53* (5).
136. Wender, P. A.; Galliher, W. C.; Goun, E. A.; Jones, L. R.; Pillow, T. H., *Advanced Drug Delivery Reviews* **2008**, *60* (4-5), 452-472.
137. Wender, P. A.; Mitchell, D. J.; Pattabiraman, K.; Pelkey, E. T.; Steinman, L.; Rothbard, J. B., *Proceedings of the National Academy of Sciences of the United States of America* **2000**, *97* (24), 13003-13008.
138. Torchilin, V.; Weissig, V., *Liposomes: A Practical Approach*. 2nd ed.; Oxford University Press: 2003.
139. Ramamoorthy, A., *Solid State Nuclear Magnetic Resonance* **2009**, *35* (4), 201-207.
140. Hallock, K. J.; Lee, D. K.; Ramamoorthy, A., *Biophysical Journal* **2003**, *84* (5), 3052-3060.
141. Hallock, K. J.; Wildman, K. H.; Lee, D. K.; Ramamoorthy, A., *Biophysical Journal* **2002**, *82* (5), 2499-2503.
142. Palermo, E.; Kuroda, K., *Biomacromolecules* **2009**, *10* (6), 1416-1428.
143. Lu, Z. R.; Kopeckova, P.; Wu, Z. C.; Kopecek, J., *Macromolecular Chemistry and Physics* **1999**, *200* (9), 2022-2030.
144. Kopecek, J.; Kopeckova, P.; Minko, T.; Lu, Z. R., *European Journal of Pharmaceutics and Biopharmaceutics* **2000**, *50* (1), 61-81.
145. Minko, T.; Kopeckova, P.; Kopecek, J., *International Journal of Cancer* **2000**, *86* (1), 108-117.
146. Sanda, F.; Koyama, E.; Endo, T., *Journal of Polymer Science Part a-Polymer Chemistry* **1998**, *36* (12), 1981-1986.

147. Thomas, J. L.; You, H.; Tirrell, D. A., *Journal of the American Chemical Society* **1995**, *117* (10), 2949-2950.
148. Chung, J. C.; Gross, D. J.; Thomas, J. L.; Tirrell, D. A.; OpsahlOng, L. R., *Macromolecules* **1996**, *29* (13), 4636-4641.
149. Lienkamp, K.; Kumar, K. N.; Som, A.; Nusslein, K.; Tew, G. N., *Chemistry-a European Journal* **2009**, *15* (43), 11710-11714.
150. Huang, J. Y.; Koepsel, R. R.; Murata, H.; Wu, W.; Lee, S. B.; Kowalewski, T.; Russell, A. J.; Matyjaszewski, K., *Langmuir* **2008**, *24* (13), 6785-6795.
151. Murata, H.; Koepsel, R. R.; Matyjaszewski, K.; Russell, A. J., *Biomaterials* **2007**, *28* (32), 4870-4879.
152. Gabriel, G. J.; Pool, J. G.; Som, A.; Dabkowski, J. M.; Coughlin, E. B.; Muthukumar, M.; Tew, G. N., *Langmuir* **2008**, *24* (21), 12489-12495.
153. Fischer, D.; Li, Y. X.; Ahlemeyer, B.; Krieglstein, J.; Kissel, T., *Biomaterials* **2003**, *24* (7), 1121-1131.
154. van de Wetering, P.; Cherng, J. Y.; Talsma, H.; Crommelin, D. J. A.; Hennink, W. E. In *2-(dimethylamino)ethyl methacrylate based (co)polymers as gene transfer agents*, 8th International Symposium on Recent Advances in Drug Delivery Systems, Salt Lake City, Utah, Feb 24-27; Salt Lake City, Utah, 1997; pp 145-153.
155. Curiel, D. T.; Wagner, E.; Cotten, M.; Birnstiel, M. L.; Agarwal, S.; Li, C. M.; Loechel, S.; Hu, P. C., *Human Gene Therapy* **1992**, *3* (2), 147-154.
156. Boussif, O.; Lezoualch, F.; Zanta, M. A.; Mergny, M. D.; Scherman, D.; Demeneix, B.; Behr, J. P., *Proceedings of the National Academy of Sciences of the United States of America* **1995**, *92* (16), 7297-7301.
157. Mukhopadhyay, K.; Whitmire, W.; Xiong, Y. Q.; Molden, J.; Jones, T.; Peschel, A.; Staubitz, P.; Adler-Moore, J.; McNamara, P. J.; Proctor, R. A.; Yeaman, M. R.; Bayer, A. S., *Microbiology-Sgm* **2007**, *153*, 1187-1197.
158. Xiong, Y. Q.; Mukhopadhyay, K.; Yeaman, M. R.; Adler-Moore, J.; Bayer, A. S., *Antimicrobial Agents and Chemotherapy* **2005**, *49* (8), 3114-3121.
159. Yaroslavov, A. A.; Kuchenkova, O. Y.; Okuneva, I. B.; Melik-Nubarov, N. S.; Kozlova, N. O.; Lobyshev, V. I.; Menger, F. M.; Kabanov, V. A., *Biochimica Et Biophysica Acta-Biomembranes* **2003**, *1611* (1-2), 44-54.
160. Epand, R. F.; Schmitt, M. A.; Gellman, S. H.; Epand, R. M., *Biochimica Et Biophysica Acta-Biomembranes* **2006**, *1758* (9), 1343-1350.
161. Sellenet, P. H.; Allison, B.; Applegate, B. M.; Youngblood, J. P., *Biomacromolecules* **2007**, *8* (1), 19-23.
162. Stratton, T. R.; Rickus, J. L.; Youngblood, J. P., *Biomacromolecules* **2009**, *ASAP on the web*.
163. Al-Badri, Z. M.; Som, A.; Lyon, S.; Nelson, C. F.; Nusslein, K.; Tew, G. N., *Biomacromolecules* **2008**, *9* (10), 2805-2810.
164. Lehrer, R. I.; Barton, A.; Ganz, T., *Journal of Immunological Methods* **1988**, *108* (1-2), 153-158.
165. Storm, D. R.; Rosenthal, K. S.; Swanson, P. E., *Annual Review of Biochemistry* **1977**, *46*, 723-763.
166. Salton, M. R. J., *Journal of General Microbiology* **1951**, *5* (2), 391-404.
167. Wu, M. H.; Maier, E.; Benz, R.; Hancock, R. E. W., *Biochemistry* **1999**, *38* (22), 7235-7242.

168. Katsu, T.; Okada, S.; Imamura, T.; Komagoe, K.; Masuda, K.; Inoue, T.; Nakao, S., *Analytical Sciences* **2008**, *24* (12), 1551-1556.
169. Sato, H.; Feix, J. B., *Biochemistry* **2006**, *45* (33), 9997-10007.
170. Bolintineanu, D.; Hazrati, E.; Davis, H. T.; Lehrer, R. I.; Kaznessis, Y. N., *Peptides* **2010**, *31* (1), 1-8.
171. Sovadinova, I.; Palermo, E. F.; Huang, R.; Thoma, L. M.; Kuroda, K., *Biomacromolecules* **2010**, DOI:10.1021/bm1011739.
172. Scherrer, R.; Beaman, T. C.; Gerhardt, P., *Journal of Bacteriology* **1971**, *108* (2), 868-&.
173. Ivanov, I.; Vemparala, S.; Pophristic, V.; Kuroda, K.; DeGrado, W. F.; McCammon, J. A.; Klein, M. L., *Journal of the American Chemical Society* **2006**, *128* (6), 1778-1779.
174. Phillips, J. C.; Braun, R.; Wang, W.; Gumbart, J.; Tajkhorshid, E.; Villa, E.; Chipot, C.; Skeel, R. D.; Kale, L.; Schulten, K., *Journal of Computational Chemistry* **2005**, *26* (16), 1781-1802.
175. Klauda, J. B.; Venable, R. M.; Freites, J. A.; O'Connor, J. W.; Tobias, D. J.; Mondragon-Ramirez, C.; Vorobyov, I.; MacKerell, A. D.; Pastor, R. W., *Journal of Physical Chemistry B* **2010**, *114* (23), 7830-7843.
176. Jorgensen, W. L.; Chandrasekhar, J.; Madura, J. D.; Impey, R. W.; Klein, M. L., *Journal of Chemical Physics* **1983**, *79* (2), 926-935.
177. Park, C. B.; Kim, H. S.; Kim, S. C., *Biochemical and Biophysical Research Communications* **1998**, *244* (1), 253-257.
178. Langer, R.; Tirrell, D. A., *Nature* **2004**, *428* (6982), 487-492.
179. Hawker, C. J.; Wooley, K. L., *Science* **2005**, *309* (5738), 1200-1205.
180. Johnson, K. P.; Brooks, B. R.; Cohen, J. A.; Ford, C. C.; Goldstein, J.; Lisak, R. P.; Myers, L. W.; Panitch, H. S.; Rose, J. W.; Schiffer, R. B.; Vollmer, T.; Weiner, L. P.; Wolinsky, J. S.; Bird, S. J.; Constantinescu, C.; Kolson, D. L.; Gonzalezscarano, F.; Brennan, D.; Pfohl, D.; Mandler, R. N.; Rosenberg, G. A.; Jeffrey, C.; Barger, G. R.; Gandhi, B.; Moore, P. M.; Rogers, L. R.; Lisak, D.; Smith, L.; Ellison, G. W.; Baumhefner, R. W.; Craig, S. L.; Jalbut, S. S.; Katz, E.; Conway, K. L.; Burns, J. B.; Shiba, C.; Giang, D. W.; Petrie, M. D.; Guarnaccia, J. B.; Anderson, S.; McKeon, A.; McCarthy, M.; Thomas, A. B.; Vriesendorp, F. J.; Austin, S. G.; Lindsey, J. W.; Dimachkie, M.; Cerreta, E.; Kachuck, N.; McCarthy, K. A.; Fleming, J.; Parnell, J. H.; Tamulevich, J.; Weasler, C.; Kadosh, S.; Halt, H.; Stark, Y.; Pinchasi, I.; Spiller, N.; Vandennoort, S.; Miller, A.; Mellits, D.; Hopkins, J.; Reingold, S.; Gomolin, I. H., *Neurology* **1995**, *45* (7), 1268-1276.
181. Novak, B. M.; Risse, W.; Grubbs, R. H., *Advances in Polymer Science* **1992**, *102*, 47-72.
182. Bielawski, C. W.; Grubbs, R. H., *Progress in Polymer Science* **2007**, *32* (1), 1-29.
183. Chiefari, J.; Chong, Y. K.; Ercole, F.; Krstina, J.; Jeffery, J.; Le, T. P. T.; Mayadunne, R. T. A.; Meijs, G. F.; Moad, C. L.; Moad, G.; Rizzardo, E.; Thang, S. H., *Macromolecules* **1998**, *31* (16), 5559-5562.
184. Wang, J. S.; Matyjaszewski, K., *Macromolecules* **1995**, *28* (23), 7901-7910.
185. Kamber, N. E.; Jeong, W.; Waymouth, R. M.; Pratt, R. C.; Lohmeijer, B. G. G.; Hedrick, J. L., *Chemical Reviews* **2007**, *107* (12), 5813-5840.
186. Hall, H. K., *Journal of the American Chemical Society* **1957**, *79* (20), 5441-5444.

187. *National Committee for Clinical Laboratory Standards. Methods for dilution antimicrobial susceptibility tests for bacteria that grow aerobically.* Villanova, PA, 2003.
188. Hancock, R. E. W. Minimal Inhibitory Concentration (MIC) Determination for Cationic Antimicrobial Peptides by Modified Microtitre Broth Dilution Method.
189. Fiske, C. H.; Subbarow, Y., *Journal of Biological Chemistry* **1925**, 66 (2), 375-400.
190. Chen, T. R., *Cytogenetics and Cell Genetics* **1988**, 48 (1), 19-24.